



UNIwersytet Przyrodniczy we Wrocławiu

Wydział Biologii i Hodowli Zwierząt

Katedra Biologii Eksperymentalnej

Dyscyplina Nauki Biologiczne

Mateusz Sikora

**Rola i znaczenie małych niekodujących cząsteczek RNA
w przebiegu regeneracji tkanki kostnej o znamionach
osteoporozy starczej na przykładzie miRNA-21-5p**

The role and importance of small non-coding RNAs in the regeneration of
bone tissue with signs of senile osteoporosis on the example of miRNA-21-5p

Praca doktorska wykonana pod kierunkiem

Promotora prof. dr hab. Krzysztofa Marycza

Promotora pomocniczego dr hab. Agnieszki Śmieszek

Wrocław, 2023

Badania przeprowadzone w niniejszej pracy zostały sfinansowane w ramach projektu:

Nowe, dwustopniowe rusztowania na bazie nanoapatytu wapnia (nHAP) inkorporowanego nanotlenkami żelaza (Fe_2O_3/Fe_3O_4) z funkcją kontrolowanego uwalniania miRNA w statycznym polu magnetycznym do regeneracji złamań kostnych u pacjentów osteoporotycznych.

Grant: Harmonia 9 UMO-2017/26/M/NZ5/01184

Kierownik projektu: Prof. dr hab. Krzysztof Marycz

Pragnę podziękować

*Panu Promotorowi **Prof. dr hab. Krzysztofowi Maryczowi** za możliwość realizacji pracy doktorskiej, opiekę merytoryczną oraz szansę rozwoju.*

*Pani Promotor Pomocniczej **Dr hab. Agnieszce Śmieszek** za nieocenione wsparcie w trakcie prowadzenia badań, niezwykle cierpliwość i poświęcony czas, a także za zaangażowanie i naukowy profesjonalizm.*

***Pracownikom i Doktorantom** Katedry Biologii Eksperymentalnej Uniwersytetu Przyrodniczego we Wrocławiu za życzliwość, pomoc oraz koleżeńską atmosferę w trakcie pracy.*

*Mojej **Rodzinie oraz Przyjaciółom** za ogromne wsparcie w trakcie kilku lat badań do pracy doktorskiej oraz za bezgraniczną wiarę w moje umiejętności. Dziękuję Wam za zrozumienie, wszystkie słowa otuchy, a także za mobilizowanie mnie do spełniania zamierzonych celów. Bez Waszego wsparcia nie znalazłbym się w miejscu, w którym jestem dzisiaj.*

Spis treści

Wykaz publikacji wchodzących w skład rozprawy doktorskiej	6
Streszczenie.....	7
Streszczenie w języku angielskim.....	9
1. Wstęp	11
2. Cel pracy	17
3. Materiały i metody.....	18
3.1. Hodowle komórkowe	18
3.2. Transfekcja komórek.....	19
3.3. Różnicowanie komórek oraz analiza macierzy zewnątrzkomórkowej	20
3.4. Ocena aktywności metabolicznej komórek	21
3.5. Testy oparte o cytometrię przepływową	21
3.6. Analizy z wykorzystaniem mikroskopii konfokalnej.....	22
3.7. Ocena poziomów transkryptów związanych z przebudową kości i aktywnością komórek kościotwórczych i kościogubnych metodą RT-qPCR.....	23
3.8. Analiza wewnątrzkomórkowej akumulacji białek metodą Western Blot	24
3.9. Badania <i>in vivo</i>	25
3.10. Analizy statystyczne	26
4. Komentarze do publikacji.....	27
4.1. Publikacja nr 1: Sikora, M., Marycz, K., & Śmieszek, A. (2020). Small and Long Non-coding RNAs as Functional Regulators of Bone Homeostasis, Acting Alone or Cooperatively. <i>Molecular Therapy-Nucleic Acids</i> , 21, 792–803. DOI: 10.1016/j.omtn.2020.07.017.....	27
4.2. Publikacja nr 2: Śmieszek, A., Marcinkowska, K., Pielok, A., Sikora, M., Valihrach, L., & Marycz, K. (2020). The Role of miR-21 in Osteoblasts-Osteoclasts Coupling In Vitro. <i>Cells</i> , 9, 1–21. DOI: 10.3390/cells9020479	28
4.3. Publikacja nr 3: Sikora, M., Śmieszek, A., & Marycz, K. (2021). Bone marrow stromal cells (BMSCs CD45-/CD44+/CD73+/CD90+) isolated from osteoporotic mice	

SAM/P6 as a novel model for osteoporosis investigation. Journal of Cellular and Molecular Medicine, 25, 6634–6651. DOI: 10.1111/jcmm.16667.....	31
4.4. Publikacja nr 4: Sikora, M., Śmieszek, A., Pielok, A., & Marycz K. (2023). MiR-21-5p regulates the dynamic of mitochondria network and rejuvenates the senile phenotype of bone marrow stromal cells (BMSCs) isolated from osteoporotic SAM/P6 mice. Stem Cell Research & Therapy, 14. DOI: 10.1186/s13287-023-03271-1	33
5. Podsumowanie.....	37
6. Wnioski.....	39
7. Literatura	41
8. Dorobek naukowy	46
9. Oświadczenia.....	52
10. Publikacje.....	57

Wykaz publikacji wchodzących w skład rozprawy doktorskiej

Publikacja nr 1 (P1):

Sikora, M., Marycz, K., & Śmieszek, A. (2020). Small and Long Non-coding RNAs as Functional Regulators of Bone Homeostasis, Acting Alone or Cooperatively. *Molecular Therapy-Nucleic Acids*, 21, 792–803. DOI: 10.1016/j.omtn.2020.07.017
IF = 8.886; MEiN = 140

Publikacja nr 2 (P2):

Śmieszek, A., Marcinkowska, K., Pielok, A., **Sikora, M.**, Valihrach, L., & Marycz, K. (2020). The Role of miR-21 in Osteoblasts-Osteoclasts Coupling In Vitro. *Cells*, 9, 1–21. DOI: 10.3390/cells9020479
IF = 6.6; MEiN = 140

Publikacja nr 3 (P3):

Sikora, M., Śmieszek, A., & Marycz, K. (2021). Bone marrow stromal cells (BMSCs CD45-/CD44+/CD73+/CD90+) isolated from osteoporotic mice SAM/P6 as a novel model for osteoporosis investigation. *Journal of Cellular and Molecular Medicine*, 25, 6634–6651. DOI: 10.1111/jcmm.16667
IF = 5.295; MEiN = 100

Publikacja nr 4 (P4):

Sikora, M., Śmieszek, A., Pielok, A., & Marycz, K. (2023). MiR-21-5p regulates the dynamic of mitochondria network and rejuvenates the senile phenotype of bone marrow stromal cells (BMSCs) isolated from osteoporotic SAM/P6 mice. *Stem Cell Research & Therapy*, 14. DOI: 10.1186/s13287-023-03271-1
IF = 7.5; MEiN = 100

Całkowity współczynnik IF publikacji, które wchodzą w skład pracy doktorskiej wynosi **28.28** oraz **480** punktów ministerialnych. Wartości współczynnika IF podane zostały w zgodzie z rokiem opublikowania. Punkty MEiN dla wszystkich artykułów zostały podane zgodnie z rokiem publikacji komunikatu Ministra Edukacji i Nauki z dnia 09.02.2021 r.

Streszczenie

Osteoporoza starcza jest najczęstszą chorobą kości występującą u pacjentów w podeszłym wieku. Zachorowalność na osteoporozę starczą rośnie w dramatycznym tempie ze względu na postępujące starzenie się społeczeństw. Co więcej, specjaliści szacują, że w ciągu kolejnych 50 lat osteoporoza osiągnie skalę światowej epidemii, a obecne metody leczenia są niewystarczające. Rozwój osteoporozy starczej związany jest z zaburzeniem równowagi między aktywnością komórek kościotwórczych i kościogubnych, a także z pogorszeniem potencjału regeneracyjnego szpikowych komórek macierzystych (BMSCs). Z tego powodu, poszukiwane są nowe metody terapeutyczne, których celem jest odtworzenie homeostazy w obrębie tkanki kostnej oraz przywrócenie potencjału regeneracyjnego komórek pacjenta. Przykładem takich terapii, są strategie oparte o wykorzystanie małych niekodujących RNA (miRNA) - zarówno jako narzędzi jak i celów terapeutycznych. Dotychczas przebadano szeroką gamę cząsteczek miRNA, do których należy miR-21-5p. Udowodniono, że cząsteczka miR-21-5p może odgrywać istotną rolę w przebudowie tkanki kostnej, ale nie zbadano dotychczas jej wpływu na mechanizmy molekularne zaangażowane w regulację aktywności komórek kościotwórczych i kościogubnych oraz utrzymanie wysokiej aktywności proliferacyjnej i metabolicznej komórek o fenotypie starczym.

Celem pracy doktorskiej było zatem zbadanie roli cząsteczki miR-21-5p w regulacji aktywności komórek tkanki kostnej o charakterze starczym w kontekście projektowania terapii celowanych ukierunkowanych na przywrócenie potencjału regeneracyjnego pacjentów chorujących na osteoporozę starczą.

Badania w ramach pracy doktorskiej zostały przeprowadzone z wykorzystaniem modelowych linii komórkowych MC3T3-E1, 4B12 oraz BMSCs izolowanych z myszy zdrowych szczepu BALB/c i unikalnego modelu myszy osteoporotycznych szczepu SAM/P6. Badania obejmowały analizy *in vitro*, *ex vivo*, a także *in vivo*. W trakcie badań za pomocą technik biologii molekularnej oceniono zaangażowanie cząsteczki miR-21-5p w kształtowaniu aktywności proliferacyjnej, metabolicznej i regeneracyjnej komórek. Kluczowym elementem badań było wskazanie szlaków molekularnych modulujących kościotwórczy potencjał komórek. Szczególną uwagę poświęcono szlakom RANKL/OPG/RANK oraz RUNX-2/TRAP. Ekspresję mRNA i miRNA analizowano przy pomocy techniki RT-qPCR, a akumulację białek za pomocą techniki Western Blot. Aktywność metaboliczną określano z wykorzystaniem technik opartych o cytometrię przepływową, a morfologię i ultrastrukturę komórek oceniano za pomocą mikroskopii

konfokalnej, elektronowej mikroskopii skaningowej (SEM) oraz technik immunocytochemicznych (ICC).

Wyniki prowadzonych badań wykazały istotny wpływ cząsteczki miR-21-5p na aktywność komórek kościotwórczych i kościogubnych. Cząsteczka miR-21-5p brała czynny udział w regulacji potencjału wydzielniczego komórek kościotwórczych oraz w dojrzewaniu komórek kościogubnych poprzez szlak RANKL/OPG/RANK. Jednocześnie potwierdzono, że BMSCs izolowane od myszy osteoporotycznych szczepu SAM/P6 charakteryzowały się upośledzonym potencjałem regeneracyjnym i zaburzonymi procesami metabolicznymi. Wykazano jednak, że cząsteczka miR-21-5p może być czynnikiem wzmagającym potencjał regeneracyjny BMSCs o fenotypie starczym. Komórki BMSC_{SAM/P6} poddane działaniu miR-21-5p charakteryzowały się przywróconą zdolnością do tworzenia wysoko zmineralizowanej macierzy zewnątrzkomórkowej w warunkach *ex vivo* i *in vivo*. Dodatkowo zaobserwowano, że pod wpływem zwiększenia ekspresji miR-21-5p, komórki izolowane od myszy osteoporotycznych przejawiały istotne zmiany w aktywności metabolicznej i w dynamice sieci mitochondrialnej. Zwiększona ekspresja miR-21-5p w BMSCs korelowała ze zwiększoną ekspresją cząsteczek odpowiedzialnych za kościotworzenie (RUNX, OPG, miR-7a-5p) oraz z obniżeniem ilości transkryptów powiązanych z resorpcją tkanki kostnej (TRAP, CTSK, miR-17-5p).

Badania zaprezentowane w ramach pracy doktorskiej wykazały, że cząsteczka miR-21-5p posiada wysoki potencjał terapeutyczny i może znaleźć zastosowanie w projektowaniu efektywnych terapii celowanych, ukierunkowanych na leczenie osteoporozy starczej i zależnej od niej złamań kości.

Streszczenie w języku angielskim

Senile osteoporosis is the most common bone disease in elderly patients. The incidence of senile osteoporosis is increasing dramatically due to the progressive aging of population. What's more, experts estimate that within next 50 years osteoporosis will reach the scale of a global epidemic, while the present therapeutic methods are insufficient. Its development is associated with the imbalance between the activity of osteoblasts and osteoclasts, as well as with the deterioration of the regenerative potential of bone marrow stem cells (BMSCs). For this reason, new therapeutic methods are investigated that will reconstruct homeostasis within the bone tissue and restore the regenerative potential of the patient's cells. An example of such therapies are strategies based on the use of small non-coding RNAs (miRNAs) - both as therapeutic tools and targets. Recently, miR-21-5p has been shown to play an important role in bone remodelling, but its molecular mechanisms that modulate the activity of osteoblasts and osteoclasts, as well as maintain high activity of cells with senile phenotype have not been yet determined.

Therefore, the aim of this doctoral thesis was to investigate the role of the miR-21-5p in the regulation of the activity of senile bone tissue cells for designing targeted therapies aimed at restoring the regenerative potential of patients suffering from senile osteoporosis.

The research was carried out using the MC3T3-E1 and 4B12 cell lines, as well as BMSCs isolated from healthy BALB/c mice and a unique model of osteoporotic SAM/P6 mice strain. The studies included *in vitro*, *ex vivo* and *in vivo* analyses. During the study, the involvement of the miR-21-5p molecule in the proliferative, metabolic and regenerative activity of cells was assessed using molecular biology techniques. The crucial part of the research was to identify molecular pathways that regulate the bone-forming potential of cells. Particular attention was paid to the RANKL/OPG/RANK and RUNX-2/TRAP pathways. mRNA and miRNA expression were analysed by RT-qPCR and protein accumulation was assessed by Western Blot. Metabolic activity was determined using techniques based on flow cytometry, and cell morphology and ultrastructure were assessed using confocal microscopy, scanning electron microscopy (SEM) and immunocytochemistry (ICC) techniques.

The results indicate a significant impact of the miR-21-5p in the regulation of the activity of osteoblasts and osteoclasts. The miR-21-5p was actively involved in the regulation of paracrine activity of osteoblasts and in the maturation of osteoclasts via the OPG/RANKL/RANK pathway. Simultaneously, it was confirmed that BMSCs isolated from osteoporotic SAM/P6 mice were characterized by impaired regenerative

potential and deteriorated metabolic activity. It has been proven that miR-21-5p reconstructs the lost regenerative potential of senile BMSCs. After the miR-21-5p upregulation, cells were characterized by a restored ability to form a highly mineralized extracellular matrix under *ex vivo* and *in vivo* conditions, as well as by significant changes in the metabolic activity and dynamics of the mitochondrial network. Upregulated expression of miR-21-5p in BMSCs correlated with enhanced expression of molecules responsible for osteogenesis (RUNX, OPG, miR-7a-5p), and decreased level of transcripts associated with bone resorption (TRAP, CTSK, miR-17-5p).

The presented research showed that miR-21-5p possesses a high therapeutic potential and can be used in the design of effective targeted therapies aimed at treating senile osteoporosis and related bone fractures.

1. Wstęp

Osteoporoza jest złożoną chorobą dotyczącą układu kostny. Ze względu na etiologię wyróżnia się dwie podstawowe formy tej choroby: osteoporozę pierwotną i osteoporozę wtórną. Osteoporoza pierwotna obejmuje trzy kategorie: osteoporozę młodzieńczą, postmenopauzalną i starczą, które związane są z naturalnymi zmianami gospodarki hormonalnej i zmianami potencjału regeneracyjnego w procesie dojrzewania i starzenia się organizmu. Osteoporoza wtórna jest natomiast wywołana dużą liczbą chorób towarzyszących i przyjmowanych leków. Częstość występowania osteoporozy pierwotnej jest większa niż osteoporozy wtórnej, natomiast osteoporoza związana z wiekiem i starzeniem się organizmu (osteoporoza starcza) stała się jednym z najbardziej istotnych problemów zdrowotnych na świecie.¹ Według najnowszych raportów zaprezentowanych przez Światową Organizację Zdrowia (WHO) oraz International Osteoporosis Foundation (IOF), osteoporozę diagnozuje się u ponad 50% kobiet w wieku menopauzalnym, 30% kobiet w wieku starczym (powyżej 75. Roku życia) oraz u 20% mężczyzn. Obecnie osteoporozą dotkniętych jest ponad 200 milionów kobiet na całym świecie.² Szacuje się także, że ze względu na szybki rozwój społeczeństw, do 2050 roku liczba złamań kości związanych z osteoporozą wzrośnie o około 310% u mężczyzn i 240% u kobiet w porównaniu do lat 90 XX wieku.³ Według raportu przedstawionego przez National Bone Health Alliance, 16.9% mężczyzn i aż 29.9% kobiet powyżej 50. roku życia spełnia najnowsze kryteria diagnostyczne warunkujące rozpoznanie osteoporozy, do których należy tzw. T-score. Osteoporozę diagnozuje się, jeśli współczynnik ten przyjmuje wartość ≤ 2.5 w odcinku lędźwiowym kręgosłupa, szyjce kości udowej lub całym biodrze na podstawie badania gęstości mineralnej kości (BMD - ang. *bone mineral density index*). Powyżej 80. roku życia takie kryteria spełnia obecnie 46.3% mężczyzn i 77.1% kobiet.⁴ Warty odnotowania jest fakt, że pacjenci cierpiący z powodu złamań kości, u podstawy których leży osteoporoza starcza, znajdują się w stanie permanentnego zagrożenia życia.⁵ Te alarmujące dane jednoznacznie wskazują, że osteoporoza starcza przybiera charakter globalnej epidemii oraz staje się narastającym problemem zdrowotnym i społeczno-ekonomicznym, zwłaszcza w wysoko rozwiniętych i starzejących się społeczeństwach.

Najważniejszym czynnikiem wpływającym na rozwój osteoporozy jest zaburzenie homeostazy immunometabolicznej w obrębie tkanki kostnej, a w szczególności w procesie jej przebudowy. Brak równowagi między regeneracją i resorpcją tkanki kostnej prowadzi do stopniowej utraty masy kostnej, co powoduje upośledzenie jej mikroarchitektoniki oraz znacząco zmniejsza gęstość kostną.^{6,7} Upośledzenie procesów przebudowy kości

spowodowane jest brakiem równowagi między aktywnością komórek kościotwórczych tj. osteoblastów, które wywodzą się z populacji komórek mezenchymalnych, a potencjałem resorpcyjnym komórek kościogubnych czyli osteoklastów, które z kolei wywodzą się z populacji komórek hematopoetycznych.⁸ W zdrowej kości osteoklasty degradują tkankę z wykorzystaniem enzymów osteolitycznych takich jak: katepsyna K (ang. *cathepsin K*), metaloproteinazy macierzy zewnątrzkomórkowej (MMPs – ang. *matrix metalloproteinases*) czy TRAP (ang. *tartrate-resistant acid phosphatase*). Za regulację aktywności komórek kościogubnych odpowiadają m.in. parathormon (PTH – ang. *parathyroid hormone*), kalcytonina (CT – ang. *calcitonin*) oraz interleukina 6 (IL-6 – ang. *interleukin 6*). Dojrzewanie osteoklastów warunkowane jest przez aktywność wydzielniczą komórek kościotwórczych, więc obie populacje komórek istotnie regulują swoją aktywność. Zresorbowana kość zostaje odbudowana dzięki aktywności komórek kościotwórczych. Do najważniejszych markerów osteoblastów odpowiedzialnych za syntezę i mineralizację macierzy zewnątrzkomórkowej należą: fosfataza alkaliczna (ALP - ang. *alkaline phosphatase*), osteokalcyna (OCL - ang. *osteocalcin*), osteoprotegeryna (OPG - ang. *osteoprotegerin*) czy ligand receptora RANK (RANKL - ang. *RANK ligand*). Etiologia osteoporozy na poziomie komórkowym uwzględnia zaburzoną relację pomiędzy komórkami kościotwórczymi, a komórkami kościogubnymi. Brak homeostazy, związany jest ze zwiększoną aktywnością osteoklastów i obniżoną osteoblastów. Niezwykle istotny jest także fakt wzajemnej regulacji dojrzewania i modulowania aktywności komórek kościotwórczych i kościogubnych. Za najważniejszy szlak sygnałowy, regulujący oddziaływania pomiędzy komórkami tworzącymi i resorbującymi kość jest szlak określany triadą RANKL/OPG/RANK. W procesie regulacji dojrzewania oraz aktywności degradacyjnej osteoklastów, receptor RANK (ang. *receptor activator of nuclear factor κ B*) znajdujący się na powierzchni ich błon komórkowych powinien zostać aktywowany przez cząsteczkę RANKL produkowaną przez osteoblasty. Cząsteczka OPG również produkowana przez osteoblasty jest inhibitorem tego wiązania, funkcjonując jako tzw. *decoy receptor*, imitujący wiązanie ze specyficznym ligandem.⁹⁻¹² Rekrutacja komórek kościotwórczych i komórek kościogubnych w miejscu przebudowy kości wymaga zatem aktywacji wielu sygnałów molekularnych regulowanych przez hormony, cytokiny czy czynniki wzrostu. W przypadku osteoporozy starczej istotne wydaje się przywrócenie prawidłowej równowagi w funkcjonowaniu osteoblastów i osteoklastów, w celu zharmonizowania procesów przebudowy tkanki kostnej. Istotną rolę pełnić mogą tutaj także niekodujące cząsteczki RNA, które aktywnie pośredniczą w interakcji między komórkami

kostnymi a komórkami progenitorowymi poprzez posttranskrypcyjną regulację ekspresji genów.

Komórki progenitorowe pochodzące ze szpiku kostnego (BMSCs – ang. *bone marrow stem/stromal cells*) opisane zostały po raz pierwszy przez zespół Alexandra Friedensteina.^{13,14} Zgodnie z wytycznymi International Society for Cellular Therapy (ISCT) BMSCs powinny charakteryzować się: (1) ekspresją markerów CD73, CD90 i CD150 oraz brakiem ekspresji markerów CD11b, CD14, CD19, CD34, CD45 i HLA-DR, (2) adhezją do plastikowych powierzchni naczyń hodowlanych, a także (3) zdolnością do różnicowania się w kierunku tkanki kostnej, chrzęstnej i tłuszczowej w warunkach *in vitro*.¹⁵ Wysoki potencjał regeneracyjny BMSCs stwarza możliwość ich potencjalnego zastosowania klinicznego – w licznych badaniach zidentyfikowano mechanizmy molekularne podkreślając ich korzystny wpływ w przebiegu regeneracji złamań tkanki kostnej.^{16–18} Komórki progenitorowe szpiku kostnego wykazują ekspresję kluczowych markerów zaangażowanych w regenerację tkanki kostnej, do których należą m.in. ALP, BMP-2/4 (ang. *bone morphogenetic protein 2/4*), OPG, RANK, RANKL, OCL, OPN (ang. *osteopontin*) czy wiele innych białek zaangażowanych w szlak molekularny Wnt – β -katenina.^{19,20} Potencjał regeneracyjny BMSCs jest również wyrażony ich wysoką aktywnością wydzielniczą poprzez uwalnianie mikropęcherzyków zewnątrzkomórkowych (ExMVs – ang. *extracellular microvesicles*), które są szczególnie bogate w czynniki wzrostu oraz szereg niekodujących cząsteczek RNA sprzyjającym procesom regeneracji.^{21–23} Jak wykazano wcześniej, niekodujące cząsteczki RNA są aktywnie zaangażowane w procesy regulujące wzajemne oddziaływanie populacji komórek kościotwórczych i komórek kościogubnych wpływając istotnie na proces przebudowy tkanki kostnej. Poprzez regulację szlaków miRNA-lncRNA-mRNA warunkują przeżycie komórek tkanki kostnej, ich różnicowanie się czy przebudowę macierzy zewnątrzkomórkowej. Z tego powodu, aktywność immunomodulacyjna BMSCs sprawia, że stanowią one obiecujące narzędzie terapeutyczne w zakresie terapii komórkowych i w leczeniu osteoporozy starczej.²⁴

Zaburzenia w równowadze metabolicznej kości związane z rozwojem osteoporozy starczej mają istotny wpływ na aktywność biologiczną BMSCs. W związku z tym, że z BMSCs rekrutowane są komórki, z których następnie różnicują się osteoblasty, zaburzenia metaboliczne towarzyszące osteoporozie mają istotny wpływ na ich rekrutację i funkcjonalne różnicowanie się. U osób chorujących na osteoporozę starczą, BMSCs przyjmują fenotyp senilny (starczy), który wyrażony jest znacznym spadkiem żywotności i obniżeniem się aktywności proliferacyjnej. Ponadto, komórki takie wykazują zmniejszony

potencjał regeneracyjny oraz akumulują i wydzielają czynniki stresu oksydacyjnego np. tlenek azotu, nadtlenuk wodoru, anion ponadtlenkowy czy tlen singletowy. BMSCs izolowane od pacjentów osteoporotycznych wykazują zwiększoną ekspresję markerów związanych z adipogenezą, a jednocześnie zmniejszoną ekspresję kluczowych genów regulujących prawidłową regenerację tkanki kostnej i niezbędnych do tworzenia się kości.^{25,26} Z tego powodu opisanie i zrozumienie szlaków molekularnych, w tym regulacji epigenetycznej z udziałem małych niekodujących RNA, stanowi istotne uzupełnienie wiedzy na temat patomechanizmów inicjowanych zaburzeniami w aktywności komórek kostnych i ich prekursorów.

Niekodujące cząsteczki RNA (ncRNA, non-coding RNA), do których należą między innymi małe niekodujące RNA (tj. mikroRNA/miRNA) zyskały uznanie jako czynniki regulujące ekspresję wielu genów. MikroRNA to małe, endogenne cząsteczki o wielkości od 19 do 25 nukleotydów, które nie zawierają informacji potrzebnej do powstania białka. Ich główną funkcją jest regulacja post-transkrypcyjnego wyciszania genów docelowych. Pojedyncza cząsteczka miRNA może być ukierunkowaną na wiele mRNA i wpływać na ekspresję setek genów zaangażowanych w funkcjonalne szlaki sygnałowe niezbędne do przeżycia, proliferacji lub różnicowania się komórek.²⁷ W procesie biogenezy cząsteczek miRNA, uzyskują one komplementarność do konkretnych sekwencji mRNA. Specyficzne wiązanie między cząsteczkami miRNA i mRNA prowadzi do zahamowania procesu translacji w wyniku degradacji mRNA.^{28,29} Najlepiej opisanym mechanizmem interakcji miRNA-mRNA jest oddziaływanie poprzez region 3' UTR (3'-untranslated region) docelowych mRNA. Do takich interakcji dochodzić może także z regionem 5' UTR, sekwencją kodującą czy promotorami genów. Finalnym efektem takiego oddziaływania jest osłabienie ekspresji genu.³⁰ Ponadto, miRNA uwalniane są także do krwioobiegu w postaci cząsteczek związanych z białkami AGO (ang. *Argonaute protein family*), w ciałach apoptotycznych, egzosomach lub lipoproteinach o dużej gęstości (HDL).³¹ Krążące miRNA (ang. *circulating miRNA*) można uznać za markery wielu chorób dotykających np. tkanki kostnej, tj. osteoporozy czy kostniakomięsaka.^{31,32} Z tego powodu rozważa się ich potencjalne zastosowanie jako wiarygodnych czynników prognostycznych i diagnostycznych.³³

Powszechnie dyskutuje się o zdolnościach cząsteczek miRNA do odgrywania kluczowej roli w rozwoju stanów patologicznych. Coraz więcej dowodów wskazuje, że miRNA odgrywają istotną rolę w procesie osteogenezy, modulując ekspresję genów niezbędnych do rekrutacji i różnicowania różnych komórek kostnych, w tym komórek

progenitorowych.³⁴⁻³⁶ Wśród szeregu przebadanych miRNA to właśnie miRNA-21-5p jest cząsteczką, która zwraca szczególną uwagę jako czynnik odgrywający ważną rolę w utrzymaniu homeostazy w obrębie tkanki kostnej.³⁷⁻³⁹ MiR-21-5p jest najczęściej opisywany jako tzw. „oncomiR”, ze względu na fakt, iż wysoką ekspresję tej cząsteczki obserwuje się w komórkach nowotworowych, np. w komórkach kostniakomięsa.^{40,41} Mimo, że molekularny mechanizm oddziaływania cząsteczki miR-21-5p jest nadal przedmiotem intensywnych badań, uznaje się ją za kluczowy regulator szlaków sygnałowych, które aktywowane są podczas różnicowania się komórek progenitorowych w kierunku komórek tkanki kostnej. Wykazano, że jednym z bezpośrednich celów cząsteczki miR-21-5p jest cząsteczka Smad7 (ang. *mothers against decapentaplegic homolog 7*), która pełni modulującą funkcję w szlaku sygnałowym indukowanym przez transformujące czynniki wzrostu, tj. TGF- β (ang. *transforming growth factor β*) i białka morfogenetyczne kości (BMPs).^{42,43} Co istotne, w badaniach opartych o komórki BMSCs wykazano, że cząsteczka miR-21-5p wpływa na ekspresję głównego regulatora kościotworzenia tj. cząsteczki RUNX-2 (ang. *runt-related transcription factor 2*). Dodatkowo, eksperymentalne zwiększenie ekspresji cząsteczki miR-21-5p znajduje odzwierciedlenie w zwiększonej ekspresji takich markerów kościotworzenia jak OCL, OPN, czy BMP-2.⁴³ Rola miR-21-5p nie ogranicza się jedynie do modulowania ekspresji genów w komórkach progenitorowych szpiku kostnego czy komórkach kościotwórczych, ale odgrywa ważną rolę w szlakach regulujących przeżycie i różnicowanie się komórek kościogubnych.^{44,45} Na szczególną uwagę zasługuje oś molekularna OPG/RANKL. Obie te cząsteczki są kluczowymi czynnikami zaangażowanymi w proces osteoklastogenezy zależnej od aktywności osteoblastów, a ich wzajemne sprzężenie opisano we wcześniejszej części wstępu.⁴⁶ Z tego powodu, terapia oparta na dostarczeniu cząsteczek miR-21-5p mogłaby potencjalnie przynieść pozytywne rezultaty w kontekście regeneracji tkanki kostnej np. w przypadku złamań kości u osób chorujących na osteoporozę starczą.^{47,48}

Dotychczas, przeprowadzono wiele badań z zakresu wyjaśnienia roli cząsteczek miRNA w procesach powiązanych z aktywacją komórek progenitorowych oraz przebudową tkanki kostnej. Jednakże, wciąż brakuje rzetelnych informacji z zakresu zaangażowania wspomnianych cząsteczek w stanie patologicznego zachwiania homeostazy w obrębie tkanki kostnej u pacjentów chorujących na osteoporozę starczą. Dodatkowo, do tej pory nie opisano w sposób wystarczający żadnego wiarygodnego modelu do badań *in vitro* oraz *in vivo*, który miałby na celu wyjaśnienie molekularnego podłoża rozwoju osteoporozy starczej oraz zaproponowanie terapii celowanych, tj. „szytych na miarę” i opartych

np. o niekodujące cząsteczki RNA. Najbardziej rozpowszechniony model do badań nad osteoporozą dotyczy gryzoni, u których wycięto jajniki (tzw. *ovariectomized model*). Model polega na indukcji osteoporozy w wyniku drastycznego spadku ekspresji estrogenu w organizmie samicy i z tego powodu nie jest to idealny model do rozważań nad osteoporozą starczą, która powiązana jest przecież z naturalnym starzeniem się organizmu i utratą potencjału regeneracyjnego komórek pacjenta. *Ovariectomized model* jest zatem wykorzystywany do badań nad osteoporozą menopauzalną.

Z tego powodu, w pracy doktorskiej podjęto się wyzwania mającego na celu zaproponowanie modelu badawczego do analizy molekularnych podstaw progresji osteoporozy starczej z wykorzystaniem myszy osteoporotycznych szczepu SAM/P6. Szczep ten uzyskano z wsobnie kojarzonych myszy, które są wykorzystywane jako zwierzęce modele do badań nad zaburzeniami związanymi z wiekiem i starzeniem się organizmu.^{49,50} W wieku 4 miesiące myszy SAM/P6 prezentują pełne spektrum objawów osteoporozy starczej: niską gęstość kośćca, upośledzony potencjał regeneracyjny komórek szpikowych, obniżenie wskaźników BMD i BV/TV, a także niski poziom wapnia i fosforu w mineralu kostnym (część nieorganiczna kości).

W pracy doktorskiej podjęto się także wyjaśnienia roli miR-21-5p, w regulacji szlaków molekularnych odzwierciedlających potencjał regeneracyjny komórek o znamionach osteoporozy starczej. Zbadano także potencjalne wskazanie tej cząsteczki jako wartościowego celu terapeutycznego w procesie projektowania nowych i spersonalizowanych metod terapeutycznych. Poznanie molekularnych mechanizmów warunkujących przebudowę osteoporetycznej tkanki kostnej jest ważnym aspektem przybliżającym nas do opracowania skutecznych terapii skoncentrowanych na pobudzeniu naturalnych procesów naprawczych i ich precyzyjnego regulowania. Duże nadzieje w tym temacie wiąże się z modulowaniem oddziaływań komórkowych i szlaków warunkujących prawidłowe funkcjonowanie komórek kości. MiRNA, a w szczególności miR-21-5p ma duży potencjał jako cząsteczka, której poziomy modelują aktywność komórek progenitorowych rezydujących w tkance kostnej poprzez regulowanie ekspresji genów o istotnym znaczeniu dla prawidłowej przebudowy kości.

2. Cel pracy

Celem pracy doktorskiej było określenie roli oraz znaczenia wybranych małych niekodujących cząsteczek RNA (miRNA/microRNA) w regeneracji tkanki kostnej o zaburzonym metabolizmie, szczególnie w przebiegu osteoporozy związanej z wiekiem i starzeniem się organizmu (tj. osteoporozy starczej). Wiodącym tematem badań była ocena funkcji miR-21-5p w regulacji aktywności metabolicznej i proliferacyjnej komórek progenitorowych tkanki kostnej, komórek kościotwórczych (osteoblastów) i komórek kościogubnych (osteoklastów). Analizy obejmowały także określenie nowych szlaków molekularnych z uwzględnieniem osi miRNA-lncRNA-mRNA. Badania prowadzone były w oparciu o cele szczegółowe:

- Poszukiwanie małych cząsteczek RNA (miRNA) istotnie zaangażowanych w zachowanie homeostazy i regulację metabolizmu w obrębie tkanki kostnej, które mogłyby służyć jako wiarygodne markery terapeutyczne w leczeniu chorób dotyczących układu kostnego.
- Określenie roli cząsteczki miR-21-5p w procesie przebudowy tkanki kostnej warunkowanej aktywnością prekursorowych i dojrzałych komórek kości.
- Scharakteryzowanie potencjału regeneracyjnego oraz aktywności metabolicznej endogennych komórek progenitorowych izolowanych ze szpiku kostnego (BMSCs) myszy z indukowaną osteoporozą starczą (szczep SAM/P6).
- Opisanie szczepu myszy SAM/P6 jako wartościowego modelu do badań *in vivo* z zakresu projektowania efektywnych i celowanych metod terapeutycznych dla osób chorujących na osteoporozę starczą.
- Określenie znaczenia miR-21-5p jako cząsteczki regulującej potencjał regeneracyjny multipotentnych komórek stromalnych szpiku (BMSC) - badania z uwzględnieniem populacji komórek o upośledzonym metabolizmie tj. BMSC_{SAM/P6}.
- Weryfikacja znaczenia miR-21-5p w regulacji homeostazy oraz przebudowy zdrowej i osteoporetycznej tkanki kostnej - badania *in vitro/in vivo* z wykorzystaniem modelu SAM/P6.
- Wskazanie cząsteczki miR-21-5p jako potencjalnego czynnika terapeutycznego przy projektowaniu terapii molekularnych, mobilizujących endogenne komórki progenitorowe kości i właściwą przebudowę tkanki, ukierunkowanych na leczenie osteoporozy starczej.

3. Materiały i metody

Poniższy rozdział zawiera informacje z zakresu metodyki prowadzonych badań. Przeprowadzone badania opierały się o wykorzystanie technik biologii molekularnej względem komórek linii MC3T3-E1 (mysie pre-osteoblasty), 4B12 (mysie pre-osteoklasty) oraz mysich komórek progenitorowych BMSCs. Szczegółowe informacje dotyczące zaimplementowanych protokołów znajdują się w publikacjach naukowych wchodzących w skład niniejszej rozprawy doktorskiej.

3.1. Hodowle komórkowe

Komórki linii MC3T3-E1 hodowane były w pożywce Minimum Essential Medium Alpha (MEM- α , Gibco™ Thermo Fisher Scientific, Warszawa, Polska) z 10% dodatkiem surowicy bydlęcej (FBS – ang. *fetal bovine serum*, Sigma-Aldrich, Monachium, Niemcy) w inkubatorze komórkowym o stałych parametrach fizycznych: temperatura 37 °C, 5% CO₂ oraz 95% wilgotności. Pożywka hodowlana wymieniana była dwa razy w tygodniu z uwzględnieniem płukania komórek z wykorzystaniem soli Hanks`a (HBSS – ang. *Hanks` Balanced Salt Solution*). W przypadku osiągnięcia 90% konfluencji w prowadzonych hodowlach, komórki pasażowane były z wykorzystaniem roztworu trypsyny (StableCell Trypsin, Sigma-Aldrich, Monachium, Niemcy).

Komórki linii 4B12 zostały wykorzystane w publikacji nr 2 dzięki uprzejmości Shigeru Amano z Meikai University School of Dentistry (Department of Oral Biology and Tissue Engineering).⁵¹ Komórki hodowano w pożywce hodowlanej składającej się z α -MEM (Sigma-Aldrich, Monachium, Niemcy) z 10% dodatkiem surowicy bydlęcej (FBS) oraz 30% CSCM (ang. *calvaria-derived stromal cell conditioned medium*). Komórki propagowano w inkubatorze komórkowym o stałych parametrach fizycznych: temperatura 37 °C, 5% CO₂ oraz 95% wilgotności. W przypadku osiągnięcia 75% konfluencji komórki pasażowano do nowych naczyń hodowlanych bez wykorzystywania roztworu trypsyny.

Dodatkowo, w publikacji nr 2 wykorzystano model ko-hodowli komórek MC3T3-E1 oraz 4B12. Komórki MC3T3-E1 wysiano na płytce 24-dołkowej oraz przeprowadzono transfekcję opisaną w punkcie 3.2. Komórki 4B12 umieszczono w komorach Boyden`a o średnicy porów równej 8 μ m i zawieszono w dołkach, w których znajdowały się wysiane wcześniej komórki MC3T3-E1. Połowa pożywki w komorach (α -MEM, 10% FBS, 30% CSCM) była wymieniana dwa razy w tygodniu w trakcie prowadzenia ko-kultury. Komórki MC3T3-E1, które inkubowano na powierzchni płytek hodowlanych różnicowano w kierunku tkanki kostnej, co zostało opisane w punkcie 3.3.

Komórki BMSCs (ang. *bone marrow stem / stromal cells*) do badań przedstawionych w publikacji nr 3 oraz 4 wyizolowano z dwóch szczepów myszy – kontrolnego szczepu myszy zdrowych BALB/c oraz myszy szczepu SAM/P6, chorujących na osteoporozę starczą. W celu izolacji komórek szpikowych zwierzęta poddano eutanazji poprzez przerwanie rdzenia kręgowego. Następnie, od myszy wypreparowano kości udowe. Szpik kostny wypłukano z jam szpikowych z wykorzystaniem strzykawek insulinowych wypełnionych solą Hanks'a. Komórki opłukano i wysiano bezpośrednio na płytki 24-dołkowe. Komórki inkubowano w pożywce hodowlanej Ham's F-12 Nutrient Mixture z 15% dodatkiem surowicy bydlęcej i 1% dodatkiem P/S. Komórki propagowano w inkubatorze komórkowym o stałych parametrach fizycznych: temperatura 37 °C, 5% CO₂ oraz 95% wilgotności. Pożywka hodowlana została wymieniona na świeżą po 24 godzinach hodowli w celu pozbycia się komórek nieadherentnych i hematopoetycznych. W trakcie hodowli komórek pożywka była wymieniana dwa razy w tygodniu z uwzględnieniem płukania komórek przy użyciu soli Hanks'a.

W trakcie prowadzenia wszystkich hodowli, komórki obserwowano z wykorzystaniem odwróconego mikroskopu świetlnego z kontrastem fazowym (Axio Observer A1, Zeiss, Oberkochen, Niemcy oraz Leica DMI1, Leica Microsystems, KAWA.SKA Sp. z o.o., Polska).

3.2. Transfekcja komórek

Badania przedstawione w publikacji nr 2 opierały się na wyciszeniu ekspresji cząsteczki miR-21-5p w komórkach linii MC3T3-E1. Transfekcję komórek przeprowadzono z wykorzystaniem inhibitora miR-21 (hsa-miR-21a-5p Anti-miR™ miRNA Inhibitor, Ambition, Thermo Fisher Scientific, Warszawa, Polska) oraz ESCORT III Transfection reagent (Sigma-Aldrich, Poznań, Polska). Odczynnik do transfekcji przygotowano w stężeniu 1:100 w pełnej pożywce hodowlanej MEM- α , a ilość inhibitora miR-21 wynosiła 50 nM. Optymalna ilość inhibitora miR-21 została określona doświadczalnie i przedstawiona w publikacji nr 2. Transfekcję komórek rozpoczęto przy konfluencji równej około 70% i przeprowadzono przez 72 godziny zgodnie z zaleceniami producenta. Komórki, w których nie wyciszano ekspresji miR-21-5p stanowiły grupę kontrolną.

W badaniach przedstawionych w publikacji nr 4 zwiększono ekspresję cząsteczki miR-21-5p w komórkach BMSCs izolowanych z myszy osteoporotycznych SAM/P6. W tym celu, po osiągnięciu około 80% konfluencji komórek, hodowle transfekowano za pomocą MISSION® miRNA miR-21 Mimic (HMI0371, Sigma-Aldrich, Monachium,

Niemcy) oraz Lipofectamine 3000 Transfection Kit (Invitrogen, Thermo Fisher Scientific, Warszawa, Polska). Odczynniki do transfekcji oraz miR-21 Mimic zostały przygotowane w pożywce OptiMEM (Gibco, Life Technologies Corporation, USA) i dodane do komórek w stężeniu 1:10. Ilość dostarczonego do komórek miR-21 Mimic wynosiła 50 nM. Transfekcję komórek przeprowadzano przez 72 godziny, zgodnie z zaleceniami producenta. Komórki, w których nie zwiększono ekspresji cząsteczki miR-21-5p stanowiły grupę kontrolną.

3.3. Różnicowanie komórek oraz analiza macierzy zewnątrzkomórkowej

Różnicowanie komórek w kierunku tkanki kostnej zostało indukowane stosując pełną pożywkę hodowlaną (MEM- α) wzbogaconą czynnikami osteogennymi – 10 nM – hydrat soli disodowej fosforanu β -glicerolu (Sigma-Aldrich, Monachium, Niemcy) i 50 g/mL kwasu askorbinowego (Sigma-Aldrich, Monachium, Niemcy). Pożywka różnicująca zmieniana była dwa razy w tygodniu. Różnicowanie komórek prowadzono przez 3, 7 i 15 dni (komórki MC3T3-E1) lub przez 10 dni (BMSCs).

Różnicowanie komórek w kierunku tkanki chrzęstnej zostało indukowane stosując StemPro Osteocyte/Chondrocyte Differentiation Basal Medium (A10069-01, Gibco, Life Technologies Corporation, USA) oraz StemPro Chondrogenesis Supplement (A10069-01, Gibco, Life Technologies Corporation, USA) w stosunku 10:1. Pożywka została wzbogacona 0.05% dodatkiem gentamycyny. Pożywka różnicująca zmieniana była dwa razy w tygodniu. Różnicowanie komórek BMSCs prowadzono przez 7 dni.

Różnicowanie komórek w kierunku tkanki tłuszczowej zostało indukowane stosując StemPro Adipogenesis Differentiation Basal Medium (A10410-01, Gibco, Life Technologies Corporation, USA) oraz StemPro Adipogenesis Supplement (A10065-01, Gibco, Life Technologies Corporation, USA) w stosunku 10:1. Pożywka została wzbogacona 0.05% dodatkiem gentamycyny. Pożywka różnicująca zmieniana była dwa razy w tygodniu. Różnicowanie komórek BMSCs prowadzono przez 7 dni.

Analizę jakościową zewnętrznej macierzy komórkowej określono za pomocą barwnika Alizarin Red, który wybarwia złogi wapnia oraz barwnika Safranina-O, który wybarwia proteoglikany. W tym celu komórki utrwalono w 4% roztworze paraformaldehydu (PFA), a następnie wybarwiono za pomocą wspomnianych barwników. Uzyskane próbki analizowano za pomocą mikroskopu odwróconego Axio Observer A1 (Zeiss, Oberkochen, Niemcy) i dokumentowano aparatem cyfrowym Canon PowerShot (Woodhatch, Wielka Brytania). Uzyskane mikrografie analizowano w programie Fiji is Just ImageJ

z wykorzystaniem wtyczki Pixel Counter (wersja 1.52n, Wayne Rasband, National Institutes of Health, USA).

Ilość kropeł tłuszczu podczas różnicowania w kierunku tkanki tłuszczowej określono za pomocą barwnika HCS LipidTOX Green Neutral Lipid Stain (H34475, Sigma-Aldrich, Monachium, Niemcy). Komórki barwiono zgodnie z zaleceniami producenta, a preparaty zamknięto na szkiełkach podstawowych za pomocą tzw. *mounting medium* (FluoroshieldTM with DAPI, Sigma-Aldrich, Monachium, Niemcy). Powstałe preparaty obserwowano przy użyciu mikroskopu konfokalnego (Leica TCS SPE, Leica Microsystems, KAWA.SKA Sp z o.o., Zalesie Górne, Poland). Uzyskane mikrofotografie analizowano w programie Fiji is Just ImageJ z wykorzystaniem wtyczki Pixel Counter (wersja 1.52n, Wayne Rasband, National Institutes of Health, USA).

3.4. Ocena aktywności metabolicznej komórek

Analiza aktywności metabolicznej komórek została przeprowadzona z wykorzystaniem testu Alamar Blue. Komórki inkubowano przez dwie godziny w warunkach standardowych (37 °C, 5% CO₂ i 95% wilgotności) w obecności roztworu resazuryny. Pod wpływem aktywności utleniania i redukcji komórek, niebieska resazuryna zostaje zredukowana do różowej resorufiny, posiadającej silne właściwości fluorescencyjne. Po inkubacji supernatant usunięto i przeniesiono na płytki 96-dołkowe. Absorbancję mierzono przy długości fali 600 i 690 nm. Aktywność metaboliczną komórek obliczono za pomocą wzoru: $\Delta A = A_{600nm} - A_{690nm}$.

3.5. Testy oparte o cytometrię przepływową

Analizy cytometryczne przeprowadzono za pomocą analizatora Guava[®] Muse[®] Cell Analyzer zgodnie z protokołami podanymi przez producentów. Każdą analizę przeprowadzono w co najmniej trzech powtórzeniach technicznych.

Analizę liczby oraz żywotności komórek przeprowadzono przy użyciu zestawu Muse[®] Count & Viability Kit (Luminex/Merck; nr kat.: MCH100102, Poznań, Polska). Analizę profilu apoptozy w prowadzonych hodowlach komórkowych przeprowadzono przy użyciu zestawu Muse[®] Annexin V & Dead Cell Kit (Luminex/Merck; nr kat.: MCH100105, Poznań, Polska). Analizę aktywacji kaspaz (enzymów proteolitycznych) przeprowadzono za pomocą zestawu Muse[®] MultiCaspase Kit (Luminex/Merck; nr kat.: MCH100109, Poznań, Polska). Analizę stopnia depolaryzacji błon mitochondrialnych przeprowadzono za pomocą zestawu

Muse[®] MitoPotential Kit (Luminex/Merck; nr kat.: MCH100110, Poznań, Polska). Analizę akumulacji reaktywnych form tlenu (ROS – ang. *reactive oxygen species*) zmierzono za pomocą zestawu Muse[®] Oxidative Stress Kit (Luminex/Merck; nr kat.: MCH100111, Poznań, Polska).

Za pomocą technik cytometrycznych oceniono także stopień akumulacji białka RUNX-2 biorącego udział w procesie regeneracji tkanki kostnej. Analizy przeprowadzono z wykorzystaniem świeżo wyizolowanych komórek BMSCs z myszy zdrowych (szczep BALB/c) oraz osteoporotycznych (szczep SAM/P6). Po izolacji szpiku kostnego komórki inokulowano na płytki 24-dółkowe. Po 24 godzinach komórki transfekowano za pomocą MISSION[®] miRNA miR-21 Mimic (HMI0371, Sigma-Aldrich, Monachium, Niemcy) przez 72 godziny. Komórki inkubowano w obecności odczynnika Fix & Perm Medium A (GAS001, Life Technologies Corporation, USA), a następnie w obecności odczynnika Fix & Perm Medium B (GAS002, Life Technologies Corporation, USA) z dodatkiem przeciwciała anti-RUNX-2 (M-70) wytworzonego w króliku (sc-10758, Santa Cruz Biotechnology) w stężeniu 1:50. Komórki inkubowano następnie z przeciwciałem drugorzędowym - anti-królicze Atto-647 wytworzone w organizmie kozy (ab150079, Abcam) w stężeniu 1:100 w PBS. Próbkę analizowano za pomocą dwulaserowego cytometru FACS Lyric Flow Cytometer (Becton Dickinson Polska, Sp. z oo, Warszawa, Polska) z oprogramowaniem FASC Suite. W każdej próbce oceniano 1000 komórek. Wyniki wizualizowano i analizowano za pomocą oprogramowania FCS Express[™] (wersja 7.08.0018, De Novo Software, Pasadena, CA, USA).

3.6. Analizy z wykorzystaniem mikroskopii konfokalnej

W celu wizualizacji morfologii i ultrastruktury komórek zastosowano komercyjnie dostępne zestawy barwników. Sieć mitochondrialną w komórkach wybarwiono przyżyciowo za pomocą barwnika Mito Red (Sigma-Aldrich, Monachium, Niemcy). Lizosomy wizualizowano również w trakcie hodowli komórek przy użyciu odczynnika LysoTracker[™] Yellow HCK-123 (Life Technologies Corporation, USA). Przed kolejnym barwieniem komórki utrwalano w 4% roztworze PFA.

Morfologię badanych komórek oceniano poprzez wizualizację jąder komórkowych przy użyciu barwnika Hoechst 33342 (I34202, Invitrogen, Thermo Fisher Scientific, Warszawa, Polska). Ponadto, cytoszkielet aktynowy barwiono roztworem falloidyny Atto-488 (49409, Sigma-Aldrich, Monachium, Niemcy). Preparaty zamknięto na szkiełkach mikroskopowych

oraz wybarwiono DAPI (4',6-diamino-2-fenoloindolem) przy użyciu mounting medium (Fluoroshield™ z DAPI, Sigma-Aldrich, Monachium, Niemcy).

Aby ocenić ekspresję badanych białek powierzchniowych oraz wewnątrzkomórkowych wykorzystano techniki oparte na immunodetekcji. Preparaty inkubowano z przeciwciałami skoniugowanymi z cząsteczkami, które posiadają zdolność do fluorescencji. W celu zastosowania technik immunocytochemicznych, komórki inkubowano przez noc z pierwszorzędowymi przeciwciałami w 4°C: anty-CD44, anty-CD45, anty-CD73, anty-CD90, anty-CD105, anty-RUNX2, anty-OPN, anty-TRAP, anty-LAMP2, anty-Ki67, anty-mTOR oraz anty-MFN1. Następnie, próbki inkubowano z przeciwciałami drugorzędowymi przez 1 godzinę w temperaturze pokojowej. Szczegółowe informacje dotyczące rodzaju oraz stężenia wykorzystanych przeciwciał pierwszo- i drugorzędowych znajdują się w odpowiednich publikacjach, które wchodzi w skład pracy doktorskiej. Preparaty zamknięto na szkiełkach mikroskopowych oraz wybarwiono DAPI przy użyciu mounting medium (Fluoroshield™ z DAPI, Sigma-Aldrich, Monachium, Niemcy).

Komórki obserwowano przy użyciu mikroskopu konfokalnego i oprogramowania Las X (11889113, Leica DMI8, Leica Microsystems, KAWA.SKA Sp. z oo, Zalesie Górne, Polska). Obrazy mikroskopowe uzyskano stosując projekcję o maksymalnej intensywności przy użyciu oprogramowania Fiji i Just ImageJ (wersja 1.52n, Wayne Rasband, National Institutes of Health, USA) oraz analizowano stosując wtyczkę Pixel Counter Plougin. Dodatkowo, do analizy morfologii mitochondriów wykorzystano oprogramowanie MicroP.⁵²

3.7. Ocena poziomów transkryptów związanych z przebudową kości i aktywnością komórek kościotwórczych i kościogubnych metodą RT-qPCR

Poziomy transkryptów dla wybranych mRNA oraz ncRNA (miRNA i lncRNA) analizowano za pomocą techniki RT-qPCR (ilościowa reakcja łańcuchowa polimerazy poprzedzona odwrotną transkrypcją). W tym celu komórki homogenizowano przy użyciu Extrazolu® (Blirt DNA, Gdańsk, Polska) oraz wyizolowano RNA metodą fenolowo-chloroformową.⁵³ Wyizolowane całkowite RNA rozcieńczono w wodzie przeznaczonej do biologii molekularnej (Sigma-Aldrich, Poznań, Polska) oraz spektrofotometrycznie oceniono jego jakość (Epoch, Biotek, Bad Friedrichshall, Niemcy). Trawienie pozostałości gDNA (genomowego DNA) przeprowadzono przy użyciu enzymu deoksyrybonukleazy I (DNaza I) wchodzącej w skład zestawu PrecisionDNase Kit (Primerdesign, BLIRT S.A., Gdańsk, Polska) zgodnie z zaleceniami producenta. cDNA (komplementarne DNA)

syntetyzowano przy użyciu zestawu Tetro cDNA Synthesis Kit (Bioline Reagents Limited, Londyn, Wielka Brytania) w termocyklerze T100 (Bio-Rad, Hercules, CA, USA). Do analizy małych niekodujących RNA (miRNA) zastosowano zestaw Mir-X™ miRNA First-Strand Synthesis Kit (Takara Clontech Laboratories, Biokom, Poznań, Polska). Procedury przeprowadzono zgodnie z zaleceniami producentów. cDNA zsyntetyzowano ze ściśle określonych ilości RNA, o których informacje znajdują się w poszczególnych publikacjach wchodzących w skład niniejszej pracy doktorskiej. Reakcje qPCR przeprowadzono przy użyciu zestawu SensiFAST SYBR® & Fluorescein Kit (Bioline Reagents Ltd., London, UK) w termocyklerze CFX Connected Real-Time PCR Detection System (Bio-Rad, Hercules, CA, USA). Reakcje przeprowadzono w co najmniej trzech powtórzeniach technicznych. Stałe warunki reakcji obejmowały: początkową denaturację (95 °C, 2 minuty) oraz 45 cykli składających się z denaturacji (95 °C, 5 sekund), hybrydyzacji starterów (10 sekund) i elongacji (72 °C, 5 sekund). W celu określenia specyficzności powstałych produktów przeprowadzono krzywą topnienia produktów stosując gradient (65 do 95 °C, szybkość ogrzewania 0,2 °C/sekundę). cDNA stanowiło zawsze 10% objętości mieszaniny reakcyjnej. Do określenia wartości ekspresji transkryptów wykorzystywano algorytm RQ_{MAX} . W celu normalizacji wyników wykorzystywano wartości ekspresji genów metabolizmu podstawowego (tzw. *housekeeping genes*): *Gapdh* (dehydrogenaza aldehydu 3-fosfoglicerynowego) oraz *B2m* (beta-2-mikroglobulina – w przypadku komórek BMSCs), a wartości ekspresji miRNA normalizowano względem genu *snU6* (small nuclear RNA U6). Normalizację przeprowadzono przy użyciu wzoru: $\Delta Ct = Ct(\text{gen b\u0119d\u0105cy przedmiotem zainteresowania}) - Ct(\text{gen metabolizmu podstawowego})$. Spośród uzyskanych wartości ΔCt otrzymano wartość maksymalną (wartość MAX), która posłużyła do standaryzacji uzyskanych wyników. Standaryzację i obliczenie ekspresji genów przeprowadzono za pomocą wzoru: $RQ_{MAX} = 2^{(\text{warto\u015bc MAX} - \Delta Ct)}$. Specyficzność otrzymanych produktów weryfikowano również względem kontroli NTC (ang. *no template control*) i NRT (ang. *no reverse transcriptase control*).

Charakterystykę zastosowanych sekwencji oligonukleotydowych (starterów) wraz z temperaturami hybrydyzacji przedstawiono w poszczególnych publikacjach wchodzących w skład pracy doktorskiej.

3.8. Analiza wewnątrzkomórkowej akumulacji białek metod\u0105 Western Blot

W celu określenia poziomu ekspresji wybranych białek wykorzystano technik\u0119 Western Blot. W tym celu hodowle kom\u00f3rkowe poddano lizie przy użyciu sch\u0142odzonego buforu

RIPA (ang. *radioimmunoprecipitation assay buffer*) uzupełnionego 1% koktajlem inhibitorów proteaz i fosfataz (Sigma-Aldrich, Monachium, Niemcy). Do określenia ilości wyizolowanego białka zastosowano zestaw Bicinchoninic Acid Assay Kit (BCA) (Sigma-Aldrich, Monachium, Niemcy). Reakcję elektroforezy (SDS-PAGE) przeprowadzono w żelu poliakrylamidowym o określonym stężeniu z wykorzystaniem Mini-PROTEAN Tetra Vertical Electrophoresis Cell (Bio-Rad, Hercules, CA, USA). Następnie próbki przeniesiono na membranę PVDF przy użyciu systemu Mini Trans-Blot® (Bio-Rad, Hercules, CA, USA). Membrany blokowano przy użyciu 5% roztworu odłuszczonego mleka w proszku w buforze TBST (Tris/NaCl/Tween), a następnie inkubowano przez noc w 4 °C z przeciwciałami pierwszorzędowymi: anty-RUNX2, anty-OPN, anty-MFN1, anty-PINK1 oraz anty-ACTβ. W czasie inkubacji z przeciwciałami drugorzędowymi wykorzystano przeciwciała skoniugowane z HRP (peroksydaza chrzanowa) w buforze TBST. Szczegółowe informacje dotyczące wykorzystanych przeciwciał pierwszo- i drugorzędowych oraz zastosowanych stężeń podano w odpowiednich publikacjach naukowych wchodzących w skład pracy doktorskiej. Membrany analizowano przy użyciu systemu Bio-Rad ChemiDoc™ XRS (Bio-Rad, Hercules, CA, USA). Sygnał chemiluminescencyjny wykryto przy użyciu substratu chemiluminescencyjnej i fluorescencyjnej peroksydazy (HRP) DuoLuX® (Vector Laboratories, Peterborough, Wielka Brytania). Intensywność sygnału i masę cząsteczkową wykrytych białek analizowano za pomocą oprogramowania Image Lab™ (Bio-Rad, Hercules, CA, USA). Ilość białka wykorzystanego w analizie, jak również stężenia żelów poliakrylamidowych podano w publikacjach wchodzących w skład pracy doktorskiej.

3.9. Badania *in vivo*

Aby potwierdzić właściwości osteo-indukcyjne cząsteczki miR-21-5p przeprowadzono badania *in vivo* z wykorzystaniem szczepu myszy SAM/P6. W tym celu wykonano procedurę obustronnego krytycznego ubytku czaszki (tzw. model CSD – ang. *critical-size cranial defect*). Zabiegi przeprowadzono u myszy osteoporotycznych szczepu SAM/P6 (n=2) pod nadzorem lekarza weterynarii, za zgodą lokalnej komisji etycznej (Lokalna Komisja Etyczna we Wrocławiu, nr decyzji: 069/2020/P1 z dnia 9.12.2020). Zwierzęta poddano ogólnemu znieczuleniu mieszaniną ksylazyny (25 mg/kg) i ketaminy (70 mg/kg). Następnie, wykonano dwa ubytki o średnicy 2 mm za pomocą cylindrycznego wiertła o niskiej prędkości. W celu dostarczenia niezdegradowanych cząsteczek miR-21 do wytworzonych ubytków, cząsteczki miR-21 zawieszono w 2% roztworze alginianu sodu.

Przed podaniem roztwór traktowano chlorkiem wapnia w celu usieciowienia i wytworzenia hydrożelu. Powstałe hydrożele alginianowe zawierające 50 nM miR-21 zostały umieszczone w ubytkach kostnych. Ubytki po lewej stronie czaszki służyły jako kontrole, do których podawano hydrożel bez zawartości miR-21. Zwierzęta poddano eutanazji dwa tygodnie po wykonaniu zabiegu w celu analizy wpływu miR-21 na regenerację tkanki kostnej.

Czaszki myszy wypreparowano w celu przeprowadzenia analiz z zakresu mikrotomografii komputerowej (μ -CT) i elektronowej mikroskopii skaningowej wraz z analizą rentgenowską dyspersji energii (SEM-EDX). Analizy μ -CT wykonano w Pracowni Mikrotomografii Rentgenowskiej Wydziału Informatyki i Inżynierii Materiałowej Uniwersytetu Śląskiego w Katowicach (Chorzów, Polska) przy użyciu systemu GE Phoenix v|tome|x (General Electric, Cincinnati, OH, USA). Skany μ -CT eksportowano jako pliki VGL i analizowano przy użyciu oprogramowania myVGL (wersja 3.3.2.170119, Volume Graphic GmbH) w celu oceny właściwości strukturalnych nowo utworzonej tkanki. Do oceny nowo wytworzonej tkanki wykorzystano program Fiji i Just ImageJ. Ponadto, czaszki analizowano za pomocą skaningowej mikroskopii elektronowej z oceną składu pierwiastkowego (SEM-EDX; SEM Evo LS 15 Zeiss, Niemcy). Mapowanie składu wapnia i fosforu wykonano za pomocą systemu Bruker Quantax 200 z detektorem BrukerXFlash 5010 i oprogramowaniem Esprit 1.8. Ponadto, zbadano ekspresję kluczowych markerów związanych z prawidłową regeneracją kości za pomocą techniki RT-qPCR, którą opisano w punkcie 3.7.

3.10. Analizy statystyczne

Każdą analizę przeprowadzono w co najmniej trzech powtórzeniach technicznych. Analizy statystyczne przeprowadzono przy użyciu oprogramowania GraphPad Prism 5 (GraphPad Software, San Diego, CA, USA). W trakcie prowadzenia analiz wykorzystano test t-Studenta oraz jednoczynnikową analizę wariancji (ANOVA) wraz z testem post-hoc Tukeya. Wyniki uznawano za istotne przy poziomie błędu mniejszym niż 5% ($p < 0,05$). Poziomy istotności oznaczano gwiazdkami: * $p < 0,05$; ** $p < 0,01$; *** $p < 0,001$. Różnice nieistotne oznaczono jako *ns*.

4. Komentarze do publikacji

4.1. Publikacja nr 1: Sikora, M., Marycz, K., & Śmieszek, A. (2020). Small and Long Non-coding RNAs as Functional Regulators of Bone Homeostasis, Acting Alone or Cooperatively. Molecular Therapy-Nucleic Acids, 21, 792–803. DOI: 10.1016/j.omtn.2020.07.017

W publikacji nr 1 został szczegółowo opisany aktualny stan wiedzy na temat funkcji niekodujących cząsteczek RNA (ncRNA: non-coding RNA) w podstawowych szlakach molekularnych i metabolicznych tkanki kostnej. Publikacja nr 1 stanowi istotne wprowadzenie teoretyczne do tematu roli niekodujących RNA w biologii tkanki kostnej oraz populacji komórek tworzących kość.

We wstępie publikacji nr 1 wskazano na poważny problem jakim są choroby dotyczące układu kostnego, ze szczególnym uwzględnieniem osteoporozy, choroby zwyrodnieniowej stawów oraz kostniakomięsaka. Wskazano na trudność diagnostyki wspomnianych jednostek chorobowych oraz na brak efektywnych i relatywnie niskobudżetowych metod ich leczenia. Z tego powodu zwraca się uwagę na alternatywne metody terapeutyczne, w szczególności terapie celowane, które opierałyby się o wykorzystanie markerów molekularnych np. niekodujących RNA.

Kolejnym tematem omówionym w manuskrypcie nr 1 jest biogeneza cząsteczek ncRNA. W szczegółowy sposób przedstawiono aktualny stan wiedzy z zakresu syntezy i funkcji zarówno małych niekodujących cząsteczek RNA (microRNA, miRNA) jak i długich niekodujących cząsteczek RNA (long non-coding RNA, lncRNA). Mechanizm powstawania oraz funkcje obydwu rodzajów RNA zostały przedstawione także w formie graficznej (P1: Ryc. 1). Szczególną uwagę zwrócono na oś molekularną lncRNA-miRNA-mRNA, ponieważ szlaki sygnałowe angażujące niekodujące RNA (na przykładzie miR-21-5p) oraz ich wpływ na ekspresję efektorowych mRNA powiązanych z procesami przebudowy tkanki kostnej były analizowane w kolejnych pracach naukowych wchodzących w skład cyklu.

Najważniejszym elementem pracy nr 1 jest szczegółowe omówienie funkcji wybranych cząsteczek miRNA oraz lncRNA w kontekście biologii komórek tkanki kostnej. Podsumowano dotychczasową wiedzę opisującą zaangażowanie wybranych cząsteczek w szlakach molekularnych, które są kluczowe dla zachowania homeostazy w obrębie tkanki kostnej. Zwrócono uwagę na zaangażowanie omawianych markerów w ekspresji istotnych czynników transkrypcyjnych powiązanych z osteogenezą np. RUNX-2. Omówiono znaczenie następujących cząsteczek miRNA: miR-21, miR-124, miR-203 oraz miR-223,

a także cząsteczek lncRNA: DANCR, TUG1, MALAT1 oraz HOTAIR. Opisano oddziaływania między wybranymi lncRNA i miRNA (tzw. *crossstalk*) oraz ich wpływ na aktywację komórek kościotwórczych (osteoblasty) lub kościogubnych (osteoklasty) (P1: Ryc. 2). Dodatkowo, w formie tabeli podsumowano zaangażowanie wybranych cząsteczek ncRNA na proces przebudowy tkanki kostnej i nowotworzenia, jak również cele molekularne powiązane z omawianymi cząsteczkami RNA, które mogą stanowić potencjalne cele diagnostyczne i terapeutyczne (P1: Tab. 1). Dodatkowo, omówiono wpływ ncRNA na aktywację morfogenów, które pełnią kluczowe funkcje w procesie różnicowania się komórek tkanki kostnej, w tym szlaki sygnałowe Wnt/ β -catenin czy białka morfogenetyczne kości (BMPs).

Podsumowując, w publikacji nr 1 omówiono dotychczasowy stan wiedzy na temat niekodujących cząsteczek RNA, które są zaangażowane w wiele istotnych procesów biologicznych, zapewniając unikalny mechanizm regulacyjny dla genów kodujących białka o istotnym znaczeniu w rozwoju kości, w tym morfogenów i czynników wzrostu, zapewniających również prawidłowy rozwój i homeostazę organizmu, zarówno na etapie życia płodowego, jak i dojrzałego organizmu. Należy podkreślić jak wartościowa jest identyfikacja i analiza powiązań między miRNA, lncRNA i domniemanymi genami docelowymi. Takie badania mogą zapewnić opracowanie nowych paneli biomarkerów, które wykazywać będą potencjał prognostyczny i diagnostyczny w przypadku chorób związanych z układem kostnym. Dodatkowo, analiza sieci molekularnych i powiązań między lncRNA-miRNA-mRNA może ujawnić nowe cele terapeutyczne, a w rezultacie umożliwić projektowanie bardziej efektywnych terapii celowanych ukierunkowanych na konkretne jednostki chorobowe.

4.2. Publikacja nr 2: Śmieszek, A., Marcinkowska, K., Pielok, A., Sikora, M., Valihrach, L., & Marycz, K. (2020). The Role of miR-21 in Osteoblasts-Osteoclasts Coupling In Vitro. Cells, 9, 1–21. DOI: 10.3390/cells9020479

Publikacja nr 2 stanowi pierwszy etap badań nad znaczeniem cząsteczki miR-21-5 w procesie regeneracji oraz zachowania homeostazy w obrębie tkanki kostnej, realizowanych w ramach pracy doktorskiej. Badania zostały przeprowadzone z wykorzystaniem komercyjnie dostępnej mysiej linii komórkowej MC3T3-E1. Komórki te zostały scharakteryzowane jako niedojrzałe komórki kościotwórcze (pre-osteoblasty). W pracy określono znaczenie miR-21-5p w kształtowaniu potencjału kościotwórczego

komórek MC3T3-E1 oraz wpływ tej cząsteczki na ich aktywność wydzielniczą. Osteoblasty odpowiedzialne są za wydzielanie czynników transkrypcyjnych, które modulują aktywność resorpcyjną komórek kościogubnych. Wzajemna regulacja osteoblastów i osteoklastów została zbadana w modelu ko-hodowli mysich komórek MC3T3-E1 z mysimi komórkami 4B12. Komórki 4B12 zostały scharakteryzowane jako niedojrzałe komórki kościogubne (pre-osteoklasty). Publikacja nr 2 jest zatem pierwszą próbą określenia roli cząsteczki miR-21-5p w procesie wzajemnej regulacji komórek kościotwórczych i kościogubnych w warunkach *in vitro*.

W pierwszym etapie badań określono znaczenie cząsteczki miR-21-5p w ekspresji markerów kościotworzenia w komórkach MC3T3-E1 inkubowanych samodzielnie oraz w ko-hodowli z komórkami 4B12. W tym celu wyciszono ekspresję miR-21-5p z wykorzystaniem cząsteczek siRNA (ang. *small interfering RNA*), które dostarczono do komórek za pomocą nośnika lipidowego. Ekspresję genów badano w trakcie różnicowania komórek w kierunku tkanki kostnej. Analiz dokonywano po 3, 7 oraz 15 dniach różnicowania. Wykazano, że po wyciszeniu ekspresji miR-21, komórki MC3T3-E1 charakteryzowały się znacznie obniżoną ilością mRNA dla takich markerów jak: OCL (ang. *osteocalcin*), OPN (ang. *osteopontin*), COLL-1 (ang. *collagen type 1*) oraz RUNX-2 (ang. *runt-related transcription factor 2*), zarówno hodowanych samodzielnie jak i w kulturze z komórkami 4B12 (P2: Ryc. 1).

Zgodnie z dotychczasową wiedzą, komórki kościotwórcze regulują dojrzewanie komórek kościogubnych poprzez zmienną ekspresję markerów OPG (ang. *osteoprotegerin*) oraz RANKL (ang. *receptor activator of nuclear factor kappa-B ligand*). Zwiększona ekspresja RANKL skutkuje dojrzewaniem komórek kościogubnych, co prowadzi do natężenia procesów degradacji tkanki kostnej. W przypadku większej ekspresji OPG, dojrzewanie komórek kościogubnych zostaje zahamowane. Z tego powodu, w publikacji nr 2 określono współczynnik ekspresji cząsteczek RANKL do OPG (poziomy transkryptów), który informuje o intensywności aktywacji komórek kościogubnych przez komórki kościotwórcze. Wykazano, że w badanych ko-kulturach współczynnik ten uległ znacznemu obniżeniu, co było rezultatem osłabionego metabolizmu komórek MC3T3, który związany był z deficytem miR-21 – efekt ten odnotowany był w każdym badanym punkcie czasowym prowadzonych ko-hodowli (P2: Ryc. 2). Można zatem wnioskować, że cząsteczka miR-21-5p odgrywa istotną rolę również w regulacji aktywności komórek kościogubnych, zależnej od prawidłowego zróżnicowania komórek kościotwórczych. Wysoka ekspresja miR-21-5p warunkuje prawidłowe dojrzewanie komórek

kościotwórczych i aktywację szlaków niezbędnych dla przeżycia komórek kościogubnych. Częsteczką miR-21-5p jest zatem czynnikiem niezbędnym dla prawidłowej przebudowy tkanki kostnej, gwarantującym homeostazę pomiędzy komórkami kościotwórczymi a kościogubnymi.

Znaczenie miR-21 oceniono również w aspekcie tworzenia funkcjonalnej macierzy zewnątrzkomórkowej w hodowlach osteogennych. Za pomocą barwników – Alizarin Red oraz Safranina-O – wybarwiono odpowiednio złogi wapnia oraz proteoglikany, w celu oceny stopnia zmineralizowania. Potwierdzono, że wyciszenie miR-21 w hodowlach komórek MC3T3-E1 skutkowało znacznym pogorszeniem jakości wytworzonej macierzy komórkowej wyrażonej zmniejszoną ilością złogów wapnia (P2: Ryc. 3) oraz proteoglikanów (P2: Ryc. 4). Jednakże, w przypadku ko-hodowli z komórkami 4B12, po wyciszeniu ekspresji cząsteczki miR-21, stopień mineralizacji macierzy wzrósł. Stanowi to kolejny dowód, że cząsteczka miR-21-5p odgrywa znaczącą rolę nie tylko w procesie aktywacji komórek kościotwórczych, ale także zaangażowana jest w regulację dojrzewania komórek kościogubnych, odpowiedzialnych za demineralizację tkanki kostnej.

W następnym etapie badań określono akumulację białek OPN oraz RUNX-2. Po rozdziale w żelu poliakrylamidowym, białko OPN rozszczepiło się na 3 podjednostki, natomiast RUNX-2 na 2 podjednostki. W przypadku białka RUNX-2 zaobserwowano jego obniżoną ekspresję po wyciszeniu miR-21 w prowadzonych ko-hodowlach komórek MC3T3-E1 i 4B12 (P2: Ryc. 5). W przypadku białka OPN stwierdzono obniżenie jego ekspresji po wyciszeniu miR-21, zarówno w hodowlach samodzielnych jak i ko-kulturach. Akumulację białka OPN określono także za pomocą technik immunofluorescencyjnych. Podczas obserwacji w mikroskopie konfokalnym potwierdzono jako mniejszą akumulację po hodowli komórek z inhibitorem miR-21 (P2: Ryc. 6).

Końcowym etapem badań była analiza komórek kościogubnych linii 4B12. Za pomocą techniki qPCR wykazano, że podczas hodowli tych komórek z linią MC3T3-E1, która potraktowana była inhibitorem cząsteczki miR-21, ekspresja kluczowych markerów powiązanych z dojrzewaniem komórek i ich aktywnością degradacyjną została obniżona (P2: Ryc. 7). Co ciekawe, wzrósł także odsetek komórek apoptotycznych. Obserwacje pod mikroskopem konfokalnym potwierdziły obniżoną akumulację białka TRAP (ang. *tartrate-resistant acid phosphatase*), które zaangażowane jest w proces degradacji tkanki kostnej (P2: Ryc. 8).

W niniejszej pracy doktorskiej, manuskrypt nr 2 stanowi pierwszy etap badań nad wyjaśnieniem roli cząsteczki miR-21-5p w procesie zachowania homeostazy w obrębie

tkanki kostnej. W pracy określono wpływ wyciszenia omawianej cząsteczki na proces różnicowania się mysich pre-osteoblastów linii MC3T3-E1 z uwzględnieniem ekspresji kluczowych markerów kościotworzenia oraz analizy formowania się funkcjonalnej, zmineralizowanej macierzy zewnątrzkomórkowej. Dodatkowo, określono wpływ miR-21 na aktywność wydzielniczą komórek kościotwórczych i regulację procesu dojrzewania komórek kościogubnych. Badania opisane w pracy nr 2 potwierdzają kluczowy wpływ cząsteczki miR-21 na procesy regeneracyjne tkanki kostnej na poziomie komórkowym oraz stanowią podwaliny do kolejnych badań z wykorzystaniem komórek progenitorowych pobranych od zwierząt, u których homeostaza tkanki kostnej została zaburzona, co zostało przedstawione w publikacji nr 3 oraz publikacji nr 4.

4.3. Publikacja nr 3: Sikora, M., Śmieszek, A., & Marycz, K. (2021). Bone marrow stromal cells (BMSCs CD45-/CD44+/CD73+/CD90+) isolated from osteoporotic mice SAM/P6 as a novel model for osteoporosis investigation. Journal of Cellular and Molecular Medicine, 25, 6634–6651. DOI: 10.1111/jcmm.16667

W publikacji nr 3 opisano i scharakteryzowano model szpikowych komórek progenitorowych (BMSCs – *bone marrow stem/stromal cells*) izolowanych z myszy szczepu SAM/P6, jako odpowiedni model do badań *in vitro* z zakresu projektowania molekularnych terapii celowanych w leczeniu osteoporozy starczej i zależnej od niej złamań kości. Badania przedstawione w publikacji 3 opierały się na charakterystyce BMSCs izolowanych z myszy osteoporotycznych, które po raz pierwszy zostały porównane względem BMSCs wyizolowanych z dzikiego szczepu myszy zdrowych – BALB/c. Manuskrypt nr 3 stanowi kontynuację badań przedstawionych w publikacji nr 2, jednak aspekt aplikacyjności został znacznie podkreślony za sprawą wykorzystania komórek izolowanych z organizmu myszy, a nie ustalonych linii komórkowych – model *ex vivo*. Jednocześnie, praca nr 3 jest wstępem do badań nad znaczeniem cząsteczki miR-21-5p z wykorzystaniem mysich osteoporotycznych komórek izolowanych ze szpiku kostnego.

We wstępie publikacji nr 3 nakreślono problem osteoporozy starczej. Zwrócono uwagę, że liczba osteoporotycznych złamań kości wzrasta w dramatycznym tempie i w przeciągu 50 lat osteoporoza przyjmie charakter globalnej epidemii. Uwagę skierowano na populację komórek progenitorowych rezydujących w szpiku kostnym (BMSCs), które odgrywają kluczową rolę w procesie regeneracji tkanki kostnej oraz zachowania homeostazy. Z tego powodu, celem pracy nr 3 było wykazanie słuszności wykorzystania modelu BMSCs,

a w szczególności komórek izolowanych z myszy osteoporotycznych, jako odpowiedniego modelu *in vitro*, który pozwoli określić zarówno molekularne podstawy rozwoju osteoporozy, jak i zaproponować nowe, bardziej skuteczne rozwiązania terapeutyczne.

Pierwszym etapem prowadzonych badań była izolacja komórek, które scharakteryzowano pod względem obecności markerów powierzchniowych typowych dla komórek mezenchymalnych, określono ich zdolność do różnicowania się oraz zmierzono aktywność metaboliczną. Wykazano, że BMSCs charakteryzowały się obecnością markerów powierzchniowych: CD44, CD73 i CD90 oraz nie posiadały markera CD45, co pozwala zaklasyfikować wyizolowane komórki do populacji progenitorowych komórek stromalnych. Na szczególną uwagę zasługuje obniżona ekspresja markerów CD44 i CD90 w komórkach wyizolowanych ze szpiku kostnego myszy osteoporotycznych SAM/P6 względem komórek wyizolowanych z myszy zdrowych BALB/c (P3: Ryc. 1). Co więcej, komórki osteoporotyczne charakteryzowały się niższą aktywnością metaboliczną zmierzoną za pomocą testu Alamar Blue oraz wykazywały znacząco niższą skłonność do różnicowania się w kierunku tkanki kostnej, jednocześnie efektywniej różnicowały się w kierunku tkanki tłuszczowej (P3: Ryc. 1). Można zatem wnioskować, że komórki BMSC izolowane od myszy SAM/P6 charakteryzują się fenotypem komórek starczych, co skutkuje obniżonym ich potencjałem regeneracyjnym.

Analizy z zakresu immunofluorescencji oraz transkryptomiki wykazały w komórkach osteoporotycznych obniżoną ekspresję markerów kościotworzenia: RUNX-2 i OPN, oraz równocześnie podwyższoną ekspresję TRAP (P3: Ryc. 2, 3, 4). Ekspresja cząsteczki TRAP związana jest przede wszystkim z degradacyjną działalnością komórek kościogubnych (osteoklastów), jednakże udowodniono, że cząsteczka ta może służyć także jako wskaźnik stanu zapalnego, który jest charakterystyczny dla procesów osteoporotycznych. Dodatkowo, komórki izolowane z myszy SAM/P6 posiadały obniżoną ekspresję późnych markerów kościotworzenia: COLL-1 i OPG (poziomy mRNA), a znacznie podwyższony poziom transkryptu lncRNA: DANCR1, który jak wskazują najnowsze badania modeluje proces degradacji tkanki kostnej (P3: Ryc. 3, 4). Warto odnotować, że komórki wyizolowane z myszy SAM/P6 charakteryzowały się podwyższoną ekspresją wybranych cząsteczek miRNA. Szczególnie istotna wydaje się różnica w poziomach transkryptu dla miR-124-3p, który opisywany jest jako kluczowa cząsteczka miRNA biorąca udział w dojrzewaniu komórek kościogubnych i progresji osteoporozy (P3: Ryc. 4).

Następnie, przeprowadzono testy funkcjonalne oparte o analizy cytometryczne, których celem była analiza żywotności komórek, profilu apoptozy, stresu oksydacyjnego, aktywności kaspaz oraz polaryzacji błon mitochondrialnych. Wykazano, że BMSCs pobrane z myszy osteoporotycznych charakteryzowały się mniejszą żywotnością, lecz znacznie podwyższonymi procesami związanymi z programowaną śmiercią komórki (apoptoza) i podwyższonym odsetkiem komórek zawierających reaktywne formy tlenu (stres oksydacyjny) (P3: Ryc. 5). Ciekawy jest fakt, że pomimo intensyfikacji apoptozy w komórkach osteoporotycznych, poziom aktywacji kaspaz był znacznie obniżony (P3: Ryc. 6). Można zatem wnioskować, że w przypadku badanych komórek kluczową rolę odgrywa tzw. śmierć komórki niezależna od kaspaz (CICD – ang. *caspase-independent cell death*). Ten mechanizm apoptozy, jak również akumulacja reaktywnych form tlenu (ROS) w komórkach pobranych od chorych myszy, znajduje bezpośrednie powiązanie z depolaryzacją błon mitochondrialnych (P3: Ryc. 6). Potwierdza to także obniżona akumulacja białek MFN-1 oraz PINK1, które odpowiedzialne są za prawidłową dynamikę sieci mitochondrialnej, w tym procesów fuzji czy mitofagii.

W manuskrypcie nr 3 opisano fenotyp BMSCs izolowanych od myszy chorujących na osteoporozę starczą. Mając na uwadze ograniczony dostęp do ludzkich komórek szpikowych o starczym fenotypie typowym dla osteoporozy, BMSCs izolowane z myszy SAM/P6 mogą z powodzeniem służyć w badaniach nad podłożem molekularnym tej jednostki chorobowej.

**4.4. Publikacja nr 4: Sikora, M., Śmieszek, A., Pielok, A., & Marycz K. (2023).
MiR-21-5p regulates the dynamic of mitochondria network and rejuvenates
the senile phenotype of bone marrow stromal cells (BMSCs) isolated from
osteoporotic SAM/P6 mice. Stem Cell Research & Therapy, 14. DOI:
10.1186/s13287-023-03271-1**

Publikacja nr 4 stanowi finalny etap badań zmierzających do wyjaśnienia biologicznej roli miR-21-5p w przebiegu regeneracji tkanki kostnej o znamionach osteoporozy starczej oraz stanowi bezpośrednią kontynuację badań przedstawionych w publikacji nr 3. Badania *ex vivo* zostały przeprowadzone w wykorzystaniu szpikowych komórek progenitorowych (BMSCs), które zostały wyizolowane z dwóch szczepów myszy, tj. z dzikiego szczepu BALB/c oraz ze szczepu SAM/P6 czyli myszy chorujących na osteoporozę starczą. Komórki wyizolowane ze szczepu BALB/c stanowiły zdrową kontrolę w stosunku do komórek

izolowanych z myszy SAM/P6. W celu określania wpływu cząsteczki miR-21-5p na potencjał regeneracyjny komórek progenitorowych zwiększano poziom jej ekspresji w komórkach pozyskanych z myszy chorujących na osteoporozę starczą (SAM/P6). Końcowym etapem eksperymentu było przeprowadzenie testów *in vivo* z wykorzystaniem modelu krytycznego ubytku czaszki (P4: Ryc. 7).

Przed przystąpieniem do badań, określono fenotyp uzyskanych komórek poprzez analizę obecności antygenów powierzchniowych celem potwierdzenia multipotentnego charakteru wyprowadzonych hodowli komórkowych. Tak jak przedstawiono w publikacji nr 3, wyizolowane komórki szpikowe charakteryzowały się obecnością markerów CD44, CD73, CD90 oraz CD105, oraz bardzo niską akumulacją markera CD45. Następnie, określono poziom ekspresji miR-21-5p w tkance kostnej u myszy BALB/c i SAM/P6. Co ciekawe, przeprowadzone badania wykazały, że u myszy SAM/P6 poziom ekspresji miR-21-5p był znacząco wyższy niż u myszy BALB/c. Fakt ten można wyjaśnić zaburzoną homeostazą w obrębie tkanki kostnej u chorujących myszy – mimo nadmiernej ekspresji miR-21 procesy związane z degradacją tkanki kostnej, tj. wzmożona aktywność komórek kościogubnych przy jednoczesnej niskiej aktywności komórek kościotwórczych, są przyczyną do rozwoju osteoporozy starczej. Dodatkowo, przed przystąpieniem do testów funkcjonalnych potwierdzono skuteczność transfekcji miR-21-5p w hodowlach komórkowych. Analizy z wykorzystaniem mikroskopii konfokalnej udowodniły, że miR-21 zwiększa aktywność proliferacyjną BMSCs wyizolowanych z myszy osteoporotycznych, co wykazano poprzez podwyższoną akumulację białka Ki67 oraz większą ilość genomowego DNA zwiualizowanego za pomocą barwnika Hoechst 33342 (P4: Ryc. 1). Dodatkowo, żywotność komórek została określona poprzez współczynnik ilości mRNA dla markera BAX względem poziomu BCL-2 (tzw. „BAX/BCL-2 ratio”). Pod wpływem miR-21 współczynnik ten obniżył się, co wskazuje na podwyższoną żywotność komórek.

W kolejnym etapie pracy badano mechanizmy metaboliczne zaangażowane w regulację potencjału regeneracyjnego komórek senilnych pod wpływem cząsteczki miR-21. Wykazano, że zwiększona ekspresja miR-21 w znacznym stopniu obniża aktywność lizosomów oraz ekspresję markera lizosomalnego LAMP-2. Lizosomy są strukturami odpowiedzialnymi za degradację określonych struktur komórkowych w procesie wzmożonej autofagii. Dodatkowo, wykazano spadek ekspresji markera PPAR γ (ang. *peroxisome proliferator-activated receptor gamma*), w przeciwieństwie do mTOR (ang. *mammalian target of rapamycin kinase*), którego poziom znacząco wzrósł. Obydwie cząsteczki są aktywnie zaangażowane w regulację procesów autofagii oraz mogą służyć jako

molekularne markery tego procesu (P4: Ryc. 2). Co istotne, wykazano, że miR-21 ma istotny wpływ na dynamikę sieci mitochondrialnych w badanych komórkach. Komórki izolowane z myszy SAM/P6 charakteryzowały się przewagą zdepolaryzowanych mitochondriów typu tubularnego (wydłużone), natomiast pod wpływem inkubacji z cząsteczkami miR-21 mitochondria przyjęły morfologię typu globularnego, które są charakterystyczne dla komórek młodych i różnicujących się.^{54,55} Analiza przy użyciu mikroskopu konfokalnego wskazała na wysoki potencjał błonowy mitochondriów na skutek działania miR-21 (P4: Ryc. 2).

Niezwykle ważnym elementem manuskryptu nr 4 było wykazanie roli miR-21-5p w procesie kościotworzenia (osteogenezy) oraz zachowania homeostazy w obrębie tkanki kostnej (P4: Ryc. 3 i 4). Wykazano, że pod wpływem miR-21 osteoporotyczne BMSCs chętniej różnicują się w kierunku tkanki kostnej, co zostało udowodnione poprzez wytworzenie wysokiej jakości macierzy zewnątrzkomórkowej bogatej w złogi wapnia oraz akumulację białka RUNX-2. Białko RUNX-2 jest wczesnym markerem procesu kościotworzenia oraz bierze aktywny udział w regulowaniu procesu regeneracji tkanki kostnej. Dodatkowo, poziomy transkryptów dla cząsteczek OPG oraz OCL, które stanowią markery później osteogenezy również wzrosły. Na szczególną uwagę zasługuje zmiana ekspresji ALPL (ang. *alkaline phosphatase*), który uważany jest za wczesny marker różnicowania – jego podwyższoną ekspresję (poziom mRNA) zaobserwowano w przypadku komórek osteoporotycznych, natomiast obecność miR-21-5p znacząco obniżyła poziom ekspresji tej cząsteczki. Na tej podstawie można wnioskować, że miR-21 aktywuje ekspresję genów powiązanych w szczególności z późniejszymi etapami różnicowania się komórek i mineralizacji macierzy zewnątrzkomórkowej (P4: Ryc. 3). Istotny jest także fakt, że zwiększona ekspresja miR-21 ma wpływ na obniżoną ekspresję markerów odpowiedzialnych za różnicowanie się komórek kościogubnych (osteoklastów) oraz procesy degradacji tkanki kostnej. W pracy skupiono się także na poziomie transkryptu oraz akumulację białka dla cząsteczki TRAP, które były znacząco obniżone pod wpływem inkubacji komórek z cząsteczkami miR-21 (P4: Ryc. 4).

Końcowym etapem badań było przeprowadzenie badań *in vivo* z wykorzystaniem modelu krytycznego ubytku czaszki. W trakcie prowadzenia badań w kościach ciemieniowych myszy wykonano dwa ubytki, które wypełniono materiałem alginianowym zawierającym cząsteczki miR-21-5p oraz kontrola niezawierająca miRNA. Analizy SEM-EDX oraz μ -CT wykazały, że obecność miR-21 w obrębie uszkodzonej tkanki w znaczącym stopniu wspomagała jej regenerację. Ubytki, w których umieszczono miR-21

charakteryzowały się większą ilością nacieków nowo powstałej tkanki kostnej oraz zwiększoną zawartością wapnia (Ca) i fosforu (P), które są podstawowymi budulcami hydroksyapatytu wchodzącego w skład tkanki kostnej.

Podsumowując, praca nr 4 stanowi końcowy efekt badań prowadzonych w ramach niniejszej pracy doktorskiej. Po raz pierwszy wykazano, że cząsteczka miR-21-5p ma istotny wpływ na metabolizm BMSCs izolowanych z myszy osteoporotycznych, w tym na ich proliferację i żywotność, a w szczególności na metabolizm mitochondrialny, wyrażony dynamiką sieci mitochondrialnej i zmianami morfologii mitochondriów. Wykazano, że miR-21 wspomaga mineralizację macierzy zewnątrzkomórkowej oraz aktywuje ekspresję markerów odpowiedzialnych za zachowanie homeostazy w obrębie tkanki kostnej. Ważnym elementem badań była analiza stopnia regeneracji tkanki kostnej z wykorzystaniem modelu *in vivo*. Wykazano, że zwiększona ekspresja miR-21 zwiększa potencjał regeneracyjny szpikowych komórek progenitorowych, co może znaleźć swoje potencjalne zastosowanie jako przykład nowej strategii terapeutycznej w leczeniu osteoporozy starczej oraz zależnej od niej złamań kości.

5. Podsumowanie

Osteoporoza starcza jest chorobą zależną od wieku, która najczęściej jest diagnozowana u osób po siedemdziesiątym roku życia i dotyczy zarówno kobiet, jak i mężczyzn. Najnowsze prognozy alarmują, że osteoporoza starcza jest drastycznie szybko rosnącym problemem zdrowotnym na całym świecie, który stał się jednym z najważniejszych zagadnień zdrowotnych i ekonomicznych. Jednakże, dostępne możliwości leczenia osteoporozy są wciąż niewystarczające.

Główną przyczyną rozwoju osteoporozy starczej jest zaburzenie homeostazy aktywności komórek kościogubnych oraz komórek kościotwórczych. Dodatkowo wykazano, że wraz z wiekiem zmniejsza się potencjał regeneracyjny organizmu, co ma olbrzymi wpływ na pogorszenie samoodnowy populacji komórek progenitorowych rezydujących w szpiku kostnym (BMSCs), odpowiedzialnych za regenerację tkanki kostnej. Do tej pory zidentyfikowano liczne szlaki molekularne zaangażowane w proces osteogenezy, jednak ich osie są rozpatrywane na nowo w kontekście regulacji procesów kościotworzenia z udziałem miRNA. Obecnie, rozważa się wykorzystanie cząsteczek miRNA jako wiarygodnych markerów diagnostycznych oraz celów terapeutycznych w procesie projektowania skutecznych terapii celowanych i ukierunkowanych na leczenie osteoporozy oraz zależnej od niej złamań kości. Cząsteczką, która zwraca uwagę badaczy w tym zakresie jest miR-21-5p. Ocena roli tej cząsteczki w procesie osteogenezy komórek o fenotypie senilnym z obniżonym potencjałem regeneracyjnym była celem tej pracy doktorskiej. Badania miały na celu określenie roli miR-21 w regulacji głównych populacji komórek tkanki kostnej – komórek kościotwórczych i kościogubnych, jak również progenitorowych mobilizowanych ze szpiku kostnego. Praca doktorska ma charakter nowatorski i złożony – aspekt merytoryczny i badawczy został zaprojektowany tak, aby móc opisać rolę miR-21 w regulacji kluczowych szlaków molekularnych związanych z przebudową kości. Tezę dowiedziono zarówno w badaniach prowadzonych w modelu *in vitro*, jak i *in vivo*.

Cykl publikacyjny został zaprojektowany w sposób celowy i rozpoczyna go praca o charakterze przeglądowym, której celem było podsumowanie wiedzy na temat znaczenia niekodujących cząsteczek RNA w biologii tkanki kostnej i rozwoju chorób dotyczących kości. Zwrócono uwagę na możliwość zastosowania wybranych miRNA jako ważnych czynników biologicznych w projektowaniu molekularnych terapii celowanych. W pracy nr 2 opisano rolę cząsteczki miR-21-5p w aktywności metabolicznej i regeneracyjnej komórek MC3T3-E1 (pre-osteoblasty). Dodatkowo, wyjaśniono znaczenie miR-21-5p w regulacji dojrzewania komórek 4B12 (pre-osteoklasty), których aktywność resorpcyjna modelowana

jest przez komórki kościotwórcze z uwzględnieniem szlaku sygnałowego OPG/RANKL/RANK. W manuskrypcie nr 3 scharakteryzowano potencjał regeneracyjny BMSCs izolowany z myszy chorujących na osteoporozę starczą szczepu SAM/P6 względem komórek izolowanych z szczepu myszy zdrowych BALB/c. Stwierdzono znacznie upośledzone mechanizmy regeneracyjne, które są charakterystyczne dla komórek o fenotypie starczym. Dodatkowo, zaproponowano modele *in vitro* oraz *in vivo*, które mogą służyć do prowadzenia badań nad molekularnym podłożem rozwoju osteoporozy starczej oraz efektywnymi terapiami. W publikacji nr 4 będącej zwięźczeniem prowadzonych badań w pracy doktorskiej, określono rolę cząsteczki miR-21-5p w regulacji potencjału BMSCs o fenotypie senilnym ze szczególnym uwzględnieniem dynamiki sieci mitochondrialnej. Udowodniono, że miR-21-5p ma istotny wpływ na przywrócenie cech charakterystycznych dla zdrowych komórek progenitorowych, takich jak: wysoki potencjał regeneracyjny, wysoka żywotność czy skłonność do różnicowania się w kierunku komórek tkanki kostnej. Badania znalazły potwierdzenie w modelu *in vivo* z wykorzystaniem myszy SAM/P6.

Praca doktorska wyjaśnia zaangażowanie cząsteczki miR-21-5p w procesie regeneracji tkanki kostnej o znamionach osteoporozy starczej ze szczególnym uwzględnieniem potencjału komórek kościotwórczych, kościogubnych oraz szpikowych komórek progenitorowych. W ramach pracy doktorskiej wykazano także zasadność wykorzystania modelu myszy senilnych szczepu SAM/P6 jako wiarygodnego modelu do badań nad podłożem osteoporozy starczej. Prowadzone badania mają zatem charakter aplikacyjny, zwracając uwagę na możliwość projektowania tzw. terapii „szytych na miarę”, które opierać się mogą o wykorzystanie biologicznie aktywnych markerów molekularnych np. mikroRNA. Co więcej, w ostatnim czasie zwraca się coraz większą uwagę na potencjał rzadkich nisz komórkowych, które mają kluczowe znaczenia dla kształtowania potencjału regeneracyjnego pacjentów. Na szczególną uwagę zasługują tzw. *skeletal stem cells* (SSCs), które dają początek innym grupom komórek macierzystych odpowiedzialnych np. za rozwój kości. Rzetelna analiza z zakresu zaangażowania tej populacji komórek w procesy przebudowy kośćca może przynieść niebagatelne korzyści w postaci alternatywnych metod terapeutycznych opierających się o przywrócenie naturalnych sił regeneracyjnych organizmu pacjenta. Z tego powodu, dalsze badania skoncentrowane nad przywróceniem naturalnego potencjału komórek macierzystych do regeneracji tkanki kostnej u pacjentów zmagających się z osteoporozą oraz zależnymi od niej złamaniami kości, wydają się w pełni uzasadnione i konieczne.

6. Wnioski

Badania zrealizowane w ramach pracy doktorskiej związane były z określeniem znaczenia małych niekodujących cząsteczek RNA (miRNA) w procesie regeneracji tkanki kostnej i przebiegu osteoporozy na przykładzie cząsteczki miR-21-5p.

Przeprowadzone badania uprawniają do sformułowania następujących wniosków końcowych:

- Cząsteczka miR-21-5p bierze istotny udział w procesie aktywacji komórek kościotwórczych. Eksperymentalne zmniejszenie ekspresji miR-21-5p w komórkach linii MC3T3-E1 powoduje utratę ich zdolności regeneracyjnych (kościotwórczych), co przejawia się m.in. obniżoną mineralizacją macierzy zewnątrzkomórkowej oraz obniżoną ekspresją istotnych markerów kościotworzenia (RUNX-2, OCL, OPN, COLL-1).
- Cząsteczka miR-21-5p zaangażowana jest w regulację aktywności komórek kościotwórczych i kościogubnych, co wyraża się przez podwyższoną ekspresję cząsteczek OPG i RANKL. Zmniejszenie ekspresji miR-21-5p obniża aktywność wydzielniczą komórek MC3T3-E1, co wiąże się z pogorszeniem żywotności komórek 4B12 oraz obniżeniem ilości transkryptów dla markerów osteolitycznych (TRAP, CTSK, CAII, MMP-9).
- BMSCs izolowane z myszy osteoporotycznych szczepu SAM/P6 przejawiają oznaki starzenia się (fenotyp senilny), co znajduje odzwierciedlenie w obniżonej żywotności komórek progenitorowych, związanej z akumulacją reaktywnych form tlenu oraz zaburzoną dynamiką sieci mitochondrialnej, a finalnie skutkuje osłabioną zdolnością do różnicowania się komórek w kierunku tkanki kostnej i chrzęstnej.
- Myszy szczepu SAM/P6, jak również pobrane z nich BMSCs mogą znaleźć zastosowanie jako wartościowe modele do badań nad molekularnym podłożem osteoporozy, jak również mogą umożliwić projektowanie nowych metod diagnostycznych i terapii celowanych dedykowanych chorobom metabolicznym kości.

- Cząsteczka miR-21-5p przywraca utracony potencjał regeneracyjny w BMSCs izolowanych z myszy SAM/P6. Zwiększenie ekspresji miR-21 w komórkach o fenotypie senilnym poprawia żywotność komórek i ich aktywność proliferacyjną, usprawnia dynamikę sieci mitochondrialnej i autofagii oraz zwiększa ekspresję markerów kościotworzenia i mineralizację macierzy zewnątrzkomórkowej (RUNX-2, COLL-1, OCL, OPG).
- Regeneracja tkanki kostnej *in situ* może być sterowana poprzez dostarczenie miR-21-5p o działaniu pro-osteogennym, które przejawia się funkcjonalnym różnicowaniem komórek kościotwórczych oraz utworzeniem zmineralizowanej tkanki kostnej.
- Implementacja cząsteczki miR-21-5p jako biologicznego czynnika modelującego prawidłową przebudowę i zachowanie homeostazy w obrębie tkanki kostnej może stanowić efektywną i celowaną formę terapii osteoporozy starczej oraz zależnej od niej złamań kości – tzw. terapia „szyta na miarę”.

7. Literatura

1. Qadir, A., Liang, S., Wu, Z., Chen, Z., Hu, L., and Qian, A. (2020). Senile Osteoporosis: The Involvement of Differentiation and Senescence of Bone Marrow Stromal Cells. *Int J Mol Sci* 21. 10.3390/ijms21010349.
2. WHO_Technical_Report.pdf.
3. Gullberg, B., Johnell, O., and Kanis, J.A. (1997). World-wide projections for hip fracture. *Osteoporos Int* 7, 407–413. 10.1007/pl00004148.
4. Sabri, S.A., Chavarria, J.C., Ackert, -Bicknell Cheryl, Swanson, C., and Burger, E. (2023). Osteoporosis: An Update on Screening, Diagnosis, Evaluation, and Treatment. *Orthopedics* 46, e20–e26. 10.3928/01477447-20220719-03.
5. Sander, R. (2007). Asymptomatic osteoporosis masks the importance of taking medication. *Nurs Older People* 19, 23. 10.7748/nop.19.10.23.s21.
6. Parra-Torres, A.Y., Valdés-Flores, M., and Velázquez-Cruz, L.O. and R. (2013). Molecular Aspects of Bone Remodeling (IntechOpen) 10.5772/54905.
7. Chen, K., Jiao, Y., Liu, L., Huang, M., He, C., He, W., Hou, J., Yang, M., Luo, X., and Li, C. (2020). Communications Between Bone Marrow Macrophages and Bone Cells in Bone Remodeling. *Front Cell Dev Biol* 8, 598263. 10.3389/fcell.2020.598263.
8. Sandhu, S.K., and Hampson, G. (2011). The pathogenesis, diagnosis, investigation and management of osteoporosis. *J Clin Pathol* 64, 1042–1050. 10.1136/jcp.2010.077842.
9. Kaur, M., Nagpal, M., and Singh, M. (2020). Osteoblast-n-Osteoclast: Making Headway to Osteoporosis Treatment. *Curr Drug Targets* 21, 1640–1651. 10.2174/1389450121666200731173522.
10. Chen, X., Wang, Z., Duan, N., Zhu, G., Schwarz, E.M., and Xie, C. (2018). Osteoblast-Osteoclast Interactions. *Connect Tissue Res* 59, 99–107. 10.1080/03008207.2017.1290085.
11. Kim, J.-M., Lin, C., Stavre, Z., Greenblatt, M.B., and Shim, J.-H. (2020). Osteoblast-Osteoclast Communication and Bone Homeostasis. *Cells* 9, 2073. 10.3390/cells9092073.
12. Park, Y., Cheong, E., Kwak, J.-G., Carpenter, R., Shim, J.-H., and Lee, J. (2021). Trabecular bone organoid model for studying the regulation of localized bone remodeling. *Sci Adv* 7, eabd6495. 10.1126/sciadv.abd6495.
13. Friedenstein, A.J. (1973). Determined and Inducible Osteogenic Precursor Cells. In *Ciba Foundation Symposium 11 - Hard Tissue Growth, Repair and Remineralization* (John Wiley & Sons, Ltd), pp. 169–185. 10.1002/9780470719947.ch9.

14. Friedenstein, A.J., Chailakhyan, R.K., and Gerasimov, U.V. (1987). Bone marrow osteogenic stem cells: in vitro cultivation and transplantation in diffusion chambers. *Cell Tissue Kinet* 20, 263–272. 10.1111/j.1365-2184.1987.tb01309.x.
15. Dominici, M., Le Blanc, K., Mueller, I., Slaper-Cortenbach, I., Marini, F., Krause, D., Deans, R., Keating, A., Prockop, D., and Horwitz, E. (2006). Minimal criteria for defining multipotent mesenchymal stromal cells. The International Society for Cellular Therapy position statement. *Cytotherapy* 8, 315–317. 10.1080/14653240600855905.
16. Huo, S.-C., and Yue, B. (2020). Approaches to promoting bone marrow mesenchymal stem cell osteogenesis on orthopedic implant surface. *World J Stem Cells* 12, 545–561. 10.4252/wjsc.v12.i7.545.
17. Yu, L., Wu, Y., Liu, J., Li, B., Ma, B., Li, Y., Huang, Z., He, Y., Wang, H., Wu, Z., et al. (2018). 3D Culture of Bone Marrow-Derived Mesenchymal Stem Cells (BMSCs) Could Improve Bone Regeneration in 3D-Printed Porous Ti6Al4V Scaffolds. *Stem Cells International* 2018, e2074021. <https://doi.org/10.1155/2018/2074021>.
18. Jin, Y.-Z., and Lee, J.H. (2018). Mesenchymal Stem Cell Therapy for Bone Regeneration. *Clin Orthop Surg* 10, 271–278. 10.4055/cios.2018.10.3.271.
19. Matsushita, Y., Nagata, M., Kozloff, K.M., Welch, J.D., Mizuhashi, K., Tokavanich, N., Hallett, S.A., Link, D.C., Nagasawa, T., Ono, W., et al. (2020). A Wnt-mediated transformation of the bone marrow stromal cell identity orchestrates skeletal regeneration. *Nat Commun* 11, 332. 10.1038/s41467-019-14029-w.
20. Frank, O., Heim, M., Jakob, M., Barbero, A., Schäfer, D., Bendik, I., Dick, W., Heberer, M., and Martin, I. (2002). Real-time quantitative RT-PCR analysis of human bone marrow stromal cells during osteogenic differentiation in vitro. *J Cell Biochem* 85, 737–746. 10.1002/jcb.10174.
21. Yu, H., Cheng, J., Shi, W., Ren, B., Zhao, F., Shi, Y., Yang, P., Duan, X., Zhang, J., Fu, X., et al. (2020). Bone marrow mesenchymal stem cell-derived exosomes promote tendon regeneration by facilitating the proliferation and migration of endogenous tendon stem/progenitor cells. *Acta Biomater* 106, 328–341. 10.1016/j.actbio.2020.01.051.
22. Zhang, Y., Liu, Y., Liu, H., and Tang, W.H. (2019). Exosomes: biogenesis, biologic function and clinical potential. *Cell Biosci* 9. 10.1186/s13578-019-0282-2.
23. Draebing, T., Heigwer, J., Juergensen, L., Katus, H.A., and Hassel, D. (2018). Extracellular Vesicle-delivered Bone Morphogenetic Proteins: A novel paracrine mechanism during embryonic development (*Developmental Biology*) 10.1101/321356.

24. Luo, Z., Lin, J., Sun, Y., Wang, C., and Chen, J. (2020). Bone Marrow Stromal Cell-Derived Exosomes promote muscle healing following contusion through macrophage polarization. *Stem Cells Dev.* 10.1089/scd.2020.0167.
25. Huang, T., Yu, Z., Yu, Q., Wang, Y., Jiang, Z., Wang, H., and Yang, G. (2020). Inhibition of osteogenic and adipogenic potential in bone marrow-derived mesenchymal stem cells under osteoporosis. *Biochemical and Biophysical Research Communications* 525, 902–908. 10.1016/j.bbrc.2020.03.035.
26. Huang, Y., Yin, Y., Gu, Y., Gu, Q., Yang, H., Zhou, Z., and Shi, Q. (2020). Characterization and immunogenicity of bone marrow-derived mesenchymal stem cells under osteoporotic conditions. *Sci China Life Sci* 63, 429–442. 10.1007/s11427-019-1555-9.
27. Lu, T.X., and Rothenberg, M.E. (2018). MicroRNA. *J Allergy Clin Immunol* 141, 1202–1207. 10.1016/j.jaci.2017.08.034.
28. Ha, M., and Kim, V.N. (2014). Regulation of microRNA biogenesis. *Nat Rev Mol Cell Biol* 15, 509–524. 10.1038/nrm3838.
29. Stavast, C.J., and Erkeland, S.J. (2019). The Non-Canonical Aspects of MicroRNAs: Many Roads to Gene Regulation. *Cells* 8. 10.3390/cells8111465.
30. O'Brien, J., Hayder, H., Zayed, Y., and Peng, C. (2018). Overview of MicroRNA Biogenesis, Mechanisms of Actions, and Circulation. *Front Endocrinol (Lausanne)* 9. 10.3389/fendo.2018.00402.
31. Foessel, I., Kotzbeck, P., and Obermayer-Pietsch, B. (2019). miRNAs as novel biomarkers for bone related diseases. *Journal of Laboratory and Precision Medicine* 4.
32. van Wijnen, A.J., van de Peppel, J., van Leeuwen, J.P., Lian, J.B., Stein, G.S., Westendorf, J.J., Oursler, M.-J., Sampen, H.-J.I., Taipaleenmaki, H., Hesse, E., et al. (2013). MicroRNA Functions in Osteogenesis and Dysfunctions in Osteoporosis. *Curr Osteoporos Rep* 11, 72–82. 10.1007/s11914-013-0143-6.
33. Bottani, M., Banfi, G., and Lombardi, G. (2019). Perspectives on miRNAs as Epigenetic Markers in Osteoporosis and Bone Fracture Risk: A Step Forward in Personalized Diagnosis. *Front. Genet.* 10. 10.3389/fgene.2019.01044.
34. Cheng, V.K.-F., Au, P.C.-M., Tan, K.C., and Cheung, C.-L. (2019). MicroRNA and Human Bone Health. *JBMR Plus* 3, 2–13. 10.1002/jbm4.10115.
35. Jia, B., Zhang, Z., Qiu, X., Chu, H., Sun, X., Zheng, X., Zhao, J., and Li, Q. (2018). Analysis of the miRNA and mRNA involved in osteogenesis of adipose-derived mesenchymal stem cells. *Exp Ther Med* 16, 1111–1120. 10.3892/etm.2018.6303.

36. Fröhlich, L.F. (2019). MicroRNAs at the Interface between Osteogenesis and Angiogenesis as Targets for Bone Regeneration. *Cells* 8, 121. 10.3390/cells8020121.
37. Zhao, Z., Li, X., Zou, D., Lian, Y., Tian, S., and Dou, Z. (2019). Expression of microRNA-21 in osteoporotic patients and its involvement in the regulation of osteogenic differentiation. *Exp Ther Med* 17, 709–714. 10.3892/etm.2018.6998.
38. Wei, F., Yang, S., Guo, Q., Zhang, X., Ren, D., Lv, T., and Xu, X. (2017). MicroRNA-21 regulates Osteogenic Differentiation of Periodontal Ligament Stem Cells by targeting Smad5. *Scientific Reports* 7, 16608. 10.1038/s41598-017-16720-8.
39. Yang, C., Liu, X., Zhao, K., Zhu, Y., Hu, B., Zhou, Y., Wang, M., Wu, Y., Zhang, C., Xu, J., et al. (2019). miRNA-21 promotes osteogenesis via the PTEN/PI3K/Akt/HIF-1 α pathway and enhances bone regeneration in critical size defects. *Stem Cell Research & Therapy* 10, 65. 10.1186/s13287-019-1168-2.
40. Hu, X., Li, L., Lu, Y., Yu, X., Chen, H., Yin, Q., and Zhang, Y. (2018). miRNA-21 inhibition inhibits osteosarcoma cell proliferation by targeting PTEN and regulating the TGF- β 1 signaling pathway. *Oncol Lett* 16, 4337–4342. 10.3892/ol.2018.9177.
41. Feng, Y.-H., and Tsao, C.-J. (2016). Emerging role of microRNA-21 in cancer (Review). *Biomedical Reports* 5, 395–402. 10.3892/br.2016.747.
42. Li, H., Yang, F., Wang, Z., Fu, Q., and Liang, A. (2015). MicroRNA-21 promotes osteogenic differentiation by targeting small mothers against decapentaplegic 7. *Molecular Medicine Reports* 12, 1561–1567. 10.3892/mmr.2015.3497.
43. Li, X., Guo, L., Liu, Y., Su, Y., Xie, Y., Du, J., Zhou, J., Ding, G., Wang, H., Bai, Y., et al. (2017). MicroRNA-21 promotes osteogenesis of bone marrow mesenchymal stem cells via the Smad7-Smad1/5/8-Runx2 pathway. *Biochem. Biophys. Res. Commun.* 493, 928–933. 10.1016/j.bbrc.2017.09.119.
44. Molténi, A., Modrowski, D., Hott, M., and Marie, P.J. (1999). Alterations of matrix- and cell-associated proteoglycans inhibit osteogenesis and growth response to fibroblast growth factor-2 in cultured rat mandibular condyle and calvaria. *Cell Tissue Res* 295, 523–536. 10.1007/s004410051258.
45. Lozano, C., Duroux-Richard, I., Firat, H., Schordan, E., and Apparailly, F. (2019). MicroRNAs: Key Regulators to Understand Osteoclast Differentiation? *Frontiers in Immunology* 10.
46. Kobayashi, Y., Udagawa, N., and Takahashi, N. (2009). Action of RANKL and OPG for Osteoclastogenesis. *CRE* 19. 10.1615/CritRevEukarGeneExpr.v19.i1.30.

47. Carthew, J., Shrestha, S., Forsythe, J.S., Donderwinkel, I., Truong, V.X., and Frith, J.E. (2019). In situ miRNA delivery from a hydrogel promotes osteogenesis of encapsulated mesenchymal stromal cells. *bioRxiv*, 712042. 10.1101/712042.
48. Meng, Y., Liu, C., Zhao, J., Li, X., Li, Z., Wang, J., Wang, R., Liu, Y., Yuan, X., Cui, Z., et al. (2016). An injectable miRNA-activated matrix for effective bone regeneration in vivo. *J. Mater. Chem. B* 4, 6942–6954. 10.1039/C6TB01790H.
49. Ichioka, N., Inaba, M., Kushida, T., Esumi, T., Takahara, K., Inaba, K., Ogawa, R., Iida, H., and Ikehara, S. (2002). Prevention of Senile Osteoporosis in SAMP6 Mice by Intrabone Marrow Injection of Allogeneic Bone Marrow Cells. *STEM CELLS* 20, 542–551. 10.1634/stemcells.20-6-542.
50. Chen, H., Zhou, X., Emura, S., and Shoumura, S. (2009). Site-specific bone loss in senescence-accelerated mouse (SAMP6): a murine model for senile osteoporosis. *Exp Gerontol* 44, 792–798. 10.1016/j.exger.2009.09.009.
51. Amano, S., Sekine, K., Bonewald, L.F., and Ohmori, Y. (2009). A novel osteoclast precursor cell line, 4B12, recapitulates the features of primary osteoclast differentiation and function: Enhanced transfection efficiency before and after differentiation. *Journal of Cellular Physiology* 221, 40–53. 10.1002/jcp.21827.
52. Peng, J.-Y., Lin, C.-C., Chen, Y.-J., Kao, L.-S., Liu, Y.-C., Chou, C.-C., Huang, Y.-H., Chang, F.-R., Wu, Y.-C., Tsai, Y.-S., et al. (2011). Automatic Morphological Subtyping Reveals New Roles of Caspases in Mitochondrial Dynamics. *PLOS Computational Biology* 7, e1002212. 10.1371/journal.pcbi.1002212.
53. Chomczynski, P., and Sacchi, N. (1987). Single-step method of RNA isolation by acid guanidinium thiocyanate-phenol-chloroform extraction. *Analytical Biochemistry* 162, 156–159. 10.1016/0003-2697(87)90021-2.
54. Ren, L., Chen, X., Chen, X., Li, J., Cheng, B., and Xia, J. (2020). Mitochondrial Dynamics: Fission and Fusion in Fate Determination of Mesenchymal Stem Cells. *Front. Cell Dev. Biol.* 8. 10.3389/fcell.2020.580070.
55. Seo, B.J., Yoon, S.H., and Do, J.T. (2018). Mitochondrial Dynamics in Stem Cells and Differentiation. *Int J Mol Sci* 19, 3893. 10.3390/ijms19123893.

8. Dorobek naukowy

Publikacje naukowe:

- 1) Bourebaba, L., Zyzak, M., **Sikora, M.**, Serwotka-Suszczak, A., Mularczyk, M., Naem, M. A., & Marycz, K. (2023). *Sex Hormone-Binding Globulin (SHBG) Maintains Proper Equine Adipose-Derived Stromal Cells (ASCs)' Metabolic Functions and Negatively Regulates their Basal Adipogenic Potential*. *Stem Cell Reviews and Reports*, 1–23. <https://doi.org/10.1007/s12015-023-10580-8>
(IF = 4.8; MEiN = 100)
- 2) Bourebaba, L., Serwotka-Suszczak, A., Pielok, A., **Sikora, M.**, Mularczyk, M., & Marycz, K. (2023). *The PTP1B inhibitor MSI-1436 ameliorates liver insulin sensitivity by modulating autophagy, ER stress and systemic inflammation in Equine metabolic syndrome affected horses*. *Frontiers in Endocrinology*, 14, 1–22. <https://doi.org/10.3389/fendo.2023.1149610>
(IF = 5.2; MEiN = 100)
- 3) **Sikora, M.**, Śmieszek, A., Pielok, A., & Marycz, K. (2023). *MiR-21-5p regulates the dynamic of mitochondria network and rejuvenates the senile phenotype of bone marrow stromal cells (BMSCs) isolated from osteoporotic SAM/P6 mice*. *Stem Cell Research & Therapy*, 14, 1–20. <https://doi.org/10.1186/s13287-023-03271-1>
(IF = 7.5; MEiN = 100)
- 4) Kosior, P., Dobrzyński, M., Zakrzewska, A., Diakowska, D., Nienartowicz, J., Blicharski, T., Nagel, S., **Sikora, M.**, Wiglusz, K., Watras, A., & Wiglusz, R. J. (2022). *Comparison of the Fluoride Ion Release from Composite and Compomer Materials under Varying pH Conditions—Preliminary In Vitro Study*. *Applied Sciences-Basel*, 12, 1–13. <https://doi.org/10.3390/app122412540>
(IF = 2.7; MEiN = 100)
- 5) **Sikora, M.**, Krajewska, K., Marcinkowska, K., Raciborska, A., Wiglusz, R., & Śmieszek, A. (2022). *Comparison of Selected Non-Coding RNAs and Gene Expression Profiles between Common Osteosarcoma Cell Lines*. *Cancers*, 14, 1–19. <https://doi.org/10.3390/cancers14184533>
(IF = 5.2; MEiN = 140)
- 6) Śmieszek, A., Marcinkowska, K., Pielok, A., **Sikora, M.**, Valihrach, L., Carnevale, E., & Marycz, K. (2022). *Obesity Affects the Proliferative Potential of Equine Endometrial Progenitor Cells and Modulates Their Molecular Phenotype Associated*

with Mitochondrial Metabolism. Cells, 11, 1–29.
<https://doi.org/10.3390/cells11091437>

(IF = 6.0; MEiN = 140)

- 7) Marycz, K., Śmieszek, A., Marcinkowska, K., **Sikora, M.**, Turlej, E., Sobierajska, P., Patej, A., Bienko, A., & Wiglusz, R. J. (2021). *Nanohydroxyapatite (nHAp) Doped with Iron Oxide Nanoparticles (IO), miR-21 and miR-124 Under Magnetic Field Conditions Modulates Osteoblast Viability, Reduces Inflammation and Inhibits the Growth of Osteoclast – A Novel Concept for Osteoporosis Treatment: Part 1*. *International Journal of Nanomedicine*, 2021, 3429–3456.
<https://doi.org/10.2147/IJN.S303412>
(IF = 7.033; MEiN = 140)
- 8) **Sikora, M.**, Śmieszek, A., & Marycz, K. (2021). *Bone marrow stromal cells (BMSCs CD45-/CD44+/CD73+/CD90+) isolated from osteoporotic mice SAM/P6 as a novel model for osteoporosis investigation*. *Journal of Cellular and Molecular Medicine*, 25, 6634–6651. <https://doi.org/10.1111/jcmm.16667>
(IF = 5.295; MEiN = 100)
- 9) Seweryn, A., Pielok, A., Ławniczak-Jabłońska, K., Pietruszka, R., Marcinkowska, K., **Sikora, M.**, Witkowski, B. S., Godlewski, M., Marycz, K., & Śmieszek, A. (2020). *Zirconium Oxide Thin Films Obtained by Atomic Layer Deposition Technology Abolish the Anti-Osteogenic Effect Resulting from miR-21 Inhibition in the Pre-Osteoblastic MC3T3 Cell Line*. *International Journal of Nanomedicine*, 15, 1595–1610. <https://doi.org/10.2147/IJN.S237898>
(IF = 6.4; MEiN = 140)
- 10) **Sikora, M.**, Marycz, K., & Śmieszek, A. (2020). *Small and Long Non-coding RNAs as Functional Regulators of Bone Homeostasis, Acting Alone or Cooperatively*. *Molecular Therapy-Nucleic Acids*, 21, 792–803.
<https://doi.org/10.1016/j.omtn.2020.07.017>
(IF = 8.886; MEiN = 140)
- 11) Śmieszek, A., Marcinkowska, K., Pielok, A., **Sikora, M.**, Valihrach, L., & Marycz, K. (2020). *The Role of miR-21 in Osteoblasts-Osteoclasts Coupling In Vitro*. *Cells*, 9, 1–21. <https://doi.org/10.3390/cells9020479>
(IF = 6.6; MEiN = 140)
- 12) Śmieszek, A., Seweryn, A., Marcinkowska, K., **Sikora, M.**, Ławniczak-Jablonska, K., Witkowski, B. S., Kuzmiuk, P., Godlewski, M., & Marycz, K. (2020). *Titanium*

- Dioxide Thin Films Obtained by Atomic Layer Deposition Promotes Osteoblasts' Viability and Differentiation Potential While Inhibiting Osteoclast Activity - Potential Application for Osteoporotic Bone Regeneration.* *Materials*, 13, 1–20. <https://doi.org/10.3390/ma13214817>
(IF = 3.623; MEiN = 140)
- 13) Targońska, S., **Sikora, M.**, Marycz, K., Śmieszek, A., & Wiglusz, R. J. (2020). *Theranostic Applications of Nanostructured Silicate-Substituted Hydroxyapatite Codoped with Eu³⁺ and Bi³⁺ Ions—A Novel Strategy for Bone Regeneration.* *ACS Biomaterials Science & Engineering*, 6, 6148–6160. <https://doi.org/10.1021/acsbiomaterials.0c00824>
(IF = 4.749; MEiN = 140)
- 14) **Sikora, M.**, Marcinkowska, K., Marycz, K., Wiglusz, R. J., & Śmieszek, A. (2019). *The Potential Selective Cytotoxicity of Poly (L- Lactic Acid)-Based Scaffolds Functionalized with Nanohydroxyapatite and Europium (III) Ions toward Osteosarcoma Cells.* *Materials*, 12, 1–20. <https://doi.org/10.3390/ma12223779>
(IF = 3.057; MEiN = 140)
- 15) Tomaszewska, A., & **Sikora, M.** (2019). *The incidence and extraction causes of third molars among young adults in Poland.* *Anthropological Review*, 82, 253–263. <https://doi.org/10.2478/anre-2019-0018>
(IF = -; MEiN = 70)

Wystąpienia konferencyjne:

- 1) Raciborska, A., Marcinkowska, K., Małas, Z., **Sikora, M.**, Weclawek-Tompol, J., Rodriguez-Galindo, C., & Śmieszek, A. (2022). *Comparison of basic cytophysiological features of three cell lines derived from progressive langerhans cell histiocytosis of bone and skin.*
38th Annual Meeting of the Histiocyte Society; 2022; Online; Szwecja. Poster.
- 2) Śmieszek, A., Marcinkowska, K., **Sikora, M.**, Pielok, A., Valihrach, L., & Marycz, K. (2021). *Obesity-induced changes in metabolism of equine endometrial multipotent stromal cells are ameliorated by seminal extracellular vesicles.*
Precision Diagnostics Europe; 2021; Online; Czechy. Wystąpienie ustne.
- 3) Pielok, A., Marcinkowska, K., **Sikora, M.**, Kucharczyk, K., Marycz, K., & Śmieszek, A. (2019). *The osteogenic effect of zirconium dioxide (ZrO₂) coatings on pre-osteoblastic cell line (MC3T3) characterized by lowered expression of miR-21.*

National Scientific Conference „Science and Young Researchers”, III edition; 2019; Łódź, Polska. Poster.

- 4) **Sikora, M.** (2019). *Cytotoksyczność biomateriałów nanohydroksyapatytowych względem wybranych linii komórkowych kostniakomięsa.*
IV Interdyscyplinarna Konferencja Nano(&)BioMateriały od teorii do aplikacji; 2019; Toruń, Polska. Wystąpienie ustne.
- 5) **Sikora, M.** (2019). Biodegradowalne biomateriały funkcjonalizowane nanohydroksyapatytem i jonami europu, jako matryce modulujące aktywność metaboliczną i transkrypcyjną komórek kostniakomięsa.
Konferencja „Biofuzje”; 2019; Warszawa, Polska. Poster.
- 6) Krajewska, K., **Sikora, M.**, Urbaniak, N., & Śmieszek, A. (2018). *Ocena ekspresji mRNA dla wybranych białek morfogenetycznych kości (BMP2, BMP7) i ich receptorów w liniach komórkowych kostniakomięsa.*
Konferencja „Młody Erudyta – Nauki Interdyscyplinarne”; 2018; Wrocław, Polska. Wystąpienie ustne.
- 7) **Sikora, M.**, Urbaniak, N., Krajewska, K., & Śmieszek, A. (2018). *Cytotoksyczność biomateriałów polilaktydowych opartych o nanohydroksyapatyt i funkcjonalizowanych europem względem wybranych linii kostniakomięsa*
Konferencja „Młody Erudyta – Nauki Interdyscyplinarne”; 2018; Wrocław, Polska. Wystąpienie ustne.
- 8) Urbaniak, N., Śmieszek, A., Krajewska, K., & **Sikora, M.** (2018). *Profil ekspresji miR-21-5p, 124-3p oraz 320-3p w komórkach zaangażowanych w regenerację tkanki kostnej.*
Konferencja „Młody Erudyta – Nauki Interdyscyplinarne”; 2018; Wrocław, Polska. Wystąpienie ustne.

Staże, kursy i szkolenia:

- 1) “Kurs przeznaczony dla osób planujących doświadczenia, wykonujących procedury i uśmiercających zwierzęta”; Polskie Towarzystwo Nauk o Zwierzętach Laboratoryjnych (PolLASA); Online; 05-21.07.2021.
- 2) „RNA-Seq Data Analysis Workshop”, ecSeq Bioinformatics GmbH; Lipsk, Niemcy; 21-24.09.2020.

- 3) Staż naukowy w Katedrze Biologii Eksperymentalnej oraz w Instytucie Niskich Temperatur i Badań Strukturalnych PAN we Wrocławiu w ramach prac badawczych w projekcie OPUS 10; 01.07.2018 – 31.07.2019.

Udział w projektach badawczych:

- 1) **Opus 22:** „*Badania nad mikrobiologicznym mechanizmem zwiększania produkcji biometanu z bioodpadów przez typowe materiały węglowe*”. Grant finansowany przez: Narodowe Centrum Nauki. Nr 2021/43/B/ST8/01924. Stypendysta.
- 2) **RegBone:** „*Ocena skuteczności i bezpieczeństwa zastosowania regorafenibu u pacjentów z opornymi na leczenie pierwotnymi nowotworami kości (REGBONE)*”. Grant finansowany przez: Agencja Badań Medycznych. Nr 2021/ABM/01/00019. Stypendysta.
- 3) **PolHisto:** „*Optymalizacja postępowania oraz leczenia małoletnich pacjentów z rozrostami z komórek histiocytarnych – pierwsze polskie niekomercyjne badanie kliniczne POL HISTIO*”. Grant finansowany przez: Agencja Badań Medycznych. Nr 2019/ABM/01/00016. Stypendysta.
- 4) **Harmonia 9:** „*Nowe, dwustopniowe rusztowania na bazie nanoapatytu wapnia (nHAP) inkorporowanego nanotlenkami żelaza (Fe₂O₃/Fe₃O₄) z funkcją kontrolowanego uwalniania miRNA w statycznym polu magnetycznym do regeneracji złamań kostnych u pacjentów osteoporotycznych*.” Grant finansowany przez: Narodowe Centrum Nauki. Nr 2017/26/M/NZ5/01184. Stażysta.
- 5) **Opus 18:** „*Rola i potencjał terapeutyczny białka wiążącego hormony płciowe (SHBG) w przebiegu insulinooporności, zapalenia, lipotoksyczności w komórkach progenitorowych tkanki tłuszczowej oraz w adipocytach u klaczy z zespołem metabolicznym (EMS)*”. Grant finansowany przez: Narodowe Centrum Nauki. Nr 2019/35/B/NZ7/03651. Stażysta.
- 6) **Opus 15:** „*Inhibicja fosfatazy tyrozynowej jako strategia uwrażliwiania na insulinę poprzez aktywację autofagii chaperonowej oraz wyciszenie odczynu zapalnego i stresu komórkowego wątroby koni z syndromem metabolicznym (EMS)*”. Grant finansowany przez: Narodowe Centrum Nauki. Nr 2018/29/B/NZ7/02662. Stażysta.
- 7) **Opus 10:** „*Otrzymywanie i badania biokompozytów na bazie nanopatyków przeznaczonych do teranostyki*”. Grant finansowany przez: Narodowe Centrum Nauki. Nr 2015/19/B/ST5/01330. Stażysta.

- 8) **Innowacyjny Doktorat:** „*Rola osi lncDANCRI - miR-21-5p na rozwój osteoporozy u osób z insulinoopornością*”. Grant finansowany przez Uniwersytet Przyrodniczy we Wrocławiu. Nr N070/0006/21. Kierownik / wykonawca.
- 9) **Bon Doktoranta:** „*Znaczenie cząsteczki CAS15 w chorobach układu kostnego*”. Grant finansowany przez Uniwersytet Przyrodniczy we Wrocławiu. Nr N020/0017/20. Kierownik / wykonawca.

9. Oświadczenia

Oświadczenia wyjaśniające rolę Autora w publikacjach naukowych będących podstawą niniejszej pracy doktorskiej.

Mateusz Sikora

imię i nazwisko

Wrocław, 01.09.2023r

miejsowość i data

Uniwersytet Przyrodniczy we Wrocławiu,
Wydział Biologii i Hodowli Zwierząt,
Katedra Biologii Eksperymentalnej,
ul. Norwida 27B, 50-375 Wrocław
afiliacja

OŚWIADCZENIE

Oświadczam, że w pracy: **Sikora, M.**, Marycz, K., & Śmieszek, A. (2020). *Small and Long Non-coding RNAs as Functional Regulators of Bone Homeostasis, Acting Alone or Cooperatively*. *Molecular Therapy-Nucleic Acids*, 21, 792–803. <https://doi.org/10.1016/j.omtn.2020.07.017> mój udział polegał na zaplanowaniu układu manuskryptu, przeglądzie literatury będącej podstawą pracy przeglądowej, zaprojektowaniu grafik wyjaśniających opisywane procesy molekularne oraz przygotowaniu manuskryptu i dyskusji z recenzentami.

08.09.23r. Sikora

data i podpis

Potwierdzam treść oświadczenia.

Podpisane elektronicznie przez Krzysztof
Mariusz Marycz (Certyfikat kwalifikowany)
w dniu 2023-09-04.

data i podpis promotora

Mateusz Sikora

imię i nazwisko

Wrocław, 01.09.2023r

miejsowość i data

Uniwersytet Przyrodniczy we Wrocławiu,

Wydział Biologii i Hodowli Zwierząt,

Katedra Biologii Eksperymentalnej,

ul. Norwida 27B, 50-375 Wrocław

afiliacja

OŚWIADCZENIE

Oświadczam, że w pracy: Śmieszek, A., Marcinkowska, K., Pielok, A., **Sikora, M.**, Valihrach, L., & Marycz, K. (2020). *The Role of miR-21 in Osteoblasts-Osteoclasts Coupling In Vitro*. Cells, 9, 1–21. <https://doi.org/10.3390/cells9020479> mój udział polegał na przeprowadzeniu analiz opartych o techniki biologii molekularnej, ze szczególnym uwzględnieniem analiz RT-qPCR (ocena ekspresji wybranych genów) wraz z ewaluacją i interpretacją uzyskanych wyników, a także pomoc w przygotowaniu manuskryptu.

01.09.23r. Sikora

data i podpis

Potwierdzam treść oświadczenia.

Podpisane elektronicznie przez
Krzysztof Mariusz Marycz (Certyfikat
kwalifikowany) w dniu 2023-09-04.

data i podpis promotora

Mateusz Sikora

imię i nazwisko

Wrocław, 01.09.2023r

miejsowość i data

Uniwersytet Przyrodniczy we Wrocławiu,

Wydział Biologii i Hodowli Zwierząt,

Katedra Biologii Eksperymentalnej,

ul. Norwida 27B, 50-375 Wrocław

afiliacja

OŚWIADCZENIE

Oświadczam, że w pracy: **Sikora, M., Śmieszek, A., & Marycz, K. (2021). Bone marrow stromal cells (BMSCs CD45-/CD44+/CD73+/CD90+) isolated from osteoporotic mice SAM/P6 as a novel model for osteoporosis investigation. Journal of Cellular and Molecular Medicine, 25, 6634–6651. <https://doi.org/10.1111/jcmm.16667>** mój udział polegał na przygotowaniu planu doświadczenia, samodzielnym przeprowadzeniu eksperymentów i wykonaniu wszystkich analiz opartych o techniki biologii molekularnej (izolacja komórek, prowadzenie hodowli komórkowych oraz ich różnicowanie, RT-qPCR, Western Blot, mikroskopia świetlna i konfokalna, testy kolorymetryczne, analizy oparte o cytometrię przepływową), a także na interpretacji uzyskanych wyników i przygotowaniu wszystkich tablic wynikowych. Mój udział polegał także na przygotowaniu manuskryptu oraz na polemice z recenzentami.

08.09.23r. Sikora

data i podpis

Potwierdzam treść oświadczenia.

Podpisane elektronicznie przez
Krzysztof Mariusz Marycz
(Certyfikat kwalifikowany) w dniu
2023-09-04.

data i podpis promotora

Mateusz Sikora

imię i nazwisko

Wrocław, 01.09.2023r

miejsowość i data

Uniwersytet Przyrodniczy we Wrocławiu,

Wydział Biologii i Hodowli Zwierząt,

Katedra Biologii Eksperymentalnej,

ul. Norwida 27B, 50-375 Wrocław

afiliacja

OŚWIADCZENIE

Oświadczam, że w pracy: **Sikora, M., Śmieszek, A., Pielok, A., & Marycz, K. (2023). *MiR-21-5p regulates the dynamic of mitochondria network and rejuvenates the senile phenotype of bone marrow stromal cells (BMSCs) isolated from osteoporotic SAM/P6 mice.* Stem Cell Research & Therapy, 14, 1–20. <https://doi.org/10.1186/s13287-023-03271-1>** mój udział polegał na przygotowaniu planu doświadczenia i abstraktu graficznego, samodzielnym przeprowadzeniu eksperymentów i wykonaniu wszystkich analiz opartych o techniki biologii molekularnej (izolacja komórek, prowadzenie hodowli komórkowych, różnicowanie komórek i ich transfekcja, RT-qPCR, mikroskopia świetlna i konfokalna, SEM-EDX, analiza morfologii mitochondriów, analiza zwapnienia macierzy zewnątrzkomórkowej, analizy cytometryczne). Asystowałem w trakcie przeprowadzania eksperymentów *in vivo* oraz analiz opartych o mikrotomografię komputerową. Mój udział polegał na interpretacji uzyskanych wyników i przygotowaniu wszystkich tablic wynikowych. Byłem również odpowiedzialny za przygotowanie manuskryptu oraz za rozbudowaną polemikę z recenzentami pracy.

08.09.23r. Sikora

data i podpis

Potwierdzam treść oświadczenia.

Podpisane elektronicznie przez
Krzysztof Mariusz Marycz (Certyfikat
kwalifikowany) w dniu 2023-09-04.

data i podpis promotora

10. Publikacje

Publikacje naukowe wchodzące w skład pracy doktorskiej.

Small and Long Non-coding RNAs as Functional Regulators of Bone Homeostasis, Acting Alone or Cooperatively

Mateusz Sikora,¹ Krzysztof Marycz,^{2,3} and Agnieszka Smieszek¹

¹Department of Experimental Biology, Faculty of Biology and Animal Science, University of Environmental and Life Sciences Wrocław, Norwida 27B Street, 50-375 Wrocław, Poland; ²International Institute of Translational Medicine, Jesionowa 11 Street, 55-124 Malin, Poland; ³Collegium Medicum, Institute of Medical Science, Cardinal Stefan Wyszyński University (UKSW), Wóycickiego 1/3, 01-938 Warsaw, Poland

Emerging knowledge indicates that non-coding RNAs, including microRNAs (miRNAs) and long-noncoding RNAs (lncRNAs), have a pivotal role in bone development and the pathogenesis of bone-related disorders. Most recently, miRNAs have started to be regarded as potential biomarkers or targets for various sets of diseases, while lncRNAs have gained attention as a new layer of gene expression control acting through versatile interactions, also with miRNAs. The rapid development of RNA sequencing techniques based on next-generation sequencing (NGS) gives us better insight into molecular pathways regulated by the miRNA-lncRNA network. In this review, we summarize the current knowledge related to the function of miRNAs and lncRNAs as regulators of genes that are crucial for proper bone metabolism and homeostasis. We have characterized important non-coding RNAs and their expression signatures, in relationship to bone. Analysis of the biological function of miRNAs and lncRNAs, as well as their network, will pave the way for a better understanding of the pathogenesis of various bone disorders. We also think that this knowledge may lead to the development of innovative diagnostic tools and therapeutic approaches for bone-related disorders.

Bone disabilities are prevalent across the life-course and affect the skeletal system. Predominantly, they can be a result of degenerative conditions, trauma, developing cancers, and infections associated with inflammations. Consequently, modern strategies of bone repair have been intensively developed, especially in terms of osteogenic and bone turnover molecular markers.¹ The proper recognition of molecular mechanisms engaged in the development of metabolic bone diseases and bone cancers is crucial for development of new treatment options. Many are commonly available, including palbociclib, which is aimed at silencing cyclin-dependent kinase (CDK)4 and CDK6 in breast cancer treatment.² However, numerous treatment methods based on molecular pathways still remain under investigation.

Recently, non-coding RNAs, including small non-coding RNAs (i.e., microRNAs [miRNAs]) and long non-coding RNAs (lncRNAs) have gained recognition as another epigenetic layer of regulation in many tissues, including bone. The biomarker validity of both circulating

and endogenous non-protein-coding RNAs is of great importance in bone-related diseases and disorders, such as osteoporosis (OP), rheumatoid arthritis (RA), or osteosarcoma (OS).³ miRNAs, as well as lncRNAs, are considered to be important regulators of gene expression. Their ability to function as key players in the development of pathological conditions has been discussed for many years. Therefore, the high degree of involvement of non-coding RNAs in transcriptional activity is closely related to their use as prognostic and diagnostic factors. Despite recent advances in non-coding RNA studies, the biology of these molecules still remains unclear.⁴ High-throughput technologies, e.g., next-generation sequencing (NGS), have led to the expansion of the understanding of the non-coding RNA world. The proper combination of multidisciplinary and interdisciplinary approaches has proven essential in revealing the complexity of the non-coding RNAs network and to support establishing the importance of their regulatory existence.⁵

The aim of this review is to highlight the connection between miRNAs and lncRNAs, which is clearly observed in the course of osteogenesis. Both miRNA and lncRNA have potential as diagnostic and prognostic markers, and thus growing evidence indicates that they can be considered as therapeutic targets in bone-related diseases. The clinical value and roles of non-coding RNAs are increasing, especially in the field of regenerative medicine. In this review, we emphasize emerging potential of non-coding RNAs as markers of bone turnover in commonly occurring bone-related diseases, such as osteoporosis, RA, and bone cancers (OS). In this review, we describe the role of several miRNAs, classified as osteo-miRs. The review summarizes the current knowledge about the function of *miR-21-5p* (*miR-21*), *miR-124-3p* (*miR-124*), *miR-203-3p* (*miR-203*), and *miR-223-3p* (*miR-223*) in bone biology. Moreover, we provide information about the role of several lncRNAs closely connected with bone metabolism. We described the function of differentiation

<https://doi.org/10.1016/j.omtn.2020.07.017>

Correspondence: Agnieszka Smieszek, Department of Experimental Biology, Faculty of Biology and Animal Science, University of Environmental and Life Sciences Wrocław, Norwida 27B Street, 50-375 Wrocław, Poland.
E-mail: agnieszka.smieszek@upwr.edu.pl



antagonizing non-protein-coding RNA (*DANCR*), taurine upregulated gene 1 (*TUG1*), metastasis-associated lung adenocarcinoma transcript 1 (*MALAT1*), and HOX transcript antisense intergenic RNA (*HOTAIR*) in order to indicate their actual therapeutic potential. Non-coding RNAs presented in the review are widely considered to be important markers affecting proper bone homeostasis in the described bone diseases.

Additionally, we have presented current information regarding crosstalk between selected miRNAs and lncRNAs, indicating their important role as regulators of molecular pathways during osteogenesis.

As of the time of this writing, only 27 original studies were identified by a literature search in PubMed's collection of articles that are related to non-coding RNA networks. The combined search terms were "lncRNA" and "miRNA" and "network" and "bone." To date, no review study has been published that referred to all of the assumed requirements. For this reason, in this review we decided to place an emphasis on the connections linking non-coding RNAs and putative mRNAs, which are essential for proper bone metabolism. In this review, we have pointed out non-coding RNAs that have gained attention as potential biomarkers of bone development or future therapeutic targets.

Biological Functions of Non-coding RNAs

Biology of miRNA

miRNAs (miRs) are small endogenous non-coding molecules, 19–25 nt in size. Their main function is regulation of post-transcriptional silencing of target genes. A single miRNA can target many mRNAs and influence the expression of hundreds of genes involved in functional signaling pathways essential for the survival, proliferation, or differentiation of cells.⁶ For example, *miR-15a* and *miR-16-1* are considered to be crucial molecules that inhibit cyclin D expression and suppress OS progression.⁷ It was proven that miRNAs regulate the expression not only of mRNA, but also other non-coding RNAs such as lncRNAs. For instance, it has been demonstrated that *miR-125b* expression is negatively correlated with *MALAT1* expression. Furthermore, the *HCA1* transcript level is highly associated with *miR-1* activity, due to a binding region for *miR-1* in the *HCA1* structure.⁸ The well-known mechanism of miRNA action reduces the expression of targeted mRNAs. The miRNAs, due to their complementarity to the sequence of mRNAs, are able to interact with them and regulate their expression. The most well-described mechanism of miRNA-mRNA interaction is via the 3' UTR region of target mRNAs, resulting in suppressed expression. Moreover, the interaction of miRNAs with other regions, such as the 5' UTR, coding sequence, and gene promoters, has also been noted.⁹ It has been shown that miRNA interaction with the promoter region may induce transcription in certain conditions.¹⁰ The described modes of miRNA-mRNA interactions are still being studied in order to depict their functional significance.

Single miRNAs may have a plethora of effects and can be regarded as pleiotropic molecules. For example, *miR-21* is a regulator of many

genes, inducing tumorigenesis, and thus is often considered to be a major onco-miR. At the same time, it is an important molecule regulating pro-osteogenic genes, facilitating the proliferation and differentiation of osteoblast precursors.^{11,12} The levels of miRNAs are regulated by mechanisms similar to other RNAs such as transcriptional activation and inhibition, epigenetic repression, and degradation. It has been proven that a miRNA expression profile changes, depending on the physiological state of the organism.¹³ Therefore, they are often used as diagnostic markers, alone or with other molecules, including mRNAs. For instance, tremendous metastatic potential of tumors is associated with a high *miR-21* level and correlates with elevated expression of cyclin D, which plays a key role during cancer cell proliferation. It is therefore a valuable prognostic marker associated with a poor prognosis.⁷

In the canonical miRNA biogenesis pathway, miRNA genes are transcribed by Pol II (polymerase II). The long primary transcripts have a local hairpin structure where the miRNA sequence is embedded. In humans, many canonical miRNAs are encoded within introns of coding and non-coding transcripts. However, some miRNAs are encoded within exonic regions.^{9,14} After transcription, the primary miRNA (pri-miRNA) is matured by a nuclear microprocessor consisting of an RNase III Drosha and a DGCR8 cofactor. The essential role of miRNA during an organism's development has been proven, because deficiency of RNase III Drosha/DGCR8 causes lethality in early embryogenesis.¹⁴ Following Drosha processing, the created pre-miRNA is exported to the cytoplasm through exportin 5 (XPO5) and forms a transcript complex with guanosine triphosphate (GTP)-binding nuclear protein. In the cytoplasm, pre-miRNA is cleaved by Dicer (RNase III endonuclease). This processing involves the removal of the terminal loop, resulting in small RNA duplex creation. Furthermore, the duplex generated by Dicer is loaded onto a protein called AGO (Argonate). This complex is known as RISC (RNA-induced silencing complex).^{9,14} Meanwhile, the passenger strand of the miRNA duplex is degraded and an active single guide strand recognizes the mRNA transcript. This specific binding inhibits translation and promotes the degradation of mRNA targets.¹⁵ The biogenesis of miRNA may also occur by alternate, non-canonical pathways, including both DROSHA-independent and DICER independent processes; however, the role of non-canonical miRNAs in bone biology is not well described.¹⁶

Furthermore, miRNAs are released into the bloodstream, in part through active secretion. About 90% of extracellular miRNAs are bound to AGO proteins, and only 10% are packed in apoptotic bodies, exosomes, or high-density lipoprotein (HDL).¹⁷ Circulating miRNAs actively regulate bone metabolism and thus can be regarded as "fingerprints" for many bone-related diseases, such as osteoporosis or bone tumors.^{17,18} Circulating miRNAs are effectively detectable in liquid biopsies, including plasma, serum, and urine. These are minimal or even non-invasive sources of biomarkers with great potential for diagnostics and clinic application, because circulating miRNAs are more stable in fluids. However, the levels of circulating miRNA are lower than those found in tissues and cells. Nevertheless, liquid

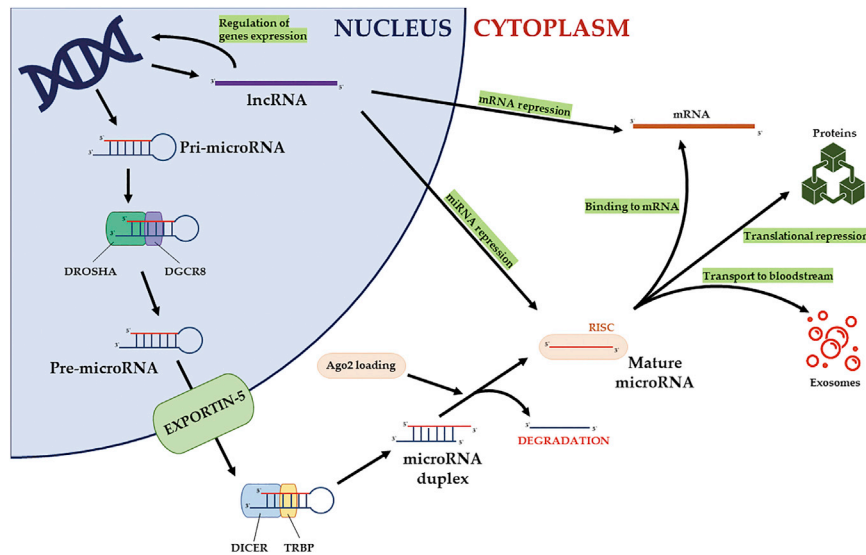


Figure 1. The Biogenesis and Mechanisms of Action of Non-protein-Coding RNAs (miRNAs and lncRNAs)

The schema of miRNA expression shows the canonical pathway of miRNA biogenesis. Additionally, there is demonstrated crosstalk between miRNA and lncRNA that ensures the variable concentration of non-coding RNAs.

gens, and have been indicated as crucial regulators of various developmental pathways during organogenesis.²⁰ For example, it was shown that lncRNAs are a vital regulator of osteogenesis induced in a progenitor derived from a mesenchymal lineage.²¹ However, lncRNAs are also identified as essential regulators of many pathological processes such as osteoporosis or osteoarthritis.²² Accumulating evidence has demonstrated that dysregulation of lncRNAs

biopsies as a source stable and reliable markers gives a huge advantage in terms of treatment of bone diseases in which biopsy may be problematic.¹⁹

Given the fact that miRNAs are engaged in the progression of many human diseases, they are a significant potential diagnostic and prognostic factor. Moreover, recent technological advances have contributed to the significant growth of miRNA validity and enhanced strategies of miRNA-dependent therapies.

Biology of lncRNAs

lncRNAs are a family of long (200–100,000 nt long) transcripts with very low protein-coding potential and a structure similar to mRNA. However, some lncRNAs can encode short peptides. Transcripts derived from lncRNAs constitute 4%–9% of the mammalian genome, in comparison to protein-coding sequences, which are 1% of the genome.⁴ Recent studies have shown that lncRNAs play a crucial role in developmental processes and that they are responsible for nuclear chromatin structure regulation as well as gene expression. Nonetheless, there are also opinions that lncRNAs are transcriptional noise and a by-product of RNA Pol II transcription.⁴ The expressed amount of different lncRNAs varies in different tissues, indicating that they are tissue-specific molecules, similarly to miRNAs. Furthermore, the general amount of expressed lncRNAs in every cell is lower than the quantity of miRNA transcripts. Moreover, interspecies homology of lncRNA sequences is relatively low compared to miRNAs. Nevertheless, a certain degree of conservation in the promoter region and exon area of lncRNAs is observed, which suggests that these molecules are biologically significant.⁴ lncRNAs are quite often abundantly expressed in a controlled manner in cells, which have open and active chromatin, such as stem or progenitor cells.²⁰ lncRNAs have been found to be highly expressed in embryonic stem cells, regulating their renewal, differentiation, and pluripotent state. Moreover, lncRNAs are expressed in a controlled manner, similarly to morpho-

is an important component in the gene regulatory networks during the development and progression of cancer. Thus, lncRNAs are being considered as potential targets in terms of cancer treatment, or biomarkers with diagnostic and prognostic potential.²³

The mechanism of lncRNA action is highly complex and has not yet been fully understood, due to initial knowledge about this type of RNA. It is thought that lncRNAs affect mRNA functionality through various pathways. It was proved that lncRNAs participate in gene expression patterns at the transcriptional and post-transcriptional levels.²⁴ First, lncRNAs can recruit a chromatin remodeling complex to specific sites and regulate the expression process. Second, lncRNAs can regulate transcriptional expression through blocking the promoter region, interacting with RNA-binding proteins, or regulating the activity of transcription factors. Moreover, lncRNAs can form double-stranded RNA complexes with mRNA at the post-transcriptional level.⁴

Many efforts are being made in terms of clarification of the biological function of lncRNAs, both as a regulator of essential developmental pathways and as regulators of tumorigenesis. In this review, we summarize the knowledge regarding the function of lncRNAs as pro-osteogenic factors (Figure 1).

The Role of Selected Non-coding RNAs in Bone Biology and Disease Pathogenesis

The maintenance of bone homeostasis is preserved by the activity of non-protein-coding RNAs. Both miRNAs and lncRNAs are extremely important factors that lead to proper cell functionality by affecting the expression of crucial genes.^{13,23} However, the supportive roles of several molecules have been explored more extensively. Apparently, this is a result of certain dependencies that link these non-coding RNAs into clear and well-established signaling pathways essential for the maintenance of homeostasis. Moreover, researchers

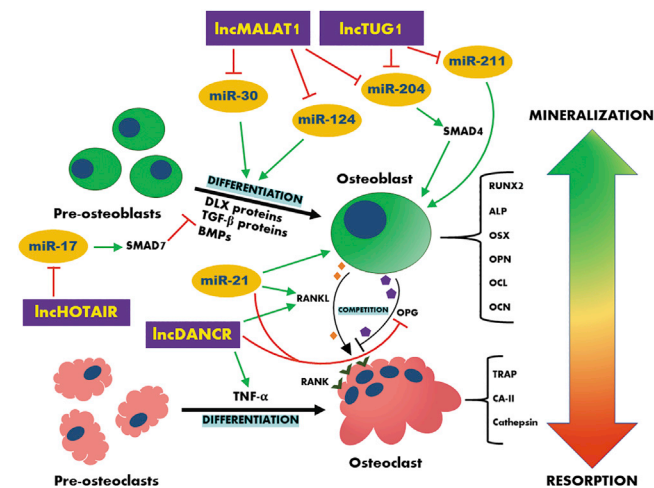


Figure 2. The Crosstalk between Selected lncRNAs, MicroRNAs, and Their Targets in Bone

Attention was paid to cell differentiation and coupling mechanism between osteoblasts and osteoclasts. Moreover, the presented signaling pathways place an emphasis on the regulating mechanisms between lncRNAs, miRNAs, and targeted mRNAs. The examined pathways indicate the close relationships between all of the presented molecules in maintaining bone homeostasis. Non-coding RNAs regulate differentiation of progenitor cells and promote survival of both osteoblasts and osteoclasts. Green arrows indicate a positive impact (elevated expression), red arrows indicate a negative connection (reduced expression).

have started to pay attention to the specific crosstalk between lncRNAs, miRNAs, and targeted mRNAs. More recent studies have started to show the great importance of specific non-coding RNAs and their relationship with regulated genes.^{23,24} Additionally, it has been proven that miRNAs significantly modulate mRNA expression, while lncRNAs are responsible for the functioning of both miRNAs and mRNAs.

The essential functions of *miR-21* and *miR-124* in bone tissue turnover were previously described in detail.^{25,26} This pair of miRNAs works in an opposite way and takes part in bone-dependent disease progression. *miR-21* is known from its engagement in the process of osteogenic differentiation of bone marrow-derived mesenchymal stem cells (BMSCs), as well as maintaining proper bone remodeling. However, it can also contribute to the development of bone neoplasms. In contrast, *miR-124* leads to aggressive osteoclast invasion, which leads to active bone resorption and bone metabolism disorders, such as osteopenia or osteoporosis. Furthermore, the potential osteogenesis modulatory abilities of *miR-203* and *miR-223* remain under investigation and need to be clarified in subsequent experimental analyses. This pair of miRNAs actively participates in both processes, i.e., bone mineralization and bone resorption; however, the regulatory roles of these molecules remain unclear. Furthermore, *TUG1*, *MALAT1*, and *HOTAIR* are lncRNAs that are among the important regulators of tumorigenesis.²¹ They are regarded as future molecular targets with extremely high prognostic and diagnostic potential. In addition, the lncRNA *DANCR* is known for its essential engagement

into the bone turnover dysregulation that leads to systemic bone disorder development, e.g., osteoporosis (Figure 2).⁴

The mechanisms of action of these molecules strictly refer to bone-related disorders, and for that reason they are broadly described in this review. Data referring to the molecular network of presented molecules is also provided.

miR-21

The role of *miR-21* as a molecule regulating osteogenesis has been widely investigated, due to an important connection between *miR-21* expression and development of bone disorders, such as osteoporosis, osteoarthritis, or bone cancers. The role of *miR-21* has been tested using various osteoprogenitor cells. For example, it was shown that *miR-21* promotes the level of osteogenic differentiation and increases matrix mineralization in osteogenic cultures of mouse pre-osteoblasts, i.e., the MC3T3-E1 cell line. The study showed that *Smad7*, which inhibits transforming growth factor β (TGF- β) signaling, is a direct target of *miR-21* in MC3T3-E1 cells. Similarly, it was shown that *miR-21* is crucial for mineralization capability of BMSCs, and that this process is also regulated by the Smad7-Smad1/5/8-runt-related transcription factor 2 (Runx2) pathway. Our recent data showed complex engagement of *miR-21* in the process of osteoblast-osteoclast coupling.²⁵ We have confirmed previous studies showing that inhibition of *miR-21* expression in MC3T3-E1 cells causes a decrease in mRNA expression of crucial osteogenic markers, such as osteocalcin (Ocl), osteopontin (Opn), collagen type I, and Runx2. Furthermore, we confirmed that MC3T3-E1 cells with lowered expression of *miR-21* did not support the osteoclastogenesis process, which might be related to the fact that its targets, such as Opn or receptor activator of nuclear factor κ B ligand (RANKL), are regulated in a dynamic manner in the process of osteogenesis.²⁵

Other studies conducted with the use of MSCs have shown similar close dependencies. In human BMSCs (huBMSCs) the elevated expression of *miR-21* affects the overexpression of typical osteogenic markers, such as *RUNX2* or osteonectin (OCN).^{27,28} Additionally, the key targets of *miR-21*, including SRY-box 2 (*SOX2*), one of the four genes promoting induced pluripotent stem cells (iPSCs), and sprout homolog 2 (*SPRY2*), negatively regulate the extracellular signal-regulated kinase-mitogen-activated protein kinase pathway.²⁷ Furthermore, the overexpression of *miR-21* can repress the expression of interleukin (IL)-6 and IL-8, which are involved in the Wnt signaling pathway. Moreover, Wnt signaling is highly engaged in cell commitment and maintenance of bone homeostasis. Therefore, therapy based on *miR-21* delivery could simultaneously relieve the symptoms of RA.^{29,30}

In contrast, *miR-21* plays a vital role in FLS (fibroblast-like synovio-cyte) invasiveness and significantly affects the expression of matrix metalloproteinases. Moreover, the inhibition of *miR-21* activity downregulates the expression of TGF- β and *Smad5* but increases the *Smad7* transcript levels.³⁰ Thus, inhibition of *miR-21* could serve as a favorable therapeutic target diminishing FLS metabolic activity

and lowering the symptoms of joint diseases. Moreover, *miR-21* seems to be a crucial factor that affects the expression of pro-inflammatory cytokines, both *in vitro* and *in vivo* during periodontitis.³¹

miR-21 is commonly known as an oncomiR and is significantly overexpressed in many cancers, including OS.¹¹ The high level of *miR-21* is correlated with initial metastasis, poor response to neoadjuvant chemotherapy, and reduced overall survival rate.³² The expression of *miR-21* is also positively correlated with the presence of lung metastases in OS patients. Therefore, it can serve as a potential biomarker for the early diagnosis of OS and considered to be a future anti-cancer target.^{32,33}

Bearing in mind the significance of *miR-21* in bone homeostasis maintenance, novel kinds of molecular therapy have been developed. *miR-21* can be used not only as diagnostic factor in cancer therapy, but especially as an important therapeutic target in many bone diseases. Modern methods based on targeted *miR-21* inhibition can improve the effectiveness of common anti-cancer therapies and increase the survivability of patients.^{34,35} Furthermore, the targeted delivery of *miR-21* can produce excellent results in the regeneration of bone fractures.^{36,37}

miR-124

miR-124 is a highly conserved miRNA, and it is overexpressed in many cancers, such as breast cancer, gastric cancer, or glioblastoma.³⁸ Other reports have demonstrated that *miR-124* has a strong inhibitory effect on various human neoplasms, such as gliomas, sarcomas, or liver cancers.^{39–41} Researchers have found various roles of *miR-124*, e.g., cell cycle arrest, epithelial-to-mesenchymal transition (EMT), cancer stem formation, induction of apoptosis, or even metastasis creation. Therefore, it might be regarded as a good target for designing novel anti-cancer therapeutic strategies.³⁸ In bone cancers, *miR-124* is considered to be potential anti-cancer agent for OS treatment, due to suppressing growth and aggressiveness of this cancer cells.^{41,42} Transfection of *miR-124* significantly decreases integrin expression and inhibits OS growth, proliferation, migration, and formation of metastases. It also attenuates OS resistance to various drugs, such as tunicamycin, by downregulation of *P53* and *Bcl-2* genes.⁴¹ Additionally, *miR-124* suppresses TGF- β expression in tumor cells.⁴¹ The inhibition of OS aggressiveness suggests that *miR-124* can be a potential anti-cancer target for OS therapy. Moreover, it was also demonstrated that *miR-124* negatively regulates the process of osteogenesis and proper bone regeneration of BMSCs.⁴³ *miR-124* negatively affects osteogenic differentiation of MSCs and *in vivo* bone formation. It acts as an endogenous attenuator of several genes belonging to the homeobox transcription factor gene family, e.g., *Dlx5*, *Dlx3*, and *Dlx2* expression, by binding the 3' UTRs of these genes.²⁶ The members of the DLX gene family are responsible for bone development and the healing of fractures. For this reason, *miR-124* is considered to be an anti-osteogenic molecular marker. In addition, *miR-124* targets *CDK2* (cyclin-dependent kinase 2) and *MPC-1* (monocyte chemotactic protein-1), which are involved in the inflammatory process in RA.⁴⁴ Previous studies have indicated

that *miR-124* directly targeted osterix (*Osx*) expression. Osterix is expressed by osteoblasts and is predominantly responsible for bone formation and homeostasis by promotion of osteoblast differentiation and maturation.⁴⁵ Therefore, the therapy based on knockdown of *miR-124* would be the most efficient in treatment of both osteoporosis and RA.

Interestingly, the high concentration of *miR-124* downregulates the expression of glycogen synthase kinase 3 β (*GSK-3 β*). This molecule is a significant marker leading to inhibited differentiation of ligament fibroblasts into osteoblasts. Hence, high expression of *miR-124* can accelerate the progression of ankylosing spondylitis, which is connected with spastic and spinal joint disabilities, as well as pathological ossification.⁴⁶

miR-203

miR-203 overexpression is primarily related to downregulation of *Runx2* expression, the key factor in osteogenesis.⁴⁷ Laxman et al.⁴⁸ proved that overexpression of *miR-203* inhibits osteoblast differentiation, whereas inhibition of *miR-203* stimulates alkaline phosphatase (ALP) activity and bone matrix mineralization. It was also shown that *miR-203* negatively regulates *BMP-2* (bone morphogenetic protein 2) expression by suppressing *Dlx5*, which is one of the key factors in bone repair. However, *miR-203* was also found to be essential in the shift from osteogenic differentiation to adipogenic differentiation of BMSCs in postmenopausal osteoporosis. The transfection of *miR-203* led to elevated expression of osteogenic genes such as *Runx2* or *ALP* in osteoporotic samples.⁴⁹ Furthermore, the *miR-203* level is up-regulated in RA-delivered tissues.⁵⁰ Elevated levels of *miR-203* lead to increased secretion of matrix metalloproteinase (MMP)-1 and IL-6 via the nuclear factor κ B (NF- κ B) pathway and in this way activate the phenotype of synovial fibroblasts in RA.⁵¹ Hence, *miR-203* plays the role of a pro-inflammatory and joint-destructive factor in RA. *miR-203* is also associated as a strong tumor suppressor. Huang et al.⁵² have shown that transfection of *miR-203* inhibits TGF- β -induced EMT, migration, and invasive ability in non-small-cell lung cancer by targeting *Smad3*. However, it was also shown that *miR-203*, predominantly associated with EMT, was significantly elevated in plasma samples of ovarian cancer patients.⁵³ Moreover, *miR-203* acts as a strong tumor suppressor in OS cells, regulating *RUNX2* and *RAB22A* expression.^{54,55} Moreover, Liu and Feng (2015) indicated anti-tumor properties of *miR-203* in OS cell lines and tissues. *miR-203* targets TANK binding kinase 1 (*TBK1*), which was found to be upregulated in OS samples.⁵⁶ In this way, *miR-203* may act as a novel molecular target in bone cancer treatments. Furthermore, analyses conducted on rat BMSCs suggested that *miR-203* is highly engaged in downregulation of phosphatidylinositol 3-kinase (PI3K) expression. Hence, it may decrease the PI3K/Akt signaling pathway and impair the viability of BMSCs, an extremely important population of progenitor cells ensuring proper bone metabolism and regeneration.⁵⁷

Nevertheless, bearing in mind the dual and complex nature of *miR-203* in osteogenic differentiation, as well as its significant impact on

the serious progression of metabolic diseases and development of various neoplasms, further in-depth analyses targeted on *miR-203* must be conducted.

miR-223

Moran-Moguel et al.⁵⁸ proved that overexpression of *miR-223* significantly inhibits osteoclastogenesis in osteoporosis patients. *miR-223* promotes osteoblast differentiation of murine MC3T3-E1 cells by regulation of HDAC2 (histone deacetylase 2). HDAC2 acts as a negative regulator of osteogenesis.⁵⁹ However, *miR-223* is additionally engaged in osteoclast differentiation by promotion of CSFR1/M-CSFR expression.¹⁸ On account of the dual effect in stimulating osteoclast differentiation and inhibiting osteoblast differentiation,⁶⁰ the role of *miR-223* as a novel therapeutic target should be further analyzed. In addition, it has been shown that *miR-223* can prevent joint destruction in RA patients, but it is significantly upregulated in serum collected from RA patients, but it is significantly upregulated in patients with anti-TNF therapy.^{61,62} When it comes to bone neoplasms, *miR-223* could be a novel pharmacological marker of OS, due to inhibition of metastasis progression.^{63,64} It was found that *miR-223* decreased the expression of PARP1, CtIP, and Pso4, which are significant components of alternative non-homologous end joining (aNHEJ). In most cells, the high level of *miR-223* represses aNHEJ, decreasing the risk of chromosomal translocation and reducing the probability of the development of malignancy.⁶⁵ However, *miR-223* represents a crucial component of multiple myeloma development. It was shown that the *miR-223* transcript level was upregulated in huBMSCs delivered from multiple myeloma patients. This could be a result of a senescence-like state that is induced by activation of stromal cells by multiple myeloma cells. Moreover, *miR-223* seems to regulate important tumor-supportive cytokines, such as VEGF and IL-6.⁶⁶

lncDANCR

The last evidence suggested that *DANCR* is one of the vital factors involved in the process of cell differentiation. It plays a crucial role in osteogenic differentiation of various types of cells, including stem cells. Furthermore, its contribution to the onset and development of osteoporosis is increasingly recognized. The downregulation of *DANCR* promotes the osteogenic differentiation of human periodontal ligament stem cells and human fetal osteoblastic cells. It has been shown that high expression of *DANCR* suppresses the differentiation of human dental pulp cells (hDPCs) by the Wnt/ β -catenin signaling pathway into odontoblast-like cells. Moreover, upregulation of the *DANCR* transcript level blocked mineralized nodule formation and the expression of crucial odontoblast markers, such as *DMP-1* and *DSPP*.⁶⁷ Additionally, *DANCR* knockdown enhances the levels of mRNA expression of osteogenic marker genes and mineralized matrix deposition in huBMSCs.^{24,68} Silva et al.⁶⁹ have demonstrated that *DANCR* is overexpressed in monocytes in osteoporosis. Importantly, research has shown that media delivered from monocytic cell cultures, which have overexpressed *DANCR*, are characterized by increasing bone-resorbing activity in mouse bone cultures. The high level of this non-coding RNA is related to a significant and sud-

den increase of TNF- α expression, which is one of the most important inflammatory markers. The high expression of TNF- α is predominantly associated with osteoclast differentiation during osteoporosis progression. Furthermore, *DANCR* promotes RANKL-induced osteoclast formation, which also affects the development of osteoporosis.⁶⁹ TNF- α is additionally strongly correlated with the development of RA, and it is called the “top of a pro-inflammatory cascade,” which means that this molecule plays a crucial role in the cytokine network of RA.⁷⁰ Inhibition of *DANCR* expression, for example using antisense molecules blocking the *DANCR* expression, may yield satisfactory results in osteoporosis, as well as RA therapy. Importantly, note that *lncDANCR* is also highly engaged in OS cell proliferation.⁷¹ It binds *miR-33a-5p*, which leads to upregulated expression of AXL (AXL receptor tyrosine kinase). AXL is abnormally expressed in OS patients, regulates tumor cell self-renewal, and indicates a poor prognosis. Additionally, due to AXL upregulation, it enhances expression of proteins in the AXL-Act pathway.⁷¹ This signaling pathway regulates colony formation and EMT of the cancer stem cells (CSCs). On account of these facts, it seems to be a key molecule in many bone pathological pathways, including bone cancers.

lncTUG1

TUG1 is an evolutionary conserved and common lncRNA present in various osteogenically induced MSCs, such as PDLSCs (periodontal ligament stem cells) or TPSCs (tendon stem/progenitor cells).^{72,73} It is considered to be a key factor facilitating the osteogenic differentiation of progenitor cells. It was shown that *TUG1* positively regulates *Runx2* expression by sponging the *miR-204-5p*. Therefore, one of the therapeutic strategies for the treatment of fractures in osteoporotic patients included a combination of pro-*TUG1* and anti-*miR-204* therapy at the same time, as a novel bone recovery approach.²⁴ Sacchetti et al.⁷⁴ have proved the validity of the *miR-204-Runx2* axis, as well as the *miR-211-Runx2* axis, in osteoporosis progression. Investigations carried out on murine MSCs indicated that enforced expression of *miR-204* inhibited osteogenesis and rescue adipogenesis of the cells. The intrinsic properties of MSCs are significantly altered in postmenopausal osteoporotic patients. They are characterized by poor osteogenic capability and increased adipogenic abilities. It is also known that osteoporosis and obesity often occur together.⁷⁵ Therefore, future treatment methods of osteoporosis should be focused not only on elevation of the osteogenic abilities of MSCs, but on their inhibition of adipogenesis as well. Similarly to *miR-204*, the *miR-211* molecule is also negatively associated with *Runx2* expression.⁷⁴ The high levels of these markers are associated with low *Runx2* level and dysregulated osteogenic processes. However, *TUG1* is abnormally overexpressed in OS cells, which pathogenically upregulates the *Runx2* transcript level and promotes the development of OS.^{24,76} Li et al.⁷⁷ indicated that the overexpression of *TUG1* is associated with *miR-132/SOX4* axis dysregulation. Lowered expression of *miR-132-3p* is associated with *TUG1* overexpression, and this has a great impact on *SOX4* upregulation and OS progression. The knockdown of *TUG1* also markedly inhibits the expression of the MET and phosphorylated (p-)AKT signaling pathway, which is revealed by increased apoptosis rate and cell growth suppression in OS cell lines Saos-2 and MG-63.

Additionally, the inhibition of *TUG1* expression significantly reduces the cisplatin resistance of these OS lines.⁷⁸ Furthermore, *TUG1* is associated with poor prognosis for osteoarthritis patients, and the elevated expression of this lncRNA promotes osteoarthritis-induced degradation of chondrocyte extracellular matrix via the *miR-195/MMP-13* axis.⁷⁹

lncMALAT1

The lncRNA *MALAT1* is a molecule predominantly considered to be an important amplifier of osteogenic differentiation of cells. *MALAT1* functions as a sponge molecule of *miR-204-5p* and upregulates the expression of *Smad4* (mothers against decapentaplegic homolog 4). The same sponging abilities against the *miR-204-5p* molecule are shown by *lncTUG1*.²⁴ *Smad4* activation promotes the expression of ALP and Ocl, considered to be essential osteogenic markers. Thus, *MALAT1* promotes bone formation and mineralization. This way, another alternative OP treatment could be based on pro-*lncMALAT1* and anti-*miR-204-5p* therapy.⁴ Moreover, *MALAT1* sponges *miR-30* and promotes osteoblast differentiation of ASCs (adipose tissue-derived MSCs) by significant promotion of *Runx2* expression.⁸⁰ Interestingly, *MALAT1* is responsible for downregulating *miR-124* expression, therefore affecting ALP, *Runx2*, and *Opn* levels and finally promoting osteogenesis of MSCs.⁸¹ The coupling mechanism between *MALAT1* and *miR-124* could be a remarkable and efficient direction for future osteoporosis therapy. Furthermore, *MALAT1* expression was proven to be reduced in synovial tissues of RA patients.⁸² Li et al.⁸² indicated that knockdown of *MALAT1* could stimulate the expression of pro-inflammatory cytokines, including IL-6, IL-10, and TNF- α . *MALAT1* could also suppress the expression of *CTNNB1* and modulate the Wnt signaling pathway. These findings suggest an inhibitory effect of *MALAT1* on the proliferation and inflammation of FLSs, which participate in the pathogenesis of RA, by inhibiting the Wnt pathway. Thus, *MALAT1* is suggested to be a perfect candidate for an OP and RA therapeutic target.

In contrast, in cartilage tissues collected from healthy and osteoarthritis patients, *MALAT1* was shown to be significantly upregulated. Moreover, *MALAT1* inhibits *miR-150-5p* expression, which has a great impact on elevated AKT3 expression. Thus, *MALAT1* is responsible for cartilage cells apoptosis, extracellular matrix degradation, and osteoarthritis development via the *miR-150-5p/AKT3* axis.⁸³ However, it was additionally proven that *MALAT1* promotes the creation of metastases in OS patients.⁸⁴ Upregulation of this molecule is associated with a high expression level of *SOX4* or activation of the Wnt/ β -catenin signaling pathway.^{85,86}

lncHOTAIR

HOTAIR is considered to be a significant diagnostic marker for many neoplasms, including breast cancer, cervical cancer, or colorectal cancer.^{87–89} Moreover, *HOTAIR* is considered to be one of the first tumor-related lncRNAs to have been discovered. It is associated with metastasis development and poor patient prognoses. In OS, *HOTAIR* was detected to be upregulated and coupled with *P53* expression. This indicates *HOTAIR* involvement in the P53-mediated

apoptosis pathway in OS cells.⁹⁰ It has been proved that *HOTAIR* promotes the proliferation and invasion of OS cells by the AKT/mTOR signaling pathway.⁹¹ However, it is also involved in bone regeneration from MSCs.⁴ *HOTAIR* reduces the expression of *miR-17-5p* and elevates the *Smad7* transcript level at the same time, and thus *Smad7* is a target of *miR-17-5p*. *Smad7* is an important factor that reduces osteogenic potential of the bone. Therefore, the knockdown of *HOTAIR* significantly upregulates the expression of *miR-17-5p*, suppresses *Smad7* activity, and finally increases the transcript levels of *Runx2*, collagen 1, and ALP.^{4,92} Furthermore, *HOTAIR* is considered to be an important factor in alleviation of RA. It was noted to be downregulated in lipopolysaccharide (LPS)-treated chondrocytes and RA mice. However, the transfection of *HOTAIR* increased cell proliferation and inhibited inflammation in RA mice. It can play a protective role in RA by regulation of the NF- κ B signaling pathway. *HOTAIR* reduces the expression of *miR-138*, which activates HDAC4/PGRN or HDAC4/NF- κ B signaling.⁹³ It also inhibits the *P65*, *Il-1 β* , and *TNF- α* transcripts,⁹⁴ which participate in the development of RA. In contrast, it has been shown that *HOTAIR* is upregulated in osteoarthritis patients and indicates elevated expression of MMPs, as well as chondrocyte apoptosis. Therefore, the silencing of lncRNA *HOTAIR* could result in better prognoses for osteoarthritis patients.⁹⁵

Table 1 summarizes the involvement of selected non-protein-coding RNAs in the maintenance of bone homeostasis. Their functionality in the course of osteogenesis and tumorigenesis is summarized. Additionally, we mention their targets and examined cell lines (Table 1).

Crosstalk between miRNAs and lncRNAs for Proper Bone Homeostasis

Non-coding RNAs are emerging as critical regulators of processes associated with bone metabolism, able to modulate complex cellular processes. Both miRNAs and lncRNAs act as fine-tuning molecules playing a crucial role in governing the expression of bone-related genes. It has been reported that lncRNAs are species-specific regulators of various metabolic processes. They may function as competing endogenous RNAs (ceRNAs) that can interact with mRNAs by competitively binding their common miRNAs. In bone tissue, non-coding RNAs are responsible for processes that are crucial for proper musculoskeletal system functions, such as bone turnover or tissue regeneration. However, minor shortcomings in the functionality of expanded networks between non-coding RNAs and mRNAs may contribute to pathological changes of the tissue structure. In addition, miRNAs and lncRNAs regulate the proliferation and differentiation of bone-forming and bone-resorbing cells.⁹⁶

lncMALAT1 serves as a sponge for *miR-30* and *miR-124* and elevates the differentiation of osteoblasts. In addition, *MALAT1* inhibits the activity of *miR-204* and thus increases the *Smad4* level, which finally leads to proper osteoblast functionality.^{4,80,81} Furthermore, *miR-204* as well as *miR-211* are blocked by *lncTUG1*.^{24,74} Therefore, *TUG1* serves as a positive factor in osteoblast activity and proper bone mineralization. *lncHOTAIR* sponges *miR-17-5p*, which leads to

Table 1. List of Selected Non-coding RNAs, Their Functions, and Targets

ncRNA	Impact on Osteogenesis	Role in Tumorigenesis	Examined Cell Lines	Targets	References
miR-17-5p	downregulation	oncogene	huASCs, MC3T3-E1, MG-63, U-2 OS, Saos-2, 143B	BRCC2, BMP-2, SMAD7, Wnt/ β -catenin signaling	100-104
miR-21	upregulation downregulation (?)	oncogene	huBMSCs, MC3T3-E1, 4B12, MG-63, U-2 OS, Saos-2, HOS, 143B	SMAD family proteins, RUNX2, OCN, OPN, OCL, COLL-1, MMP-9, OPG, RANKL, RANK, IL-6, IL-8	25,27,29,30,105
miR-124	downregulation	suppressor gene	huBMSCs, MG-63	TGF- β family proteins, DLX family proteins, OSX, CDK2, MPC-1	26,41,43-45
miR-149	downregulation	suppressor gene	raBMSCs, MG-63, U-2 OS, Saos-2, HOS, 143B	ERK/MAPK signaling, SDF-1, PI3K/AKT pathway	106-108
miR-203	upregulation downregulation	suppressor gene	huBMSCs, huH226, MG-63, U-2 OS, Saos-2	RUNX2, DLX5, MMP-1, SMAD3, TGF- β family proteins, IL-6, RAB22A, TBK1	47,49,51,54-56
miR-223	upregulation downregulation	suppressor gene	MC3T3-E1, huBMSCs, 143B, U-2 OS	HDAC2, CSFR1/M-CSFR, CDH6	18,58,59,63,109
lncDANCR	downregulation	oncogene	huBMSCs, human monocytes, 143B	TNF- α , RANKL, miR-33a-5p, miR-216a-5p/SOX5	69,70,110
lncTUG1	upregulation	oncogene	huPDLSCs, huTPSCs, huBMSCs, MG-63, U-2 OS	miR-204, miR-211, miR-132/SOX4, RUNX2,	24,74,77
lncMALAT1	upregulation	oncogene	huASCs, huFLSs huFOB1.19, MG-63, U-2 OS, Saos-2	miR-204, SMAD4, miR-30, miR-124, IL-6, IL-10, TNF- α , CTNBN1	4,81,82
lncHOTAIR	downregulation	oncogene	huBMSCs, huAVICs, MG-63	miR-138, miR-204, miR17-5p/SMAD7 axis, Wnt/ β -catenin signaling, NF- κ B signaling	4,92,94,111
lncH19	upregulation	oncogene	raBMSCs, raEMSCs, MG-63, U-2 OS, Saos-2, HOB	Wnt/ β -catenin signaling, miR-138, miR-149/SDF-1 axis	107,112-115

ERK, extracellular signal-regulated kinase; MAPK, mitogen-activated protein kinase; AVIC, aortic valve interstitial cell.

increased *Smad7* transcript levels. This signaling pathway results in downregulated osteogenic potential of the bone.⁴ *lncDANCR* positively regulates osteoclast differentiation by upregulating *TNF- α* . Furthermore, *DANCR* elevates the RANKL/OPG ratio via sponging *OPG* and downregulating *RANKL*. It leads to upregulated osteoclast activity and facilitates bone resorption.⁶⁹ Moreover, *miR-21* also elevates the RANKL/OPG ratio; however, it is also considered to be a crucial factor that positively affects osteoblast activity and enhances the mineralization of bone tissue.²⁵

Despite the critical driving force of the non-coding RNA network in bone-dependent disease progression, attention is more often paid to single nucleotide polymorphism (SNP), which is a common genetic variation. This is considered to be an important factor that modulates susceptibility to serious diseases, e.g., cancers.⁹⁷ For instance, it has been proven that the SNP of *miR-124a* significantly affects the risk and determines the prognosis of OS.⁹⁸ Moreover, a single miRNA can differ at the 5' or 3' terminus by minor changes. This can result in the formation of isoform of specific miRNA (iso-miR). The numerous variants of single miRNAs could be associated with disease progression; however, more in-depth studies are required to explore iso-miRs as future therapeutic targets.⁹⁹

Conclusions

It is estimated that around 70%–90% of mammalian genomes are transcribed, but the vast majority of transcripts do not code proteins.

The rapid development of molecular biology techniques, especially next-generation sequencing technologies such as RNA sequencing (RNA-seq), makes it possible to verify that non-coding transcripts are not only junk or “transcriptional noise,” but also essential regulators of gene expression. Non-coding RNAs are engaged in many important biological processes, providing a unique regulatory mechanism for genes coding proteins, including morphogens and growth factors, which assure the proper development as well as homeostasis of an organism. There is a great need to explore this enormous world of functional classes of non-coding RNAs. In our opinion, special attention should be devoted to the identification and analysis of crosstalk between miRNAs, lncRNAs, and putative target genes. Evaluation of this functional network is crucial, notably in the view of better understanding of the molecular basis for the pathogenesis of lifestyle diseases, such as osteoporosis and RA. The analysis may also provide novel panels of biomarkers showing prognostic and diagnostic potential for bone-related diseases. Importantly, analysis of miRNA-lncRNA-mRNA crosstalk and networks may disclose new targets and allow the design of better therapies and therapeutic approaches, such as personalized medicine for bone disorders.

In this review, we have presented current knowledge related to the biology and function of miRNAs and lncRNAs that are involved in the process of osteogenesis and may find application as novel biomarkers for bone-related diseases. Several biotypes of non-coding RNAs, including miRNAs and lncRNAs, were identified in the cargo

of extracellular vesicles released to the biological fluids. Thus, non-coding RNAs can act locally (in a paracrine and autocrine manner), as well as on adjacent cells. This is an important biological aspect that allows us to describe full panels of biomarkers, with paramount clinical importance in terms of personalized regenerative medicine for bone. It was shown that *MALAT1* and *TUG1* can serve as vital therapeutic targets, especially for osteoporosis patients. Due to affecting *miR-30*, *miR-124*, *miR-204*, and *miR-211*, presented lncRNAs are significantly engaged in the process of proper bone mineralization. Moreover, *HOTAIR*, by affecting *miR-17-5p* expression, may serve as a remarkable diagnostic and prognostic factor for tumor development and osteoporosis progression. Additionally, *DANCR* can act as another essential therapeutic target, especially for the treatment of bone metabolic diseases. We strongly believe that the presented information on selected non-protein-coding RNA molecules will serve as an important impetus for preclinical investigations.

AUTHOR CONTRIBUTIONS

Concept of the Review, M.S. and AS; Graphical Work, M.S.; Writing – Original Draft, M.S. and A.S.; Writing – Review & Editing, M.S., A.S., and K.M. All authors have read and agreed to the published version of the manuscript.

CONFLICTS OF INTEREST

The authors declare no competing interests.

ACKNOWLEDGMENTS

Substantive and financial support was obtained during the course of the completion of the Harmonia 10 project titled “New, two-stage scaffolds based on calcium nanoapatite (nHAP) incorporated with iron nanotoxides ($\text{Fe}_2\text{O}_3/\text{Fe}_3\text{O}_4$) with the function of controlled release of miRNA in a static magnetic field for the regeneration of bone fractures in osteoporotic patients” (National Science Center (NCN) in Poland grant no. UMO 2017/26/M/NZ5/01184) is gratefully acknowledged. This work was co-financed under the Leading Research Groups support project from the subsidy increased for the period 2020–2025 in the amount of 2% of the subsidy referred to Art. 387 (3) of the Law of 20 July 2018 on Higher Education and Science, obtained in 2019.

REFERENCES

1. Ansari, M. (2019). Bone tissue regeneration: biology, strategies and interface studies. *Prog. Biomater.* 8, 223–237.
2. Turner, N.C., Ro, J., André, F., Loi, S., Verma, S., Iwata, H., Harbeck, N., Loibl, S., Huang Bartlett, C., Zhang, K., et al.; PALOMA3 Study Group (2015). Palbociclib in hormone-receptor-positive advanced breast cancer. *N. Engl. J. Med.* 373, 209–219.
3. Hackl, M., Heilmeier, U., Weilner, S., and Grillari, J. (2016). Circulating microRNAs as novel biomarkers for bone diseases—complex signatures for multifactorial diseases? *Mol. Cell. Endocrinol.* 432, 83–95.
4. Peng, S., Cao, L., He, S., Zhong, Y., Ma, H., Zhang, Y., and Shuai, C. (2018). An overview of long noncoding RNAs involved in bone regeneration from mesenchymal stem cells. *Stem Cells Int.* 2018, 8273648.
5. Jathar, S., Kumar, V., Srivastava, J., and Tripathi, V. (2017). Technological developments in lncRNA biology. *Adv. Exp. Med. Biol.* 1008, 283–323.
6. Lu, T.X., and Rothenberg, M.E. (2018). MicroRNA. *J. Allergy Clin. Immunol.* 141, 1202–1207.
7. Cai, C.-K., Zhao, G.-Y., Tian, L.-Y., Liu, L., Yan, K., Ma, Y.-L., Ji, Z.W., Li, X.X., Han, K., Gao, J., et al. (2012). miR-15a and miR-16-1 downregulate CCND1 and induce apoptosis and cell cycle arrest in osteosarcoma. *Oncol. Rep.* 28, 1764–1770.
8. Mohr, A.M., and Mott, J.L. (2015). Overview of microRNA biology. *Semin. Liver Dis.* 35, 3–11.
9. O'Brien, J., Hayder, H., Zayed, Y., and Peng, C. (2018). Overview of microRNA biogenesis, mechanisms of actions, and circulation. *Front. Endocrinol. (Lausanne)* 9, 402.
10. Dharap, A., Pokrzywa, C., Murali, S., Pandi, G., and Vemuganti, R. (2013). MicroRNA miR-324-3p induces promoter-mediated expression of RelA gene. *PLoS ONE* 8, e79467.
11. Hua, Y., Jin, Z., Zhou, F., Zhang, Y.-Q., and Zhuang, Y. (2017). The expression significance of serum miR-21 in patients with osteosarcoma and its relationship with chemosensitivity. *Eur. Rev. Med. Pharmacol. Sci.* 21, 2989–2994.
12. Li, X., Guo, L., Liu, Y., Su, Y., Xie, Y., Du, J., Zhou, J., Ding, G., Wang, H., Bai, Y., and Liu, Y. (2017). MicroRNA-21 promotes osteogenesis of bone marrow mesenchymal stem cells via the Smad7-Smad1/5/8-Runx2 pathway. *Biochem. Biophys. Res. Commun.* 493, 928–933.
13. Gulyaeva, L.F., and Kushlinskiy, N.E. (2016). Regulatory mechanisms of microRNA expression. *J. Transl. Med.* 14, 143.
14. Ha, M., and Kim, V.N. (2014). Regulation of microRNA biogenesis. *Nat. Rev. Mol. Cell Biol.* 15, 509–524.
15. Stavast, C.J., and Erkeland, S.J. (2019). The non-canonical aspects of microRNAs: many roads to gene regulation. *Cells* 8, 1465.
16. Havens, M.A., Reich, A.A., Duelli, D.M., and Hastings, M.L. (2012). Biogenesis of mammalian microRNAs by a non-canonical processing pathway. *Nucleic Acids Res.* 40, 4626–4640.
17. Foessel, I., Kotzbeck, P., and Obermayer-Pietsch, B. (2019). miRNAs as novel biomarkers for bone related diseases. *J. Lab. Precis. Med.* 4, 2.
18. van Wijnen, A.J., van de Peppel, J., van Leeuwen, J.P., Lian, J.B., Stein, G.S., Westendorf, J.J., Oursler, M.J., Im, H.J., Taipaleenmäki, H., Hesse, E., et al. (2013). MicroRNA functions in osteogenesis and dysfunctions in osteoporosis. *Curr. Osteoporos. Rep.* 11, 72–82.
19. Bottani, M., Banfi, G., and Lombardi, G. (2019). Perspectives on miRNAs as epigenetic markers in osteoporosis and bone fracture risk: a step forward in personalized diagnosis. *Front. Genet.* 10, 1044.
20. Aich, M., and Chakraborty, D. (2020). Role of lncRNAs in stem cell maintenance and differentiation. *Curr. Top. Dev. Biol.* 138, 73–112.
21. Tye, C.E., Boyd, J.R., Page, N.A., Falcone, M.M., Stein, J.L., Stein, G.S., and Lian, J.B. (2018). Regulation of osteogenesis by long noncoding RNAs: an epigenetic mechanism contributing to bone formation. *Connect. Tissue Res.* 59 (Suppl), 35–41.
22. Li, D., Yang, C., Yin, C., Zhao, F., Chen, Z., Tian, Y., Dang, K., Jiang, S., Zhang, W., Zhang, G., and Qian, A. (2020). lncRNA, important player in bone development and disease. *Endocr. Metab. Immune Disord. Drug Targets* 20, 50–66.
23. Jiang, M.-C., Ni, J.-J., Cui, W.-Y., Wang, B.-Y., and Zhuo, W. (2019). Emerging roles of lncRNA in cancer and therapeutic opportunities. *Am. J. Cancer Res.* 9, 1354–1366.
24. Zhang, J., Hao, X., Yin, M., Xu, T., and Guo, F. (2019). Long non-coding RNA in osteogenesis: a new world to be explored. *Bone Joint Res.* 8, 73–80.
25. Smieszek, A., Marcinkowska, K., Pielok, A., Sikora, M., Valihrach, L., and Marycz, K. (2020). The role of miR-21 in osteoblasts-osteoclasts coupling in vitro. *Cells* 9, 479.
26. Qadir, A.S., Um, S., Lee, H., Baek, K., Seo, B.M., Lee, G., Kim, G.S., Woo, K.M., Ryoo, H.M., and Baek, J.H. (2015). miR-124 negatively regulates osteogenic differentiation and in vivo bone formation of mesenchymal stem cells. *J. Cell. Biochem.* 116, 730–742.




27. Valenti, M.T., Dalle Carbonare, L., and Mottes, M. (2018). Role of microRNAs in progenitor cell commitment and osteogenic differentiation in health and disease (Review). *Int. J. Mol. Med.* *41*, 2441–2449.
28. Yang, N., Wang, G., Hu, C., Shi, Y., Liao, L., Shi, S., Cai, Y., Cheng, S., Wang, X., Liu, Y., et al. (2013). Tumor necrosis factor α suppresses the mesenchymal stem cell osteogenesis promoter miR-21 in estrogen deficiency-induced osteoporosis. *J. Bone Miner. Res.* *28*, 559–573.
29. Liu, X.-G., Zhang, Y., Ju, W.-F., Li, C.-Y., and Mu, Y.-C. (2019). miR-21 relieves rheumatoid arthritis in rats via targeting Wnt signaling pathway. *Eur. Rev. Med. Pharmacol. Sci.* *23* (3, Suppl), 96–103.
30. Xiong, G., Huang, Z., Jiang, H., Pan, Z., Xie, J., and Wang, S. (2016). Inhibition of microRNA-21 decreases the invasiveness of fibroblast-like synoviocytes in rheumatoid arthritis via TGF β /Smads signaling pathway. *Iran. J. Basic Med. Sci.* *19*, 787–793.
31. Zhou, W., Su, L., Duan, X., Chen, X., Hays, A., Upadhyayula, S., Shivde, J., Wang, H., Li, Y., Huang, D., and Liang, S. (2018). MicroRNA-21 down-regulates inflammation and inhibits periodontitis. *Mol. Immunol.* *101*, 608–614.
32. Nakka, M., Allen-Rhoades, W., Li, Y., Kelly, A.J., Shen, J., Taylor, A.M., Barkauskas, D.A., Yustein, J.T., Andrusis, I.L., Wunder, J.S., et al.; TARGET osteosarcoma consortium (2017). Biomarker significance of plasma and tumor miR-21, miR-221, and miR-106a in osteosarcoma. *Oncotarget* *8*, 96738–96752.
33. Zhao, H., Yan, P., Wang, J., Zhang, Y., Zhang, M., Wang, Z., Fu, Q., and Liang, W. (2019). Clinical significance of tumor miR-21, miR-221, miR-143, and miR-106a as biomarkers in patients with osteosarcoma. *Int. J. Biol. Markers* *34*, 184–193.
34. Lee, T.J., Yoo, J.Y., Shu, D., Li, H., Zhang, J., Yu, J.-G., Jaime-Ramirez, A.C., Acunzo, M., Romano, G., Cui, R., et al. (2017). RNA nanoparticle-based targeted therapy for glioblastoma through inhibition of oncogenic miR-21. *Mol. Ther.* *25*, 1544–1555.
35. Ding, T., Cui, P., Zhou, Y., Chen, C., Zhao, J., Wang, H., Guo, M., He, Z., and Xu, L. (2018). Antisense oligonucleotides against miR-21 inhibit the growth and metastasis of colorectal carcinoma via the DUSP8 pathway. *Mol. Ther. Nucleic Acids* *13*, 244–255.
36. Carthew, J., Donderwinkel, I., Shrestha, S., Truong, V.X., Forsythe, J.S., and Frith, J.E. (2020). In situ miRNA delivery from a hydrogel promotes osteogenesis of encapsulated mesenchymal stromal cells. *Acta Biomater.* *101*, 249–261.
37. Meng, Y., Liu, C., Zhao, J., Li, X., Li, Z., Wang, J., Wang, R., Liu, Y., Yuan, X., Cui, Z., and Yang, X. (2016). An injectable miRNA-activated matrix for effective bone regeneration in vivo. *J. Mater. Chem. B Mater. Biol. Med.* *4*, 6942–6954.
38. Moghadasi, M., Alivand, M., Fardi, M., Moghadam, K.S., and Solali, S. (2020). Emerging molecular functions of microRNA-124: cancer pathology and therapeutic implications. *Pathol. Res. Pract.* *216*, 152827.
39. Yue, X., Cui, Y., You, Q., Lu, Y., and Zhang, J. (2019). MicroRNA-124 negatively regulates chloride intracellular channel 1 to suppress the migration and invasion of liver cancer cells. *Oncol. Rep.* *42*, 1380–1390.
40. Lang, F.M., Hossain, A., Gumin, J., Momin, E.N., Shimizu, Y., Ledbetter, D., Shahar, T., Yamashita, S., Parker Kerrigan, B., Fueyo, J., et al. (2018). Mesenchymal stem cells as natural biofactories for exosomes carrying miR-124a in the treatment of gliomas. *Neuro-oncol.* *20*, 380–390.
41. Yu, B., Jiang, K., and Zhang, J. (2018). MicroRNA-124 suppresses growth and aggressiveness of osteosarcoma and inhibits TGF- β -mediated AKT/GSK-3 β /SNAIL-1 signaling. *Mol. Med. Rep.* *17*, 6736–6744.
42. Meng, Q., Zhang, W., Xu, X., Li, J., Mu, H., Liu, X., Qin, L., Zhu, X., and Zheng, M. (2018). The effects of TRAF6 on proliferation, apoptosis and invasion in osteosarcoma are regulated by miR-124. *Int. J. Mol. Med.* *41*, 2968–2976.
43. Tang, J., Lin, X., Zhong, J., Xu, F., Wu, F., Liao, X., Cui, R.R., Li, F., and Yuan, L.Q. (2019). miR-124 regulates the osteogenic differentiation of bone marrow-derived mesenchymal stem cells by targeting Sp7. *Mol. Med. Rep.* *19*, 3807–3814.
44. Maeda, Y., Farina, N.H., Matzelle, M.M., Fanning, P.J., Lian, J.B., and Gravallesse, E.M. (2017). Synovium-derived microRNAs regulate bone pathways in rheumatoid arthritis. *J. Bone Miner. Res.* *32*, 461–472.
45. Fiscalletti, M., Biggin, A., Bennetts, B., Wong, K., Briody, J., Pacey, V., Birman, C., and Munns, C.F. (2018). Novel variant in Sp7/Osx associated with recessive osteogenesis imperfecta with bone fragility and hearing impairment. *Bone* *110*, 66–75.
46. Tang, S.-L., Huang, Q.-H., Wu, L.-G., Liu, C., and Cai, A.-L. (2018). miR-124 regulates osteoblast differentiation through GSK-3 β in ankylosing spondylitis. *Eur. Rev. Med. Pharmacol. Sci.* *22*, 6616–6624.
47. Tu, B., Liu, S., Yu, B., Zhu, J., Ruan, H., Tang, T., and Fan, C. (2016). miR-203 inhibits the traumatic heterotopic ossification by targeting Runx2. *Cell Death Dis.* *7*, e2436.
48. Laxman, N., Mallmin, H., Nilsson, O., and Kindmark, A. (2016). miR-203 and miR-320 regulate bone morphogenetic protein-2-induced osteoblast differentiation by targeting distal-less homeobox 5 (*Dlx5*). *Genes (Basel)* *8*, 4.
49. Qiao, L., Liu, D., Li, C.-G., and Wang, Y.-J. (2018). miR-203 is essential for the shift from osteogenic differentiation to adipogenic differentiation of mesenchymal stem cells in postmenopausal osteoporosis. *Eur. Rev. Med. Pharmacol. Sci.* *22*, 5804–5814.
50. Ciancio, G., Ferracin, M., Negrini, M., and Govoni, M. (2013). The role of micro-RNAs in rheumatic diseases: an update. In *Innovative Rheumatology*, H. Matsuno, ed. (IntechOpen), <https://www.intechopen.com/books/innovative-rheumatology/the-role-of-micro-rnas-in-rheumatic-diseases-an-update>.
51. Stanczyk, J., Ospelt, C., Karouzakis, E., Filer, A., Raza, K., Kolling, C., Gay, R., Buckley, C.D., Tak, P.P., Gay, S., and Kyburz, D. (2011). Altered expression of microRNA-203 in rheumatoid arthritis synovial fibroblasts and its role in fibroblast activation. *Arthritis Rheum.* *63*, 373–381.
52. Huang, W., Wu, Y., Cheng, D., and He, Z. (2020). Mechanism of epithelial-mesenchymal transition inhibited by miR-203 in non-small cell lung cancer. *Oncol. Rep.* *43*, 437–446.
53. Márton, É., Lukács, J., Penyige, A., Janka, E., Hegedüs, L., Soltész, B., Méhes, G., Póka, R., Nagy, B., and Szilágyi, M. (2019). Circulating epithelial-mesenchymal transition-associated miRNAs are promising biomarkers in ovarian cancer. *J. Biotechnol.* *297*, 58–65.
54. Yang, D., Liu, G., and Wang, K. (2015). miR-203 acts as a tumor suppressor gene in osteosarcoma by regulating RAB22A. *PLoS ONE* *10*, e0132225.
55. Lin, W., Zhu, X., Yang, S., Chen, X., Wang, L., Huang, Z., Ding, Y., Huang, L., and Lv, C. (2017). MicroRNA-203 inhibits proliferation and invasion, and promotes apoptosis of osteosarcoma cells by targeting Runt-related transcription factor 2. *Biomed. Pharmacother.* *91*, 1075–1084.
56. Liu, S., and Feng, P. (2015). miR-203 determines poor outcome and suppresses tumor growth by targeting TBK1 in osteosarcoma. *Cell. Physiol. Biochem.* *37*, 1956–1966.
57. Liu, T., Fu, N.-N., Song, H.-L., Wang, Y.-L., Wu, B.-J., and Shen, Z.-Y. (2014). Suppression of microRNA-203 improves survival of rat bone marrow mesenchymal stem cells through enhancing PI3K-induced cellular activation. *IUBMB Life* *66*, 220–227.
58. Moran-Moguel, M.C., Petarra-Del Rio, S., Mayorquin-Galvan, E.E., and Zavala-Cerna, M.G. (2018). Rheumatoid arthritis and miRNAs: a critical review through a functional view. *J. Immunol. Res.* *2018*, 2474529.
59. Chen, J., He, G., Wang, Y., and Cai, D. (2019). MicroRNA-223 promotes osteoblast differentiation of MC3T3-E1 cells by targeting histone deacetylase 2. *Int. J. Mol. Med.* *43*, 1513–1521.
60. Xie, Y., Zhang, L., Gao, Y., Ge, W., and Tang, P. (2015). The multiple roles of microRNA-223 in regulating bone metabolism. *Molecules* *20*, 19433–19448.
61. Castro-Villegas, C., Pérez-Sánchez, C., Escudero, A., Filipescu, I., Verdu, M., Ruiz-Limón, P., Aguirre, M.A., Jiménez-Gomez, Y., Font, P., Rodríguez-Ariza, A., et al. (2015). Circulating miRNAs as potential biomarkers of therapy effectiveness in rheumatoid arthritis patients treated with anti-TNF α . *Arthritis Res. Ther.* *17*, 49.
62. Dunaeva, M., Blom, J., Thurlings, R., and Puijn, G.J.M. (2018). Circulating serum miR-223-3p and miR-16-5p as possible biomarkers of early rheumatoid arthritis. *Clin. Exp. Immunol.* *193*, 376–385.
63. Ji, Q., Xu, X., Song, Q., Xu, Y., Tai, Y., Goodman, S.B., Bi, W., Xu, M., Jiao, S., Maloney, W.J., and Wang, Y. (2018). miR-223-3p inhibits human osteosarcoma metastasis and progression by directly targeting CDH6. *Mol. Ther.* *26*, 1299–1312.
64. Dong, J., Liu, Y., Liao, W., Liu, R., Shi, P., and Wang, L. (2016). miRNA-223 is a potential diagnostic and prognostic marker for osteosarcoma. *J. Bone Oncol.* *5*, 74–79.
65. Srinivasan, G., Williamson, E.A., Kong, K., Jaiswal, A.S., Huang, G., Kim, H.-S., Schärer, O., Zhao, W., Burma, S., Sung, P., and Hromas, R. (2019). miR223-3p

- promotes synthetic lethality in BRCA1-deficient cancers. *Proc. Natl. Acad. Sci. USA* 116, 17438–17443.
66. Berenstein, R., Nogai, A., Waechter, M., Blau, O., Kuehnel, A., Schmidt-Hieber, M., Kunitz, A., Pezzutto, A., Dörken, B., and Blau, I.W. (2016). Multiple myeloma cells modify VEGF/IL-6 levels and osteogenic potential of bone marrow stromal cells via Notch/miR-223. *Mol. Carcinog.* 55, 1927–1939.
 67. Chen, L., Song, Z., Huang, S., Wang, R., Qin, W., Guo, J., and Lin, Z. (2016). lncRNA DANCR suppresses odontoblast-like differentiation of human dental pulp cells by inhibiting wnt/ β -catenin pathway. *Cell Tissue Res.* 364, 309–318.
 68. Zhang, J., Tao, Z., and Wang, Y. (2017). Long non-coding RNA DANCR regulates the proliferation and osteogenic differentiation of human bone-derived marrow mesenchymal stem cells via the p38 MAPK pathway. *Int. J. Mol. Med.* 41, 213–219.
 69. Silva, A.M., Moura, S.R., Teixeira, J.H., Barbosa, M.A., Santos, S.G., and Almeida, M.I. (2019). Long noncoding RNAs: a missing link in osteoporosis. *Bone Res.* 7, 10.
 70. Feldmann, M. (2002). Development of anti-TNF therapy for rheumatoid arthritis. *Nat. Rev. Immunol.* 2, 364–371.
 71. Jiang, N., Wang, X., Xie, X., Liao, Y., Liu, N., Liu, J., Miao, N., Shen, J., and Peng, T. (2017). lncRNA DANCR promotes tumor progression and cancer stemness features in osteosarcoma by upregulating AXL via miR-33a-5p inhibition. *Cancer Lett.* 405, 46–55.
 72. He, Q., Yang, S., Gu, X., Li, M., Wang, C., and Wei, F. (2018). Long noncoding RNA TUG1 facilitates osteogenic differentiation of periodontal ligament stem cells via interacting with Lin28A. *Cell Death Dis.* 9, 455.
 73. Yu, Y., Chen, Y., Zheng, Y.J., Weng, Q.H., Zhu, S.P., and Zhou, D.S. (2020). lncRNA TUG1 promoted osteogenic differentiation through promoting bFGF ubiquitination. *In Vitro Cell. Dev. Biol. Anim.* 56, 42–48.
 74. Sacchetti, B., Fatica, A., Sorci, M., Sorrentino, A., Signore, M., Cerio, A., Felicetti, F., Feo, A., Pelosi, E., Caré, A., et al. (2017). Effect of miR-204&211 and RUNX2 control on the fate of human mesenchymal stromal cells. *Regen. Med. Res.* 5, 2.
 75. Pino, A.M., Rosen, C.J., and Rodríguez, J.P. (2012). In osteoporosis, differentiation of mesenchymal stem cells (MSCs) improves bone marrow adipogenesis. *Biol. Res.* 45, 279–287.
 76. Sheng, K., and Li, Y. (2019). lncRNA TUG1 promotes the development of osteosarcoma through RUNX2. *Exp. Ther. Med.* 18, 3002–3008.
 77. Li, G., Liu, K., and Du, X. (2018). Long non-coding RNA TUG1 promotes proliferation and inhibits apoptosis of osteosarcoma cells by sponging miR-132-3p and up-regulating SOX4 expression. *Yonsei Med. J.* 59, 226–235.
 78. Zhou, Q., Hu, T., and Xu, Y. (2020). Anticancer potential of TUG1 knockdown in cisplatin-resistant osteosarcoma through inhibition of MET/Akt signalling. *J. Drug Target.* 28, 204–211.
 79. Tang, L.-P., Ding, J.-B., Liu, Z.-H., and Zhou, G.-J. (2018). lncRNA TUG1 promotes osteoarthritis-induced degradation of chondrocyte extracellular matrix via miR-195/MMP-13 axis. *Eur. Rev. Med. Pharmacol. Sci.* 22, 8574–8581.
 80. Yi, J., Liu, D., and Xiao, J. (2019). lncRNA MALAT1 sponges miR-30 to promote osteoblast differentiation of adipose-derived mesenchymal stem cells by promotion of Runx2 expression. *Cell Tissue Res.* 376, 113–121.
 81. Zhang, Y., Guo, H., Ma, L., Zhu, J., Guo, A., and He, Y. (2020). [Study on adsorption of microRNA-124 by long chain non-coding RNA MALAT1 regulates osteogenic differentiation of mesenchymal stem cells]. *Zhongguo Xiu Fu Chong Jian Wai Ke Za Zhi* 34, 240–245.
 82. Li, G.-Q., Fang, Y.-X., Liu, Y., Meng, F.-R., Wu, X., Zhang, C.-W., Zhang, Y., Liu, D., and Gao, B. (2019). MALAT1-driven inhibition of Wnt signal impedes proliferation and inflammation in fibroblast-like synoviocytes through CTNNB1 promoter methylation in rheumatoid arthritis. *Hum. Gene Ther.* 30, 1008–1022.
 83. Zhang, Y., Wang, F., Chen, G., He, R., and Yang, L. (2019). lncRNA MALAT1 promotes osteoarthritis by modulating miR-150-5p/AKT3 axis. *Cell Biosci.* 9, 54.
 84. Chen, Y., Huang, W., Sun, W., Zheng, B., Wang, C., Luo, Z., Wang, J., and Yan, W. (2018). lncRNA MALAT1 promotes cancer metastasis in osteosarcoma via activation of the PI3K-Akt signaling pathway. *Cell. Physiol. Biochem.* 51, 1313–1326.
 85. Sun, Z., Zhang, T., and Chen, B. (2019). Long non-coding RNA metastasis-associated lung adenocarcinoma transcript 1 (MALAT1) promotes proliferation and metastasis of osteosarcoma cells by targeting c-Met and SOX4 via miR-34a/c-5p and miR-449a/b. *Med. Sci. Monit.* 25, 1410–1422.
 86. Yang, G., Zhang, C., Wang, N., and Chen, J. (2019). miR-425-5p decreases lncRNA MALAT1 and TUG1 expressions and suppresses tumorigenesis in osteosarcoma via Wnt/ β -catenin signaling pathway. *Int. J. Biochem. Cell Biol.* 111, 42–51.
 87. Tornesello, M.L., Faraonio, R., Buonaguro, L., Annunziata, C., Starita, N., Cerasuolo, A., Pezzuto, F., Tornesello, A.L., and Buonaguro, F.M. (2020). The role of microRNAs, long non-coding RNAs, and circular RNAs in cervical cancer. *Front. Oncol.* 10, 150.
 88. Chen, S., Zhang, C., and Feng, M. (2020). Prognostic value of lncRNA HOTAIR in colorectal cancer: a meta-analysis. *Open Med. (Wars.)* 15, 76–83.
 89. Mozdarani, H., Ezzatizadeh, V., and Rahbar Parvaneh, R. (2020). The emerging role of the long non-coding RNA HOTAIR in breast cancer development and treatment. *J. Transl. Med.* 18, 152.
 90. Zheng, H., and Min, J. (2016). Role of long noncoding RNA HOTAIR in the growth and apoptosis of osteosarcoma cell MG-63. *BioMed Res. Int.* 2016, 5757641.
 91. Han, J., and Shen, X. (2020). Long noncoding RNAs in osteosarcoma via various signaling pathways. *J. Clin. Lab. Anal.* 34, e23317.
 92. Wei, B., Wei, W., Zhao, B., Guo, X., and Liu, S. (2017). Long non-coding RNA HOTAIR inhibits miR-17-5p to regulate osteogenic differentiation and proliferation in non-traumatic osteonecrosis of femoral head. *PLoS ONE* 12, e0169097.
 93. Shao, L., and Hou, C. (2019). miR-138 activates NF- κ B signaling and PGRN to promote rheumatoid arthritis via regulating HDAC4. *Biochem. Biophys. Res. Commun.* 519, 166–171.
 94. Zhang, H.-J., Wei, Q.-F., Wang, S.-J., Zhang, H.-J., Zhang, X.-Y., Geng, Q., Cui, Y.H., and Wang, X.H. (2017). lncRNA HOTAIR alleviates rheumatoid arthritis by targeting miR-138 and inactivating NF- κ B pathway. *Int. Immunopharmacol.* 50, 283–290.
 95. Zhu, J., Yu, W., Wang, Y., Xia, K., Huang, Y., Xu, A., Chen, Q., Liu, B., Tao, H., Li, F., and Liang, C. (2019). lncRNAs: function and mechanism in cartilage development, degeneration, and regeneration. *Stem Cell Res. Ther.* 10, 344.
 96. Chen, H., and Chen, L. (2020). An integrated analysis of the competing endogenous RNA network and co-expression network revealed seven hub long non-coding RNAs in osteoarthritis. *Bone Joint Res.* 9, 90–98.
 97. Cong, J., Zhang, S., and Gao, X. (2014). Quantitative assessment of the associations between CD28 T > C polymorphism (rs3116496) and cancer risk. *Tumour Biol.* 35, 9195–9200.
 98. Shi, Z.-W., Wang, J.-L., Zhao, N., Guan, Y., and He, W. (2016). Single nucleotide polymorphism of hsa-miR-124a affects risk and prognosis of osteosarcoma. *Cancer Biomark.* 17, 249–257.
 99. Dhanoa, J.K., Verma, R., Sethi, R.S., Arora, J.S., and Mukhopadhyay, C.S. (2019). Biogenesis and biological implications of isomiRs in mammals—a review. *ExRNA* 1, 3.
 100. Li, H., Li, T., Wang, S., Wei, J., Fan, J., Li, J., Han, Q., Liao, L., Shao, C., and Zhao, R.C. (2013). miR-17-5p and miR-106a are involved in the balance between osteogenic and adipogenic differentiation of adipose-derived mesenchymal stem cells. *Stem Cell Res. (Amst.)* 10, 313–324.
 101. Zhou, M., Ma, J., Chen, S., Chen, X., and Yu, X. (2014). MicroRNA-17-92 cluster regulates osteoblast proliferation and differentiation. *Endocrine* 45, 302–310.
 102. Jia, J., Feng, X., Xu, W., Yang, S., Zhang, Q., Liu, X., Feng, Y., and Dai, Z. (2014). miR-17-5p modulates osteoblastic differentiation and cell proliferation by targeting SMAD7 in non-traumatic osteonecrosis. *Exp. Mol. Med.* 46, e107.
 103. Yang, H., Peng, Z., Liang, M., Zhang, Y., Wang, Y., Huang, T., Jiang, Y., Jiang, B., and Wang, Y. (2018). The miR-17-92 cluster/QKI2/ β -catenin axis promotes osteosarcoma progression. *Oncotarget* 9, 25285–25293.
 104. Wang, W., Zhang, L., Zheng, K., and Zhang, X. (2016). miR-17-5p promotes the growth of osteosarcoma in a BRCC2-dependent mechanism. *Oncol. Rep.* 35, 1473–1482.
 105. Vanas, V., Haigl, B., Stockhammer, V., and Sutterlüty-Fall, H. (2016). MicroRNA-21 increases proliferation and cisplatin sensitivity of osteosarcoma-derived cells. *PLoS ONE* 11, e0161023.

106. Wang, L., and Yu, J. (2019). The regulatory effect of Mir-149 on bone marrow mesenchymal stem cells in osteoporosis rats and its related mechanisms. *J. Biomater. Tissue Eng.* 9, 1127–1132.
107. Li, G., Yun, X., Ye, K., Zhao, H., An, J., Zhang, X., Han, X., Li, Y., and Wang, S. (2020). Long non-coding RNA-H19 stimulates osteogenic differentiation of bone marrow mesenchymal stem cells via the microRNA-149/SDF-1 axis. *J. Cell. Mol. Med.* 24, 4944–4955.
108. Xu, R.-D., Feng, F., Yu, X.-S., Liu, Z.-D., and Lao, L.-F. (2018). miR-149-5p inhibits cell growth by regulating TWEAK/Fn14/PI3K/AKT pathway and predicts favorable survival in human osteosarcoma. *Int. J. Immunopathol. Pharmacol.* 32, 2058738418786656.
109. Zhang, S., Liu, Y., Zheng, Z., Zeng, X., Liu, D., Wang, C., and Ting, K. (2018). MicroRNA-223 suppresses osteoblast differentiation by inhibiting DHRS3. *Cell. Physiol. Biochem.* 47, 667–679.
110. Pan, Z., Wu, C., Li, Y., Li, H., An, Y., Wang, G., Dai, J., and Wang, Q. (2020). lncRNA DANCR silence inhibits SOX5-mediated progression and autophagy in osteosarcoma via regulating miR-216a-5p. *Biomed. Pharmacother.* 122, 109707.
111. Carrion, K., Dyo, J., Patel, V., Sasik, R., Mohamed, S.A., Hardiman, G., and Nigam, V. (2014). The long non-coding *HOTAIR* is modulated by cyclic stretch and WNT/ β -CATENIN in human aortic valve cells and is a novel repressor of calcification genes. *PLoS ONE* 9, e96577.
112. Gong, Y.-Y., Peng, M.-Y., Yin, D.-Q., and Yang, Y.-F. (2018). Long non-coding RNA H19 promotes the osteogenic differentiation of rat ectomesenchymal stem cells via Wnt/ β -catenin signaling pathway. *Eur. Rev. Med. Pharmacol. Sci.* 22, 8805–8813.
113. Wu, J., Zhao, J., Sun, L., Pan, Y., Wang, H., and Zhang, W.-B. (2018). Long non-coding RNA H19 mediates mechanical tension-induced osteogenesis of bone marrow mesenchymal stem cells via FAK by sponging miR-138. *Bone* 108, 62–70.
114. Zhao, J., and Ma, S.-T. (2018). Downregulation of lncRNA H19 inhibits migration and invasion of human osteosarcoma through the NF- κ B pathway. *Mol. Med. Rep.* 17, 7388–7394.
115. Stuhlmüller, B., Kunisch, E., Franz, J., Martinez-Gamboa, L., Hernandez, M.M., Pruss, A., Ulbrich, N., Erdmann, V.A., Burmester, G.R., and Kinne, R.W. (2003). Detection of oncofetal h19 RNA in rheumatoid arthritis synovial tissue. *Am. J. Pathol.* 163, 901–911.

Article

The Role of miR-21 in Osteoblasts–Osteoclasts Coupling In Vitro

Agnieszka Smieszek ^{1,*}, Klaudia Marcinkowska ¹, Ariadna Pielok ¹, Mateusz Sikora ¹,
Lukas Valihrach ² and Krzysztof Marycz ^{1,3,4}

¹ Department of Experimental Biology, The Faculty of Biology and Animal Science, University of Environmental and Life Sciences, 50-375 Wrocław, Poland; klaudia.marcinkowska@upwr.edu.pl (K.M.); ariadna.pielok@upwr.edu.pl (A.P.); mateusz.sikora@upwr.edu.pl (M.S.); krzysztof.marycz@upwr.edu.pl (K.M.)

² Laboratory of Gene Expression, Institute of Biotechnology CAS, Biocev, 25250 Vestec, Czech Republic; lukas.valihrach@ibt.cas.cz

³ International Institute of Translational Medicine, Jesionowa 11 St, 55-124 Malin, Poland

⁴ Collegium Medicum, Cardinal Stefan Wyszyński University (UKSW), Woycickiego 1/3, 01-938 Warsaw, Poland

* Correspondence: agnieszka.smieszek@upwr.edu.pl; Tel.: +48-71-320-52-48

Received: 29 December 2019; Accepted: 18 February 2020; Published: 19 February 2020



Abstract: MiR-21 is being gradually more and more recognized as a molecule regulating bone tissue homeostasis. However, its function is not fully understood due to the dual role of miR-21 on bone-forming and bone-resorbing cells. In this study, we investigated the impact of miR-21 inhibition on pre-osteoblastic cells differentiation and paracrine signaling towards pre-osteoclasts using indirect co-culture model of mouse pre-osteoblast (MC3T3) and pre-osteoclast (4B12) cell lines. The inhibition of miR-21 in MC3T3 cells (MC3T3_{inh21}) modulated expression of genes encoding osteogenic markers including collagen type I (*Coll-1*), osteocalcin (*Ocl*), osteopontin (*Opn*), and runt-related transcription factor 2 (*Runx-2*). Inhibition of miR-21 in osteogenic cultures of MC3T3 also inflected the synthesis of OPN protein which is essential for proper mineralization of extracellular matrix (ECM) and anchoring osteoclasts to the bones. Furthermore, it was shown that in osteoblasts miR-21 regulates expression of factors that are vital for survival of pre-osteoclast, such as receptor activator of nuclear factor κB ligand (RANKL). The pre-osteoclast cultured with MC3T3_{inh21} cells was characterized by lowered expression of several markers associated with osteoclasts' differentiation, foremost tartrate-resistant acid phosphatase (*Trap*) but also receptor activator of nuclear factor-κB ligand (*Rank*), cathepsin K (*Ctsk*), carbonic anhydrase II (*CaII*), and matrix metalloproteinase (*Mmp-9*). Collectively, our data indicate that the inhibition of miR-21 in MC3T3 cells impairs the differentiation and ECM mineralization as well as influences paracrine signaling leading to decreased viability of pre-osteoclasts.

Keywords: miR-21-5p; osteogenesis; differentiation; precursor cells; osteoblasts; osteoclasts

1. Introduction

MicroRNAs (miRNAs) are a class of non-coding, single stranded RNAs with average length around 22 nucleotides. The molecules are highly conserved across species and have various biological functions that are connected with the regulation of gene expression by targeting 3'-untranslated region (3'-UTR) of messenger RNA [1,2]. MiRNAs regulate multiple processes crucial for homeostasis maintenance, such as cell proliferation, differentiation, survival and apoptosis. Mounting evidence indicates that miRNAs play a vital role during osteogenesis process by modulating expression of genes

essential for recruitment and differentiation of various bone cells, including progenitor and mature cells [2,3]. MiRNAs are also important molecules that control the process of extracellular matrix (ECM) mineralization. For instance, miR-29b-dependent suppression of collagen occurs at the late stage of differentiation, which facilitates the maturation of collagen fibrillar matrix for mineral deposition [4]. Furthermore, therapeutic usefulness of miRNAs in terms of bone-associated diseases treatment is widely discussed [5].

MiR-21 represents a molecule that has gained attention as a factor with an important role in bone homeostasis maintenance [1,6,7]. This molecule is predominantly characterized as “oncomiR”, due to the fact that its overexpression was observed in several cancers, including prostate and breast cancer, as well as osteosarcoma [8–10]. Most recently, it was shown that miR-21 may promote differentiation of multipotent stromal cells (MSCs) derived from bone-marrow (BMSCs).

The mechanism of miR-21 action is still under debate, nevertheless it was recognized as an important regulator of signaling pathways activated during differentiation of progenitor cells toward osteogenic cells. It has been shown that one of the direct targets of miR-21 is an inhibitory protein Smad7, which modulates signal transduction pathway that is induced by members of transforming growth factor family, i.e., TGF- β and bone morphogenetic proteins (BMPs) [11,12]. A study performed by Li et al. [12] showed that miR-21 deficiency significantly weakened osteogenic potential of BMSCs. Observed effect was associated with decreased expression of master regulator for osteogenesis, i.e., transcription factor *Runx-2* (runt-related transcription factor 2). As a result of miR-21 deficiency, BMSCs showed attenuated osteogenic differentiation and formed poorly mineralized matrix. Moreover, impaired formation of calvarial bone was noted in miR-21-knockout mice [12].

Most recently, it has been demonstrated that miR-21 may promote migration and osteogenic differentiation of BMSCs via PTEN/PI3K/Akt/HIF-1 α pathway [7]. MiR-21 exogenously added to BMSCs cultures accelerated the osteogenesis process which resulted not only in increased expression of *Runx-2*, but also secretion of key osteogenic markers such as osteocalcin (OCL), osteopontin (OPN) and BMP-2. Valenti et al. showed that miR-21, derived from sera collected from runners after intense exercise, had an anti-apoptotic effect on BMSCs and promoted their osteogenic potential by targeting PTEN and SMAD7 [13]. Moreover, miR-21 was shown to promote differentiation of MSCs derived not only from bone-marrow. Meng et al. found that miR-21 plays an important role in osteogenic differentiation of umbilical cord blood mesenchymal stem cells (UCBMSCs) via PI3K-AKT-GSK3 β pathway and in activating transcription of *Runx-2* [14]. However, there are also contradictory results showing that miR-21 inhibits activation of key osteogenesis regulators. For example, in MSCs derived from periodontal ligament tissue (PDLSCs) overexpression of miR-21 was correlated with decreased expression of alkaline phosphatase (ALP), as well as *Runx-2* [6]. The study showed that miR-21 decreased osteogenic potential of PDLSCs by targeting Smad5 molecule, a component of BMPs signaling pathway that is activated during osteoblastogenesis. Furthermore, Wei et al. showed that transfection of cells with miR-21 inhibitor stimulated the osteogenic differentiation of hPDLSCs and improved mineralization of ECM [6].

The role of miR-21 has been studied also in bone resorbing cells (osteoclasts). Suppression of miR-21 was associated with upregulation of osteoclast suppressor programmed cell death protein 4 (PDCD4), and downregulation of osteoclast marker cathepsin K (CTSK) [15]. Thus, miR-21 may be involved in bone biology, not only via promoting mobilization of osteoblast precursors, but also by regulation of osteoclast survival and differentiation [16]. It was also shown that miR-21 knockout mice are characterized by normal skeletal phenotype during development and maintain osteoblastogenesis in vivo. However, miR-21-knockout mice showed increased expression of receptor activator of nuclear factor κ B ligand (RANKL) accompanied by decreased level of osteoprotegerin (OPG). Both molecules are major osteoblastic mediators of osteoclastogenesis. RANKL is an essential cytokine promoting differentiation and maturation of osteoclasts, while OPG acts as a decoy receptor for RANKL. OPG inhibits osteoclast differentiation by blocking the interaction between RANKL and RANK, which is a receptor of RANKL [17].

Bearing in mind all this emerging information about the dual function of miR-21 in the process of osteogenesis, we studied the effect of miR-21 inhibition on differentiation of mice pre-osteoblast cell line (MC3T3). Specifically, we analysed the impact of miR-21 down-regulation in MC3T3 cell line (MC3T3_{inh21}) on their osteogenic potential and paracrine activity towards osteoclast precursors.

We used indirect co-culture system of MC3T3_{inh21} and osteoclast precursor cell line 4B12 established by professor Amano's group [18]. The pre-osteoclastic 4B12 mouse cell line is a model that faithfully recapitulates features of primary osteoclast differentiation showing high expression of c-Fms (macrophage colony-stimulating factor receptor) and RANK (receptor activator of nuclear factor κ B) [18,19]. To our best knowledge this is the first study showing the consequences of miR-21 inhibition in osteoblasts on pre-osteoclasts activity. Using the model of indirect co-culture system, we were able to determine the paracrine interplay between MC3T3_{inh21} and pre-osteoclasts. The analysis included evaluation of matrix mineralization and composition, as well as the analysis of key osteogenic markers expression determined by using reverse transcription quantitative PCR (RT-qPCR), Western blot and immunocytochemical staining.

2. Materials and Methods

2.1. Pre-osteoblastic Mouse Cell Line MC3T3

MC3T3 cells were cultured in Minimum Essential Media Alpha (MEM- α , Gibco™ Thermo Fisher Scientific, Warsaw, Poland) supplemented with 10% FBS (Fetal Bovine Serum, Sigma Aldrich, Munich, Germany) at constant conditions in incubator at 37 °C, 5% CO₂ and 95% humidity. Cells were passaged with trypsin solution (StableCell Trypsin, Sigma Aldrich, Munich, Germany). The protocol of MC3T3 detachment included culture washing using Hanks' Balanced Salt Solution (HBSS) without calcium and magnesium. Following this step, trypsin solution was added to the culture dish in the volume allowing complete coverage of monolayer. The cultures were incubated with the trypsin solution for 5 min at 37 °C in CO₂ incubator. Detachment of MC3T3 from culture dishes was monitored under inverted microscope with phase contrast (Axio Observer A.1 Zeiss, Oberkochen, Germany). The passage was performed when cultures reached 90% confluence. The MC3T3 used for further experiments were at passage 19 (p19).

2.2. Transfection of miR-21 Inhibitor

MC3T3 cells were transfected with miR-21 inhibitor (hsa-miR-21a-5p Anti-miR™ miRNA Inhibitor, Ambition, Thermo Fisher Scientific, Warsaw, Poland) using ESCORT III Transfection reagent (Sigma-Aldrich Sp. z o. o. Poznan, Poland). The transfection reagent was prepared in dilution 1:100, while miR-21 inhibitor was used at concentration equal to 50 nM, which was established based on screening assay results (Figure S1, Supplementary Materials). The reagents were prepared in Minimum Essential Medium Eagle—Alpha Modification (MEM- α). The transfection protocol was followed accordingly to manufacturer's specification. For the purpose of transfection cells were seeded in 24-well plates at density equal to 20,000 cells per well. Transfection of cells was performed when cultures reached 70% confluence. Cells were used for experiment after 72 h following the transfection. The experiment was divided into two experimental groups: MC3T3 (control) and MC3T3_{inh21} (miR-21 inhibitor transfected cells).

The effectiveness of miR-21 inhibition was assessed using Two-tailed RT-qPCR. Levels of miR-21 were determined using a protocol described by Androvic et al. [20,21]. Sequences of primers used for the analysis were published previously [22]. Moreover, expression of Runt-related transcription factor 2 was determined as follows: the mRNA levels of Runx-2 were determined by RT-qPCR, while protein expression was detected with Western-blot technique using protocols described below.

2.3. Osteogenic Conditions

Osteogenic differentiation of MC3T3 was induced using medium consisted of complete growth medium (MEM- α) supplemented with osteogenic factors—10 nM β -glycerol phosphate disodium salt hydrate (Sigma Aldrich, Munich, Germany) and 50 μ g/mL ascorbic acid (Sigma Aldrich, Munich, Germany). The osteogenic medium was changed twice a week, and cultures were maintained in osteogenic medium for 3, 7, and 15 days. After differentiation, the cultures were collected for further analysis.

2.4. Co-culture with Pre-osteoclastic Cell Line 4B12

The osteoclast precursor cell line 4B12 used in the experiment was kindly provided by Shigeru Amano from Department of Oral Biology and Tissue Engineering, Meikai University School of Dentistry [18]. The cultures were propagated in complete growth medium (CGM_{4B12}) consisting of α -MEM (Sigma Aldrich, Munich, Germany) supplemented with 10% of FBS and 30% of calvaria-derived stromal cell conditioned medium (CSCM). The 4B12 cultures were maintained in incubator at constant conditions (37 °C, 5% CO₂, and 95% humidity). The cultures of pre-osteoclasts were passaged after reaching confluence of 75%, and then detached from flask by gentle pipetting. The 4B12 used for co-culture experiment were at passage eighteen (p18). Pre-osteoclasts in co-culture system were inoculated at density equal to 3.5×10^4 into upper chamber of 8 μ m transwell system (Corning, Biokom, Warsaw, Poland). The cells were maintained in 0.3 mL of CGM_{4B12}. Half of the culture medium was changed twice a week. The lower chamber was pre-seeded with MC3T3 pre-osteoblast maintained under osteogenic conditions as indicated in Section 2.3.

2.5. Evaluation of Extracellular Matrix Composition

Osteogenic cultures were fixed using 4% paraformaldehyde (PFA) for 15 min at room temperature. Afterwards, cultures were specifically stained with Alizarin Red for calcium deposits detection, and with Safranin O dye for evaluation of proteoglycan content. Staining of extracellular matrix was performed as described previously [23,24]. Obtained specimens were analyzed using inverted microscope Axio Observer A1 (Zeiss, Oberkochen, Germany) and documented with Canon PowerShot digital camera (Woodhatch, UK). The signals obtained after staining were determined using ImageJ and Pixel Counter plugin (version 1.6.0, U. S. National Institutes of Health, Bethesda, MD, USA) as described previously [25–27]. The chemical composition of extracellular matrix was evaluated using scanning electron microscope with the energy-dispersive X-ray spectroscopy (SEM-EDX) using the protocol published previously [28].

2.6. Detection of Osteogenic Markers Using RT-qPCR

After the experiment, cultures after 3, 7 and 15 days of differentiation were homogenized using 1 mL of Extrazol[®] (Blirt DNA, Gdansk, Poland). RNA isolation procedure was performed according to manufacturer's instruction, which is a modified version of the phenol-chloroform method described by Chomczyński and Sacchi [29]. Total RNA was diluted in molecular grade water (Sigma Aldrich, Poznan, Poland). RNA quantity and purity was determined spectrophotometrically at 260 and 280 nm wavelengths (Epoch, Biotek, Bad Friedrichshall, Germany). Total RNA (500 ng) was treated with DNase I using PrecisionDNase kit (Primerdesign, BLIRT S.A, Gdansk, Poland) before reverse transcription. cDNA synthesis was performed using Tetro cDNA Synthesis Kit (Bioline Reagents Limited, London, UK). Digestion of DNA and cDNA synthesis were performed accordingly to the instructions provided by manufacturer in T100 Thermal Cycler (Bio-Rad, Hercules, CA, USA). RT-qPCR analysis was carried out using the SensiFAST SYBR[®]&Fluorescein Kit (Bioline Reagents Ltd., London, United Kingdom) in CFX Connect Real-Time PCR Detection System (Bio-Rad, Hercules, CA, USA). Each reaction mixture included 1 μ L of cDNA in final volume of 10 μ L, while primers were used at 0.5 μ M concentration. The reactions proceeded according to the following conditions: initial denaturation

at 95 °C for 2 min, followed by 45 cycles at 95 °C for 5 s, annealing for 10 s, and elongation at 72 °C for 5 s. The analysis of the dissociation curves was performed to determine the specificity of PCR products. The melting curve was obtained using a gradient from 65 to 95 °C, and the heating rate was 0.2 °C/s. Reaction conditions were described previously [22,27]. Primer sequences are summarized in Table S1. All reactions were performed in at least three repetitions. The expression of genes was calculated using RQ_{MAX} algorithm and converted into log₂ scale as described previously [22]. The transcript levels were normalized to the housekeeping gene – *Gapdh* (glyceraldehyde 3-phosphatedehydrogenase).

2.7. Western Blotting Detection of Osteopontin and Runx-2

The cultures were lysed using ice-cold RIPA buffer containing 1% protease and phosphatase inhibitor mix (Sigma Aldrich, Munich, Germany). The concentration of protein was evaluated using the Bicinchoninic Acid Assay Kit (Sigma Aldrich, Munich, Germany). The procedure of the reaction was established previously [22,30]. The concentration of proteins loaded per well was equal to 20 µg. Samples were separated in 12% sodium dodecyl sulphate-polyacrylamide gel by electrophoresis (SDS-PAGE; 100V, 90 min) and transferred into PVDF membrane (100 V, 60 min) in Transfer buffer (Tris-base/Glycine, Sigma Aldrich, Munich, Germany) using the Mini Trans-Blot[®] system (Bio-Rad, Hercules, CA, USA). After the transfer, the membranes were blocked for 1 h with 5% skim milk (Sigma Aldrich, Munich, Germany). Then, the membranes were incubated overnight at room temperature with primary antibodies detecting osteopontin in dilution of 1:1000 (OPN, ab8448, Abcam, Cambridge, UK), RUNX-2 in dilution of 1:100 (F-2: sc-390351, Santa Cruz Biotechnology, Dallas, Texas, USA), and β-actin in dilution of 1:1000 (A2066, Sigma Aldrich, Munich, Germany). The antibodies were diluted in 5% of skim milk prepared in TBST buffer (Tris/NaCl/Tween). Next, the membranes were washed five times for 5 min with TBST buffer. After washing, the membranes were incubated with secondary antibody conjugated with HRP (Sigma Aldrich, Munich, Germany) for 60 min at room temperature. The secondary antibody was diluted at concentration 1:2500 in TBST. After incubation with secondary antibody the membranes were washed, as indicated above and analyzed using Bio-Rad ChemiDoc[™] XRS system. The reaction was performed using DuoLuX[®] Chemiluminescent and Fluorescent Peroxidase (HRP) Substrate (Vector Laboratories, Peterborough, United Kingdom). The intensity of signals was quantified using Image Lab[™] Software (Bio-Rad, Hercules, CA, USA).

2.8. Immunocytochemical Detection of Osteopontin and Tartrate-Resistant Acid Phosphatase (TRAP)

Immunostaining reaction was performed according to methods described previously [27,31]. Before the analysis, cells were cultured under experimental conditions, within 24-well dishes coated with glass cover slides. After the experiment, cultures were fixed with 4% PFA (30 min at room temperature) for the immunocytochemical detection. Following fixation, cultures were washed three times with HBSS and permeabilized with 0.2% PBS-Tween solution for 15 min. Next, specimens were washed 3 times in HBSS and incubated overnight at 4 °C with primary antibodies and 10% goat serum in order to block nonspecific protein–protein interactions. The following antibodies were used: anti-osteopontin antibody produced in rabbit (ab8448, Abcam, Cambridge, UK) and anti-TRAP antibody (D-3) mouse monoclonal IgG1. (sc-376875, Santa Cruz Biotechnology, Dallas, Texas, USA). Primary antibodies were diluted to concentration of 1:50 (TRAP) and 1:1000 (OPN). After incubation with primary antibody, samples were washed as described previously and incubated with secondary antibody for 1 h at room temperature. Concentration of secondary antibodies was 1:1000. After incubation with the secondary antibodies, samples were washed (as above) and fixed on slides using mounting medium with DAPI (4',6-diamidino-2-phenylindole) as a nuclear counterstain (ProLong[™] Diamond Antifade Mountant with DAPI, Thermo Fisher Scientific, Warsaw, Poland). Specimens were analyzed using confocal microscope (Leica TCS SPE, Leica Microsystems, KAWA.SKA Sp. z o.o., Zalesie Gorne, Poland) at 0.5 µm steps up to a final depth of 25 µm. Images were processed using Fiji is just ImageJ (ImageJ 1.52n, Wayne Rasband, National Institute of Health, USA) [27,32]. The microscopic images were obtained using maximum intensity projection (Z-projection).

2.9. Statistical Analysis

Experimental values are presented as the mean obtained from at least three technical repetitions. Mean values are presented with standard deviation (\pm SD). The data were analyzed using t-Student test or One-way analysis of variance and Dunnett's post hoc test. The data were analyzed using GraphPad Software (Prism 8.20, CA, USA). Differences with a probability of $p < 0.05$ were considered as significant.

3. Results

3.1. The Influence of miR-21 Inhibition on mRNA Expression of Osteogenic Markers

The expression of osteogenic markers was monitored after 3, 7, and 15 days of differentiation since their profiles are known to be highly modulated during the early stages of osteogenesis (Figure 1).

No significant differences in terms of osteocalcin (*Ocl*) levels were noted between MC3T3 cultures and MC3T3_{inh21} after 3 days of osteogenesis. However, in MC3T3_{inh21} co-cultured with 4B12 we noted significant increase of *Ocl* transcripts following 3 days of differentiation (Figure 1a). Significantly reduced mRNA levels for *Ocl*, in response to miR-21 inhibition were noted after 7 and 15 days of MC3T3 differentiation, both in monolayer, as well as in the co-culture system (Figure 1b,c). Further, we determined the mRNA levels for collagen type 1 (*Coll-1*). Analysis revealed that inhibition of miR-21 in MC3T3 cultures do not affect the *Coll-1* expression after 3 and 7 days of differentiation (Figure 1d,e). The significant decrease in mRNA levels for *Coll-1*, following miR-21 inhibition were noted after 15 days of culture ($p < 0.05$, Figure 1f). In co-culture model of MC3T3 with 4B12, inhibition of miR-21 had influence on *Coll-1* levels only after 7 days of differentiation. In these cultures we observed significant ($p < 0.01$) increase of *Coll-1* transcripts in MC3T3_{inh21}/4B12 cultures. The higher mRNA level for *Coll-1* was also noted in MC3T3_{inh21}/4B12 cultures following 15 days of osteogenic differentiation, however the observed differences were not statistically significant (Figure 1d,e). The mRNA levels for osteopontin (*Opn*) measured in MC3T3 after 3 days of osteogenic cultures were not affected by miR-21 inhibition (Figure 1g). In turn, after 7 and 15 days of culture we observed significant decrease of *Opn* transcripts (Figure 1h,i). Significantly decreased mRNA levels for *Opn* were determined during 3, 7, and 15 days of osteogenic cultures of MC3T3_{inh21} with 4B12 (Figure 1g–i). The inhibition of miR-21 significantly influenced on mRNA levels of runt-related transcription factor 2 (*Runx2*) in MC3T3 cell line. The decrease expression of *Runx-2* following miR-21 inhibition was noted during 3, 7, and 15 days of osteogenesis (Figure 1j–l). In co-culture of MC3T3 with 4B12, the inhibition of miR-21 had no influence on *Runx-2* levels after 3 and 15 days of culture (Figure 1j,l), however lowered expression of miR-21 was correlated with increased mRNA level for *Runx-2*, noted after 7 days of osteogenic differentiation (Figure 1k).

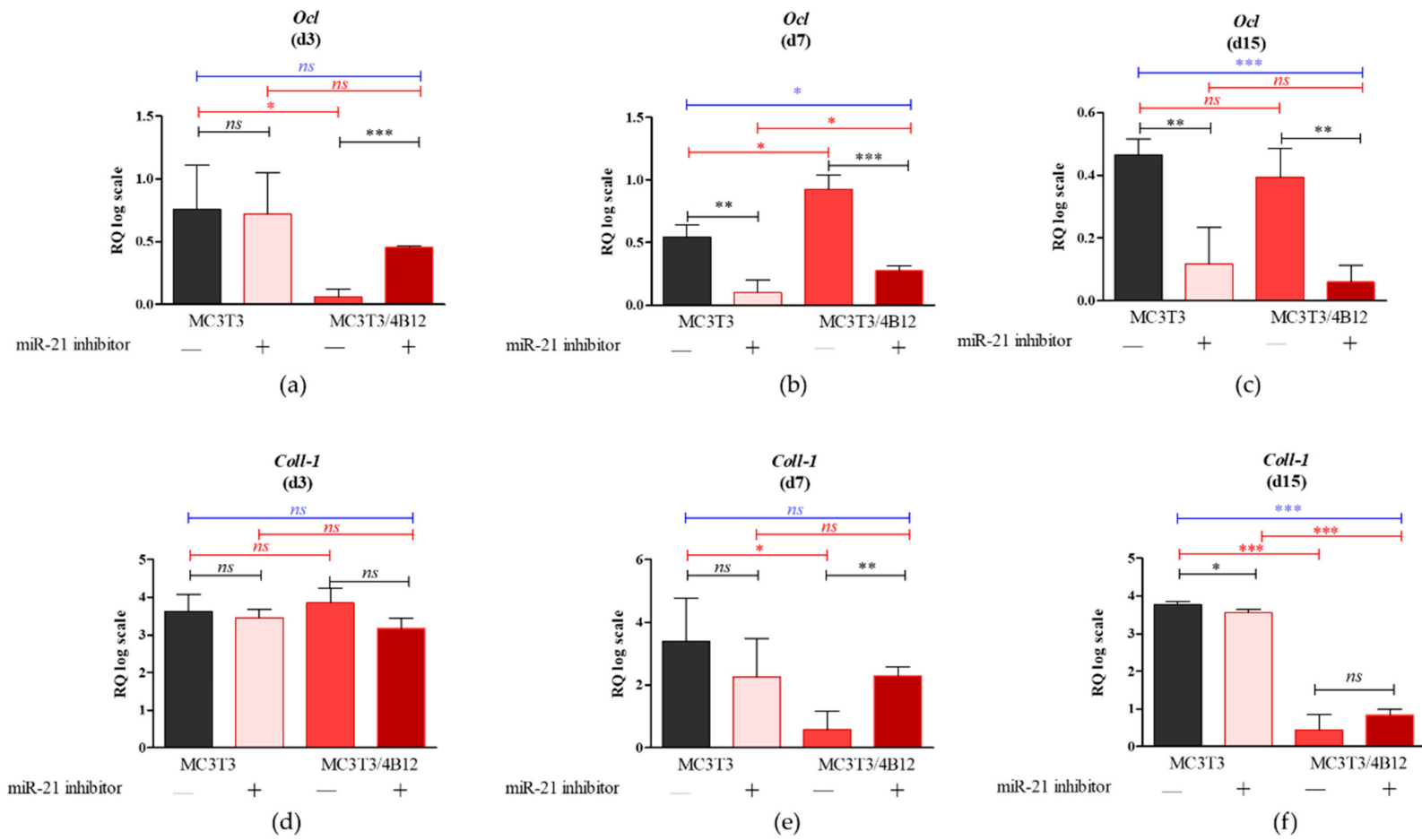


Figure 1. Cont.

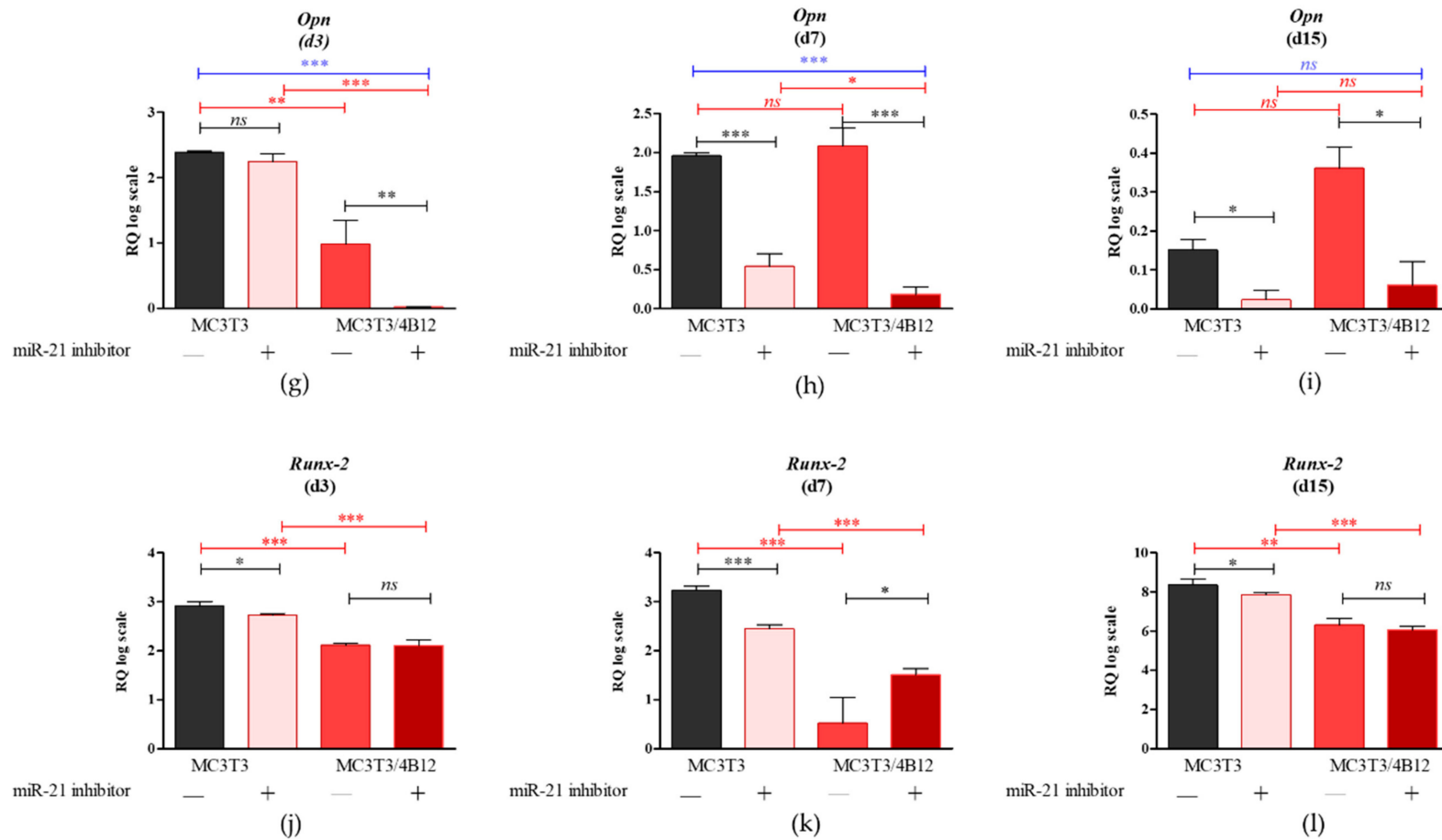


Figure 1. The results of RT-qPCR analysis showing the mRNA levels of key osteogenic markers measured after 3 (a,d,g,j), 7 (b,e,h,k), and 15 days (c,f,i,l) of osteogenic cultures (d3 d7 and d15 respectively). Following osteogenic markers were determined: osteocalcin (*Ocl*) (a–c), collagen type I (*Coll-1*) (d–f), osteopontin (*Opn*) (g–i) and runt-related transcription factor 2 (*Runx2*) (j–l). Significant differences are indicated with asterisks (* $p < 0.05$; ** $p < 0.01$ and *** $p < 0.001$), while non-significant differences are marked as *ns*. The comparisons between groups are marked with square brackets.

3.2. The Analysis of mRNA Transcripts of RANKL-OPG Axis

As the relation between *Rankl* and *Opg* expression levels in osteoblasts determines differentiation of osteoclasts [17], we decided to analyze the influence of the miR-21 inhibition on *Rankl/Opg* ratio. Obtained results showed that miR-21 inhibition do not influence on *Rankl/Opg* ratio during 3 and 7 days of culture under osteogenic conditions (Figure 2a and b). Significantly increased *Rankl* levels ($p < 0.05$) were noted in MC3T3_{inh21} cultures after 15 days of osteogenesis (Figure 2c).

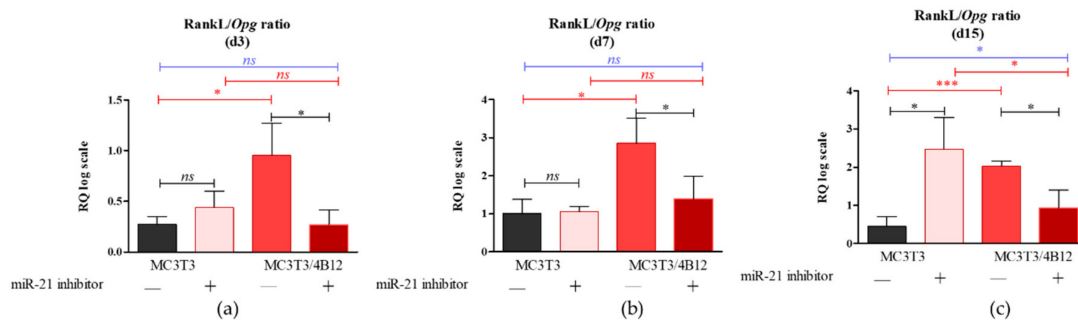


Figure 2. The *Rankl/Opg* ratio determined in experimental osteogenic cultures on days 3 (a), 7 (b), and 15 (c). Significant differences are indicated with asterisks ($* p < 0.05$ and $*** p < 0.001$), while non-significant differences are marked as *ns*. The comparisons between groups are marked with square brackets.

In turn we observed decreased expression of *Rankl* in co-cultures of MC3T3_{inh21} with 4B12. Decreased *Rankl/Opg* ratio in MC3T3_{inh21}/4B12 was maintained during the osteogenesis, on days 3, 7, and 15 (Figure 2a-c).

3.3. The Influence of miR-21 Inhibition on Extracellular Matrix Composition

Calcium deposition in extracellular matrix is a marker of late osteogenesis and reflects maturation of osteoblasts precursors [1,11,33], thus we decided to determine the extracellular matrix composition after 15 days of osteogenesis. Largely distributed calcium deposits were detected in pre-osteoblasts (M3CT3) maintained under osteogenic conditions, indicating that cells properly underwent the differentiation process (Figure 3a). The inhibition of miR-21 caused a decrease in extracellular matrix mineralization. The MC3T3_{inh21} cells formed dense networks, however we did not observe the formation of characteristic nodules stained with Alizarin Red (Figure 3b). Furthermore, the osteoclasts presence significantly lowered osteogenic differentiation of MC3T3. In co-culture of MC3T3 with 4B12 we observed a decreased number of mineralized areas (Figure 3c). In turn, the production of extracellular calcium deposits in co-cultures of MC3T3_{inh21} with 4B12 was more apparent (Figure 3d). Spectrophotometric analysis of dye absorption and statistical analysis of the obtained results, confirmed the observations made under microscope. SEM-EDX analysis confirmed lowered calcium and phosphorous deposition in MC3T3 cultures with decreased expression of miR-21 and in co-culture model (Figure S2, Supplementary Materials).

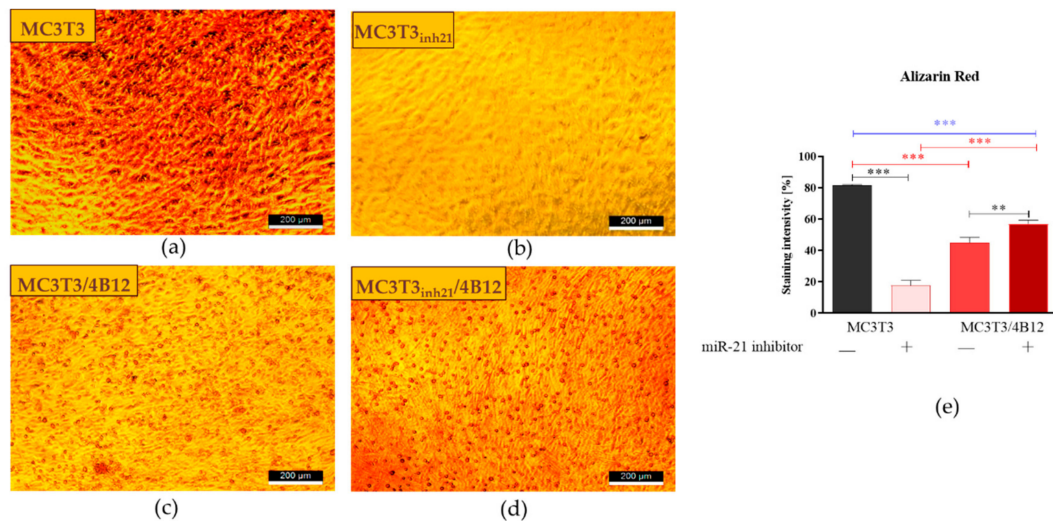


Figure 3. Representative images showing the results of Alizarin Red staining for calcium deposit detection. The mineralized extracellular matrix is stained with the dye. The images show an effect of miR-21 inhibition on mineralization of extracellular matrix formed by pre-osteoblast. The analysis included the determination of osteoclast precursors' activity (co-culturing with 4B12) on MC3T3 osteogenic differentiation. Osteogenic differentiation of MC3T3 was manifested by red calcium deposits (a). The decreased mineralization was observed in cultures of MC3T3 with blocked activity of miR-21 (b). The influence of 4B12 pre-osteoclast presence during osteogenic differentiation was monitored both in co-culture with MC3T3 (c) and MC3T3_{inh21} (d). Images were taken under 100-fold magnification (scale bar indicated). Staining intensity was determined using ImageJ software with Pixel Counter application, as indicated in Materials and Methods section (e). Significant differences are marked using an asterisks (** $p < 0.01$ and *** $p < 0.001$), while non-significant differences are described as *ns*. The comparisons between groups are marked with square brackets.

We also determined the influence of miR-21 inhibition on proteoglycan content in extracellular matrix formed by the cells under osteogenic conditions (d15). Images obtained after Safranin-O staining (Figure 4) coincide with the results of Alizarin Red analysis (Figure 2). The most abundant accumulation of proteoglycans was observed in osteogenic cultures of MC3T3 (Figure 4a). Transfection of pre-osteoblasts with the miR-21 inhibitor, as well as co-culture of MC3T with 4B12 pre-osteoclasts diminished the synthesis of proteoglycans and their deposition in the extracellular matrix (Figure 4b,c). The intense reaction indicating high proteoglycan content was noted in MC3T3_{inh21} co-cultured with pre-osteoclasts (Figure 4d). Comparative analysis of staining intensity confirmed microscopic observations (Figure 4e).

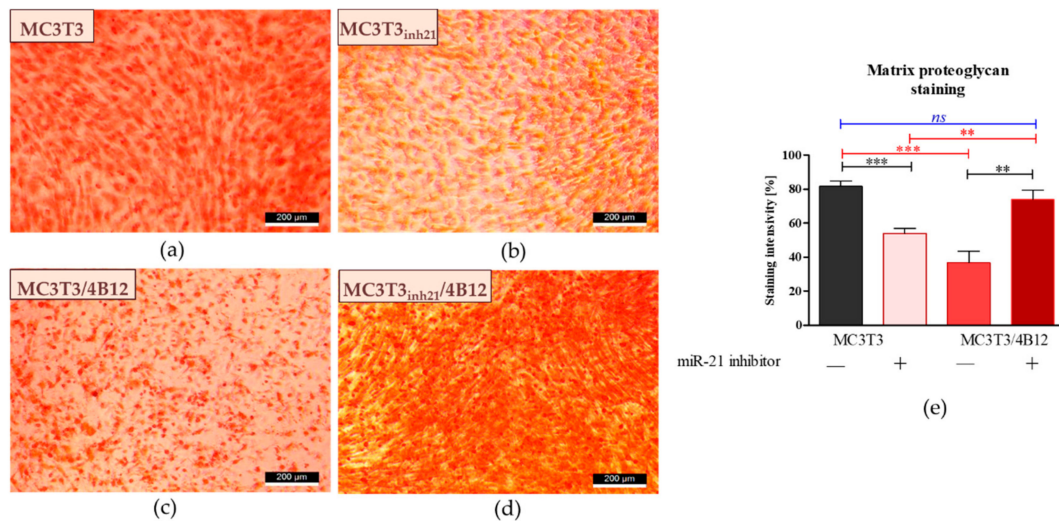


Figure 4. Representative images showing detection of proteoglycans with Safranin-O. The images show the effect of miR-21 inhibition on proteoglycan accumulation within the extracellular matrix formed by pre-osteoblasts under osteogenic conditions. Additionally, influence of osteoclast precursors on MC3T3 differentiation was evaluated. Osteogenic differentiation of MC3T3 was associated with increased accumulation of proteoglycans (a). The decreased content of proteoglycans was observed in cultures of MC3T3 transfected with miR-21 inhibitor (b). The influence of 4B12 pre-osteoclast presence during osteogenic differentiation of MC3T3 was monitored. The analysis revealed that osteoclasts presence decreased the accumulation of proteoglycans (c). In turn, extracellular matrix which formed in co-cultures of MC3T3_{inh21} with osteoclasts was rich in proteoglycans (d). Images were taken under 100-fold magnification (scale bar indicated). The staining intensity was determined using ImageJ software with Pixel Counter application, as indicated in Materials and Methods section (e). Significant differences are indicated with asterisks (** $p < 0.01$ and *** $p < 0.001$), while non-significant differences are marked as *ns*. The comparisons between groups are marked with square brackets.

3.4. The Influence of miR-21 Inhibition on Intracellular Accumulation of OPN and RUNX-2 in MC3T3 after 15 Days of Osteogenesis

Western blot analysis was performed to determine the influence of the miR-21 inhibition on intracellular expression of OPN and RUNX-2 in pre-osteoblast maintained under osteogenic conditions. The analysis indicated the presence of three different immunoreactive bands for OPN having various molecular weight: 66 kDa resembling full-length protein, as well as 30 kDa and 24 kDa bands resulting from the full-length protein cleavage (Figure 5a). The densitometry analysis of band intensities indicated that the inhibition of miRNA-21 decreases the expression of 66 kDa OPN, however the differences were not statistically significant (Figure 5b). Furthermore, the presence of osteoclast precursors in osteogenic cultures of MC3T3 (co-cultures) resulted in significant accumulation of 66 kDa OPN. Next, we analyzed the levels of 30 kDa OPN, and we observed that the band intensity is not altered by miR-21 inhibition for cells cultured in the monolayer system (Figure 4c). In the co-culture of MC3T3 with 4B12 we noted significant increase of 30 kDa protein. In contrast to that, we determined the significant decrease of protein in homogenates derived from MC3T3_{inh21} cultured with osteoclasts. The expression of 25 kDa OPN was notably increased in the osteogenic cultures of MC3T3, the protein level significantly decreased after miR-21 inhibition also in the presence of osteoclasts (Figure 5d). The expression of 65 kDa and 55 kDa RUNX-2 decreased after miR-21 inhibition (Figure 5e,f), however significant difference in terms of signal intensity was noted only for 65 kDa bands. The expression of RUNX-2 decreased in the co-culture system of MC3T3/4B12. The inhibition of miR-21 expression in MC3T3 cultured with pre-osteoclast had no effect on RUNX-2 intracellular accumulation.

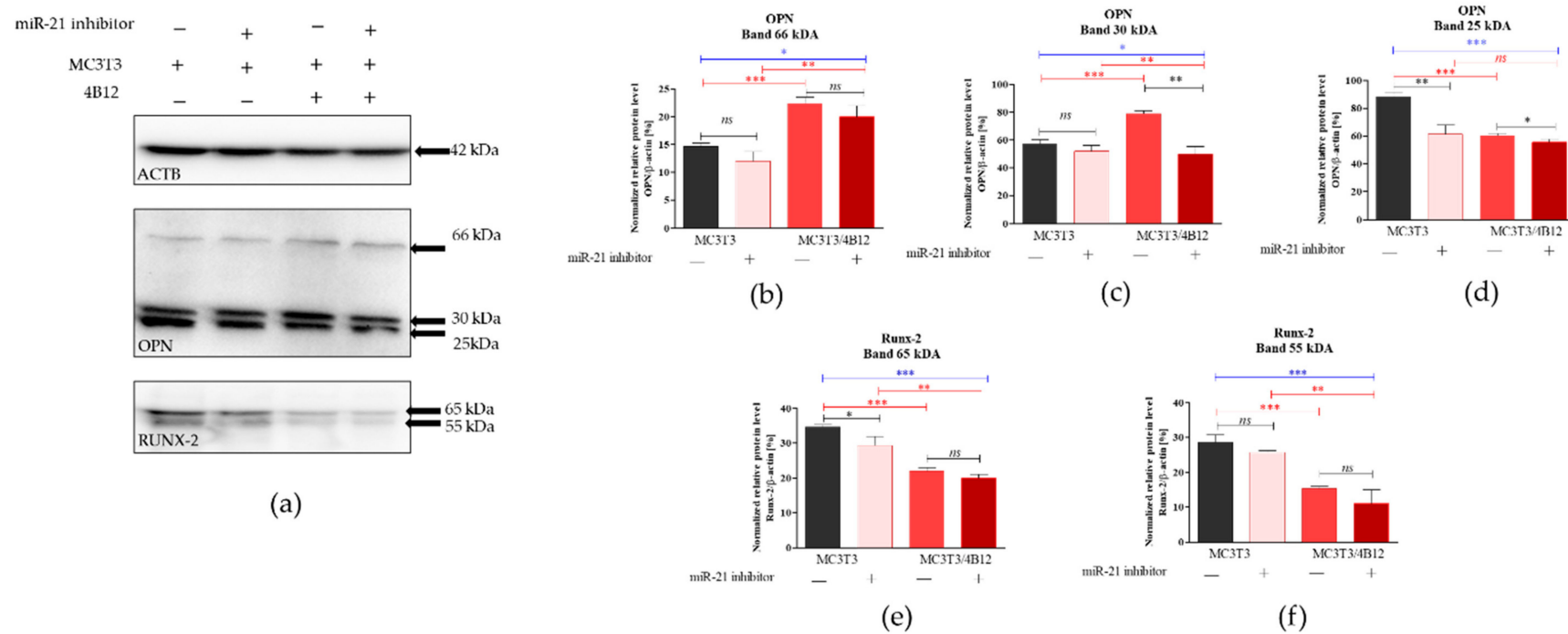


Figure 5. Intracellular accumulation of osteopontin (OPN) and runt-related transcription factor 2 (*Runx-2*). The β -actin (ACTB) was used as a housekeeping protein for normalization. The representative blots are shown in graph (a) and molecular weights of the detected proteins are indicated on the right. Results of statistical analysis performed on normalized values are shown in graphs (b–f). Significant differences are indicated with asterisks (* $p < 0.05$; ** $p < 0.01$ and *** $p < 0.001$), while non-significant differences are marked as *ns*. The comparisons between groups are marked with square brackets.

Immunocytochemistry was used to determine the OPN cellular localization (Figure 6). Images obtained with confocal microscope confirmed that OPN expression decreases after the miR-21 inhibition. Moreover, the increase of OPN expression was confirmed in MC3T3/4B12 cultures. The visualization of actin cytoskeleton indicated that under osteogenic conditions, MC3T3 are characterized by well-developed network supporting intracellular connections. The inhibition of miR-21 caused the alteration in cytoskeleton organization by weakening the architecture of actin network. In the co-culture system of MC3T3 and 4B12, the loss of intracellular connections was noted. Images obtained for MC3T3_{inh21}/4B12 co-cultures indicated an increase in number of osteoblasts and maintenance of intracellular connections between pre-osteoblast.

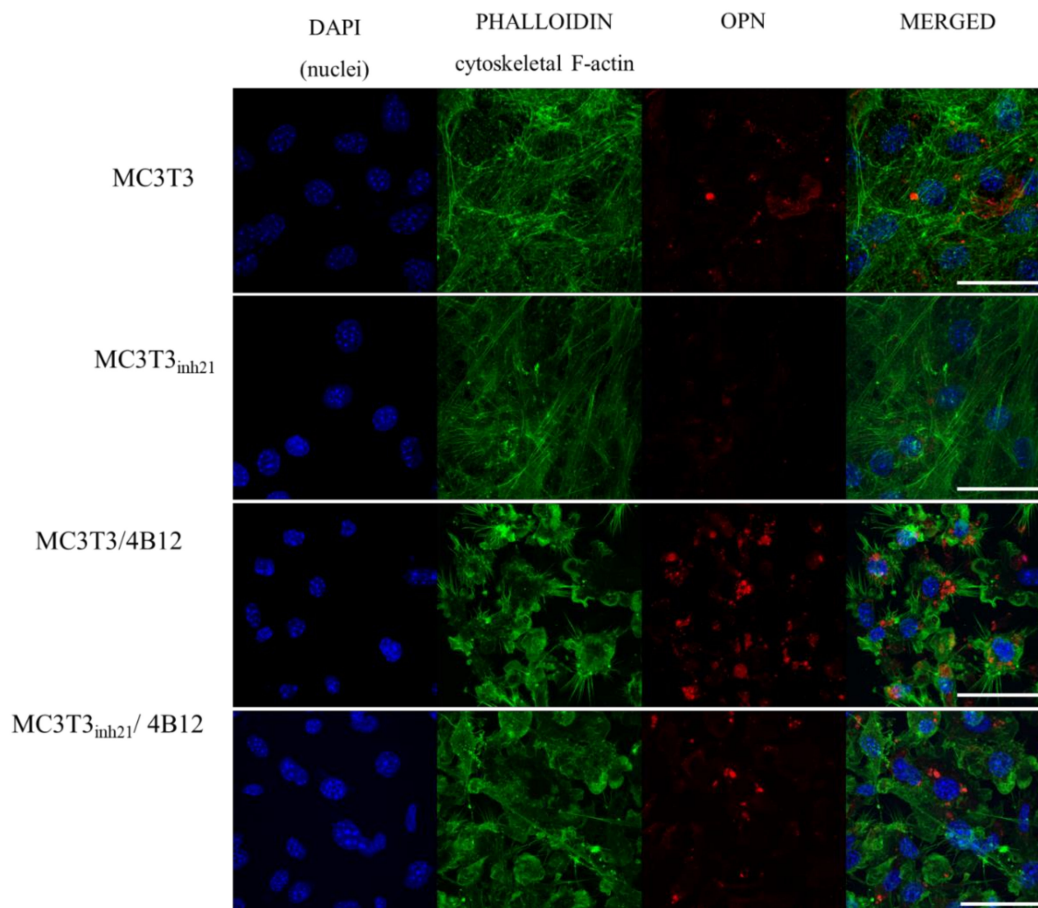


Figure 6. Representative images (Z-projects) showing co-localization of OPN (red signal) with nuclei (blue, DAPI stained) and cytoskeleton (green, phalloidin atto-488 stained). The images were taken under 60-fold magnification. The scale bar is equal to 50 μ m.

3.5. The Analysis of Markers Associated with Differentiation and Bone Resorption Activity of Osteoclasts

Bearing in mind the *Rankl/Opg* profile expression obtained for MC3T3 cultures after 15 days of osteogenesis, we were interested in an analysis of markers that are strictly characteristic for the activity of osteoclast cells, as well as for their survival. The analysis included measurement of mRNA levels for receptor activator of nuclear factor κ B (*Rank*), tartrate-resistant acid phosphatase (*Trap*), cathepsin K (*Ctsk*), carbonic anhydrase II (*Call*), and matrix metalloproteinase 9 (*Mmp-9*), as well as genes from B-cell lymphoma 2 family associated with apoptosis, i.e., pro-apoptotic *Bax* and anti-apoptotic *Bcl-2*. Obtained results showed significantly increased levels of transcripts for *Rank*, *Trap*, *Ctsk*, *Call*, and *Mmp-9* in 4B12 co-cultured with MC3T3 without inhibitor (Figure 7a–d) which indicates increased pre-osteoclasts activity. In contrast, the osteoclasts cultured with MC3T3_{inh21} expressed pro-apoptotic profile related to increased levels of mRNA for *Bax* and decreased for *Bcl-2* (Figure 7e).

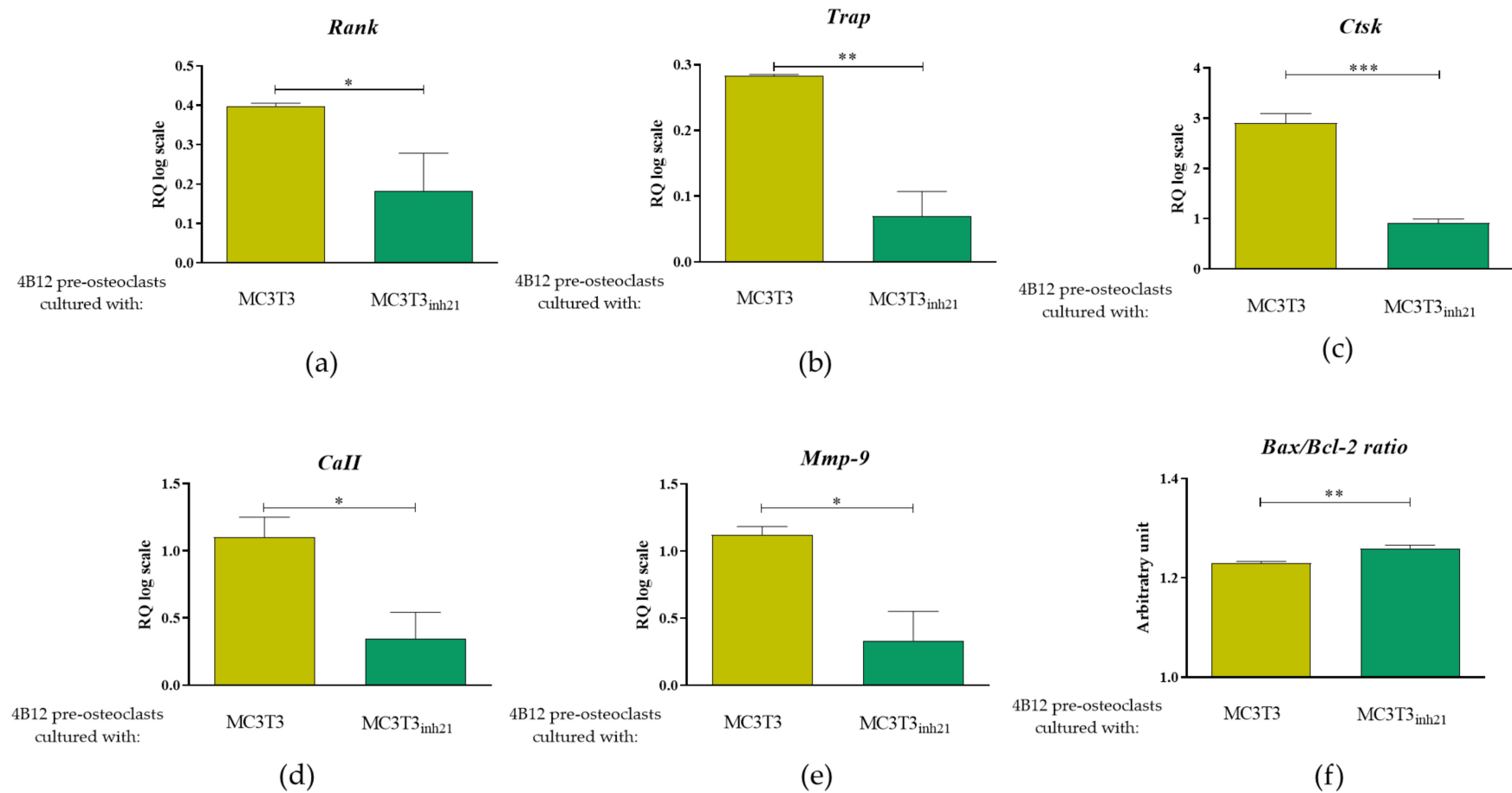


Figure 7. The expression of mRNA for typical osteoclast markers and molecules associated with apoptosis. The analysis included determination of transcript levels for receptor activator of nuclear factor κ B (a), tartrate-resistant acid phosphatase (b), cathepsin K (c), carbonic anhydrase II (d) and matrix metalloproteinase 9 (e). Moreover, the ratio of pro-apoptotic *Bax* and anti-apoptotic *Bcl-2* gene was calculated (f). Significant differences between groups are indicated with asterisks (* $p < 0.05$; ** $p < 0.01$ and *** $p < 0.001$), while non-significant differences are marked as *ns*.

Following that, TRAP expression was studied using immunocytochemistry technique. We did not observe a specific signal derived from TRAP positive cells in MC3T3 and MC3T3_{inh21} cultures (Figure S3, Supplementary materials). In turn, the analysis of the TRAP expression performed on co-cultures of pre-osteoblast and 4B12 revealed that occurrence of TRAP positive cells increased in the MC3T3/4B12 co-culture system, while decreasing in MC3T3_{inh21}/4B12 (Figure 8), which confirms the results obtained by RT-qPCR (Figure 7b).

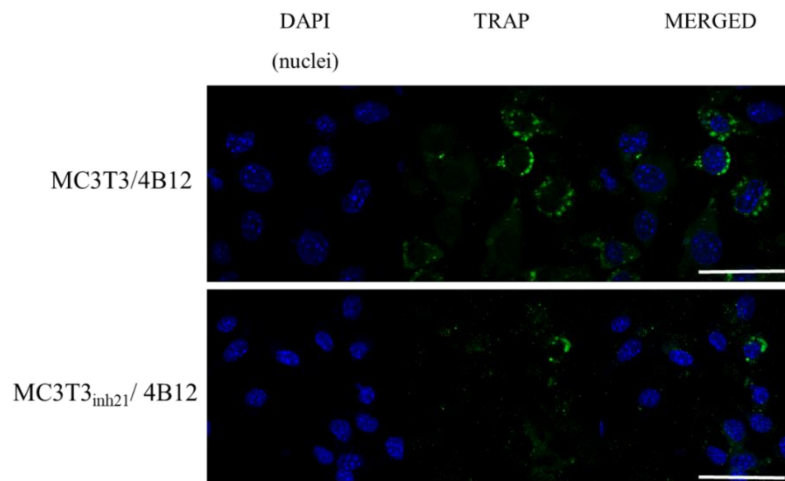


Figure 8. Representative images showing co-localization of tartrate-resistant acid phosphatase (TRAP) (green signal) with nuclei (blue, DAPI stained). The images were taken under 60-fold magnification. The scale bar is equal to 50 μ m.

4. Discussion

The number of studies related to function of miR-21 in bone homeostasis maintenance has grown rapidly over the past few years. Despite the efforts, the function of miR-21 in the biology of bone forming and bone-resorbing cells has not been fully elucidated. The aim of this study was to investigate the role of miR-21 during differentiation of osteoblast precursors—MC3T3 cell line. In addition, we determined the effect of miR-21 inhibition on osteoblast interaction with osteoclasts precursors using indirect co-culture system of MC3T3_{inh21} and semi-adherent pre-osteoclasts cell line 4B12 [18]. This model allowed us to study paracrine interactions between differentiating osteoblasts and osteoclasts [34]. We used this strategy to monitor individual phenotype changes and gene expression characteristics, both in osteoblast and osteoclast, which is difficult in the condition of direct co-culturing. Moreover, the indirect co-culture model is more accurate for cells with different characteristics of growth [35,36].

Various research groups put forward compelling evidence that miR-21 promotes differentiation of progenitor cells toward osteoblasts. The function of miR-21 as an essential molecule promoting bone regeneration was determined for example using model of multipotent stromal cells (MSCs) [2,7,12,14]. However, discussed results were inconsistent and contradictory, indicating that miR-21 may promote, as well as inhibit osteogenic differentiation, what can be correlated with diverse cellular plasticity of MSCs and their origin. To minimize this issue, we used the model of pre-osteoblast MC3T3 cell line that represents a stable and reproducible model for studies related with signaling pathways crucial for proliferation and differentiation of osteoblast [37–41]. Furthermore, under osteogenic conditions MC3T3 pre-osteoblasts synthesize and assemble collagenous extracellular matrix with organization and mineralization that resembles bone [37]. Previously, it was shown that overexpression of miR-21 in MC3T3 pre-osteoblast improves matrix mineralization, whereas the miR-21 inhibition was correlated with lowered calcium deposition [11]. The results are in good agreement with our data, confirming that miR-21 inhibition is associated with decreased deposition of calcium and lowered proteoglycan content in extracellular matrix (ECM).

We have also noted reduced mineralization of ECM in the co-culture model of MC3T3/4B12, which correlates with high occurrence of TRAP positive cells and increased mRNA levels for *Rank*, and other osteoclastic bone resorption-related genes like MMP-9, cathepsin K (*Ctsk*) and carbonic anhydrase II (*CaII*). In turn, the activity of TRAP-positive cells was reduced in co-cultures of MC3T3_{inh21}/4B12, indicating that inhibition of miR-21 in osteoblast may reduce paracrine signals necessary for pre-osteoclasts survival [42]. Thus, the mineralization of ECM in MC3T3_{inh21}/4B12 culture was less influenced by osteoclasts activity.

As miR-21 regulates the process of osteogenesis at the molecular level, we decided to determine the mRNA expression of main osteogenic markers after 3, 7, and 15 days of osteogenic stimulation. We showed that miR-21 inhibition is associated with decreased mRNA levels for collagen I (*Coll-1*), osteocalcin (*Ocl*) and *Runx-2*, which was previously reported by Li et al. [11]. We also studied the influence of miR-21 inhibition on the mRNA levels of osteopontin (*Opn*). This molecule plays a crucial role in bone remodeling by influencing differentiation of osteoblasts and determining survival of osteoclasts. An effect of miR-21 overexpression on *Opn* mRNA levels was recently studied using BMSCs model [7]. Authors showed that *Opn* expression increases in BMSCs as a result of miR-21 upregulation [7]. Our results confirmed the role of miR-21 as a molecule regulating *Opn* expression. MC3T3 with downregulated expression of miR-21 had lowered *Opn* expression, measured at 7 and 15 days of in vitro osteogenesis. Nevertheless, we observed that *Opn* mRNA level increases in the co-culture of MC3T3 with 4B12 cells. This is in agreement with studies showing that osteopontin plays crucial role in modulating osteoclast-osteoblast interactions, both in vivo and in vitro. Boskey et al. [43] showed that OPN knockout mice are characterized by elevated mineral content and crystallinity in bone, while OPN knockout osteoblasts formed matrix with increased mineral deposition [44]. This observation may explain the improvement of matrix mineralization in model of MC3T3_{inh21} propagated with 4B12 pre-osteoblasts.

Having the results obtained on mRNA level, we decided to determine the expression of OPN using Western blot technique. We detected three different immunoreactive bands of OPN, i.e., 66 kDa, as well as 30 and 25 kDa. We observed that in the co-culture system the expression of OPN at molecular weight equal to 66 kDa (doublets) increases, in contrast to the monolayer cultures. The miR-21 inhibition does not have any influence on OPN expression at 66 kDa. However, in MC3T3/4B12 cultures we observed the increased expression of OPN at 35 kDa, and its levels significantly decreased in the co-cultures of MC3T3_{inh21}/4B12. Obtained results confirm previous data, indicating that OPN produced by osteoblasts can activate bone resorption by osteoclasts [45]. The OPN expression after miR-21 inhibition may explain the images obtained after ECM staining, showing the improvement in matrix biomineralization in MC3T3_{inh21}/4B12 cultures. Osteogenic cultures of MC3T3 were characterized by increased expression of smaller molecular-weight OPN protein—25 kDa. The function of low molecular weight OPN is not properly described in the literature, however it was shown that this protein may be a product of OPN cleavage with matrix metalloproteinases [46]. We also determined the intracellular localization of OPN in the experimental cultures, and the results of analysis were consistent with data obtained using RT-qPCR, showing decrease of OPN after miR-21 inhibition in MC3T3 cells as well as increase of OPN expression in the co-cultures of MC3T3 with 4B12 pre-osteoclasts.

Further, we confirmed that the miR-21 inhibition may significantly reduce the intracellular accumulation of RUNX-2, which is a common regulator of osteogenesis [47,48]. The obtained results are consistent with recent studies showing that BMSCs after transfection with the miR-21 inhibitor exhibit lowered accumulation of intracellular RUNX-2 on both mRNA [1] and protein level [12].

A study performed by Li et al. indicated that miR-21 regulates differentiation of progenitor cells into bone forming cells via the Smad7-Smad1/5/8-Runx2 pathway. Moreover, it was shown that miR-21 deficiency impaired the bone formation of calvarial bone defects, what might result from deterioration of osteogenic potential of endogenous progenitor cells. Multipotent stromal cells derived from bone marrow of miR-21 knock-out mice, exhibited lowered osteogenic potential associated with decreased mRNA levels for Runx-2 [12]. Additionally, Meng et al. showed that miR-21 promotes osteogenic

differentiation of human umbilical cord mesenchymal stem cells (hUMSCs) through PI3K/ β -catenin pathway, activating the transcription of RUNX-2 [14]. However expression of *Runx-2* is modulated at multiply levels during the osteogenesis. *Runx-2* expression profile strictly depends on differentiation stage of the cells. It was previously indicated that *Runx-2* may act as a positive regulator during early stages of osteoblast differentiation and negative regulator at later stage of osteogenesis [47–49]. Given the stage-dependent shift of *Runx2* expression, the role of miRNA-21 as a regulator of *Runx-2* should be monitored at early, mid and late stage of osteogenesis, what was also confirmed in our study.

It was speculated previously, that RUNX-2 controls RANKL expression and that this interaction conveys molecular background for the linkage between osteoblast and osteoclast formation [50]. Our results confirmed this dependency. We have shown that RANKL/OPG ratio is increased in MC3T3 pre-osteoblasts transfected with the miR-21 inhibitor, thus we expected the increased osteoclast formation and activity in this condition. However, in the co-culture system of MC3T3_{inh21}/4B12 we observed the decrease of RANKL/OPG ratio. Obtained result confirmed the study of Pitari et al. who showed that co-culture of multiple myeloma cells with BMSCs under constitutive inhibition of miR-21 may result in the restoration of RANKL/OPG balance and impair the resorbing activity of mature osteoclasts [51]. This implies, that the miR-21 inhibition may affect the activity of pre-osteoclasts and their survival regulating RANKL expression. This is in agreement with studies of Sutherland et al. [52], showing that RANKL protects osteoclasts from the apoptosis-inducing and anti-resorptive effects of bisphosphonates in vitro, via anti-apoptotic protein Mcl-1. In turn, in our study we showed that the inhibition of miR-21 in pre-osteoblast is associated with the lowered expression of *Rankl*, and increased *Bax/Bcl-2* ratio. Obtained results coincide with research of Hu et al. showing that pro-osteoclastic effect of miR-21 may be associated with its function during regulation of programmed cell death [53]. Moreover, the most recent research of Luukkonen et al. [54] showed that the inhibition of miR-21 associated with decreased OPN accumulation affects survival of pre-osteoclasts. The OPN is essential for osteoclasts attachment to the resorbed matrix and the cell surface receptor. Luukkonen et al. showed that OPN produced in the resorption pits may inhibit bone mineralization, what also confirms the suppressive effect of OPN on osteoblast physiology emerging from autocrine/paracrine signals. Of note, confocal analysis of MC3T3_{inh21}/4B12 co-cultures showed decreased TRAP expression which was also evidenced at mRNA level. This result is in line with study of Ek-Rylander and Andersson, who indicated that TRAP could regulate the extent of ECM degradation including depth and area at each bone resorption site [55]. The study showed that TRAP modulates OPN-dependent osteoclasts migration and triggers osteoclast detachment facilitating their subsequent movement on the bone surface. Given the increased apoptosis of pre-osteoclasts cultured with MC3T3_{inh21}, we hypothesize that lowered viability of TRAP positive pre-osteoclasts could be solely due to altered osteoblast signaling.

5. Conclusions

In summary, we demonstrated that decreased expression of miR-21 in MC3T3 pre-osteoblasts cell line results in loss of their bone forming capability, what was evidenced by poor mineralization of extracellular matrix in vitro and lowered expression of essential bone markers. Moreover, the inhibition of miR-21 expression attenuated paracrine activity of pre-osteoblast, which was associated with increased apoptosis of pre-osteoclasts in the co-culture model. The observed effect may be related with the function of miR-21 as a regulator of key molecules regulating osteoblastogenesis and osteoclastogenesis. MiR-21 may have a dual role in the process of osteoblast-osteoclast coupling, probably due to the fact that its targets (eg. *Rankl* and *Opn*) are regulated in a dynamic manner during the process of osteogenesis. Thus, analysis of regulatory effect of miR-21 should be determined at different stages of osteogenesis in order to elucidate its influence on genes expressed during early osteogenic commitment (d3, d7, and d15). Obtained results are in line with other studies indicating the emerging role of miR-21 in terms of regulation of bone metabolism and homeostasis. Profound characterization of miR-21 function in osteoblast-osteoclast coupling may account for development of novel therapies directly influencing bone cell differentiation and the process of bone remodeling.

Supplementary Materials: The following are available online at <http://www.mdpi.com/2073-4409/9/2/479/s1>. Table S1. Sequences of the primers used in the experiment. Figure S1. Analysis of effectiveness of miR-21 inhibition in MC3T3 cell line. Figure S2. The influence of transfection with miR21 inhibitor on MC3T3 proliferative activity. Figure S3. The results showing a specific action of miR-21 inhibitor in osteogenic cultures. Figure S4. The analysis of calcium (Ca) and phosphorus (P) content deposited in extracellular matrix formed by MC3T3. Figure S5. The influence of miR-21 inhibition on TRAP expression in the MC3T3 osteoblasts.

Author Contributions: Conceptualization, A.S. and K.M. (Krzysztof Marycz); methodology, A.S., K.M. (Klaudia Marcinkowska); software, A.S., K.M. (Klaudia Marcinkowska) and A.P.; validation, A.S., L.V. and K.M. (Krzysztof Marycz); formal analysis, A.S.; investigation, A.S., K.M. (Klaudia Marcinkowska), A.P.; M.S.; resources, K.M. (Krzysztof Marycz); data curation, A.S., K.M. (Klaudia Marcinkowska); writing—original draft preparation, A.S., K.M. (Klaudia Marcinkowska), A.P. and L.V.; writing—review and editing, A.S., K.M. (Klaudia Marcinkowska) and L.V.; visualization, A.S. and L.V.; supervision, A.S. and L.V.; project administration A.S. and K.M. (Krzysztof Marycz); funding acquisition, L.V. and K.M. (Krzysztof Marycz)”, please turn to the CRediT taxonomy for the term explanation. Authorship must be limited to those who have contributed substantially to the work reported. All authors have read and agreed to the published version of the manuscript.

Funding: Financial support from the National Science Centre over the course of the realization of the project Harmonia 10 titled “New, two-stage scaffolds based on calcium nanoapatite (nHAP) incorporated with iron nanotoxides ($\text{Fe}_2\text{O}_3/\text{Fe}_3\text{O}_4$) with the function of controlled release of miRNA in a static magnetic field for the regeneration of bone fractures in osteoporotic patients” (Grant No. UMO 2017/26/M/NZ5/01184) is gratefully acknowledged. This study is supported by following grants: Czech Science Foundation GACR 18-21942S, RVO 86652036 and BIOCEV CZ.1.05/1.1.00/02.0109.

Acknowledgments: The research is co-financed under the Leading Research Groups support project from the subsidy increased for the period 2020–2025 in the amount of 2% of the subsidy referred to Art. 387 (3) of the Law of 20 July 2018 on Higher Education and Science, obtained in 2019.

Conflicts of Interest: The authors declare no conflict of interest.

References

- Zhao, Z.; Li, X.; Zou, D.; Lian, Y.; Tian, S.; Dou, Z. Expression of microRNA-21 in osteoporotic patients and its involvement in the regulation of osteogenic differentiation. *Exp. Ther. Med.* **2019**, *17*, 709–714. [[CrossRef](#)] [[PubMed](#)]
- Cheng, V.K.; Au, P.C.; Tan, K.C.; Cheung, C. MicroRNA and Human Bone Health. *JBMR Plus* **2018**, *3*, 2–13. [[CrossRef](#)] [[PubMed](#)]
- Jia, B.; Zhang, Z.; Qiu, X.; Chu, H.; Sun, X.; Zheng, X.; Zhao, J.; Li, Q. Analysis of the miRNA and mRNA involved in osteogenesis of adipose-derived mesenchymal stem cells. *Exp. Ther. Med.* **2018**, *16*, 1111–1120. [[CrossRef](#)] [[PubMed](#)]
- Li, Z.; Hassan, M.Q.; Jafferji, M.; Aqeilan, R.I.; Garzon, R.; Croce, C.M.; van Wijnen, A.J.; Stein, J.L.; Stein, G.S.; Lian, J.B. Biological Functions of miR-29b Contribute to Positive Regulation of Osteoblast Differentiation. *J. Biol. Chem.* **2009**, *284*, 15676–15684. [[CrossRef](#)] [[PubMed](#)]
- Fröhlich, L.F. MicroRNAs at the Interface between Osteogenesis and Angiogenesis as Targets for Bone Regeneration. *Cells* **2019**, *8*, 121. [[CrossRef](#)]
- Wei, F.; Yang, S.; Guo, Q.; Zhang, X.; Ren, D.; Lv, T.; Xu, X. MicroRNA-21 regulates Osteogenic Differentiation of Periodontal Ligament Stem Cells by targeting Smad5. *Sci. Rep.* **2017**, *7*, 1–12. [[CrossRef](#)]
- Yang, C.; Liu, X.; Zhao, K.; Zhu, Y.; Hu, B.; Zhou, Y.; Wang, M.; Wu, Y.; Zhang, C.; Xu, J.; et al. miRNA-21 promotes osteogenesis via the PTEN/PI3K/Akt/HIF-1 α pathway and enhances bone regeneration in critical size defects. *Stem Cell Res. Ther.* **2019**, *10*, 65.
- Feng, Y.-H.; Tsao, C.-J. Emerging role of microRNA-21 in cancer. *Biomed. Rep.* **2016**, *5*, 395–402. [[CrossRef](#)]
- Medina, P.P.; Nolde, M.; Slack, F.J. OncomiR addiction in an in vivo model of microRNA-21-induced pre-B-cell lymphoma. *Nature* **2010**, *467*, 86–90. [[CrossRef](#)]
- Hu, X.; Li, L.; Lu, Y.; Yu, X.; Chen, H.; Yin, Q.; Zhang, Y. miRNA-21 inhibition inhibits osteosarcoma cell proliferation by targeting PTEN and regulating the TGF- β 1 signaling pathway. *Oncol. Lett.* **2018**, *16*, 4337–4342. [[CrossRef](#)]
- Li, H.; Yang, F.; Wang, Z.; Fu, Q.; Liang, A. MicroRNA-21 promotes osteogenic differentiation by targeting small mothers against decapentaplegic 7. *Mol. Med. Rep.* **2015**, *12*, 1561–1567. [[CrossRef](#)] [[PubMed](#)]

12. Li, X.; Guo, L.; Liu, Y.; Su, Y.; Xie, Y.; Du, J.; Zhou, J.; Ding, G.; Wang, H.; Bai, Y.; et al. MicroRNA-21 promotes osteogenesis of bone marrow mesenchymal stem cells via the Smad7-Smad1/5/8-Runx2 pathway. *Biochem. Biophys. Res. Commun.* **2017**, *493*, 928–933. [[CrossRef](#)] [[PubMed](#)]
13. Valenti, M.T.; Deiana, M.; Cheri, S.; Dotta, M.; Zamboni, F.; Gabbiani, D.; Schena, F.; Dalle Carbonare, L.; Mottes, M. Physical Exercise Modulates miR-21-5p, miR-129-5p, miR-378-5p, and miR-188-5p Expression in Progenitor Cells Promoting Osteogenesis. *Cells* **2019**, *8*, 742. [[CrossRef](#)] [[PubMed](#)]
14. Meng, Y.-B.; Li, X.; Li, Z.-Y.; Zhao, J.; Yuan, X.-B.; Ren, Y.; Cui, Z.-D.; Liu, Y.-D.; Yang, X.-J. microRNA-21 promotes osteogenic differentiation of mesenchymal stem cells by the PI3K/ β -catenin pathway. *J. Orthop. Res.* **2015**, *33*, 957–964. [[CrossRef](#)] [[PubMed](#)]
15. Molténi, A.; Modrowski, D.; Hott, M.; Marie, P.J. Alterations of matrix- and cell-associated proteoglycans inhibit osteogenesis and growth response to fibroblast growth factor-2 in cultured rat mandibular condyle and calvaria. *Cell Tissue Res.* **1999**, *295*, 523–536. [[CrossRef](#)] [[PubMed](#)]
16. Lozano, C.; Duroux-Richard, I.; Firat, H.; Schordan, E.; Apparailly, F. MicroRNAs: Key Regulators to Understand Osteoclast Differentiation? *Front. Immunol.* **2019**, *10*. [[CrossRef](#)]
17. Kobayashi, Y.; Udagawa, N.; Takahashi, N. Action of RANKL and OPG for osteoclastogenesis. *Crit. Rev. Eukaryot. Gene Exp.* **2009**, *19*, 61–72. [[CrossRef](#)]
18. Amano, S.; Sekine, K.; Bonewald, L.; Ohmori, Y. A Novel Osteoclast Precursor Cell Line, 4B12, Recapitulates the Features of Primary Osteoclast Differentiation and Function: Enhanced Transfection Efficiency Before and After Differentiation. *J. Cell Physiol.* **2009**, *221*, 40–53. [[CrossRef](#)]
19. Amano, S.; Chang, Y.-T.; Fukui, Y. ERK5 Activation Is Essential for Osteoclast Differentiation. *PLoS ONE* **2015**, *10*, e0125054. [[CrossRef](#)]
20. Androvic, P.; Valihrach, L.; Elling, J.; Sjoback, R.; Kubista, M. Two-tailed RT-qPCR: A novel method for highly accurate miRNA quantification. *Nucleic Acids Res.* **2017**, *45*, e144. [[CrossRef](#)]
21. Androvic, P.; Romanyuk, N.; Urdzikova-Machova, L.; Rohlova, E.; Kubista, M.; Valihrach, L. Two-tailed RT-qPCR panel for quality control of circulating microRNA studies. *Sci. Rep.* **2019**, *9*, 1–9. [[CrossRef](#)] [[PubMed](#)]
22. Smieszek, A.; Kornicka, K.; Szłapka-Kosarzewska, J.; Androvic, P.; Valihrach, L.; Langerova, L.; Rohlova, E.; Kubista, M.; Marycz, K. Metformin Increases Proliferative Activity and Viability of Multipotent Stromal Stem Cells Isolated from Adipose Tissue Derived from Horses with Equine Metabolic Syndrome. *Cells* **2019**, *8*, 80. [[CrossRef](#)] [[PubMed](#)]
23. Smieszek, A.; Tomaszewski, K.A.; Kornicka, K.; Marycz, K. Metformin Promotes Osteogenic Differentiation of Adipose-Derived Stromal Cells and Exerts Pro-Osteogenic Effect Stimulating Bone Regeneration. *J. Clin. Med.* **2018**, *7*, 482. [[CrossRef](#)] [[PubMed](#)]
24. Zimoch-Korzycka, A.; Śmieszek, A.; Jarmoluk, A.; Nowak, U.; Marycz, K. Potential Biomedical Application of Enzymatically Treated Alginate/Chitosan Hydrosols in Sponges-Biocompatible Scaffolds Inducing Chondrogenic Differentiation of Human Adipose Derived Multipotent Stromal Cells. *Polymers* **2016**, *8*, 320. [[CrossRef](#)]
25. Schindelin, J.; Arganda-Carreras, I.; Frise, E.; Kaynig, V.; Longair, M.; Pietzsch, T.; Preibisch, S.; Rueden, C.; Saalfeld, S.; Schmid, B.; et al. Fiji: An open-source platform for biological-image analysis. *Nat. Methods* **2012**, *9*, 676–682. [[CrossRef](#)]
26. Jensen, E.C. Quantitative analysis of histological staining and fluorescence using ImageJ. *Anat. Rec. Hoboken* **2013**, *296*, 378–381. [[CrossRef](#)]
27. Śmieszek, A.; Stręk, Z.; Kornicka, K.; Grzesiak, J.; Weiss, C.; Marycz, K. Antioxidant and Anti-Senescence Effect of Metformin on Mouse Olfactory Ensheathing Cells (mOECs) May Be Associated with Increased Brain-Derived Neurotrophic Factor Levels—An Ex Vivo Study. *Int. J. Mol. Sci.* **2017**, *18*, 872. [[CrossRef](#)]
28. Śmieszek, A.; Szydłarska, J.; Mucha, A.; Chrapiec, M.; Marycz, K. Enhanced cytocompatibility and osteoinductive properties of sol-gel-derived silica/zirconium dioxide coatings by metformin functionalization. *J. Biomater. Appl.* **2017**, *32*, 570–586. [[CrossRef](#)]
29. Chomczynski, P.; Sacchi, N. Single-step method of RNA isolation by acid guanidinium thiocyanate-phenol-chloroform extraction. *Anal. Biochem.* **1987**, *162*, 156–159. [[CrossRef](#)]
30. Smieszek, A.; Marycz, K.; Szustakiewicz, K.; Kryszak, B.; Targonska, S.; Zawisza, K.; Watras, A.; Wiglusz, R.J. New approach to modification of poly (l-lactic acid) with nano-hydroxyapatite improving functionality of

- human adipose-derived stromal cells (hASCs) through increased viability and enhanced mitochondrial activity. *Mater. Sci. Eng. C* **2019**, *98*, 213–226.
31. Marycz, K.; Weiss, C.; Śmieszek, A.; Kornicka, K. Evaluation of Oxidative Stress and Mitophagy during Adipogenic Differentiation of Adipose-Derived Stem Cells Isolated from Equine Metabolic Syndrome (EMS) Horses. *Stem Cells Int.* **2018**, *2018*, 1–18. [[CrossRef](#)] [[PubMed](#)]
 32. Marycz, K.; Sobierajska, P.; Smieszek, A.; Maredziak, M.; Wiglusz, K.; Wiglusz, R.J. Li⁺ activated nanohydroxyapatite doped with Eu³⁺ ions enhances proliferative activity and viability of human stem progenitor cells of adipose tissue and olfactory ensheathing cells. Further perspective of nHAP:Li⁺, Eu³⁺ application in theranostics. *Mater. Sci. Eng. C Mater. Biol. Appl.* **2017**, *78*, 151–162. [[CrossRef](#)] [[PubMed](#)]
 33. Jeon, J.; Lee, M.S.; Yang, H.S. Differentiated osteoblasts derived decellularized extracellular matrix to promote osteogenic differentiation. *Biomater. Res.* **2018**, *22*, 4. [[CrossRef](#)]
 34. Zhu, S.; Ehnert, S.; Rouß, M.; Häussling, V.; Aspera-Werz, R.H.; Chen, T.; Nussler, A.K. From the Clinical Problem to the Basic Research—Co-Culture Models of Osteoblasts and Osteoclasts. *Int. J. Mol. Sci.* **2018**, *19*, 2284. [[CrossRef](#)]
 35. Janardhanan, S.; Wang, M.O.; Fisher, J.P. Coculture Strategies in Bone Tissue Engineering: The Impact of Culture Conditions on Pluripotent Stem Cell Populations. *Tissue Eng. Part B Rev.* **2012**, *18*, 312–321. [[CrossRef](#)] [[PubMed](#)]
 36. Owen, R.; Reilly, G.C. In vitro Models of Bone Remodelling and Associated Disorders. *Front. Bioeng. Biotechnol.* **2018**, *6*, 134. [[CrossRef](#)] [[PubMed](#)]
 37. Addison, W.; Nelea, V.; Chicatun, F.; Chien, Y.; Tran-Khanh, N.; Buschmann, M.; Nazhat, S.; Kaartinen, M.; Vali, H.; Tecklenburg, M.; et al. Extracellular matrix mineralization in murine MC3T3-E1 osteoblast cultures: An ultrastructural, compositional and comparative analysis with mouse bone. *Bone* **2015**, *71*, 244–256. [[CrossRef](#)]
 38. Peng, J.; Huang, N.; Huang, S.; Li, L.; Ling, Z.; Jin, S.; Huang, A.; Lin, K.; Zou, X. Effect of miR-21 down-regulated by H₂O₂ on osteogenic differentiation of MC3T3-E1 cells. *Zhongguo Xiu Fu Chong Jian Wai Ke Za Zhi* **2018**, *32*, 276–284.
 39. Chai, X.; Zhang, W.; Chang, B.; Feng, X.; Song, J.; Li, L.; Yu, C.; Zhao, J.; Si, H. GPR39 agonist TC-G 1008 promotes osteoblast differentiation and mineralization in MC3T3-E1 cells. *Artif. Cells Nanomed. Biotechnol.* **2019**, *47*, 3569–3576. [[CrossRef](#)]
 40. Liu, L.; Wang, D.; Qin, Y.; Xu, M.; Zhou, L.; Xu, W.; Liu, X.; Ye, L.; Yue, S.; Zheng, Q.; et al. Astragalin Promotes Osteoblastic Differentiation in MC3T3-E1 Cells and Bone Formation in vivo. *Front. Endocrinol. Lausanne* **2019**, *10*, 228. [[CrossRef](#)]
 41. Sterner, R.M.; Kremer, K.N.; Dudakovic, A.; Westendorf, J.J.; van Wijnen, A.J.; Hedin, K.E. Tissue-Nonspecific Alkaline Phosphatase Is Required for MC3T3 Osteoblast-Mediated Protection of Acute Myeloid Leukemia Cells from Apoptosis. *J. Immunol.* **2018**, *201*, 1086–1096. [[CrossRef](#)] [[PubMed](#)]
 42. Chen, X.; Wang, Z.; Duan, N.; Zhu, G.; Schwarz, E.M.; Xie, C. Osteoblast-osteoclast interactions. *Connect. Tissue Res.* **2018**, *59*, 99–107. [[CrossRef](#)] [[PubMed](#)]
 43. Boskey, A.L.; Spevak, L.; Paschalis, E.; Doty, S.B.; McKee, M.D. Osteopontin deficiency increases mineral content and mineral crystallinity in mouse bone. *Calcif. Tissue Int.* **2002**, *71*, 145–154. [[CrossRef](#)] [[PubMed](#)]
 44. Holm, E.; Gleberzon, J.S.; Liao, Y.; Sørensen, E.S.; Beier, F.; Hunter, G.K.; Goldberg, H.A. Osteopontin mediates mineralization and not osteogenic cell development in vitro. *Biochem. J.* **2014**, *464*, 355–364. [[CrossRef](#)]
 45. Rittling, S.R.; Matsumoto, H.N.; Mckee, M.D.; Nanci, A.; An, X.-R.; Novick, K.E.; Kowalski, A.J.; Noda, M.; Denhardt, D.T. Mice Lacking Osteopontin Show Normal Development and Bone Structure but Display Altered Osteoclast Formation In Vitro. *J. Bone Mineral. Res.* **1998**, *13*, 1101–1111. [[CrossRef](#)]
 46. Denhardt, D.T.; Guo, X. Osteopontin: A protein with diverse functions. *FASEB J.* **1993**, *7*, 1475–1482. [[CrossRef](#)]
 47. Pregizer, S.; Baniwal, S.K.; Yan, X.; Borok, Z.; Frenkel, B. Progressive recruitment of Runx2 to genomic targets despite decreasing expression during osteoblast differentiation. *J. Cell Biochem.* **2008**, *105*, 965–970. [[CrossRef](#)]
 48. Bruderer, M.; Richards, R.G.; Alini, M.; Stoddart, M.J. Role and regulation of RUNX2 in osteogenesis. *Eur. Cell Mater.* **2014**, *28*, 269–286. [[CrossRef](#)]
 49. Xu, J.; Li, Z.; Hou, Y.; Fang, W. Potential mechanisms underlying the Runx2 induced osteogenesis of bone marrow mesenchymal stem cells. *Am. J. Transl. Res.* **2015**, *7*, 2527–2535.
 50. O'Brien, C.A. Control of RANKL Gene Expression. *Bone* **2010**, *46*, 911–919. [[CrossRef](#)]

51. Pitari, M.R.; Rossi, M.; Amodio, N.; Botta, C.; Morelli, E.; Federico, C.; Gullà, A.; Caracciolo, D.; Di Martino, M.T.; Arbitrio, M.; et al. Inhibition of miR-21 restores RANKL/OPG ratio in multiple myeloma-derived bone marrow stromal cells and impairs the resorbing activity of mature osteoclasts. *Oncotarget* **2015**, *6*, 27343–27358. [[CrossRef](#)] [[PubMed](#)]
52. Sutherland, K.A.; Rogers, H.L.; Tosh, D.; Rogers, M.J. RANKL increases the level of Mcl-1 in osteoclasts and reduces bisphosphonate-induced osteoclast apoptosis in vitro. *Arthritis Res. Ther.* **2009**, *11*, R58. [[CrossRef](#)] [[PubMed](#)]
53. Hu, C.-H.; Sui, B.-D.; Du, F.-Y.; Shuai, Y.; Zheng, C.-X.; Zhao, P.; Yu, X.-R.; Jin, Y. miR-21 deficiency inhibits osteoclast function and prevents bone loss in mice. *Sci. Rep.* **2017**, *7*, 1–14. [[CrossRef](#)] [[PubMed](#)]
54. Luukkonen, J.; Hilli, M.; Nakamura, M.; Ritamo, I.; Valmu, L.; Kauppinen, K.; Tuukkanen, J.; Lehenkari, P. Osteoclasts secrete osteopontin into resorption lacunae during bone resorption. *Histochem. Cell Biol.* **2019**, *151*, 475–487. [[CrossRef](#)] [[PubMed](#)]
55. Ek-Rylander, B.; Andersson, G. Osteoclast migration on phosphorylated osteopontin is regulated by endogenous tartrate-resistant acid phosphatase. *Exp. Cell Res.* **2010**, *316*, 443–451. [[CrossRef](#)] [[PubMed](#)]



© 2020 by the authors. Licensee MDPI, Basel, Switzerland. This article is an open access article distributed under the terms and conditions of the Creative Commons Attribution (CC BY) license (<http://creativecommons.org/licenses/by/4.0/>).

Bone marrow stromal cells (BMSCs CD45⁻/CD44⁺/CD73⁺/CD90⁺) isolated from osteoporotic mice SAM/P6 as a novel model for osteoporosis investigation

Mateusz Sikora¹  | Agnieszka Śmieszek¹ | Krzysztof Marycz^{1,2} 

¹The Department of Experimental Biology, The Faculty of Biology and Animal Science, University of Environmental and Life Sciences Wrocław, Wrocław, Poland

²International Institute of Translational Medicine, Malin, Poland

Correspondence

Krzysztof Marycz, The Department of Experimental Biology, The Faculty of Biology and Animal Science, University of Environmental and Life Sciences Wrocław, Norwida 27B St, 50-375 Wrocław, Poland. Email: krzysztof.marycz@upwr.edu.pl

Funding information

Narodowe Centrum Nauki, Grant/Award Number: UMO 2017/26/M/NZ5/01184

Abstract

Available therapies aimed at treating age-related osteoporosis are still insufficient. Therefore, designing reliable in vitro model for the analysis of molecular mechanisms underlying senile osteoporosis is highly required. We have isolated and characterized progenitor cells isolated from bone marrow (BMSCs) of osteoporotic mice strain SAM/P6 (BMSC_{SAM/P6}). The cytophysiology of BMSC_{SAM/P6} was for the first time compared with BMSCs isolated from healthy BALB/c mice (BMSC_{BALB/c}). Characterization of the cells included evaluation of their multipotency, morphology and determination of specific phenotype. Viability of BMSCs cultures was determined in reference to apoptosis profile, metabolic activity, oxidative stress, mitochondrial membrane potential and caspase activation. Additionally, expression of relevant biomarkers was determined with RT-qPCR. Obtained results indicated that BMSC_{SAM/P6} and BMSC_{BALB/c} show the typical phenotype of mesenchymal stromal cells (CD44⁺, CD73⁺, CD90⁺) and do not express CD45. Further, BMSC_{SAM/P6} were characterized by deteriorated multipotency, decreased metabolic activity and increased apoptosis occurrence, accompanied by elevated oxidative stress and mitochondria depolarisation. The transcriptome analyses showed that BMSC_{SAM/P6} are distinguished by lowered expression of molecules crucial for proper osteogenesis, including *Coll-1*, *Opg* and *Opn*. However, the expression of *Trap*, *DANCR1* and miR-124-3p was significantly up-regulated. Obtained results show that BMSC_{SAM/P6} present features of progenitor cells with disturbed metabolism and could serve as appropriate model for in vitro investigation of age-dependent osteoporosis.

KEYWORDS

bone marrow, bone marrow stromal cells, cellular model, osteogenic markers, senile osteoporosis, stromal cells

This is an open access article under the terms of the Creative Commons Attribution License, which permits use, distribution and reproduction in any medium, provided the original work is properly cited.

© 2021 The Authors. *Journal of Cellular and Molecular Medicine* published by Foundation for Cellular and Molecular Medicine and John Wiley & Sons Ltd.

1 | INTRODUCTION

Osteoporosis represents the most common bone disease in elderly patients of both sexes and all races, occurring worldwide.¹ Moreover, its incidents are more frequent in well-developed and ageing societies.² Notably, more than 200 million citizens worldwide currently suffer from osteoporosis, and ~8.9 million fractures are caused by osteoporosis-related fractures.³ Furthermore, the specialists estimate that within 50 years, osteoporosis will reach the scale of global epidemic. The sudden termination of physical activity of osteoporotic patients, especially those suffering from bone fractures, becomes an even higher sociological cost that eliminates them from social life.⁴ Therefore, the investigation of novel concepts improving knowledge about the molecular mechanism of osteoporosis occurrence is critical for developing new therapeutic strategies and very much needed.

Osteoporosis is characterized by low bone mass as a result of impaired bone mineralisation, leading to reduced bone mechanical properties, increasing fracture risk.⁵ The pathophysiological mechanism of osteoporosis includes the deterioration of bone metabolisms. It is a consequence of several factors, including the advantage of bone resorption over bone formation process. The impairment of bone remodelling is caused by an imbalance between osteoclasts and osteoblasts, that is between bone-degrading and bone-producing cells.⁶ The recruitment of osteoclasts and osteoblast at the bone remodelling site requires activation of the plethora of molecular signals including hormones, cytokines, growth factors and non-coding RNAs, including long non-coding RNA (lncRNA) and microRNA (miRNA), which mediates the interaction between bone cells and progenitor cells.⁷ Moreover, the recruitment of bone marrow stromal cells (BMSCs), which are a source of progenitor cells at the bone remodelling site, guarantees a supportive role during new bone formation.

Bone marrow-derived stromal cells (BMSCs) are multipotent stem cells with self-renewal capacity.⁸ The population of showing features of BMSCs was described for the first time by Alexander Friedenstein and colleagues.^{9,10} Since that time, the knowledge regards BMSCs biology and nature are still extensively investigated.^{8,11} According to the current statement of *International Society for Cellular Therapy* (ISCT) BMSCs as a mesenchymal stromal stem cell are characterized by: (a) expression of CD73, CD90 and CD150 and lack of expression of CD11b, CD14, CD19, CD34, CD45 and HLA-DR molecules, (b) adhesion to the plastic surface of culture dish under standard culture condition and (c) possesses the ability for differentiation into chondrocytes, osteoblasts and adipocytes in vitro.¹² The self-renewal potential, associated with increased proliferative capacity, shed a promising light for various clinical application of BMSCs transplants. Numerous studies identified the molecular mechanisms of BMSCs, emphasizing their beneficial effects in the course of fractures bone regeneration.¹³⁻¹⁵ The progenitor cells of bone marrow express critical markers for new bone formation, which included alkaline phosphatase (ALP), bone morphogenetic protein 2/4 (BMP-2/4), osteoprotegerin

(OPG), receptor activator of nuclear factor B (RANK), RANK ligand (RANKL), osteocalcin (OCL), osteopontin (OPN), wntless-type MMTV integration site family (Wnt) proteins and signalling through parathyroid hormone receptors.^{16,17}

The pro-regenerative potential of BMSCs is also mediated by their paracrine activity and shedding the extracellular microvesicles (ExMV's), which are particularly rich in growth factors, miRNAs or lncRNAs.¹⁸⁻²⁰ Moreover, various miRNA and lncRNA have been shown recently to be involved in the mediation of balance between cell populations of osteoblast-like or osteoclast-like nature.^{7,21} Recent data suggest that the immunomodulatory activity of BMSCs makes them an even more promising therapeutic tool in terms of cell-based therapies in osteoporosis treatment.²²

However, the metabolic imbalance associated with osteoporosis affects the activity of BMSCs. The cells are losing their valuable biological properties, such as proliferative activity and multipotency. Moreover, BMSCs isolated from osteoporotic patients show apoptotic phenotype and accumulation of oxidative stress factors, which seriously reduce their viability. BMSCs isolated from osteoporotic rat show increased expression of several markers related to adipogenesis and simultaneously reduced expression of master regulators essential for bone formation.^{23,24} Thus, BMSCs are currently extensively investigated since understanding their molecular nature under osteoporosis might bring us closer to understanding the molecular mechanism involved in osteoporosis development.

For that reason, in this study, for the first time, we have isolated BMSCs derived from osteoporotic mice strain SAM/P6 (BMSC_{SAM/P6}) and described it as a genuine and relevant in vitro model, allowing determination of the molecular basis of osteoporosis development. Current models rely on BMSCs isolated from ovariectomized rats^{23,24} or patients with osteoporosis^{17,25,26} However, still the molecular aspects of BMSCs cytophysiology affected by osteoporosis has not been fully elucidated. Here, we have characterized BMSC_{SAM/P6} proliferative and metabolic activity and determined the expression of common phenotype markers, critical for stemness. Moreover, using cytometric-based tests, we have confirmed lowered metabolism of the cells, associated with depolarization of the mitochondrial membrane, intracellular accumulation of reactive oxygen species (ROS), accompanied with down-regulation of mitofusin 1 (MFN-1) protein expression in osteoporotic BMSCs compared with BMSCs isolated from healthy tissue. Additionally, we have evaluated the multipotency of BMSC_{SAM/P6} and determined the expression profile of bone-related markers (lncRNA-miRNA-mRNA axis). The molecular pattern of miRNAs expression, for example miR-21-5p or miR-124-3p in osteoporotic murine BMSCs has not been previously evaluated by other authors. Moreover, the analysed miRNAs were referred to the expression of lncRNA (*DANCR1*) and mRNAs, including *Runx-2* (runt-related transcription factor 2), *Trap* (tartrate-resistant acid phosphatase) or *Opn* (osteopontin). Obtained results were compared with BMSCs isolated from healthy BALB/c mice (BMSC_{BALB/c}). Here, we characterized novel bone marrow multipotent stem cells that could be used in future research regarding osteoporosis, especially attributed to ageing.

2 | MATERIALS AND METHODS

2.1 | Isolation procedure and propagation of bone marrow-delivered progenitor stem cells

The bone marrow-derived stromal cells were isolated from long bones of mice collected from lower limbs. After removal, bones were washed twice in Hank's Balanced Salt Solution (HBSS) with 1% addition of antibiotics (P/S—penicillin and streptomycin). The distal parts of every bone were cut out. Following that, bone marrow was isolated by its flushing from the medullary canal with an insulin syringe U-40 (29G X 1/2" needle) filled with HBSS as described previously.²⁷ The cells were collected and centrifuged two times (300 × g, 4 min). Subsequently, the isolated cells were counted by Muse[®] Count & Viability Kit (Merck[®]; cat. no.: MCH100102, Poznan, Poland). The procedure was carried out following protocol provided by the manufacturer. Further, the cells were inoculated on the 24-well dishes at density 800 000 cells/well and suspended in 500 μL of complete growth medium (CGM), consisted of Ham's F-12 Nutrient Mixture (F-12) supplemented with 15% of foetal bovine serum (FBS) and 1% of antibiotics (P/S). The cultures were propagated in sterile conditions using CO₂ incubator with constant parameters: 5% CO₂, 37°C and 95% humidity. After 24 hours of culture, the media were removed and replaced by the fresh media in order to eliminate hematopoietic cell lineage.²⁸ All reagents used for cell cultures (media, HBSS, antibiotics, FBS) were derived from Sigma-Aldrich (Poznan, Poland).

During propagation culture condition, growth pattern, as well as cells morphology were monitored using Axio Observer A1-inverted microscope (Zeiss, Oberkochen, Germany) and documented with Canon PowerShot digital camera (Woodhatch, UK). The photographs were taken under 100× and 400× magnification.

2.2 | Analysis of BMSCs metabolic activity

The analysis of BMSC_{BALB/c} and BMSC_{SAM/P6} metabolic activity was carried out by the use of well-established Alamar Blue test. After five days of cultures propagation, the cells were washed once with HBSS and 350 μL of CGM with 10% addition of resazurin dye solution (Tox8-1KT, Sigma-Aldrich, Munich, Germany) was added. Subsequently, the cultures were incubated for 2 hours in 37°C (5% CO₂ and 95% humidity). After incubation, the supernatant was removed and transported to the 96-well dish in six repetitions. The absorbance was measured at the wavelengths of 600 and 690 nm. The metabolic activity of BMSCs was calculated using formula: $\Delta A = A_{600nm} - A_{690nm}$.

2.3 | Immunocytochemical detection of CD44, CD73, CD90 and CD45

In order to characterize the isolated cells, surface markers typical for BMSCs were stained. After reaching ~80% of confluency, the

cells were fixed with 4% PFA (paraformaldehyde) for 30 minutes at room temperature. Further, cultures were washed three times with HBSS and permeabilised with 0.2% PBS-Tween solution with 10% addition of goat serum for 1 hour. Subsequently, specimens were washed 3 times with HBSS and incubated overnight at 4°C with primary antibodies: anti-CD44 (hpa005785, Sigma-Aldrich, Munich, Germany) in the dilution of 1:1000; anti-CD73 (ab54217, Abcam, Cambridge, UK) in the dilution of 0.1 μg/100 μL; anti-CD90 (ab92574, Abcam, Cambridge, UK) in the dilution of 1:100; and anti-CD45 (sc-53047, Santa Cruz Biotechnology, Dallas, Texas, USA) in the dilution of 1:100. Anti-CD44, anti-CD90 antibodies were produced in rabbit and anti-CD73, anti-CD45 antibodies were produced in mouse. After the overnight incubation, the specimens were washed 3 times with HBSS. Following washing, specimens were incubated for 1 hour at room temperature with secondary antibodies: anti-mouse IgG—Atto 594 antibody produced in goat (76085, Sigma-Aldrich, Munich, Germany) and anti-rabbit IgG—Atto 594 antibody produced in goat (77671, Sigma-Aldrich, Munich, Germany). The concentration of secondary antibodies was 1:1000. Finally, specimens were washed (as above) and fixed on slides using the mounting medium with DAPI (4',6-diamino-2-phenolindole) as a nuclear counterstain (Fluoroshield[™] with DAPI, Sigma-Aldrich, Munich, Germany). The specimens were analysed using a confocal microscope (Leica TCS SPE, Leica Microsystems, KAWA.SKA Sp z o.o., Zalesie Górne, Poland). The microscopic images were obtained by application of maximum intensity projection (Z-Project). The photographs were captured under 630× magnification. Obtained signals after cell surface antigens staining were measured using Fiji is just ImageJ and Pixel Counter plugin (version 1.52n, Wayne Rasband, National Institutes of Health, USA). The differences between the amount of colour pixels in CD44, CD45, CD73 and CD90 staining were determined in three technical repetitions and using three different thresholds (29, 30 and 31) within ImageJ Software.

2.4 | Chondrogenic, osteogenic and adipogenic differentiation of BMSCs

In order to prove the multipotent abilities of isolated BMSCs, chondrogenic, osteogenic and adipogenic differentiation of cultures were performed with differentiation media.

The chondrogenic medium was prepared using StemPro Osteocyte/Chondrocyte Differentiation Basal Medium (A10069-01, Gibco, Life Technologies Corporation, USA) and StemPro Chondrogenesis Supplement (A10069-01, Gibco, Life Technologies Corporation, USA) in the ratio of 10:1, respectively. The adipogenic medium was prepared using StemPro Adipogenesis Differentiation Basal Medium (A10410-01, Gibco, Life Technologies Corporation, USA) and StemPro Adipogenesis Supplement (A10065-01, Gibco, Life Technologies Corporation, USA) in the ratio of 10:1, respectively. The chondrogenic and adipogenic media were supplemented with 0.05% of gentamycin, according to the manufacturer's protocol.

The fresh chondrogenic and adipogenic media were changed twice a week and maintained for 7 days.

The osteogenic medium was prepared using Minimum Essential Medium Eagle—Alpha Modification (MEM- α), supplemented with osteogenic factors as was described previously²¹: 50 $\mu\text{g}/\text{mL}$ of ascorbic acid (Sigma-Aldrich, Munich, Germany) and 10 nmol/L of β -glycerol phosphate disodium salt hydrate (Sigma-Aldrich, Munich, Germany). The fresh osteogenic medium was changed twice a week. The osteogenic conditions were maintained for 10 days. After the differentiation process, the cultures were collected for subsequent analyses.

2.5 | Evaluation of BMSCs extracellular matrix composition and neutral lipids staining after differentiation conditions

The protocol of extracellular matrix staining was described previously.^{21,29} Briefly, differentiated cultures of BMSCs were fixed with 4% paraformaldehyde (PFA) for 15 minutes at room temperature and stained with specific dyes. Safranin-O was used for proteoglycans detection and Alizarin Red for calcium deposits detection. Obtained specimens were analysed using Axio Observer A1-inverted microscope (Zeiss, Oberkochen, Germany) and documented with Canon PowerShot digital camera (Woodhatch, UK). The photographs of visualized proteoglycan and calcium deposits were taken under 100 \times magnification. In order to visualize the neutral lipid droplets, HCS LipidTOX Green Neutral Lipid Stain was used according to manufacturer's protocol (H34475, Sigma-Aldrich) and observed under a confocal microscope (Leica TCS SPE, Leica Microsystems, KAWA.SKA Sp z o.o., Zalesie Górne, Poland). The photographs of visualized neutral lipid droplets were taken under 630 \times magnification. Obtained signals were measured using Fiji (ImageJ) and Pixel Counter plugin (version 1.52n, Wayne Rasband, National Institutes of Health, USA) as described previously.³⁰ The differences between the amount of colour pixels were determined in three technical repetitions and using three different thresholds (osteogenesis/chondrogenesis—239, 240 and 241; adipogenesis—48, 50 and 51) within ImageJ Software.

2.6 | Immunocytochemical detection of RUNX-2, OPN and TRAP

The procedure of RUNX-2, OPN and TRAP protein staining using confocal microscopy was mentioned in Section 2.3. and was described previously in detail.^{21,31} The used primary antibody were anti-RUNX-2 antibody (F-2) produced in mice (sc-390351, Santa Cruz Biotechnology, Dallas, Texas, USA) diluted to concentration 1:50 in HBSS; anti-OPN antibody produced in rabbit (ab8448, Abcam, Cambridge, UK) diluted to concentration 1:100 in HBSS; and anti-TRAP antibody (D-3) mouse monoclonal IgG1 (sc-376875, Santa Cruz Biotechnology, Dallas, Texas, USA) diluted to concentration 1:50 in HBSS. Following incubation with primary antibody, samples were washed three times with HBSS and incubated with secondary antibody (anti-mouse or anti-rabbit IgG—Atto

594 antibody produced in goat, Sigma-Aldrich, Munich, Germany) for 1 hour at room temperature. The concentration of secondary antibodies was 1:1000. The analysis of the samples was described in Section 2.3. The differences between the amount of colour pixels in RUNX-2, OPN and TRAP staining were determined in three technical repetitions and using three different thresholds (29, 30 and 31) within ImageJ Software.

2.7 | Analysis of BMSCs apoptosis profile and viability

Analysis of apoptosis profile and viability in BMSC cultures was carried out using the Muse™ Annexin V & Dead Cell Kit (Merck®; cat. no.: MCH100105, Poznań, Poland). The procedure was performed according to the producer's protocol after five days of culture propagation. Before the test cultures were trypsinised (StableCell Trypsin, Sigma-Aldrich, Munich, Germany) and suspended in 100 μL of phosphate-buffered saline (PBS) supplemented with 1% of FBS. Further, 100 μL of Muse™ Annexin V & Dead Cell Reagent was added to the cells and they were incubated at room temperature for 20 minutes. The reagent provided by the manufacturer consisted of two dyes: Annexin V and 7-Aminoactinomycin D (7-AAD). The apoptosis profile and percentage of viable cells were determined by the use of Muse™ Cell Analyzer. Each analysis was performed in triplicate. The gating procedure of cells' populations was based on the positive and negative controls.³²⁻³⁴

2.8 | Analysis of BMSCs caspase activation profile

The activation of caspases was determined using the Muse™ MultiCaspase Kit (Merck®; cat. no.: MCH100109, Poznań, Poland). The whole procedure was performed accordingly to manufacturer's protocol and our previous experiment.³⁵ Briefly, Caspase buffer was diluted 10 \times in DEPC-treated water and the MultiCaspase Reagent Stock Solution was diluted in 50 μL of DMSO. Other reagents were prepared for the analysis as it was described elsewhere.³⁵ According to manufacturer instructions, the analysis of caspases activation was based on membrane permeable VAD-peptide that can detect multiple caspases for example caspase 1, -3, -4, -5, -6 -7, -8 and -9. Stained samples were incubated for 30 min (37°C, 95% humidity, 5% CO_2) and 150 μL of Muse™ 7-AAD Working Solution was added in order to detect dead cells. The caspases activity profile was measured using Muse™ Cell Analyzer. Each analysis was performed in triplicate. The gating procedure of cells' populations was based on the positive and negative controls.³²⁻³⁴

2.9 | Analysis of BMSCs reactive oxygen species activation

The analysis of reactive oxygen species activation (ROS) was measured using the Muse™ Oxidative Stress Kit (Merck®; cat. no.:

MCH100111, Poznań, Poland). The staining procedure was performed accordingly to producer's protocol and described previously.³² Briefly, after trypsinisation 10 μ L of cells were added to 190 μ L of Muse Oxidative Stress Working Solution and incubated 30 minutes in 37°C. The staining reagent was provided by manufacturer and based on dihydroethidium (DHE), which is widely used for ROS detection in many cell cultures.³⁶ Then, the oxidative stress was measured using Muse™ Cell Analyzer. Each analysis was performed in triplicate. The gating procedure of cells' populations was based on the positive and negative controls.³²⁻³⁴

2.10 | Analysis of BMSCs mitochondrial membrane depolarisation status

The measurements of mitochondrial membrane depolarisation were determined using the Muse™ MitoPotential Kit (Merck®; cat. no.: MCH100110, Poznań, Poland). Firstly, Muse™ MitoPotential working solution was prepared by diluting MitoPotential Dye with 1X Assay Buffer in concentration of 1:1000. The MitoPotential Dye is a cationic, lipophilic solution that detects the changes in mitochondrial membrane potential and was provided by the manufacturer. Further, 95 μ L of prepared dye was added to 100 μ L of the cells and incubated 20 minutes in 37°C. After the incubation, 5 μ L of Muse™ 7-AAD was added to the samples in order to stain dead cells. After 5 minutes of incubation in room temperature, the depolarisation of cells' mitochondrial membrane was measured using Muse™ Cell Analyzer. Each analysis was performed in triplicate. The gating procedure of cells' populations was based on the positive and negative controls.³²⁻³⁴

2.11 | Analysis of MFN-1 and PINK1 protein expression in BMSCs

In order to determine the extracellular level of accumulated proteins, the cell cultures were lysed by the use of ice-cold RIPA buffer supplemented with 1% of protease and phosphatase inhibitor cocktail (Sigma-Aldrich, Munich, Germany). The Bicinchoninic Acid Assay Kit was used to determine the amount of isolated protein (Sigma-Aldrich, Munich, Germany). The samples containing 8 μ g of protein were mixed with 4 \times Laemmli loading buffer and incubated at 95°C for 5 min in T100 Thermal Cycler (Bio-Rad, Hercules, CA, USA). The electrophoresis reaction (SDS-PAGE) was performed in 11% sodium dodecyl sulphate-polyacrylamide gel for 90 minutes at 100V using Mini-PROTEAN Tetra Vertical Electrophoresis Cell (Bio-Rad, Hercules, CA, USA). Subsequently, the samples were transferred into polyvinylidene difluoride membrane (PVDF) using the Mini Trans-Blot® system (Bio-Rad, Hercules, CA, USA) for 1h at 100V. Then, membranes were blocked by the use of 5% skim milk powder in TBST buffer for 1h and then incubated overnight at 4°C with primary antibodies. The used primary antibodies were anti MFN-1 antibody produced in rabbit (orb11040,

Biorbyt) in dilution 1:500 and anti PINK1 antibody produced in rabbit (orb331223, Biorbyt) in dilution 1:250. The reference was anti β -ACT antibody produced in rabbit (a5441, Sigma-Aldrich) in dilution 1:2500. Membranes were washed 5 times for 5 min in TBST buffer. The incubation with secondary antibodies was performed for 1h at 4°C (Goat Anti-Rabbit IgG Antibody in dilution 1:2500, ap156p, Sigma-Aldrich). Subsequently, membranes were washed 5 times as described previously and analysed using Bio-Rad ChemiDoc™ XRS system (Bio-Rad, Hercules, CA, USA). The chemiluminescent signal was detected by the use of DuoLuX® Chemiluminescent and Fluorescent Peroxidase (HRP) Substrate (Vector Laboratories). The signal intensity and molecular weight of detected proteins was analysed using Image Lab™ Software (Bio-Rad, Hercules, CA, USA).

2.12 | Analysis of mRNA, miRNA and lncRNA expression

The transcripts levels for selected mRNA, miRNA and lncRNA were evaluated using reverse transcription quantitative polymerase chain reaction (RT-qPCR). After experiment, cultures were homogenized using 1 mL of Extrazol® (Blirt DNA, Gdańsk, Poland). The isolation procedure of RNA was performed accordingly to manufacturer's protocol. After isolation, total RNA was diluted in molecular grade water (Sigma-Aldrich, Poznan, Poland). The quantity and purity was evaluated spectrophotometrically at 260 and 280 nm wavelength (Epoch, BioTek, Bad Friedrichshall, Germany). The gDNA was digested by total RNA treatment with DNase I using PrecisionDNase Kit (Primerdesign, BLIRT SA, Gdańsk, Poland). Synthesis of cDNA was performed from 190 ng of isolated RNA applying Tetro cDNA Synthesis Kit (Bioline Reagents Limited, London, UK). The procedure was carried out accordingly to manufacturers' protocol in T100 Thermal Cycler (Bio-Rad, Hercules, CA, USA). Moreover, Mir-X™ miRNA First-Strand Synthesis Kit (Takara Clontech Laboratories, Biokom, Poznań, Poland) was used to evaluate non-coding RNA levels. For this purpose, 150 ng of RNA was used and the procedure was carried out according to the manufacturer's protocol.

RT-qPCR was performed with SensiFAST SYBR®&Fluorescein Kit (Bioline Reagents Ltd., London, UK) in CFX Connected Real-Time PCR Detection System (Bio-Rad, Hercules, CA, USA). The reaction for mRNA and lncRNA was carried out according to presented conditions: 95°C for 2 minutes (initial denaturation), then 45 cycles at 95°C for 5 s, annealing for 10 s and 72°C for 5 s (elongation). The melting curve using a gradient protocol (65°C–95°C with heating rate 0.2°C/s). For miRNA levels detection, all reaction conditions maintain the same; however, annealing temperature was always 58.8 °C. All reactions were performed in at least three repetitions. Relative values of transcripts were calculated using RQ_{MAX} algorithm and presented in the graphs after conversion into log₂ scale. The transcripts levels for mRNA and lncRNA were normalized to the house-keeping gene *Gapdh* (glyceraldehyde 3-phosphatehydrogenase) and

B2m (beta-2-microglobulin). The transcript levels for miRNA were calculated in relation to a snU6 gene. The list of used primers are enclosed in Table 1.

2.13 | Statistical analyses

Experimental values are presented as means of obtained from at least three technical repetitions and they supplemented with standard deviation (\pm SD). The statistical calculations and data presentation was done with GraphPad Prism 5 (GraphPad Software, San Diego, CA, USA). The data were analysed using Student's *t* test. Differences were considered as statistically significant at $P < .05$.

Significant differences between groups were indicated with asterisks: * $P < .05$, ** $P < .01$, *** $P < .001$. Non-significant differences were marked as *ns*.

3 | RESULTS

3.1 | Characterization of isolated BMSCs—growth pattern, metabolic activity and multipotency

Isolated BMSCs, derived both from SAM/P6 and BALB/c mice, were successfully cultured in the monolayer system in sterile plastic dishes and maintained in the CO₂ incubator with constant conditions:

TABLE 1 The list of primers used for RT-qPCR

Gene	Primer Sequence 5'-3'	Annealing [°C]	Amplicon length [bp]	Accession no.
Igf-1	F:AGAGCCTGCGCAATGGAATA R:TGCTGATTTCCCATCGCT	58,8	152	NM_010512.5
Bcl-2	F:ATCGCCCTGTGGATGACTGAG R:CAGCCAGGAGAAATCAAACAGAGG	58,8	129	NM_000633.2
Bax	F:ACCAAGAAGCTGAGCGAGTGTC R:ACAAAGATGGTCACGGTCTGCC	58,8	414	NM_001291428.1
Mmp-9	F:GATGCCAACCTCCTCAACGA R:GGAAGCGGTCCAGGTAGTTC	60	211	NM_053056.2
Runx-2	F:TCCGAAATGCCTCTGCTGTT R:GCCACTTGGGGAGGATTTGT	58,8	130	NM_001271630.1
Coll-1	F:CAGGGTATTGCTGGACAACGTG R:GGACCTTGTTGCCAGTTCA	61,4	107	NM_007742.4
Opn	F:AGACCATGCAGAGAGCGAG R:GCCCTTCCGTTGTTGCTCT	57,3	340	NM_001204203.1
Ocl	F:GGTGCAGACCTAGCAGACACCA R:CGCTGGGCTTGGCATCTGTAA	57	100	NM_001032298.3
Opg	F:AGCCACGCAAAAGTGTGGAA R:TCCTCTTACTACTCTCGGCA	58,8	149	NM_008764.3
Trap	F:GTCTCTGGGGGACAATTTCTACT R:GTTTGTACGTGGAATTTGAAGC	60	241	XM_006509945.3
Rankl	F:ACGCAGATTTGCAGGACTCGAC R:TTCGTGCTCCCTCCTTCATC	58,8	493	NM_011613.3
Gapdh	F:GTCAGTGGTGGACCTGACCT R:CACCACCCTGTTGCTGTAGC	58,8	256	NM_001289746.1
DANCR1	F:GCCACTATGTAGCGGGTTTC R:ACCTGCGCTAAGAAGTACTGAGG	58,8	129	NR_024031.2
miR-7a-5p	TGGAAGACTAGTGATTTTGTGT	58,8	-	MIMAT0000677
miR-17-5p	CAAAGTGCTTACAGTGCAGGTAG	58,8	-	MIMAT0000649
miR-21a-5p	TAGCTTATCAGACTGATGTTGA	58,8	-	MIMAT0000530
miR-124-3p	TAAGGCACGCGGTGAATGCC	58,8	-	MIMAT0000134
miR-145-5p	GTCCAGTTTTCCAGGAATCCCT	58,8	-	MIMAT0000437
miR-203a-3p	GTGAAATGTTTAGGACCACTAG	58,8	-	MIO000283
miR-223-3p	TGTCAGTTTGTCAAATACCCCA	58,8	-	MIMAT0000280

37°C, 5% CO₂ and 95% of humidity (Figure 1A). The morphology and growth pattern of BMSC cultures were characteristic for heterogenic population of multipotent stromal cells, with the predominant presence of fibroblast-like, spindle-shaped cells. The primary cultures of BMSC_{SAM/P6} had lowered confluency when compared to BMSC_{BALB/c}, what was also reflected by their decreased proliferative activity. The metabolic activity of isolated BMSCs, measured by the use of Alamar Blue assay, showed that BMSC_{SAM/P6} metabolic rate was reduced ($P < .05$), and culture growth was impeded (Figure 1A and B).

Immunocytochemical staining showed that BMSC_{SAM/P6} and BMSC_{BALB/c} expressed typical cell surface confirming their mesenchymal origin (CD44, CD73 and CD90) and did not express CD45 characteristic for haematopoietic cells (Figure 1C). Importantly, the expression of CD44 and CD90 in BMSC_{SAM/P6} decreased ($P < .05$ and $P < .001$, respectively), compared with BMSC_{BALB/c} (Figure 1D).

After reaching around 80% of confluency, the cultures were differentiated under chondrogenic, osteogenic and adipogenic conditions (Figure 1E, F and G). When the differentiation process was finished, the extracellular matrix (ECM) formed in cultures was stained by specific dyes in order to analyse the amount of proteoglycans deposits (Safranin-O staining), calcium deposits (Alizarin Red staining) and lipid droplets (LipidTox staining). No differences were noticed in the potential of both, BMSC_{SAM/P6} and BMSC_{BALB/c}, to differentiate into cartilage tissue (Figure 1F and I). However, the analyses of ECM composition indicated on lower potential ($P < .001$) of BMSC_{SAM/P6} to differentiate into bone tissue, compared with BMSC_{BALB/c} (Figure 1E and H). Simultaneously, BMSC_{SAM/P6} presented increased potential ($P < .001$) for lipid droplets formation and accumulation, when compared to BMSC_{BALB/c} (Figure 1G and J).

3.2 | The BMSCs ultrastructure and expression of osteogenic markers

Confocal imaging of cultures showed that the cytoskeleton network in BMSC_{SAM/P6} is less developed than in BMSC_{BALB/c}. Additionally, the formation of cytoplasmic projections was less visible in BMSC_{SAM/P6} than in BMSC_{BALB/c}. Poorly established actin cytoskeleton and intracellular connections influenced decreased confluency (cell to cell contact) in BMSC_{SAM/P6} cultures (Figures 1A and 2A). However, significant differences were noticed in the expression of osteogenesis-dependent proteins: RUNX-2 (runt-related transcription factor 2), OPN (osteopontin) and TRAP (tartrate-resistant acid phosphatase). The BMSCs isolated from SAM/P6 mice were characterized by lowered expression of RUNX-2 ($P < .05$) and OPN ($P < .001$) proteins, key factors regulating osteogenic potential of progenitor cells (Figure 2B and D). Simultaneously, the expression of an osteoclastic marker, that is TRAP was increased ($P < .001$) in BMSC_{SAM/P6}, while BMSC_{BALB/c} cultures showed reversed phenotype. (Figure 2F). Obtained results are consistent with decreased deposition of calcium in ECM formed by BMSC_{SAM/P6} (Figure 1E and H).

3.3 | Decreased expression of osteogenic markers is characteristic for BMSC derived from mice with osteoporotic phenotype

The analysis performed by the use of RT-qPCR technique indicated that BMSC_{SAM/P6} are characterized by the reduced level of transcripts associated with proper osteogenesis and bone homeostasis. It has been shown that BMSC_{SAM/P6} had decreased mRNA level of *Coll-1* ($P < .05$; collagen type 1), *Opg* ($P < .05$; osteoprotegerin) and *Opn* ($P < .01$; osteopontin) (Figure 3B, C and E). Moreover, the tendency of the expression of *Runx-2* (runt-related transcription factor 2) and *Ocl* (osteocalcin) in BMSCs indicated on the osteoporotic phenotype of BMSCs derived from SAM/P6 mice strain (Figure 3A and D).

3.4 | Increased levels of Trap and osteogenesis-dependent non-coding RNAs distinguish BMSC derived from osteoporotic mice

The RT-qPCR analysis of mRNAs and non-coding RNAs associated with osteoclastogenesis and bone loss confirmed the osteoporotic phenotype of BMSC_{SAM/P6} cultures. The expression level of non-coding *DANCR1* (differentiation antagonizing non-protein coding RNA 1) was significantly up-regulated ($P < .05$) in BMSC_{SAM/P6} (Figure 4A). Moreover, it has been shown that the expression of *Trap* (tartrate-resistant acid phosphatase) in BMSC_{SAM/P6} was significantly elevated ($P < .01$), compared with BMSC_{BALB/c} (Figure 4B). Furthermore, the analyses showed that the levels of typical miRNAs, characteristic for osteoporotic bone, were highly expressed in BMSC_{SAM/P6}. We noted elevated levels of miR-124-3p ($P < .05$; Figure 4D), miR-7a-5p ($P < .001$; Figure 4E), miR-17-5p ($P < .001$; Figure 4F), miR-145-3p ($P < .001$; Figure 4G), miR-203a ($P < .001$; Figure 4H) and miR-223-3p ($P < .001$; Figure 4I). The difference in the level of miR-21-5p, known from its dual activity towards bone cells, was insignificant (Figure 4C).

The expression profile of transcripts determined in BMSC_{BALB/c} and BMSC_{SAM/P6} was also presented as a heatmap in Supporting Information (Figure S1).

3.5 | BMSC from osteoporotic mice are characterized by apoptotic phenotype and increased oxidative stress

It has been shown that BMSCs delivered from osteoporotic SAM/P6 mice were characterized by a lower ratio of viable cells ($P < .01$; Figure 5A and B) and a greater ratio of dead cells ($P < .01$; Figure 5A and C), compared with BMSC_{BALB/c}. Moreover, BMSC_{SAM/P6} had a significantly greater ratio of cells that undergo apoptosis ($P < .01$; Figure 5A and D). The analysis performed by the use of RT-qPCR technique showed no differences in the expression of important markers associated with programmed cell death, that is

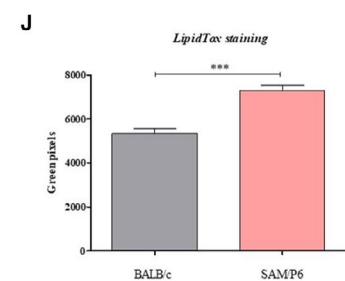
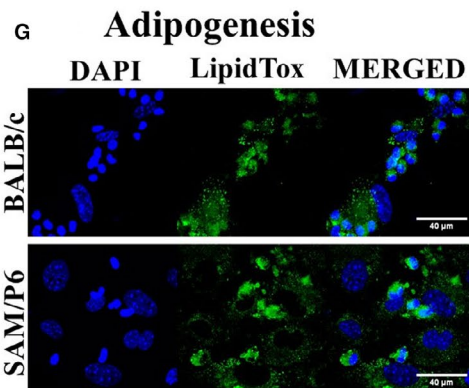
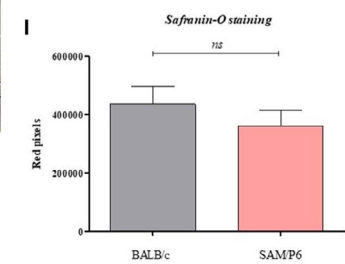
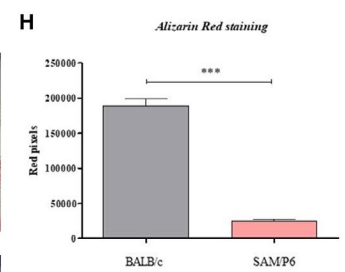
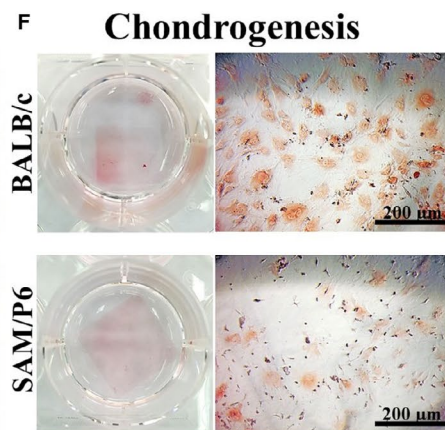
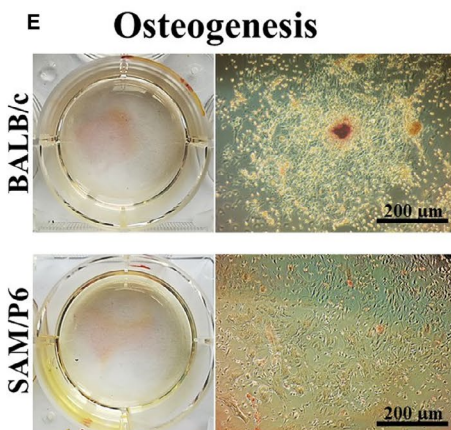
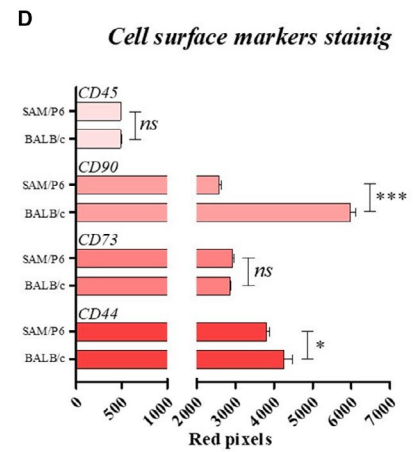
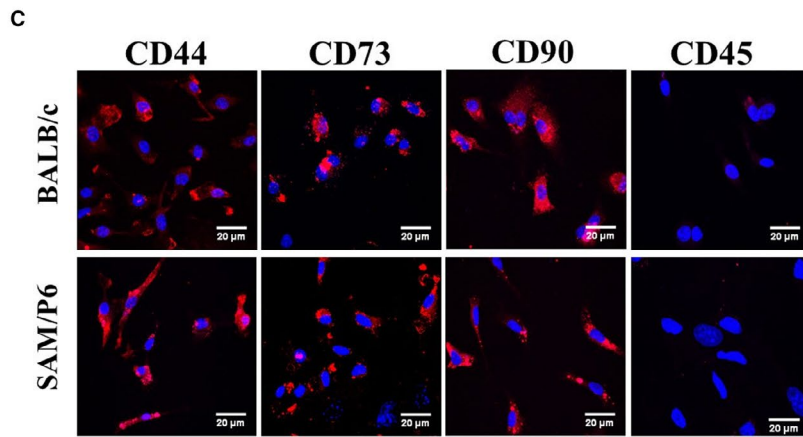
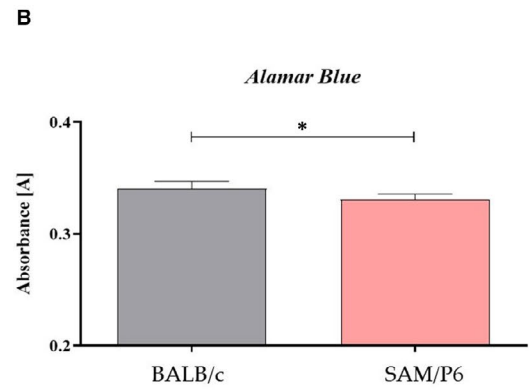
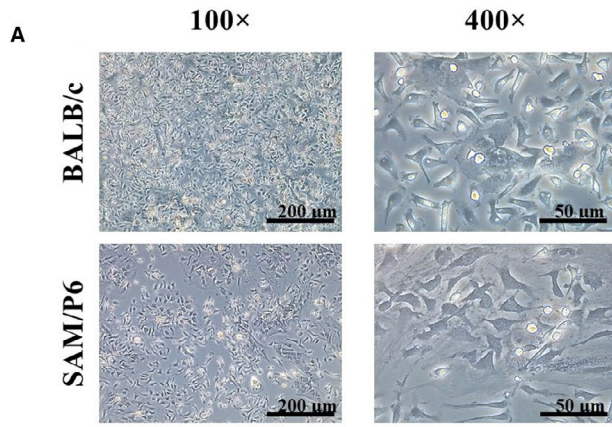


FIGURE 1 Characterization of BMSCs: The inverted light microscope images of BMSC_{BALB/c} and BMSC_{SAM/P6}. The photographs were captured under 100- and 400-fold magnification. The scale bars are equal 200 μm and 50 μm , respectively (A). The results of metabolic assay (Alamar Blue) determined for both tested population of BMSCs (B). The visualization of cells' surface markers: CD44, CD73, CD90 and CD45. The microphotographs were taken using confocal microscope under 630 \times magnification. The scale bar is equal 20 μm (C). The comparative analysis based on staining intensity of surface markers presented as grouped bar graph (D). The images of BMSCs differentiated under osteogenic (E), chondrogenic (F) and adipogenic conditions (G). The photographs of cultures that undergo chondro- and osteogenesis were taken by the use of inverted light microscope under 100-fold magnification, and the scale bar is equal 200 μm . The photographs of cultures that undergo adipogenesis were taken using confocal microscopy in order to visualize cells' nuclei (DAPI) and lipid droplets (LipidTox). The confocal images were captured under 630-fold magnification, and the scale bar is equal 40 μm . The stainings intensity measured in differentiated cultures was presented as bar graphs (H, I and J). Significant differences between groups are indicated with asterisks: * $P < .05$, ** $P < .01$, *** $P < .001$. Non-significant differences are marked as *ns*

pro-apoptotic *Bax* (Bcl-2-associated X protein) and anti-apoptotic *Bcl-2* (B-cell lymphoma 2) (Figure 5F and G). However, BMSC_{SAM/P6} expressed more transcript for *Mmp-9* ($P < .05$; metalloproteinase 9), an additional marker of apoptotic cells.³⁷

The examination of oxidative stress in the isolated BMSCs indicated an increased accumulation of reactive oxygen species (ROS) in BMSC_{SAM/P6} ($P < .01$; Figure 5H and J). In turn, the reactivity of ROS in BMSC_{BALB/c} was lesser ($P < .01$; Figure 5H and I). Furthermore, it has been shown that BMSC_{SAM/P6} accumulates more transcripts for *Igf-1* ($P < .001$; insulin-like growth factor 1). In correspondence with increased ROS, the up-regulated *Igf-1* may be associated with the pro-inflammatory activity of progenitor cells derived from bone marrow of SAM/P6 mice (Figure 5K).

3.6 | Decreased viability of BMSC from osteoporotic mice can be a caspase-independent process

The flow cytometry-based measurements showed that BMSC_{SAM/P6} were characterized by a lower cell ratio with activated caspases ($P < .01$; Figure 6A and D). However, the ratio of viable cells was decreased ($P < .01$) in BMSC_{SAM/P6} (Figure 6A and B) and ratio of dead cells was increased in BMSC_{SAM/P6} ($P < .001$; Figure 6A and C), compared with BMSC_{BALB/c}. Obtained data suggested that the deteriorated viability of BMSC_{SAM/P6} is not a result of caspase-dependent processes.

3.7 | BMSCs with osteoporotic phenotype are characterized by mitochondrial membrane depolarisation and impaired dynamics of mitochondrial network

The mitochondrial membrane depolarisation status indicated on elevated cell ratio with depolarised mitochondrial membrane ($P < .05$) in BMSC isolated from SAM/P6 mice (Figure 7A and D). Thus, lowered activity of caspases and decreased viability of BMSC_{SAM/P6} may be associated with mitochondrial-dependent pathway. The analysis of BMSC_{SAM/P6} viability, based on mitochondrial membrane potential, confirmed the increased death occurrence ($P < .01$) in those cultures (Figure 7A and C). Moreover, it has been shown that

osteoporotic BMSC_{SAM/P6} were characterized by down-regulation of protein levels for MFN-1 (mitofusin 1; Figure 7E and F; $P < .05$) and PINK1 (PTEN-induced kinase 1; Figure 7E and G; $P < .05$) compared with healthy BMSC_{BALB/c}.

4 | DISCUSSION

A new bone formation requires constant replenishment of the osteoblast from progenitor/stem cells mobilized from bone marrow. That cell lineage population needs to proliferate, differentiate and finally deposit a tissue-specific extracellular matrix to create well-developed and functional tissue. Numerous research groups worldwide study the biology of bone marrow-derived stromal cells (BMSCs) in terms of osteoporosis development. Such studies are aimed to explore the cellular and molecular mechanisms involved in the progress of osteoporosis. So far, the ovariectomised rat derived BMSCs model has been extensively used for investigation of postmenopausal osteoporosis.^{38,39} However, there are limited data regarding the biology of BMSCs characterized by senescence phenotype. Complete characterization of such population is needed to describe an appropriate model for investigating molecular and therapeutic targets of age-related osteoporosis development.

Thus, for the first time in this study, we demonstrated and characterized a novel bone marrow-derived stromal cells population isolated from senescence-accelerated mouse strain prone 6 (BMSC_{SAM/P6}) that resemble age-dependent osteoporosis. Isolated cells exhibited senescence-like phenotype, reduced proliferative and metabolic activity and seriously impaired multilineage differentiation potential comparing to the wild-type BMSCs delivered from healthy BALB/c mice (BMSC_{BALB/c}). The isolated BMSCs were characterized by typical markers such as CD44, CD73 and CD90, confirming their mesenchymal origin and indicating stemness. Moreover, obtained BMSCs showed lack of CD45 expression, which excludes their hematopoietic origin. Notably, BMSC_{SAM/P6} were characterized by reduced expression of CD44 and CD90, which are markers critical for multipotency of stromal cells and are related to progenitor cells' proliferative activity.⁴⁰ Obtained data are in line with previous research performed on BMSCs derived from patients with senile osteoporosis. The study showed that bone-marrow progenitor cells of patients with age-related osteoporosis are characterized by reduced proliferative activity,

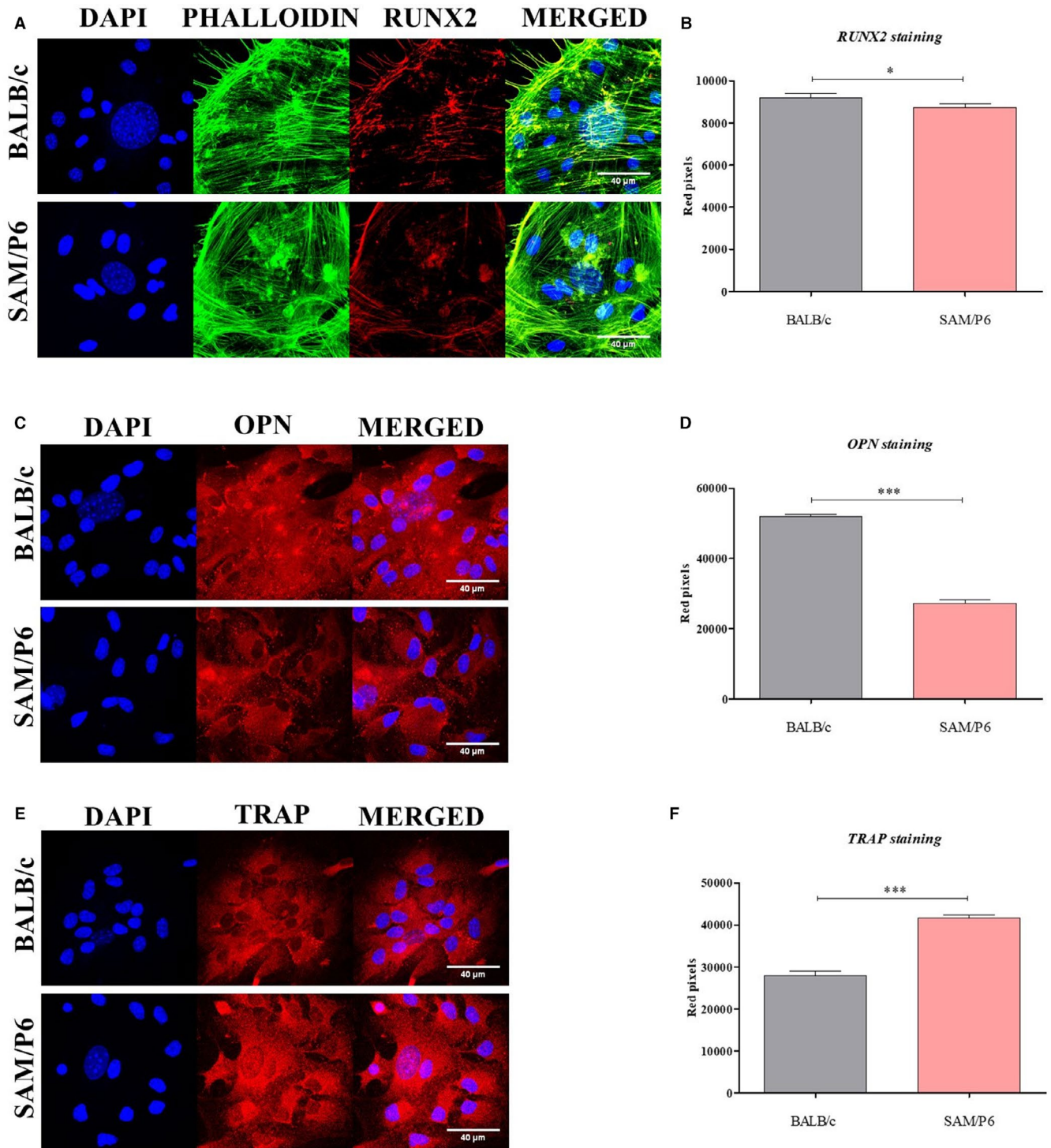


FIGURE 2 The morphology of BMSCs and expression of important osteogenic markers. The images show representative photographs (Z-stacks) of: cells' nuclei (DAPI) with actin cytoskeleton (Phalloidin) and co-localisation of RUNX-2 protein (A); cell's nuclei with co-localisation of OPN protein (C); cells' nuclei with co-localisation of TRAP protein (E). The photographs were taken under 630-fold magnification. The scale bar is equal to 40 μ m. Moreover, the staining intensity (amount of red pixels) of visualized RUNX-2, OPN and TRAP proteins were analysed and presented as bar graphs (B, D and F). Significant differences between groups are indicated with asterisk: * $P < .05$, ** $P < .01$, *** $P < .001$. Non-significant differences are marked as ns

impaired phenotype, what affected disturbed recruitment and reduced regenerative potential.²⁶ Numerous studies confirmed that increased patient age correlates with decreased beneficial properties of progenitor cells, namely "stemness" depending on lowered

self-renewal potential and causing defective extracellular matrix formation.^{41,42}

Moreover, progenitor cells with senescence phenotype exhibit seriously deteriorated multilineage differentiation potential, limiting

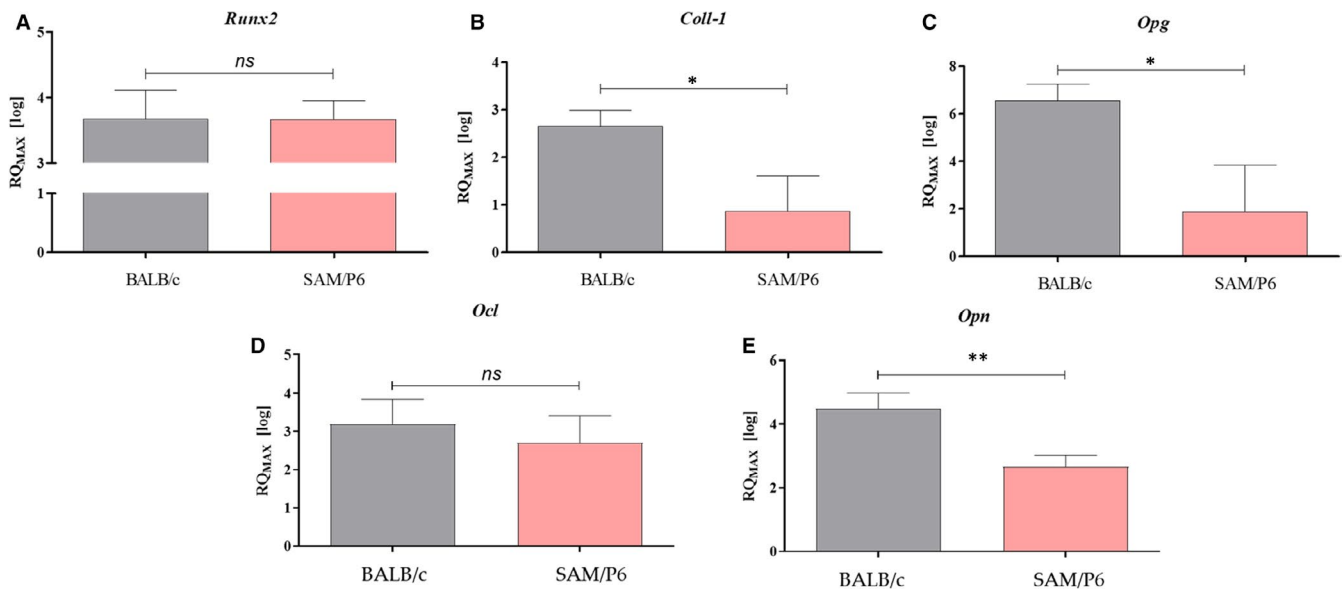


FIGURE 3 The analysis of genes' transcriptomes (mRNA) associated with osteogenesis and bone homeostasis. The measurements were performed with RT-qPCR technique, calculated using RQMAX method and presented in a log scale. The analysed targets were Runx-2 (A); Coll-1 (B); Opg (C); Ocl (D) and Opn (E). Significant differences between groups are indicated with asterisk: * $P < .05$, ** $P < .01$, *** $P < .001$. Non-significant differences are marked as ns

their clinical application.^{25,43} We have found that $\text{BMSC}_{\text{SAM/P6}}$ were prone to accumulate lipid droplets and showed enhanced adipogenic differentiation. That indicates an advantage of adipogenic over osteogenic and/or chondrogenic-like phenotype of BMSCs derived from patients suffering from senile osteoporosis. The loss of osteogenic potential of $\text{BMSC}_{\text{SAM/P6}}$ was also related to decreased expression of RUNX-2 and OPN expression and increased TRAP levels, characteristic for osteolytic cells.

Furthermore, cytometric-based analyses of BMSCs' viability indicated on the apoptotic profile of $\text{BMSC}_{\text{SAM/P6}}$. Cells isolated from osteoporotic SAM/P6 mice were characterized by a lowered ratio of viable cells, simultaneously with a greater ratio of dead and apoptotic cells. Moreover, $\text{BMSC}_{\text{SAM/P6}}$ expressed increased mRNA levels for *Mmp-9* (gelatinase B), which can serve as an additional marker of cells that undergo apoptosis.^{37,44} It has been shown that MMP-9 may modulate the viability of cells, affecting pro-apoptotic and anti-apoptotic signals and proteins, such as BAX, BCL-2, PARP or CASP-3. However, MMP-9 influence on the viability of BMSC has not been yet elucidated.

The decreased viability of $\text{BMSC}_{\text{SAM/P6}}$ was also associated with the accumulation of reactive oxygen species (ROS) and corresponded to up-regulated expression of *Igf-1*. It has been proven that oxidative stress influences inflammatory cytokines like TNF- α or interleukins, which orchestrated synergy plays a key role during intercellular redox state, leading to important alterations of the differentiation process and osteoporosis development.^{45,46} Notably, $\text{BMSC}_{\text{SAM/P6}}$ were characterized by significant depolarisation of the mitochondrial membrane, which also correlates with an apoptotic phenotype of $\text{BMSC}_{\text{SAM/P6}}$. However, the analyses of caspases activation suggested that the apoptosis of $\text{BMSC}_{\text{SAM/P6}}$ is not a caspase-dependent process. It has been shown that caspase-independent cell

death (CICD) is an alternative pathway of programmed cell death. Although CICD proceeds in slower kinetics than classic apoptosis, it is related to large-scale cytoplasmic vacuolisation, peripheral nuclear condensation and autophagosome accumulation.^{47,48} Importantly, this mechanism of apoptosis is also reflected by depolarisation of the mitochondrial membrane. Nevertheless, more insightful examination needs to be performed to specify the apoptosis phenotype of $\text{BMSC}_{\text{SAM/P6}}$ in detail.

The mitochondrial depolarization accompanied with accumulation of ROS, characteristic for $\text{BMSC}_{\text{SAM/P6}}$ stands in line with lowered expression of mitofusin 1 (MFN-1) and PTEN-induced kinase 1 (PINK1) protein. It has been previously shown that MFN-1 plays a vital role in the process of mitochondria fusion, thus maintaining proper mitochondrial dynamics.^{49,50} Importantly, the impaired mitochondrial functionality caused by knockout of MFN-1 in BMSCs has been previously associated with enhanced apoptosis and suppression of osteogenesis.⁵¹ Moreover, previous studies have distinguished PINK1 as an essential regulator of mitochondria quality control, protecting against oxidative stress and disposal of damaged mitochondria.^{52,53} Moreover, Feng et al (2021) have noted that PINK1 was highly engaged in the process of mitophagy in the rat BMSCs and proven its importance in maintaining the BMSCs' stemness.⁵⁴

Our previous study has shown that increased patient age corresponds with adipogenic and osteoclasts like phenotype of multipotent stromal cells, associated with high expression of p53.⁴³ However, the mechanism of that phenomenon is still poorly investigated. For that reason, in this study, we investigated the expression of critical transcripts involved in regulating osteogenesis on mRNA, miRNA, and lncRNA. We have found, that $\text{BMSC}_{\text{SAM/P6}}$ expressed higher osteoclasts related transcripts including *Trap* and long non-coding RNA *DANCR1* together with elevated expression of miR-7a-5p, miR-17-5p,

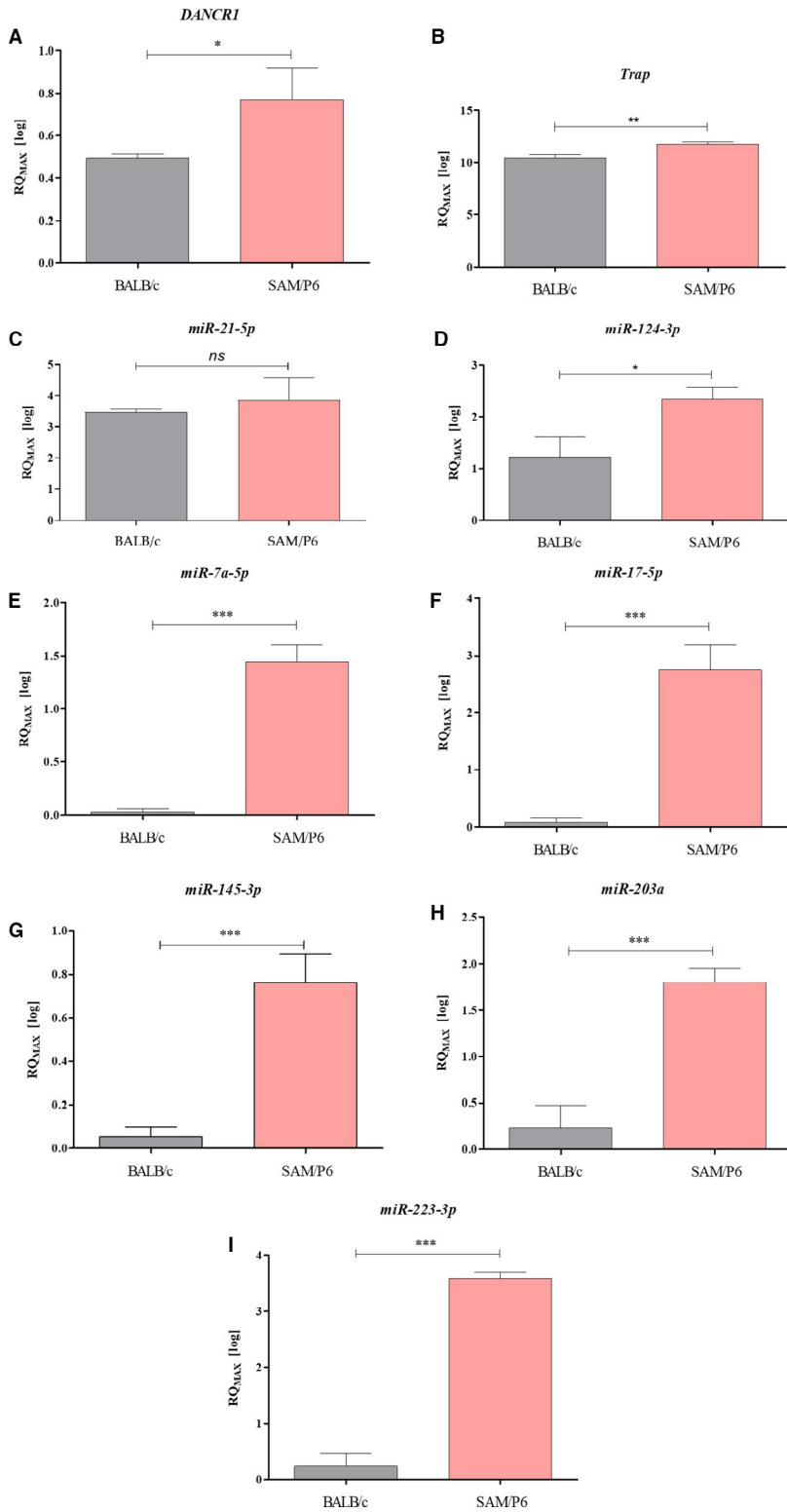
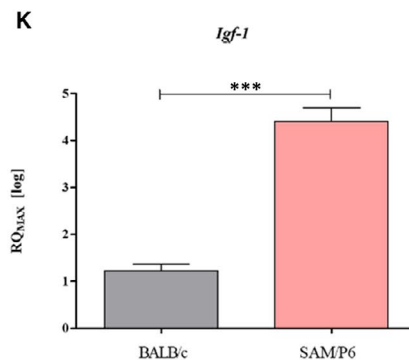
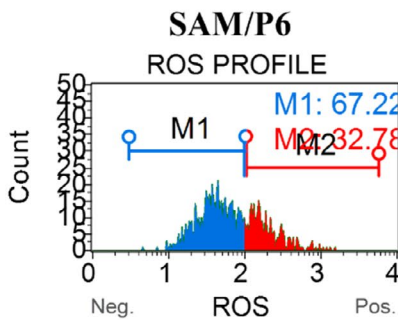
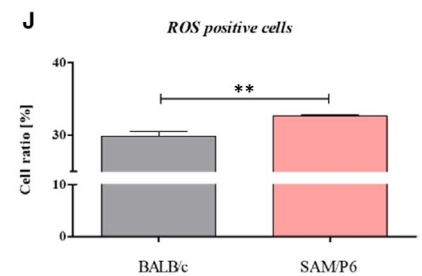
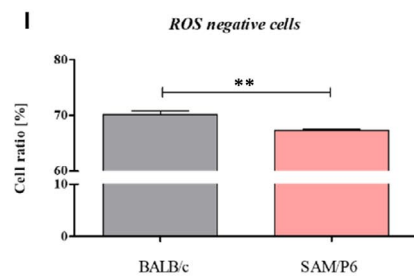
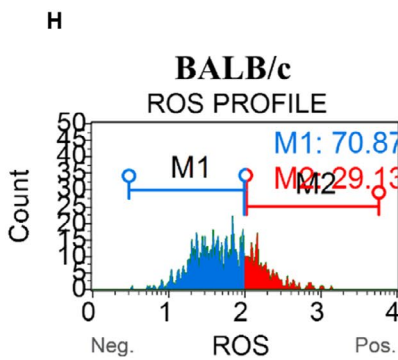
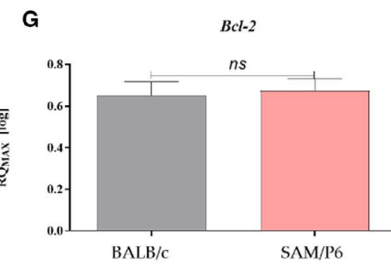
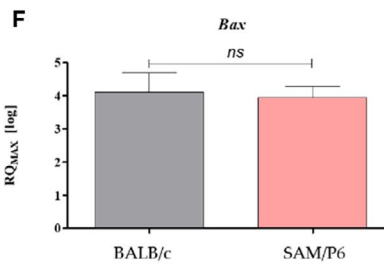
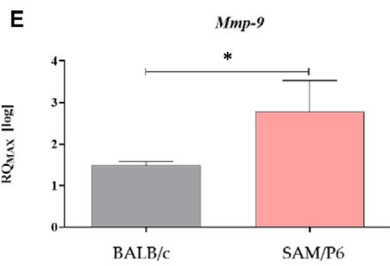
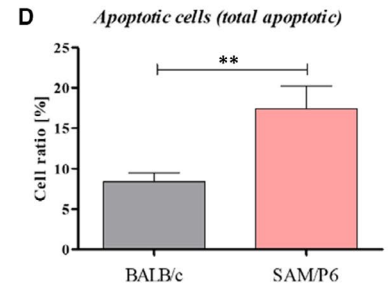
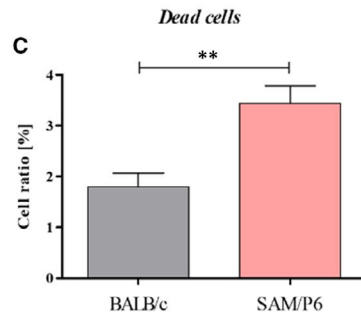
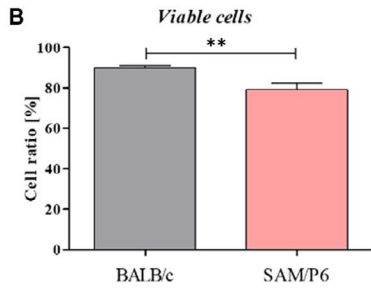
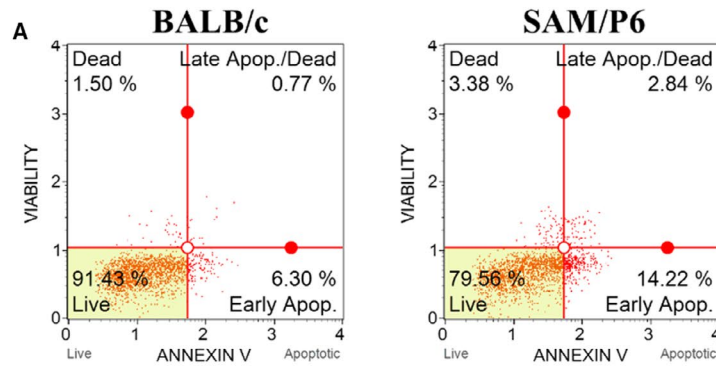


FIGURE 4 The analysis of genes' transcriptomes (mRNA and non-coding RNA) associated with osteoporosis and bone loss. The measurements were performed with RT-qPCR technique, calculated using RQMAX method and presented in a log scale. The analysed targets were *DANCR1* (A); *Trap* (B); *miR-21-5p* (C); *miR-124-3p* (D); *miR-7a-5p* (E); *miR-17-5p* (F); *miR-145-3p* (G); *miR-203a* (H) and *miR-223-3p* (I). Significant differences between groups are indicated with asterisk: * $P < .05$, ** $P < .01$, *** $P < .001$. Non-significant differences are marked as *ns*

FIGURE 5 The BMSCs' apoptosis profile and oxidative stress. The representative graphs of cells' populations divided into four groups related to apoptosis profile (A): *live* (left bottom corner), *dead* (left upper corner), *early apoptosis* (right bottom corner) and *late apoptosis* (right upper corner). The comparison analysis of viable cells (B), dead cells (C) and apoptotic cells (D). The representative graphs of cells' populations divided into two groups related to reactive oxygen species activation (H): ROS-negative cells (blue colour) and ROS-positive cells (red colour). The comparison analysis of ROS-negative cells (I) and ROS-positive cells (J). The mRNA expression of genes associated with cells' viability and inflammation: *Mmp-9* (E), *Bax* (F), *Bcl-2* (G) and *Igf-1* (K). The genes' transcript levels were measured using RT-qPCR technique, calculated with RQMAX method and presented in log scale. Significant differences between groups are indicated with asterisk: * $P < .05$, ** $P < .01$, *** $P < .001$. Non-significant differences are marked as *ns*



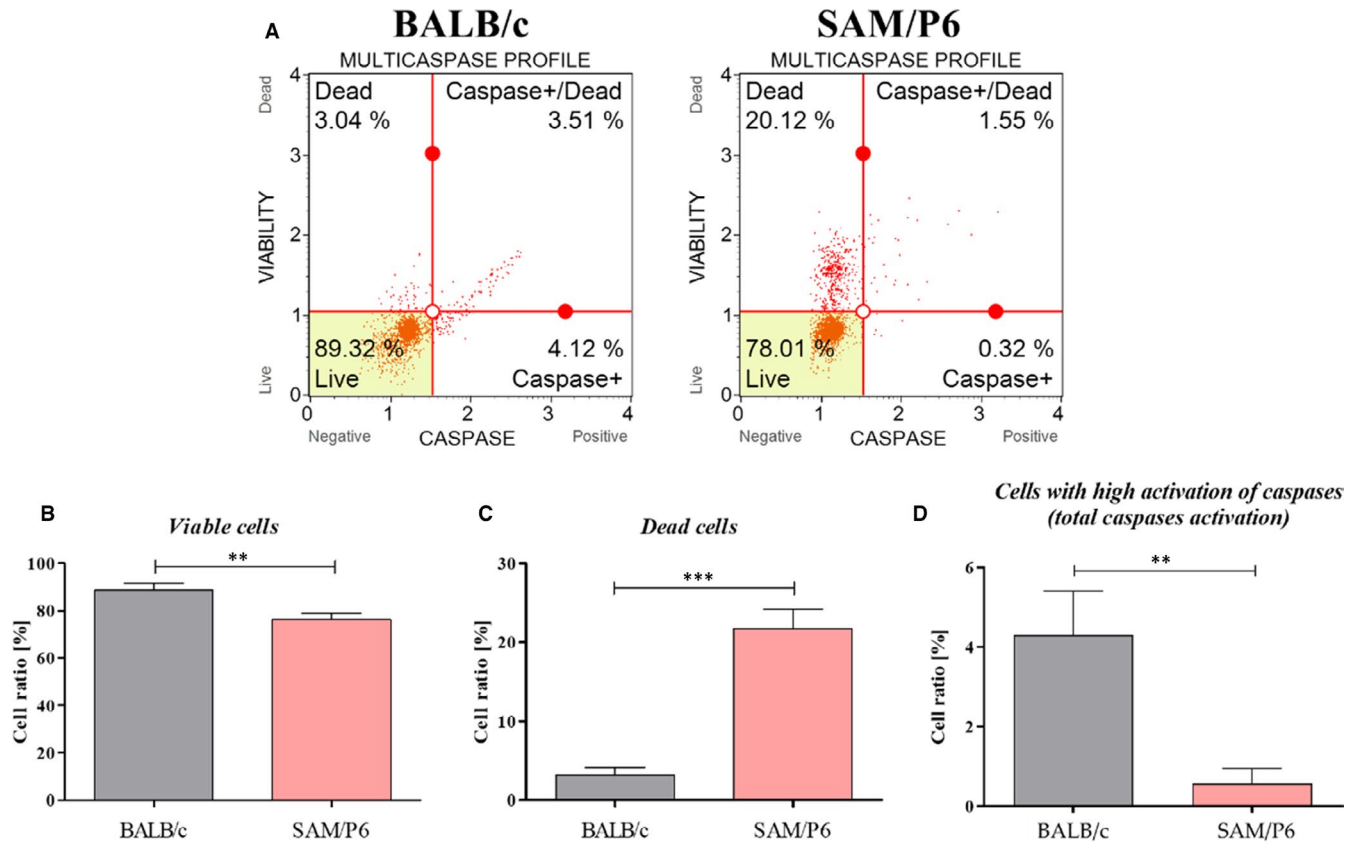


FIGURE 6 The activation of caspases in BMSCs. The representative graphs of cells' populations divided into four groups (A): *live* (left bottom corner), *dead* (left upper corner), *viable cells with activated caspases* (right bottom corner) and *dead cells with activated caspases* (right upper corner). The comparison analysis of viable cells (B), dead cells (C) and cells with activated caspases (D). Significant differences between groups are indicated with asterisk: * $P < .05$, ** $P < .01$, *** $P < .001$. Non-significant differences are marked as *ns*

miR-124-3p, miR145-3p, miR-203a and miR-223-3p, which are critical for modulation of osteogenesis. *Trap* belongs to the most common bone resorption markers naturally secreted by osteoclasts⁵⁵ within resorption sites. The increased expression of TRAP was characteristic for BMSC_{SAM/P6} and determined both at mRNA, as well as protein level. TRAP activity correlates not only with resorptive activity of osteoclasts, but also might be implicated in autoimmune disorders.⁵⁶ The complex role of TRAP has been explained by its key role in both bone homeostasis and the immune system.^{56,57} Many papers indicated that TRAP is not only the typical marker of osteoclasts, but also a significant player during chronic inflammation.⁵⁸ Moreover, Solberg et al showed that *Trap* expression in osteoblasts and osteocytes could be related to the capability of this enzyme to phosphorylate the pro-osteogenic proteins widely expressed by this cell types.⁵⁹ Thus, the molecular significance of *Trap* expression in multiple cell types has not been yet well elucidated.

Additionally, in this study, the high correlation between *Trap* and lncRNA *DANCR1* has been shown. Recent data indicate the critical role of *DANCR1* in osteoclastogenesis and osteoblasts differentiation.⁶⁰ The high expression of *DANCR1* in BMSC_{SAM/P6} might underline their similarity to osteoporotic human BMSCs that acquires osteoclast-like phenotype. It was shown that lncDANCR is highly expressed in osteoporotic patients and promotes IL-6 and TNF- α expression at mRNA and protein level in human blood mononuclear

cells (MNC). The lncDANCR1 increased resorbing activity of MNC, which can serve as a source of osteoclasts.⁶⁰ Therefore, we believe that *DANCR1*, as a result of its involvement in osteoporosis pathology in humans, may also serve as a biomarker for osteoporosis in BMSC_{SAM/P6}.

Moreover, we have established the profile of small non-coding RNAs profile (miRNA/miR), involved in the epigenetic regulation of bone development and homeostasis. We have found that BMSC_{SAM/P6} exhibit significantly increased miR levels including miR-7a-5p, miR-17-5p, miR-124-3p, miR145-3p, miR-203pa and miR-223-3p. Those molecules are associated with senescence- and age-dependent osteoporosis.⁶¹⁻⁶⁸ Mentioned miRNAs were highly expressed in osteoporotic BMSCs, however, in our previous articles, we have proven the dual role of the several miRNAs, including miR-124-3p, miR-203a and miR-223-3p.^{7,21} For that reason, the miRNAs biology needs to be determined. The miRNAs can be encapsulated in extracellular exosomes and/or microvesicles and released into osteoporotic tissue microenvironment. Moreover, mounting evidence show that miRNAs delivered through exosomes are present in body fluids, for example in blood, saliva and urine, thus influence distant cells of different types and may serve as diagnostic and prognostic markers.⁶⁹⁻⁷¹

Finally, as a result of the accumulation of the high amount of ROS and depolarised mitochondrial membrane, BMSC_{SAM/P6} defectively expressed master regulators of osteogenesis including

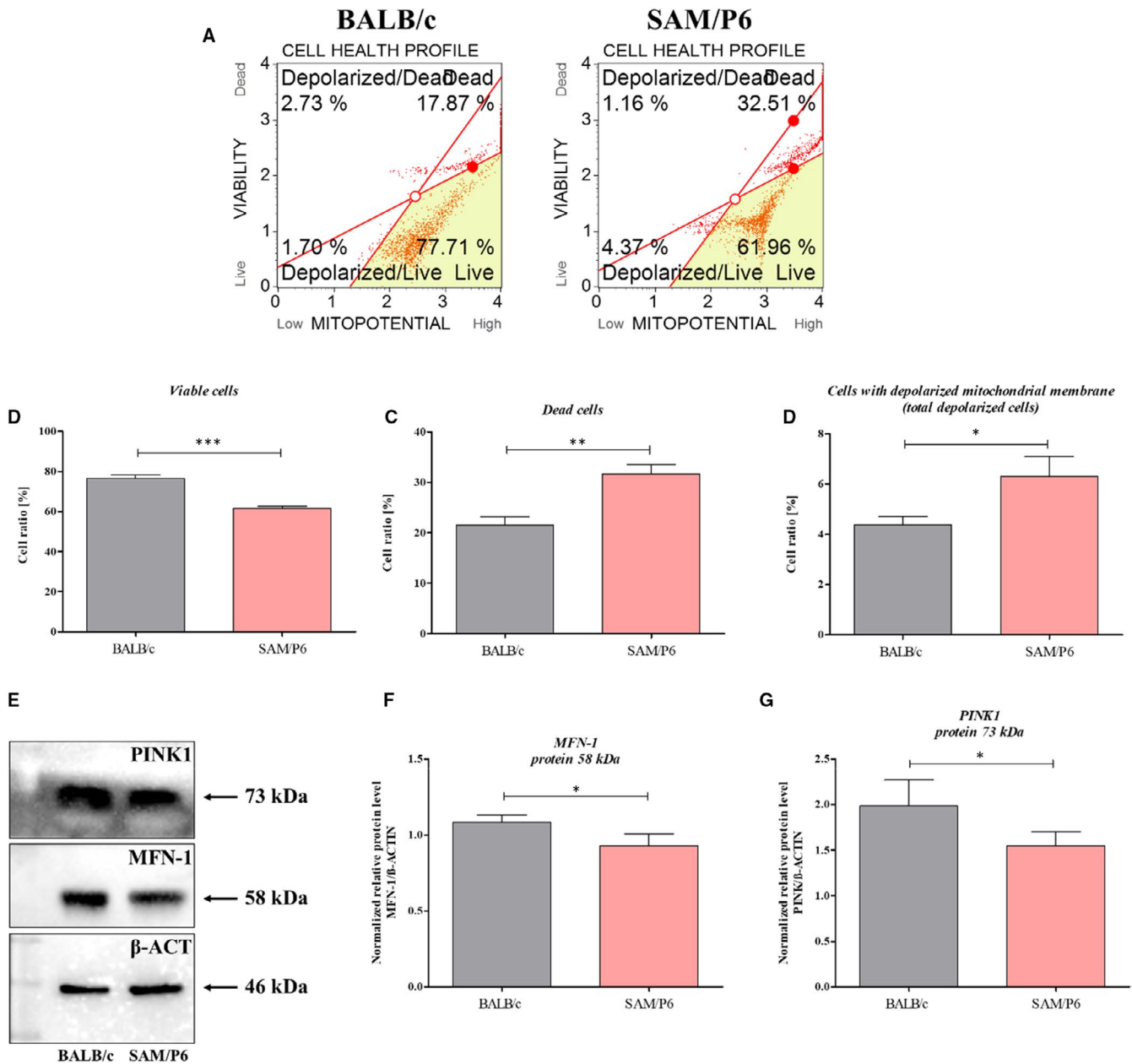


FIGURE 7 The electrostatic potential of mitochondrial membrane and mitochondrial dynamics in BMSCs. The representative graphs of cells' populations divided into four groups (A): *live* (right bottom corner), *dead* (right upper corner), *depolarised/live* (left bottom corner) and *depolarised/dead* (left upper corner). The comparison analysis of viable cells (B), dead cells (C) and cells with depolarised mitochondrial membrane (D). The representative graph of Western blot (E). The mitochondrial dynamics was evaluated by protein level of MFN-1 (F) and PINK1 (G). Significant differences between groups are indicated with asterisk: * $P < .05$, ** $P < .01$, *** $P < .001$. Non-significant differences are marked as *ns*

Coll-1, *Opg* and *Opn*, leading to the reduction in extracellular matrix mineralisation. The reduced expression of *Coll-1*, *Opg* and *Opn* has been previously shown in ovariectomised rat or human BMSCs derived from osteoporosis patients.⁷²⁻⁷⁵ Our data confirmed that senile osteoporosis influence the expression of OPN, both at mRNA and protein level. Previously, OPN was described as a protective factor against postmenopausal osteoporosis development, while OPG is a well-known inhibitor of osteoclastogenesis that protects against age-dependent osteoporosis development. Thus, reduced

expression of both *Opn* and *Opg* noted in BMSC_{SAM/P6} confirms a similar mechanism that modulates bone resorption in humans with senile osteoporosis.

Interestingly, mRNA expression for transcription factor *Runx-2* noted in BMSC_{SAM/P6} and BMSC_{BALB/c} was comparable. However, the analysis of RUNX-2 protein expression also confirmed disturbed osteogenic potential of BMSC_{SAM/P6}. A similar tendency has been observed by Corrigan and colleagues²⁶ indicating the impaired osteoblast differentiation of human BMSCs derived from the osteoporotic

patients. Moreover, Zannata et al showed that RUNX-2 regulates bone formation and remodelling throughout life, and its expression profile is age-dependent and correlates with bone mineral density (BMD).⁷⁶

This study indicates that BMSC_{SAM/P6} exhibit a high similarity with progenitor cells isolated from osteoporotic human patients, thus becoming a novel model for in vitro study to develop new and efficient therapeutic strategies for age-related (senile) osteoporosis. The SAM/P6 model of osteoporosis has a valuable impact on the preclinical examinations of age-related osteoporosis and might help to develop more effective strategies of treatment. Here, we have performed profound characteristic of BMSC_{SAM/P6} cytophysiology, with particular attention on self-renewal and multilineage potential. The BMSC_{SAM/P6} show features of ageing and senescent cells, with lowered pro-regenerative function, related to decreased osteogenic potential and enhanced accumulation of a lipid vacuoles. Given the limited access to human cells with age-related and senescence phenotype typical for senile osteoporosis, the BMSC_{SAM/P6} can be used successfully as a reliable model to explore and establish novel agents for osteoporosis treatment.

ACKNOWLEDGEMENTS

The publication is financed under the Leading Research Groups support project from the subsidy increased for the period 2020–2025 in the amount of 2% of the subsidy referred to Art. 387 (3) of the Law of 20 July 2018 on Higher Education and Science, obtained in 2019. Substantive and financial support obtained over the course of the completion of the Harmonia 10 project titled “New, two-stage scaffolds based on calcium nanoapatite (nHAP) incorporated with iron nanotoxides (Fe₂O₃/Fe₃O₄) with the function of controlled release of miRNA in a static magnetic field for the regeneration of bone fractures in osteoporotic patients” (Grant No. UMO 2017/26/M/NZ5/01184) is thankfully gratefully acknowledged. Moreover, acknowledgements go to Ariadna Pielok for the help with animals' killings, as well as Klaudia Marcinkowska for the guidance during *in vitro* procedures.

CONFLICTS OF INTEREST

The authors declare no conflict of interest.

AUTHOR CONTRIBUTION

Mateusz Sikora: Data curation (equal); Formal analysis (equal); Investigation (equal); Methodology (equal); Resources (equal); Software (equal); Validation (equal); Visualization (equal); Writing-original draft (equal); Writing-review & editing (equal). **Agnieszka Smieszek:** Conceptualization (equal); Data curation (equal); Formal analysis (equal); Investigation (equal); Methodology (equal); Resources (equal); Software (equal); Supervision (equal); Validation (equal); Visualization (equal); Writing-original draft (equal); Writing-review & editing (equal). **Krzysztof Marycz:** Conceptualization (equal); Funding acquisition (lead); Project administration (lead); Supervision (equal); Validation (equal); Writing-original draft (equal); Writing-review & editing (equal).

DATA AVAILABILITY STATEMENT

The data sets used in this study are available from the first author and corresponding author on reasonable request.

ORCID

Mateusz Sikora  <https://orcid.org/0000-0002-9965-587X>

Krzysztof Marycz  <https://orcid.org/0000-0003-3676-796X>

REFERENCES

- Porter JL, Varacallo M. Osteoporosis. In: *StatPearls*. StatPearls Publishing; 2020. Accessed January 2, 2021. <http://www.ncbi.nlm.nih.gov/books/NBK441901/>
- Johnston CB, Dagar M. Osteoporosis in older adults. *Med Clin North Am*. 2020;104(5):873-884. <https://doi.org/10.1016/j.mcna.2020.06.004>
- Hernlund E, Svedbom A, Ivergård M, et al. Osteoporosis in the European Union: medical management, epidemiology and economic burden. A report prepared in collaboration with the International Osteoporosis Foundation (IOF) and the European Federation of Pharmaceutical Industry Associations (EFPIA). *Arch Osteoporos*. 2013;8(1-2):136. <https://doi.org/10.1007/s11657-013-0136-1>
- Compston J. Osteoporosis: social and economic impact. *Radiol Clin North Am*. 2010;48(3):477-482. <https://doi.org/10.1016/j.rcl.2010.02.010>
- Föger-Samwald U, Dovjak P, Azizi-Semrad U, Kersch-Schindl K, Pietschmann P. Osteoporosis: Pathophysiology and therapeutic options. *EXCLI J*. 2020;19:1017-1037. <https://doi.org/10.17179/excli.2020-2591>
- Sandhu SK, Hampson G. The pathogenesis, diagnosis, investigation and management of osteoporosis. *J Clin Pathol*. 2011;64(12):1042-1050. <https://doi.org/10.1136/jcp.2010.077842>
- Sikora M, Marycz K, Smieszek A. Small and long non-coding RNAs as functional regulators of bone homeostasis, acting alone or cooperatively. *Molecular Therapy - Nucleic Acids*. 2020;21:792-803. <https://doi.org/10.1016/j.omtn.2020.07.017>
- Zhou C-C, Wu Z-P, Zou S-J. The study of signal pathway regulating the osteogenic differentiation of bone marrow mesenchymal stem cells. *Sichuan Da Xue Xue Bao Yi Xue Ban*. 2020;51(6):777-782. <https://doi.org/10.12182/20201160103>
- Friedenstein AJ. Determined and Inducible Osteogenic Precursor Cells. In: *Ciba Foundation Symposium 11 - Hard Tissue Growth, Repair and Remineralization*. John Wiley and Sons. Ltd; 1973:169-185. <https://doi.org/10.1002/9780470719947.ch9>
- Friedenstein AJ, Chailakhyan RK, Gerasimov UV. Bone marrow osteogenic stem cells: in vitro cultivation and transplantation in diffusion chambers. *Cell Tissue Kinet*. 1987;20(3):263-272. <https://doi.org/10.1111/j.1365-2184.1987.tb01309.x>
- Qadir A, Liang S, Wu Z, Chen Z, Hu L, Qian A. Senile osteoporosis: the involvement of differentiation and senescence of bone marrow stromal cells. *Int J Mol Sci*. 2020;21(1):349. <https://doi.org/10.3390/ijms21010349>
- Dominici M, Le Blanc K, Mueller I, et al. Minimal criteria for defining multipotent mesenchymal stromal cells. The International Society for Cellular Therapy position statement. *Cytotherapy*. 2006;8(4):315-317. <https://doi.org/10.1080/14653240600855905>
- Huo S-C, Yue B. Approaches to promoting bone marrow mesenchymal stem cell osteogenesis on orthopedic implant surface. *World J Stem Cells*. 2020;12(7):545-561. <https://doi.org/10.4252/wjsc.v12.i7.545>
- Yu L, Wu Y, Liu J, et al. 3D culture of bone marrow-derived mesenchymal stem cells (BMSCs) could improve bone regeneration in 3D-printed porous Ti6Al4V scaffolds. *Stem Cells Int*. 2018;2018:1-13. <https://doi.org/10.1155/2018/2074021>

15. Jin Y-Z, Lee JH. Mesenchymal stem cell therapy for bone regeneration. *Clin Orthop Surg*. 2018;10(3):271-278. <https://doi.org/10.4055/cios.2018.10.3.271>
16. Matsushita Y, Nagata M, Kozloff KM, et al. A Wnt-mediated transformation of the bone marrow stromal cell identity orchestrates skeletal regeneration. *Nat Commun*. 2020;11(1):332. <https://doi.org/10.1038/s41467-019-14029-w>
17. Frank O, Heim M, Jakob M, et al. Real-time quantitative RT-PCR analysis of human bone marrow stromal cells during osteogenic differentiation in vitro. *J Cell Biochem*. 2002;85(4):737-746. <https://doi.org/10.1002/jcb.10174>
18. Yu H, Cheng J, Shi W, et al. Bone marrow mesenchymal stem cell-derived exosomes promote tendon regeneration by facilitating the proliferation and migration of endogenous tendon stem/progenitor cells. *Acta Biomater*. 2020;106:328-341. <https://doi.org/10.1016/j.actbio.2020.01.051>
19. Zhang Y, Liu Y, Liu H, Tang WH. Exosomes: biogenesis, biologic function and clinical potential. *Cell Biosci*. 2019;9: <https://doi.org/10.1186/s13578-019-0282-2>
20. Draebing T, Heigwer J, Juergensen L, Katus HA, Hassel D. Extracellular vesicle-delivered bone morphogenetic proteins: a novel paracrine mechanism during embryonic development. *bioRxiv*. 2018. <https://doi.org/10.1101/321356>
21. Smieszek A, Marcinkowska K, Pielok A, Sikora M, Valihrach L, Marycz K. The Role of miR-21 in osteoblasts-osteoclasts coupling in vitro. *Cells*. 2020;9(2):479. <https://doi.org/10.3390/cells9020479>
22. Luo Z, Lin J, Sun Y, Wang C, Chen J. Bone marrow stromal cell-derived exosomes promote muscle healing following contusion through macrophage polarization. *Stem Cells Dev*. 2021;30(3):135-148. <https://doi.org/10.1089/scd.2020.0167>
23. Huang T, Yu Z, Yu Q, et al. Inhibition of osteogenic and adipogenic potential in bone marrow-derived mesenchymal stem cells under osteoporosis. *Biochem Biophys Res Comm*. 2020;525(4):902-908. <https://doi.org/10.1016/j.bbrc.2020.03.035>
24. Huang Y, Yin Y, Gu Y, et al. Characterization and immunogenicity of bone marrow-derived mesenchymal stem cells under osteoporotic conditions. *Sci China Life Sci*. 2020;63(3):429-442. <https://doi.org/10.1007/s11427-019-1555-9>
25. Coipeau P, Rosset P, Langonné A, et al. Impaired differentiation potential of human trabecular bone mesenchymal stromal cells from elderly patients. *Cytotherapy*. 2009;11(5):584-594. <https://doi.org/10.1080/14653240903079385>
26. Corrigan MA, Coyle S, Eichholz KF, Riffault M, Lenehan B, Hoey DA. Aged osteoporotic bone marrow stromal cells demonstrate defective recruitment, mechanosensitivity, and matrix deposition. *CTO*. 2019;207(2):83-96. <https://doi.org/10.1159/000503444>
27. Śmieszek A, Czyrek A, Basinska K, et al. effect of metformin on viability, morphology, and ultrastructure of mouse bone marrow-derived multipotent mesenchymal stromal cells and Balb/3T3 embryonic fibroblast cell line. *Biomed Res Int*. 2015;2015:1-14. <https://doi.org/10.1155/2015/769402>
28. Soleimani M, Nadri S. A protocol for isolation and culture of mesenchymal stem cells from mouse bone marrow. *Nat Protoc*. 2009;4(1):102-106. <https://doi.org/10.1038/nprot.2008.221>
29. Śmieszek A, Tomaszewski K, Kornicka-Garbowska K, Marycz K. Metformin promotes osteogenic differentiation of adipose-derived stromal cells and exerts pro-osteogenic effect stimulating bone regeneration. *Journal of Clinical Medicine*. 2018;7:482. <https://doi.org/10.3390/jcm7120482>
30. Śmieszek A, Stręż K, Kornicka K, Grzesiak J, Weiss C, Marycz K. Antioxidant and anti-senescence effect of metformin on mouse olfactory ensheathing cells (mOECs) may be associated with increased brain-derived neurotrophic factor levels—an ex vivo study. *Int J Mol Sci*. 2017;18(4):872. <https://doi.org/10.3390/ijms18040872>
31. Marycz K, Weiss C, Śmieszek A, Kornicka K. Evaluation of oxidative stress and mitophagy during adipogenic differentiation of adipose-derived stem cells isolated from equine metabolic syndrome (EMS) horses. *Stem Cells Int*. 2018;2018:1-18. <https://doi.org/10.1155/2018/5340756>
32. Targonska S, Sikora M, Marycz K, Smieszek A, Wiglusz RJ. Theranostic Applications of Nanostructured Silicate-Substituted Hydroxyapatite Codoped with Eu³⁺ and Bi³⁺ Ions—A Novel Strategy for Bone Regeneration. *ACS Biomater Sci Eng*. Published online September 22, 2020. <https://doi.org/10.1021/acsbomaterials.0c00824>
33. Seweryn A, Pielok A, Lawniczak-Jablonska K, et al. Zirconium oxide thin films obtained by atomic layer deposition technology abolish the anti-osteogenic effect resulting from miR-21 inhibition in the pre-osteoblastic MC3T3 cell line. *Int J Nanomedicine*. 2020;15:1595-1610. <https://doi.org/10.2147/IJN.S237898>
34. Smieszek A, Seweryn A, Marcinkowska K, et al. Titanium dioxide thin films obtained by atomic layer deposition promotes osteoblasts' viability and differentiation potential while inhibiting osteoclast activity—potential application for osteoporotic bone regeneration. *Materials*. 2020;13(21):4817. <https://doi.org/10.3390/ma13214817>
35. Sikora M, Marcinkowska K, Marycz K, Wiglusz RJ, Śmieszek A. The potential selective cytotoxicity of poly (L- lactic acid)-based scaffolds functionalized with Nanohydroxyapatite and Europium (III) ions toward osteosarcoma cells. *Materials (Basel)*. 2019;12(22): <https://doi.org/10.3390/ma12223779>
36. Bindokas VP, Jordán J, Lee CC, Miller RJ. Superoxide production in rat hippocampal neurons: selective imaging with hydroethidine. *J Neurosci*. 1996;16(4):1324-1336.
37. Vu TH, Shipley J, Michael B, Bergers G, et al. MMP-9/Gelatinase B Is a key regulator of growth plate angiogenesis and apoptosis of hypertrophic chondrocytes. *Cell*. 1998;93(3):411-422.
38. Kadiroğlu ET, Akbalık ME, Karaöz E, et al. Calvarial bone defects in ovariectomized rats treated with mesenchymal stem cells and demineralised freeze-dried bone allografts. *Folia Morphologica*. 2020;79(4):720-735. <https://doi.org/10.5603/FM.a2020.0001>
39. Yousefzadeh N, Kashfi K, Jeddi S, Ghasemi A. Ovariectomized rat model of osteoporosis: a practical guide. *EXCLI J*. 2020;19:89-107. <https://doi.org/10.17179/excli2019-1990>
40. Petrenko Y, Vackova I, Kekulova K, et al. A Comparative analysis of multipotent mesenchymal stromal cells derived from different sources, with a focus on neuroregenerative potential. *Sci Rep*. 2020;10(1):4290. <https://doi.org/10.1038/s41598-020-61167-z>
41. Infante A, Rodríguez CI. Osteogenesis and aging: lessons from mesenchymal stem cells. *Stem Cell Res Ther*. 2018;9(1):244. <https://doi.org/10.1186/s13287-018-0995-x>
42. Alicka M, Kornicka-Garbowska K, Kucharczyk K, Kępska M, Röcken M, Marycz K. Age-dependent impairment of adipose-derived stem cells isolated from horses. *Stem Cell Res Ther*. 2020;11(1):4. <https://doi.org/10.1186/s13287-019-1512-6>
43. Kornicka K, Marycz K, Tomaszewski KA, Marędzia M, Śmieszek A. The effect of age on osteogenic and adipogenic differentiation potential of human adipose derived stromal stem cells (hASCs) and the impact of stress factors in the course of the differentiation process. *Oxid Med Cell Longev*. 2015;2015:1-20. <https://doi.org/10.1155/2015/309169>
44. Chen Y, Wang W, Liu F, Tang L, Tang R, Li W. Apoptotic effect of matrix metalloproteinases 9 in the development of diabetic retinopathy. *Int J Clin Exp Pathol*. 2015;8(9):10452-10459.
45. Abdollahi M, Larijani B, Rahimi R, Salari P. Role of oxidative stress in osteoporosis. *Therapy*. 2005;2(5):787-796. <https://doi.org/10.2217/14750708.2.5.787>
46. Domazetovic V, Marcucci G, Iantomasi T, Brandi ML, Vincenzini MT. Oxidative stress in bone remodeling: role of antioxidants. *Clin Cases*

- Miner Bone Metab.* 2017;14(2):209-216. <https://doi.org/10.11138/ccmbm/2017.14.1.209>
47. Tait SWG, Green DR. Caspase-independent cell death: leaving the set without the final cut. *Oncogene.* 2008;27(50):6452-6461. <https://doi.org/10.1038/onc.2008.311>
 48. Kroemer G, Martin SJ. Caspase-independent cell death. *Nat Med.* 2005;11(7):725-730. <https://doi.org/10.1038/nm1263>
 49. Ishihara N, Eura Y, Mihara K. Mitofusin 1 and 2 play distinct roles in mitochondrial fusion reactions via GTPase activity. *J Cell Sci.* 2004;117(Pt 26):6535-6546. <https://doi.org/10.1242/jcs.01565>
 50. Belov SV, Lobachevsky YP, Danilejko YK, et al. The role of mitochondria in the dual effect of low-temperature plasma on human bone marrow stem cells: from apoptosis to activation of cell proliferation. *Appl Sci.* 2020;10(24):8971. <https://doi.org/10.3390/app10248971>
 51. Ren L, Chen X, Chen X, Li J, Cheng B, Xia J. Mitochondrial dynamics: fission and fusion in fate determination of mesenchymal stem cells. *Front Cell Dev Biol.* 2020;8. <https://doi.org/10.3389/fcell.2020.580070>
 52. Bingol B, Sheng M. Mechanisms of mitophagy: PINK1, Parkin, USP30 and beyond. *Free Radic Biol Med.* 2016;100:210-222. <https://doi.org/10.1016/j.freeradbiomed.2016.04.015>
 53. Matsuda S, Kitagishi Y, Kobayashi M. Function and characteristics of PINK1 in mitochondria. *Oxid Med Cell Longev.* 2013;2013:1-6. <https://doi.org/10.1155/2013/601587>
 54. Feng X, Yin W, Wang J, Feng L, Kang YJ. Mitophagy promotes the stemness of bone marrow-derived mesenchymal stem cells. *Exp Biol Med (Maywood).* 2021;246(1):97-105. <https://doi.org/10.1177/1535370220964394>
 55. Kuo T-R, Chen C-H. Bone biomarker for the clinical assessment of osteoporosis: recent developments and future perspectives. *Biomark Res.* 2017;5. <https://doi.org/10.1186/s40364-017-0097-4>
 56. Hayman AR. Tartrate-resistant acid phosphatase (TRAP) and the osteoclast/immune cell dichotomy. *Autoimmunity.* 2008;41(3):218-223. <https://doi.org/10.1080/08916930701694667>
 57. Ginaldi L, Di Benedetto MC, De Martinis M. Osteoporosis, inflammation and ageing. *Immun Ageing.* 2005;2:14. <https://doi.org/10.1186/1742-4933-2-14>
 58. Park JK, Rosen A, Saffitz JE, et al. Expression of cathepsin K and tartrate-resistant acid phosphatase is not confined to osteoclasts but is a general feature of multinucleated giant cells: systematic analysis. *Rheumatology.* 2013;52(8):1529-1533. <https://doi.org/10.1093/rheumatology/ket184>
 59. Solberg LB, Brorson S-H, Stordalen GA, Bækkevold ES, Andersson G, Reinholt FP. Increased tartrate-resistant acid phosphatase expression in osteoblasts and osteocytes in experimental osteoporosis in rats. *Calcif Tissue Int.* 2014;94(5):510-521. <https://doi.org/10.1007/s00223-013-9834-3>
 60. Tong X, Gu P, Xu S, Lin X. Long non-coding RNA-DANCR in human circulating monocytes: a potential biomarker associated with postmenopausal osteoporosis. *Biosci Biotechnol Biochem.* 2015;79(5):732-737. <https://doi.org/10.1080/09168451.2014.998617>
 61. Zhou M, Ma J, Chen S, Chen X, Yu X. MicroRNA-17-92 cluster regulates osteoblast proliferation and differentiation. *Endocrine.* 2014;45(2):302-310. <https://doi.org/10.1007/s12020-013-9986-y>
 62. Tang L, Yin Y, Liu J, Li Z, Lu X. MiR-124 attenuates osteoclastogenic differentiation of bone marrow monocytes via targeting Rab27a. *Cell Physiol Biochem.* 2017;43(4):1663-1672. <https://doi.org/10.1159/000484027>
 63. Tang J, Lin X, Zhong J, et al. miR-124 regulates the osteogenic differentiation of bone marrow-derived mesenchymal stem cells by targeting Sp7. *Mol Med Rep.* 2019;49. <https://doi.org/10.3892/mmr.2019.10054>
 64. Hao W, Liu H, Zhou L, et al. MiR-145 regulates osteogenic differentiation of human adipose-derived mesenchymal stem cells through targeting FoxO1. *Exp Biol Med (Maywood).* 2018;243(4):386-393. <https://doi.org/10.1177/1535370217746611>
 65. Jin Y, Hong F, Bao Q, et al. MicroRNA-145 suppresses osteogenic differentiation of human jaw bone marrow mesenchymal stem cells partially via targeting semaphorin 3A. *Connect Tissue Res.* 2020;61(6):577-585. <https://doi.org/10.1080/03008207.2019.1643334>
 66. Tang Y, Zheng L, Zhou J, et al. MiR-203-3p participates in the suppression of diabetes-associated osteogenesis in the jaw bone through targeting Smad. *Int J Mol Med.* 2018;41. <https://doi.org/10.3892/ijmm.2018.3373>
 67. Zhang S, Liu Yi, Zheng Z, et al. MicroRNA-223 suppresses osteoblast differentiation by inhibiting DHRS3. *Cell Physiol Biochem.* 2018;47(2):667-679. <https://doi.org/10.1159/000490021>
 68. Li X, Zheng Y, Zheng Y, et al. Circular RNA CDR1as regulates osteoblastic differentiation of periodontal ligament stem cells via the miR-7/GDF5/SMAD and p38 MAPK signaling pathway. *Stem Cell Res Ther.* 2018;9(1):232. <https://doi.org/10.1186/s13287-018-0976-0>
 69. Cheng L, Sun X, Scicluna BJ, Coleman BM, Hill AF. Characterization and deep sequencing analysis of exosomal and non-exosomal miRNA in human urine. *Kidney Int.* 2014;86(2):433-444. <https://doi.org/10.1038/ki.2013.502>
 70. Gallo A, Tandon M, Alevizos I, Illei GG. The majority of microRNAs detectable in serum and saliva is concentrated in exosomes. *PLoS One.* 2012;7(3):e30679. <https://doi.org/10.1371/journal.pone.0030679>
 71. Zhao F, Cheng LI, Shao Q, et al. Characterization of serum small extracellular vesicles and their small RNA contents across humans, rats, and mice. *Sci Rep.* 2020;10(1):4197. <https://doi.org/10.1038/s41598-020-61098-9>
 72. Ma Z-P, Zhang Z-F, Yang Y-F, Yang Y. Sesamin promotes osteoblastic differentiation and protects rats from osteoporosis. *Med Sci Monit.* 2019;25:5312-5320. <https://doi.org/10.12659/MSM.915529>
 73. Liu X, Bao C, Xu HHK, et al. Osteoprotegerin gene-modified BMSCs with hydroxyapatite scaffold for treating critical-sized mandibular defects in ovariectomized osteoporotic rats. *Acta Biomater.* 2016;42:378-388. <https://doi.org/10.1016/j.actbio.2016.06.019>
 74. Meng B, Wu D, Cheng Y, et al. Interleukin-20 differentially regulates bone mesenchymal stem cell activities in RANKL-induced osteoclastogenesis through the OPG/RANKL/RANK axis and the NF- κ B, MAPK and AKT signalling pathways. *Scand J Immunol.* 2020;91(5):e12874. <https://doi.org/10.1111/sji.12874>
 75. He W, Chen L, Huang Y, et al. Synergistic effects of recombinant Lentiviral-mediated BMP2 and TGF-beta3 on the osteogenic differentiation of rat bone marrow mesenchymal stem cells in vitro. *Cytokine.* 2019;120:1-8. <https://doi.org/10.1016/j.cyt.2019.03.020>
 76. Zanatta M, Valenti MT, Donatelli L, Zucal C, Dalle CL. Runx-2 gene expression is associated with age-related changes of bone mineral density in the healthy young-adult population. *J Bone Miner Metab.* 2012;30(6):706-714. <https://doi.org/10.1007/s00774-012-0373-1>

SUPPORTING INFORMATION

Additional supporting information may be found online in the Supporting Information section.

How to cite this article: Sikora M, Śmieszek A, Marycz K. Bone marrow stromal cells (BMSCs CD45⁻/CD44⁺/CD73⁺/CD90⁺) isolated from osteoporotic mice SAM/P6 as a novel model for osteoporosis investigation. *J Cell Mol Med.* 2021;00:1-18. <https://doi.org/10.1111/jcmm.16667>

RESEARCH

Open Access



MiR-21-5p regulates the dynamic of mitochondria network and rejuvenates the senile phenotype of bone marrow stromal cells (BMSCs) isolated from osteoporotic SAM/P6 mice

Mateusz Sikora¹ , Agnieszka Śmieszek¹, Ariadna Pielok¹ and Krzysztof Marycz^{2,3*}

Abstract

Background Progression of senile osteoporosis is associated with deteriorated regenerative potential of bone marrow-derived mesenchymal stem/stromal cells (BMSCs). According to the recent results, the senescent phenotype of osteoporotic cells strongly correlates with impaired regulation of mitochondria dynamics. Moreover, due to the ageing of population and growing osteoporosis incidence, more efficient methods concerning BMSCs rejuvenation are intensely investigated. Recently, miR-21-5p was reported to play a vital role in bone turnover, but its therapeutic mechanisms in progenitor cells delivered from senile osteoporotic patients remain unclear. Therefore, the goal of this paper was to investigate for the first time the regenerative potential of miR-21-5p in the process of mitochondrial network regulation and stemness restoration using the unique model of BMSCs isolated from senile osteoporotic SAM/P6 mice model.

Methods BMSCs were isolated from healthy BALB/c and osteoporotic SAM/P6 mice. We analysed the impact of miR-21-5p on the expression of crucial markers related to cells' viability, mitochondria reconstruction and autophagy progression. Further, we established the expression of markers vital for bone homeostasis, as well as defined the composition of extracellular matrix in osteogenic cultures. The regenerative potential of miR-21 in vivo was also investigated using a critical-size cranial defect model by computed microtomography and SEM-EDX imaging.

Results MiR-21 upregulation improved cells' viability and drove mitochondria dynamics in osteoporotic BMSCs evidenced by the intensification of fission processes. Simultaneously, miR-21 enhanced the osteogenic differentiation of BMSCs evidenced by increased expression of *Runx-2* but downregulated *Trap*, as well as improved calcification of extracellular matrix. Importantly, the analyses using the critical-size cranial defect model indicated on a greater ratio of newly formed tissue after miR-21 application, as well as upregulated content of calcium and phosphorus within the defect site.

Conclusions Our results demonstrate that miR-21-5p regulates the fission and fusion processes of mitochondria and facilitates the stemness restoration of senile osteoporotic BMSCs. At the same time, it enhances the expression of

*Correspondence:

Krzysztof Marycz

kmmarycz@ucdavis.edu

Full list of author information is available at the end of the article



© The Author(s) 2023. **Open Access** This article is licensed under a Creative Commons Attribution 4.0 International License, which permits use, sharing, adaptation, distribution and reproduction in any medium or format, as long as you give appropriate credit to the original author(s) and the source, provide a link to the Creative Commons licence, and indicate if changes were made. The images or other third party material in this article are included in the article's Creative Commons licence, unless indicated otherwise in a credit line to the material. If material is not included in the article's Creative Commons licence and your intended use is not permitted by statutory regulation or exceeds the permitted use, you will need to obtain permission directly from the copyright holder. To view a copy of this licence, visit <http://creativecommons.org/licenses/by/4.0/>. The Creative Commons Public Domain Dedication waiver (<http://creativecommons.org/publicdomain/zero/1.0/>) applies to the data made available in this article, unless otherwise stated in a credit line to the data.

RUNX-2, while reduces TRAP accumulation in the cells with deteriorated phenotype. Therefore, miR-21-5p may bring a novel molecular strategy for senile osteoporosis diagnostics and treatment.

Keywords miR-21, Senile osteoporosis, Bone regeneration, Mitochondria dynamic, BMSCs, SAM/P6 mice

Background

Senile osteoporosis (OP) belongs to the progressive skeletal system diseases, manifested by disproportionate bone loss. Osteoporosis development results from the imbalance between bone resorption and bone formation, leading to gradual losses of bone mass and deteriorated density due to its demineralization [1–3]. As reported by World Health Organization (WHO) and International Osteoporosis Foundation (IOF), more than 200 million women worldwide are affected by this disability. Moreover, OP is diagnosed in more than 75 million people in Europe, Japan and the USA [4]. It is estimated that by 2050 osteoporosis-dependent bone fractures will increase to 310% in men and 240% in women when compared to the '90 s [5]. Furthermore, patients suffering from osteoporosis-related fractures are life-threatening, since they usually become bedridden and require constant medical health care [6]. This alarming data clearly indicate that OP is a progressing epidemic affecting people worldwide and require the development of intelligent pharmaceutical strategies to reverse this unfavourable trend.

Recently, bone marrow-derived mesenchymal stem/stromal cells (BMSCs) have been proposed to have clinical potential for osteoporosis-related bone fractures regeneration due to their unique physiological properties [7, 8]. Numerous studies showed that BMSCs compared to the other stem cells populations exhibit a higher ability to stimulate and enhance bone regeneration due to their paracrine activity [9, 10]. BMSCs were also identified as osteogenic stem/progenitor cells, demonstrating high osteoblast differentiation potential, hence their therapeutic potential is mainly associated with bone tissue regeneration [9, 11]. However, MSCs (mesenchymal stem cells) are losing their regenerative ability with age, and MSCs derived from elderly patients have limited regenerative potential [12–14]. Importantly, we have previously shown that BMSCs obtained from senile accelerated osteoporotic SAM/P6 mice were characterised by poor regenerative potential accompanied with stemness deterioration, which contributes to osteoporosis progression and might become a pharmaceutical target to prevent OP development [8]. Further, we have indicated an upregulated accumulation of reactive oxygen species (ROS) and a greater ratio of mitochondria with depolarized membrane potential within osteoporotic BMSCs that indicate on deteriorated cytophysiological processes

[8]. Furthermore, osteoporotic BMSCs presented inflammatory features, e.g. upregulation of TRAP expression, which undeniably links osteoporosis state with ongoing inflammation [8, 15–17]. Therefore, searching for an effective therapeutic solution that would target BMSCs rejuvenation and stemness restoration seems to be fully justified.

Recently, microRNAs (miRNAs) have been shown to play an essential regulatory role in bone cells growth, differentiation potential, metabolic activity, regulation of multipotency, as well as mitochondrial dynamics [2, 18]. MiR-21-5p (miR-21) is differentially expressed in many diseases, leading to pathological changes. The miR-21-5p level was reported to be reduced in serum and bone tissue of osteoporotic patients, hence may serve as a potential diagnostic biomarker of OP in liquid biopsies [19]. However, it has never been elucidated if the upregulation of miR-21 could affect the stemness restoration by the regulation of the mitochondria network in bone tissue milieu of senile osteoporotic patients. Nonetheless, our previous studies provide evidence that regulation of miR-21 expression may contribute to proper bone homeostasis, e.g. by modulating the expression of markers that regulate osteoblasts differentiation and drive their interplay with osteoclasts [2, 20, 21]. Concluding, we hypothesised that miR-21-5p may serve as an important factor with the evident capability to recover the deteriorated stemness of BMSCs in senile osteoporotic patients, e.g. by the regulation of mitochondria network dynamic that affects the cells' capability for bone homeostasis maintenance.

In this study, we assess whether the application of miR-21-5p rescues bone marrow mesenchymal stem/stromal cells (BMSC_{SAM/P6}) from senile phenotype and defective osteogenesis. The BMSC_{SAM/P6} and BMSC_{SAM/P6+miR-21} were compared to healthy BMSCs isolated from wild-type BALB/c mice (BMSC_{BALB/c}). We have analysed for the first time the impact of miR-21 on the regulation of mitochondrial network dynamic evidenced by differences in fusion and fission processes, as well as restoration of cells' stemness, including the potential for osteogenic differentiation. Therefore, we also focused on the miR-21-5p role in BMSCs metabolism and autophagy. Moreover, we have examined the cells' capability to differentiate into bone tissue by assessing the expression of markers associated with bone remodelling, both on RNA and protein levels. Finally, we have evaluated the miR-21 impact on

bone regeneration *in vivo*, using a critical-size cranial defect model (CSD) accompanied by computed microtomography (μ -CT) and SEM–EDX analyses. Given the obtained results, we speculate that miR-21-5p might become a potential therapeutic molecule for treating osteoporotic-related fractures by senile BMSCs rejuvenation. Our studies provide evidence that miR-21-5p has a pro-osteogenic function restoring the differentiation potential of progenitor cells with deteriorated metabolism. These results indicate that miR-21-5p is a promising target which can be modulated in order to regulate BMSCs metabolism and mitochondria network dynamic, thus, to restore the loss regenerative potential of BMSC for treatment of senile osteoporosis.

Methods

Model of senescence-accelerated mice prone 6

SAM/P6 mice strain (senescence-accelerated mice prone 6) was used as an animal model of senile osteoporosis. The strain belongs to SAM group of inbred mouse strains that are used as animal models of senescence acceleration, as well as age-related disorders. The SAM/P6 strain was obtained by Dr. Takeda during brother-sister mating of AKR/J mice in Kyoto University. In the age of 4 months, SAM/P6 mice presents the full spectrum of senile osteoporosis symptoms: low global bone density, deteriorated osteogenesis of bone marrow, deficits in endocortical mineralizing surface, reduction of BMD index and BV/TV index, as well as reduced calcium and phosphorus level. In addition, SAM/P6 mice are characterised by age-dependent inhibition of osteoblastogenesis and osteoclastogenesis but enhanced adipogenesis, which results in early disturbances of bone homeostasis [22–24].

The procedure of isolation and propagation of bone marrow-delivered mesenchymal stem/stromal cells

Long bones of mice lower limbs (femurs) were isolated in order to collect bone marrow-delivered mesenchymal stem/stromal cells (BMSCs). In order to collect the bones, the mice had to be sacrificed. Before the sacrifice procedure, the animals were given an aesthetic (mixture of xylazine—15 mg/kg and ketamine—50 mg/kg) in order to minimize the stress and suffering of animals. 15 min after administration of anaesthetics, animals were euthanized by the disruption of the spinal cord. The procedure was performed by a person qualified to kill animals. The death of each animal was confirmed by a veterinarian. The cells were isolated from two mice strains: healthy BALB/c mice ($n=15$ mice, 4 months old) and senescence-accelerated mice prone 6—SAM/P6 ($n=15$ mice, 4 months old). Collected bones (two bones per mouse) were washed two times using Hank's Balanced Salt

Solution (HBSS) with 1% addition of P/S (penicillin & streptomycin). The bone marrows were isolated by flushing it from medullary canals by the use of insulin syringes U-40 (29G X 1/2" needle) filled with HBSS and the samples were pooled together within the strains. After double centrifugation ($300\times g$, 4 min), they were counted using Muse[®] Count & Viability Kit (Merck[®]; cat. no.: MCH100102, Poznan, Poland) accordingly to manufacturers' instructions. Then, the isolated cells were inoculated on the 24-well dishes (800 000 cell/well) in 500 μ L of Ham's F-12 Nutrient Mixture (F-12) supplemented with 15% of foetal bovine serum (FBS) and 1% of P/S. The cells were maintained in CO₂ incubator (5% CO₂, 37 °C and 95% humidity). The culture media were removed and replaced with fresh media after 24 h of propagation in order to eliminate non-adherent hematopoietic cell lineage [25–27]. During cells propagation, the media were changed every 3–4 days.

Transfection with miR-21 Mimic

For the purpose of transfection, BMSCs were trypsinized at least once and propagated on the 24-well plates until reaching approximately 80% of confluency. Then, BMSCs isolated from SAM/P6 mice were transfected using MISSION[®] miRNA miR-21 Mimic (HMI0371, Sigma-Aldrich, Munich, Germany) and Lipofectamine 3000 Transfection Kit (L3000-008, Invitrogen, Thermo Fisher Scientific, Warsaw, Poland). The procedure of transfection was conducted accordingly to manufacturers protocol. The Lipofectamine 3000 Reagent and MISSION[®] miR-21 miRNA Mimic were prepared in OptiMEM medium (31985-070, Gibco, Life Technologies Corporation, USA) and mixed as described in producer's instructions. The transfection reagent was added to the cultures in the dilution 1:10. MiR-21 was used at the final concentration of 50 nM. The procedure of cells' transfection has been carried out for 72 h. BMSCs isolated from SAM/P6 mice that were not transfected with miR-21-5p, as well as BMSCs isolated from healthy BALB/c mice served as references during the experiment. After transfection, the cells were collected or maintained for osteogenic differentiation.

Cytometric evaluation of proteins related to bone homeostasis

In order to analyse the presence of proteins related to bone homeostasis, cytometric evaluation was performed. After the bone marrow isolation, the cells were inoculated on the 24-well plates. After 24 h, the cells were washed with HBSS and immediately transfected with miR-21 Mimic for 72 h, as described previously. Further, the cells were trypsinized, centrifuged (1300 RPM, 5 min, 4 °C), washed in PBS (Phosphate Buffered Saline) with 2%

addition of FBS and centrifuged for the second time (1300 RPM, 5 min, 4 °C). Finally, the cells were washed with PBS without FBS and centrifuged for the third time (1300 RPM, 5 min, 4 °C). In order to lyse the remained erythrocytes, 1 mL of NH₄Cl was added to the samples and centrifuged (1300 RPM, 5 min, 4 °C). Then, the samples were incubated with NH₄Cl for 15 min and centrifuged (1300 RPM, 5 min, 4 °C). Next, 100 µL of Fix & Perm Medium A (GAS001, Life Technologies Corporation, USA) was added to the cells and incubated for 15 min. Then, the cells were washed with 3 mL of PBS with 5% addition of FBS and centrifuged (350×g, 5 min). After that, the cells were incubated in the dark for 30 min with Fix & Perm Medium B (GAS002, Life Technologies Corporation, USA) with the addition of anti-RUNX-2 (M-70) antibody produced in rabbit (sc-10758, Santa Cruz Biotechnology) in the dilution 1:50. The cells were washed in 3 mL of PBS with 5% addition of FBS and centrifuged (350×g, 5 min). The secondary antibody—Anti-rabbit Atto-647 produced in goat (ab150079, Abcam)—was diluted in the PBS at the concentration 1:100 and incubated with the samples for 30 min in the dark. The samples were washed in 3 mL of PBS without FBS and centrifuged (350×g, 5 min). The cells were resuspended in 500 µL of fresh PBS and proceeded for cytometric evaluation. The samples were analysed using two-laser FACS Lyric Flow Cytometer (Becton Dickinson Polska, Sp. z o.o., Warsaw, Poland) with FACS Suite software. In each sample, 1000 of cells were evaluated. The results were visualised and analysed using FCS Express™ Software (version 7.08.0018, De Novo Software, Pasadena, CA, USA).

Osteogenesis induced in BMSCs

In order to induce the osteogenic differentiation of BMSCs, the cultures were propagated in the osteogenic medium prepared as described previously [20, 25]: MEM- α medium (Minimum Essential Medium Eagle—Alpha Modification) was supplemented with ascorbic acid (50 µg/mL), β glycerol phosphate disodium salt hydrate (10 nM) and 15% addition of FBS. The osteogenesis was performed for 10 days, and the media were changed twice a week. After differentiation, the cells were collected for analysis.

Evaluation of extracellular matrix composition

After osteogenic differentiation, the cells were fixed with 4% PFA (paraformaldehyde) for 15 min at room temperature. To visualise the calcium deposits, the specimens were stained with Alizarin Red for 20 min at room temperature as described previously [20, 28]. Then, the specimens were washed three times with distilled water and observed under Axio Observer A1 inverted microscope (3832000970, Zeiss, Oberkochen, Germany). The

photographs were taken by Canon PowerShot digital camera (Woodhatch, UK) under 100× magnification. The resolution of obtained images was: 3648 × 2736 pixels. The differences in staining intensity between the specimens were based on the number of colour pixels. The number of colour pixels was determined in three technical repetitions and using three different thresholds in Pixel Counter plugin (ImageJ Software version 1.52n, Wayne Rasband, National Institutes of Health, USA).

Immunocytochemical detection of proteins accumulation and cells' ultrastructure

The immunocytochemical staining technique was used to visualise the cells' ultrastructure and protein accumulation, as described previously [8] and accordingly to manufacturers' instructions. Mitochondrial network was stained using Mito Red dye (Sigma-Aldrich, Munich, Germany) at the concentration of 1:1000 in CGM (complete growth medium) for 30 min at 37 °C. The lysosomes were visualised using LysoTracker™ Yellow HCK-123 (Life Technologies Corporation, USA) at the concentration of 1:10,000 in CGM for 30 min at 37 °C. Before subsequent stainings, the cells were fixed with 4% PFA for 15 min and washed three times with HBSS. Afterwards, the specimens were permeabilized using 0.2% PBS-Tween solution with 10% addition of goat serum for 1 h and washed 3 times with HBSS. The cells' integrity was assessed by nuclei visualisation using Hoechst 33,342 (I34202, Invitrogen, Thermo Fisher Scientific, Warsaw, Poland) dye that was performed by incubation of specimens at 37 °C for 5 min. The reagent was diluted to the concentration 2 µg/mL. Moreover, the actin cytoskeleton was stained using phalloidin solution (49409, Sigma-Aldrich, Munich, Germany) at the concentration 1:800 for 40 min at 37 °C. Then, cells were incubated overnight with primary antibodies at 4 °C. The antibodies used for staining were diluted in HBSS: anti-RUNX-2 antibody (F-2) produced in mice (sc-390351, Santa Cruz Biotechnology, Dallas, Texas, USA) at the concentration 1:50 and anti-TRAP antibody (D-3) mouse monoclonal IgG1 (sc-376875, Santa Cruz Biotechnology, Dallas, Texas, USA) at the concentration 1:50. RUNX-2 and TRAP are initial markers of bone homeostasis and participate in bone turnover processes. Additionally, the specimens were stained with anti-LAMP2 antibody (H4B4) produced in mouse (ab25631, Abcam, Cambridge, UK) at the concentration 1:100 that serves as a marker of selective autophagy; anti-Ki67 antibody produced in rabbit (ab15580, Abcam, Cambridge, UK) at the concentration 1:1000 that is cells' proliferation marker; anti mTOR antibody (nb100-240) produced in rabbit (Novus Biologicals, Bio-Techne) at the concentration 1:100; and anti-MFN-1 antibody produced in rabbit (orb11040,

Biorbyt) at the concentration 1:250 which is a mediator of mitochondria fusion. For the purpose of BMSCs immunophenotyping, the following antibodies were used: anti-CD44 produced in rabbit (hpa005785, Sigma-Aldrich, Munich, Germany) at the concentration 1:1000; anti-CD45 produced in mouse (sc-53047, Santa Cruz Biotechnology, Dallas, Texas, USA) at the concentration 1:100; anti-CD73 produced in mouse (ab54217, Abcam, Cambridge, UK) at the concentration 0.1 µg/100µL; anti-CD90 produced in rabbit (ab92574, Abcam, Cambridge, UK) at the concentration 1:100 and anti-CD105 produced in rabbit (ab107595, Abcam, Cambridge, UK) at the concentration 1:100. Subsequently, the specimens were washed three times with HBSS and incubated with secondary antibodies: IgG—Atto 594 antibody produced in goat (anti-mouse or anti-rabbit) at the concentration 1:100 (Sigma-Aldrich, Munich, Germany) for 1 h at room temperature. The specimens were washed three times with HBSS and stained with DAPI (4',6-diamino-2-phenolindole) using a mounting medium (Fluoroshield™ with DAPI, Sigma-Aldrich, Munich, Germany). The cells were observed using a confocal microscope and Las X software (11889113, Leica DMI8, Leica Microsystems, KAWA.SKA Sp. z o.o., Zalesie Górne, Poland). The images were captured under 630 × and 1000 × magnification. The microscopic images were obtained by applying maximum intensity projection using Fiji is just ImageJ Software (version 1.52n, Wayne Rasband, National Institutes of Health, USA). The obtained images resolution was 768 × 256 pixels. The differences in staining intensity between the specimens were evaluated based on the number of colour pixels from images captured in three technical repetitions and using three different thresholds (thresholds: 49, 50, 51) in Pixel Counter plugin (ImageJ Software). Additionally, the MicroP Software was used to analyse the mitochondria morphology [29].

Evaluation of miRNA and mRNA expression in BMSCs cultures

The miRNA and mRNA transcripts levels were analysed using RT-qPCR (reverse transcription quantitative polymerase chain reaction) technique as described previously in detail [8, 28]. The cells were homogenised using 1 mL of Extrazol® (Blirt DNA, Gdańsk, Poland). Then, RNA was isolated using the phenol–chloroform method. The isolated RNA was diluted in molecular grade water (Sigma-Aldrich, Poznan, Poland) and evaluated spectrophotometrically (Epoch, Biotek, Bad Friedrichshall, Germany). Digestion of gDNA was performed using PrecisionDNase Kit (Primerdesign, BLIRT S.A., Gdańsk, Poland). cDNA was synthesised using Tetro cDNA Synthesis Kit (Bioline Reagents Limited, London, UK) in T100 Thermal Cycler (Bio-Rad, Hercules, CA,

USA). For non-coding RNAs analysis, Mir-X™ miRNA First-Strand Synthesis Kit (Takara Clontech Laboratories, Biokom, Poznań, Poland) was used. The procedures were conducted accordingly to manufacturers' instructions. The cDNA was synthesised from 150 ng of RNA. The qPCR reactions were performed using SensiFAST SYBR®&Fluorescein Kit (Bioline Reagents Ltd., London, UK) and CFX Connected Real-Time PCR Detection System (Bio-Rad, Hercules, CA, USA). The reactions were performed at least in triplicate. The reaction conditions: initial denaturation (95 °C, 2 min) and 45 cycles consisting of denaturation (95 °C, 5 s), annealing (10 s) and elongation (72 °C, 5 s). The melting curve was performed using a gradient protocol (65 to 95 °C, heating rate 0.2 °C/s). RQMAX algorithm was used to calculate the values of transcripts expression. Expression values of *Gapdh* (glyceraldehyde 3-phosphatehydrogenase) and *B2m* (beta-2-microglobulin) genes were used for the purpose of normalisation; however, miRNA expression values were normalised to snU6 gene. The normalisation was performed using the formula: $\Delta Ct = Ct(\text{gene of interest}) - Ct(\text{housekeeping gene})$. Among obtained ΔCt values, a maximum value was emerged (MAX value), which was used for standardisation of obtained results. The standardisation and calculation of gene expression was performed using the formula $RQMAX = 2^{(MAX\ value - \Delta Ct)}$. The characterisation of used primers is presented in Table 1. The accession numbers presented in Table 1 refer to specific nucleotides and can be found in the official database of National Center for Biotechnology Information (<https://www.ncbi.nlm.nih.gov/>).

The effectiveness of new bone formation in vivo

The in vivo study was conducted with the full approval of the Local Ethics Committee for Animal Experiments in Wrocław (Resolution no.069/2020/P1, 9.12.2020). The guidelines included in the Act on the Protection of Animals Used for Scientific or Educational Purposes from 15 of January 2015, which implements Directive 2010/63/EU of the European Parliament and the Council of 22 September 2010, were fully followed during the study. Moreover, the procedures of PN-EN ISO 10993–2:2006 standards were used. Senescence accelerated osteoporotic SAM/P6 mice were purchased from Envigo (Indianapolis, IN, USA). One-week period of acclimatisation was preceded before the experiment. The mice were housed under a 12 h light/dark cycle with constant temperature (22 ± 2 °C) and humidity ($50 \pm 10\%$), as well as fed with a standard chow diet and ad libitum access to water.

A bilateral cranial defect was performed to assess the osteoinductive properties of miR-21. The procedure of cranial defect model conduction was described previously and performed in two (n=2) SAM/P6 mice [30].

Table 1 The characteristic of primers used in RT-qPCR

Gene	Primer Sequence 5'-3'	Annealing [°C]	Accession No
<i>Ppar-γ</i>	F:CTCTGCTGGGGATCTGAAGG R:GGAATGCGAGTGGTCTTCCA	58.8	NM_001308354.1
<i>mTOR</i>	F:CTTGAGAAACCAGCCATAA R:CTGGTTTCACCAAACCGTCT	60.0	NM_020009.2
<i>Lamp2</i>	F:CTTAGCTTCTGGGATGCCCC R:TCATCCAGCGAACACTCCTG	60.0	NM_001017959.2
<i>Mfn-1</i>	F:ATCACTGCAATCTTCGGCCA R:AGCAGTTGGTTGTGTGACCA	60.0	NM_024200.4
<i>Mff</i>	F:TCACATTTGGTGAGTGGGGC R:TTTTCCGGGACCCTCATTG	60.0	NM_001372412.1
<i>Bcl-2</i>	F:ATCGCCCTGTGGATGACTGAG R:CAGCCAGGAGAAATCAAACAGAGG	58.8	NM_000633.2
<i>Bax</i>	F:ACCAAGAAGCTGAGCGAGTGTC R:ACAAAGATGGTCACGGTCTGCC	58.8	NM_001291428.1
<i>Mmp-9</i>	F:GATGCCAACCTCCTCAACGA R:GGAAGCGGTCCAGGTAGTTC	60.0	NM_053056.2
<i>Runx-2</i>	F:TCCGAAATGCCTCTGCTGTT R:GCCACTTGGGGAGGATTTGT	58.8	NM_001271630.1
<i>Coll-1</i>	F:CAGGTATTGCTGGACAACGTG R:GGACCTTGTTCAGGTTCA	61.4	NM_007742.4
<i>Opn</i>	F:AGACCATGCAGAGAGCGAG R:GCCCTTCCGTTGTTGTCCT	57.3	NM_001204203.1
<i>Ocl</i>	F:GGTGCAGACCTAGCAGACACCA R:CGCTGGGCTTGGCATCTGTAA	57.0	NM_001032298.3
<i>Opg</i>	F:AGCCACGCAAAAAGTGTGGAA R:TCCTCTCTACACTCTCGGCA	58.8	NM_008764.3
<i>Alpl</i>	F:TTCATAAGCAGCGGGGGAG R:TGAGATTCGTCCTCGCTGG	60.0	NM_007431.3
<i>Bmp-2</i>	F:CTACAGGGAGAACACCCGGA R:GGGGAAGCAGCAACTAGAA	60.0	NM_007553.3
<i>Trap</i>	F:GTCTCTGGGGACAATTTCTACT R:GTTTGACGTGGAATTTGAAGC	60.0	XM_006509945.3
<i>Ctsk</i>	F:TAACAGCAAGGTGGATGAAATCT R:CTGTAGGATCGAGAGGGAGGTAT	60.0	NM_011613.3
<i>Nfatc-1</i>	F:TTCGAGTTCGATCAGAGCGG R:AGGTGACACTAGGGGACACA	60.0	NM_001164112.1
<i>Pu.1</i>	F:GAGAAGCTGATGGCTTGGAG R:TTGTGCTTGGACGAGAACTG	60.0	NM_001378899.1
<i>Gapdh</i>	F:GTCAGTGGTGGACCTGACCT R:CACCACCCTGTTGCTGTAGC	58.8	NM_001289746.1
<i>B2m</i>	F:CATACGCCTGCAGAGTTAAGCA R:GATCACATGTCTCGATCCCAGTAG	58.8	NM_009735.3
<i>miR-7a-5p</i>	TGGAAGACTAGTGATTTTGTGT	58.8	MIMAT0000677
<i>miR-17-5p</i>	CAAAGTGCTTACAGTCAGGTAG	58.8	MIMAT0000649
<i>miR-21a-5p</i>	TAGCTTATCAGACTGATGTTGA	58.8	MIMAT0000530
<i>miR-124-3p</i>	TAAGGCACGCGGTGAATGCC	58.8	MIMAT0000134
<i>miR-145-5p</i>	GTCAGTTTTCCAGGAATCCCT	58.8	MIMAT0000437
<i>miR-203a-3p</i>	GTGAAATGTTTAGGACCACTAG	58.8	MI0000283
<i>miR-223-3p</i>	TGTCAGTTTGTCAAATACCCCA	58.8	MIMAT0000280

The procedures were performed under the supervision of a veterinarian. The animals were subjected to general anaesthesia with the mixture of xylazine (25 mg/kg) and ketamine (70 mg/kg) and placed in a prone position. The type of anaesthesia was recommended due to the severe nature of the procedure and to minimise the suffering of the animals. The operating site was disinfected with a chlorhexidine solution. Then, the scalp and the periosteum on both sides of the parietal bone were incised. The periosteum was removed to expose the skull bone. The circular cranial defect (2 mm in diameter) was drilled using a cylindrical low-speed carbide bur with 1 mm of diameter. In order to deliver undegraded miR-21 to the defect site, a fully biocompatible and biodegradable biomaterial based on sodium alginate was prepared. Briefly, 2% solution of sodium alginate was prepared in NaCl and filtrated using 0.45 and 0.22 μm syringe filters. Simultaneously, 0.5 M solution of CaCl_2 was prepared. MISSION[®] miRNA miR-21 Mimic (HMI0371, Sigma-Aldrich, Munich, Germany) was added to the sodium alginate solution at the concentration 50 nM and mixed for 10 s using the vortex. Shortly before the procedure, the sodium alginate and CaCl_2 solution were mixed in a ratio 1:1 in order to synthesise a hydrogel. The alginate-based biomaterials with 50 nM of miR-21 were allocated in the right defect sites during the procedure. Left defect sites serve as controls, where hydrogels without miR-21 were administered. The procedure was performed in the presence of a heat lamp and the cuts were closed with 6–0 synthetic seams. Every 12 h, for three days after surgery, animals received painkillers i.e. buprenorphine (0.03 mg/kg) and meloxicam (1 mg/kg). Further, mice were sacrificed two weeks after the cranial defect procedure to analyse the formation of novel bone tissue. Before the sacrifice procedure, the animals were given an aesthetic (mixture of xylazine—15 mg/kg and ketamine—50 mg/kg) in order to minimize the stress and suffering of animals. 15 min after administration of anaesthetics, animals were euthanized by the disruption of the spinal cord. The procedure was performed by a person qualified to kill animals. The death of each animal was confirmed by a veterinarian.

Mice skulls were dissected for the μ -CT and SEM-EDX analyses. The computed microtomography measurements were performed in the X-ray Microtomography Laboratory at the Faculty of Computer Science and Materials Science, University of Silesia in Katowice (Chorzów, Poland) using the GE Phoenix v|tome|x microtomography system (General Electric, Cincinnati, OH, USA) at voltage 140 kV and current intensity 40 μA . The voxel size was 5.5 μm^3 . Detector sensitivity $\times 2$ and binning $\times 1$. Tomographic reconstructions were based on projection of 1800 images equally spaced through 360°

(exposure time 500 ms). The μ -CT scans were exported as VGL files and analysed using myVGL software (version 3.3.2.170119, Volume Graphic GmbH) in order to assess the structural properties of newly formed tissue. The initial resolution of obtained images was: 652 \times 456 pixels. For evaluating new tissue contribution, Fiji is just ImageJ Software was used. Moreover, the skulls were analysed using scanning electron microscopy with energy-dispersive X-ray analysis (SEM-EDX; SEM Evo LS 15 Zeiss, Germany) operating at 10 000 V and work distance 11 mm. The photographs of the defect sites were taken under 35 \times magnification. The images resolution was: 1024 \times 768 pixels. The mapping of calcium, phosphorus and hydroxyapatite composition was performed using Bruker Quantax 200 System with BrukerXFlash 5010 detector and Esprit 1.8 Software. Each analysis was performed under 35 \times magnification for 120 s operating at 20 000 V and a working distance set at 8.5 mm. Furthermore, the expression of crucial markers related to proper bone regeneration was examined using RT-qPCR technique as described in the previous paragraph.

Statistical analyses

Each analysis was performed in three technical repetitions. The material for the ex vivo experiments was delivered from 15 BALB/c and 15 SAM/P6 mice. The statistical analyses were performed using GraphPad Prism 5 (GraphPad Software, San Diego, CA, USA). The data were obtained using one-way analysis of variance (ANOVA) with Tukey's post hoc test. Differences were considered as statistically significant at $p < 0.05$. The significance levels were indicated with asterisks: * $p < 0.05$, ** $p < 0.01$, *** $p < 0.001$. Non-significant differences were marked as *ns*.

Results

miR-21 improves viability and proliferative activity in senile osteoporotic BMSCs

We confirmed the presence of BMSC population based on the expression of cell surface antigens typical for mesenchymal stem cells. Obtained cultures were characterised by accumulation of CD44, CD73, CD90 and CD105, while there was no presence of CD45 marker (Fig. 1A). Importantly, the accumulation of presented antigens was reduced in BMSCs delivered from osteoporotic SAM/P6 mice (Fig. 1B). The loss of the expression of cell surface markers may be correlated with senescent-like phenotype of BMSC_{SAM/P6}. Further, the miR-21-5p level was assessed in bone tissue collected from BALB/c and SAM/P6 mice, as well as in BMSCs. We noticed a higher transcript level of miR-21 in SAM/P6 mice when compared to BALB/c in both bone tissue and cells samples (Fig. 1C, D). It is known that non-coding RNAs are one of many

factors that affect the cells status, thus does not direct their biology independently. Although miR-21-5p expression was noticed to be upregulated in BMSCs and bones delivered from SAM/P6 mice, the activity of other crucial markers (senile phenotype, high activity of osteoclasts) affects the bone homeostasis that finally leads the mice into osteoporotic state. In addition, we confirmed the transfection efficiency that was observed by upregulation of miR-21-5p expression in the treated BMSC_{SAM/P6+miR-21} comparing to non-transfected BMSC_{SAM/P6} (Fig. 1D). Senile osteoporotic BMSC_{SAM/P6} were characterised by decreased DNA level (Hoechst positive cells) that was additionally manifested by deteriorated proliferative potential (Ki67 positive cells) when compared to healthy BMSC_{BALB/c}. However, it was noted that miR-21 increased the DNA level, thus improving proliferative potential of BMSC_{SAM/P6+miR-21} (Fig. 1E–G). Furthermore, miR-21 improved the viability of BMSC_{SAM/P6+miR-21} evidenced by downregulation of *Bax/Bcl-2* ratio (Bcl-2 associated X protein / B-cell lymphoma 2) (Fig. 1H–J). *Bax* and *Bcl-2* are both key players during intrinsic apoptotic pathway triggered by mitochondrial dysfunction. It was shown that *Bax* initialise cell death, while *Bcl-2* prevents apoptosis by inhibiting the activity of *Bax*.

MiR-21 reduces autophagy and regulates mitochondria dynamics in senile osteoporotic BMSCs

Obtained results demonstrated that upregulated expression of miR-21 in senile osteoporotic BMSC_{SAM/P6} impedes autophagy in bone marrow-derived mesenchymal stem/stromal cells. It has been evidenced by the decreased intensity of lysosomes and LAMP2 (lysosome-associated membrane protein 2) protein staining but greater intensity of mTOR (mammalian target of rapamycin kinase) staining in BMSC_{SAM/P6+miR-21}, when compared to BMSC_{SAM/P6} (Fig. 2A–D). Further, it has been noticed that BMSC_{SAM/P6} were characterised by upregulated expression of *PPAR-γ* (peroxisome proliferator-activated receptor gamma) and *Lamp2* (Fig. 2E, G), which serve as markers of selective autophagy. Notably, the expression of *PPAR-γ* was significantly downregulated in BMSC_{SAM/P6+miR-21} compared to BMSC_{SAM/P6} (Fig. 2E). Moreover, the expression level of

mTOR in osteoporotic BMSC was elevated after miR-21 upregulation (Fig. 2F). It is known that the activation of mTOR pathway inhibits the pathological induction of autophagy. No significant changes were observed in *Lamp2* expression (Fig. 2G).

The presence of miR-21 within BMSCs cultures significantly regulated the dynamic of the mitochondrial network, which was evidenced by the modulation of fusion and fission processes. In senile osteoporotic BMSC_{SAM/P6}, the mitochondria were characterised by their tubular-shape morphology observed in the senescent cells. However, after miR-21 upregulation, the mitochondria underwent fission processes evidenced by the decreased percentage of tubular-shape mitochondria in favour of globular-shape mitochondria (Fig. 2H, I). This crucial finding indicates the ongoing selective macroautophagy (mitophagy), which is responsible for degradation of defective mitochondria and maintain cellular homeostasis. Moreover, mitochondrial network activity reflected by a signal from MitoRed staining revealed that osteoporotic BMSC_{SAM/P6} show signs of depolarization. However, miR-21 upregulation improved mitochondrial activity, which was correlated with an enhanced MitoRed signal. Simultaneously reduced signal intensity of stained MFN-1 protein (mitofusin-1), as well as downregulated *Mfn-1* and *Mff* (mitochondria fission factor) expression, were characteristic for BMSC_{SAM/P6+miR-21} compared to BMSC_{SAM/P6} (Fig. 2H, J, K, L, M).

The complementary results regarding the modifications of mitochondria phenotype as a result of miR-21 upregulation were presented in Additional file 1: Figure S1. The prevalence of elongated and tubular-shaped mitochondria corresponded to their low number noted in BMSC_{SAM/P6}. The upregulation of miR-21 increased the number of mitochondria that stayed in line with the modification of mitochondria phenotype (Additional file 1: Figure S1A). The detailed analysis of fission and fusion processes has shown that BMSC_{SAM/P6} were characterised by an increased occurrence of mitochondria classified as simple tubes simultaneously accompanied by a lowered ratio of branching tubes and small globules when compared to BMSC_{BALB/c}. The addition of miR-21 drove the mitochondria reconstruction, evidenced by a decreased percentage of simple tubes, while upregulated

(See figure on next page.)

Fig. 1 MiR-21 improves viability and proliferative activity in BMSCs isolated from senile osteoporotic SAM/P6 mice. **A** The representative photographs (z-stack) of cells surface markers (CD44, CD45, CD73, CD90 and CD105) in BMSCs isolated from BALB/c and SAM/P6 mice. The staining intensity of visualised antigens was presented as bar graph **(B)**. The level of miR-21-5p was analysed in bone tissue samples delivered from BALB/c and SAM/P6 mice **(C)**, as well as in cell cultures after transfection with miR-21 mimic **(D)**. **E** The representative photographs (z-stacks) of cells stained with Hoechst 33342 and Ki67 protein in BMSCs isolated from BALB/c and SAM/P6 mice. The staining intensity of visualised **F** nuclei and **G** Ki67 protein were presented as bar graphs. The RT-qPCR technique was used to present the gene expression of **H** *Bax*, **I** *Bcl-2* and **J** *Bax/Bcl-2* ratio. The RT-qPCR measurements were performed using RQMAX method and presented in a log scale. The confocal microscope photographs were taken under 630-fold & 1000-fold magnification and the scale bars are equal to 40 μm and 10 μm, respectively. Significant differences between groups are indicated with asterisk: * $p < 0.05$, ** $p < 0.01$, *** $p < 0.001$. Non-significant differences are marked as ns

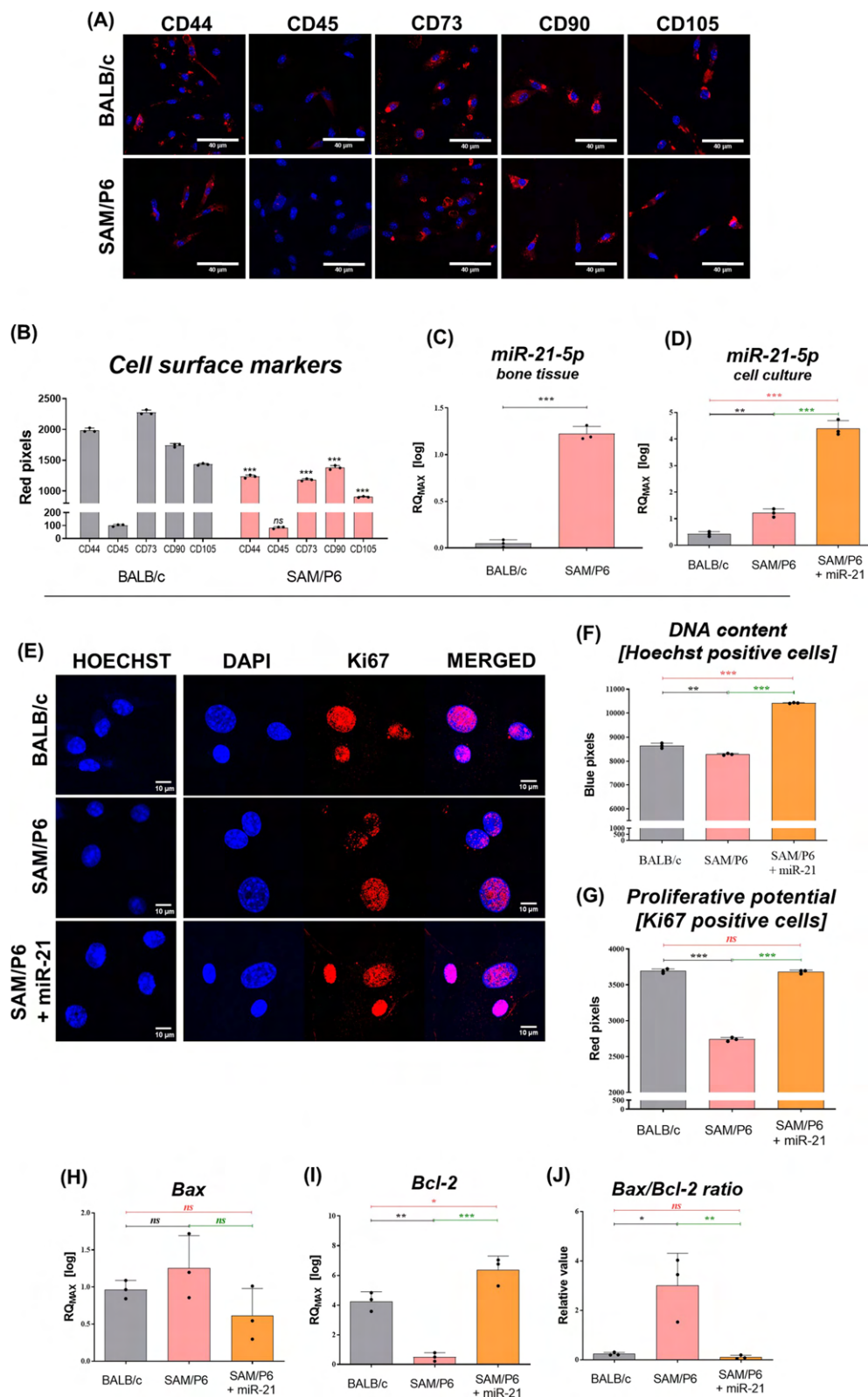


Fig. 1 (See legend on previous page.)

branching tubes and small globules (Additional file 1: Figure S1B–D).

MiR-21 improves osteogenic differentiation in senile osteoporotic BMSCs

The extracellular matrix (ECM) composition after BMSCs osteogenic differentiation indicated lowered osteogenic potential of senile BMSC_{SAM/P6} compared to healthy BMSC_{BALB/c}. However, improved quantity and quality of calcium deposits in BMSC_{SAM/P6+miR-21} cultures showed pro-osteogenic properties of miR-21 (Fig. 3A, C). At the same time, the actin cytoskeleton was poorly developed in BMSC_{SAM/P6} cultures which led to impaired cell–cell contact, lowered cells' confluency and finally deteriorated differentiation. Moreover, the signal intensity of stained RUNX-2 (runt-related transcription factor 2) protein was poorer in BMSC_{SAM/P6}, when compared to BMSC_{BALB/c}. The upregulation of miR-21 improved the development of the actin cytoskeleton in osteoporotic BMSCs and caused an increased protein expression of RUNX-2 during osteogenic differentiation (Fig. 3B, D). Importantly, miR-21 affected the expression of crucial osteogenic markers during BMSCs differentiation. Osteoporotic BMSC_{SAM/P6} were characterised by lower expression of *Runx-2* and *Coll-1* (collagen type 1), but elevated transcripts level of *Alpl* (alkaline phosphatase) and *Bmp-2* (bone morphogenetic protein 2), which serve as early osteogenic markers. The upregulation of miR-21 increased the expression of *Runx-2*, *Coll-1* and *Bmp-2* in BMSC_{SAM/P6+miR-21}, but downregulated the transcript level of *Alpl* (Fig. 3E, F, G, H). Additionally, BMSC_{SAM/P6} expressed less transcripts of late osteogenic markers, such as *Opn* (osteopontin) and *Opg* (osteoprotegerin), when compared to BMSC_{BALB/c}. Interestingly, BMSC_{SAM/P6} were also characterised by higher expression of *Ocl* (osteocalcin). Upregulation of miR-21 promoted osteogenesis in BMSC_{SAM/P6} which was manifested by increased expression of *Opn*, *Opg* and *Ocl* transcripts (Fig. 3I–K). Moreover, cytometric evaluation of isolated bone marrow cells revealed that miR-21 upregulates the expression of RUNX-2 protein in BMSC_{SAM/P6} (Fig. 3L, M).

(See figure on next page.)

Fig. 2 MiR-21 reduces autophagy and regulates mitochondria dynamics in BMSCs isolated from senile osteoporotic SAM/P6 mice. **A** The representative photographs (z-stacks) of cells' nuclei stained with lysosomes, LAMP2 and mTOR protein in BMSCs isolated from BALB/c and SAM/P6 mice. The staining intensity of visualised **B** lysosomes, **C** LAMP2 protein and **D** mTOR protein were presented as bar graphs. The RT-qPCR technique was used to present the gene expression of **E** *Ppar-γ*, **F** *mTOR* and **G** *Lamp2*. **H** The representative photographs (z-stacks) of nuclei with stained MFN-1 protein and mitochondrial network in BMSCs isolated from BALB/c and SAM/P6 mice. The images were supplemented with MicroP visualisation of mitochondria morphology and presented as a bar graph **I**. The staining intensity of visualised **J** MFN-1 protein and **K** mitochondria network were presented as bar graphs. The RT-qPCR technique was used to present the gene expression of **L** *Mfn-1* and **M** *Mff*. The RT-qPCR measurements were performed using RQMAX method and presented in a log scale. The confocal microscope photographs were taken under 630-fold and 1000-fold magnification and the scale bar is equal to 40 μm. Significant differences between groups are indicated with asterisk: **p* < 0.05, ***p* < 0.01, ****p* < 0.001. Non-significant differences are marked as *ns*

MiR-21 inhibits osteoclastogenesis in senile osteoporotic BMSCs

It has been shown that miR-21 inhibits the maturation of osteoclasts and impede the expression of osteoclastic markers. After miR-21 upregulation, the signal of TRAP-positive cells during microscopic analyses in osteoporotic BMSCs was significantly reduced (Fig. 4A, B). Moreover, after miR-21 upregulation, the expression of *Trap*, *Ctsk* (cathepsin K) and *Nfatc-1* (nuclear factor of activated T-cells, cytoplasmic 1) in osteoporotic BMSCs was significantly decreased (Fig. 4C, D, F). Simultaneously, the level of *Pu.1* (transcription factor PU.1) in BMSC_{SAM/P6+miR-21} was downregulated (Fig. 4G), but *Mmp-9* (matrix metalloproteinase 9) level was upregulated (Fig. 4E), when compared to BMSC_{SAM/P6}.

MiR-21 affects the expression of non-protein-coding RNAs in BMSCs isolated from senile osteoporotic SAM/P6 mice

It has been noticed that miR-21 promotes the osteogenic potential of senile osteoporotic BMSCs, thus we decided to evaluate if miR-21 affects the miRNAs essential for bone homeostasis. After miR-21 upregulation, the level of *miR-7a-5p*, *miR-145-3p* and *miR-223-3p* was significantly elevated (Fig. 5A, D, F). At the same time, the level of *miR-17-5p* went down (Fig. 5B). The level of *miR-124-3p* and *miR-203a* did not change significantly (Fig. 5C, E).

MiR-21 improves bone regeneration in senile osteoporotic SAM/P6 mice

The in vivo study performed using senile osteoporotic SAM/P6 mice strain confirmed the pro-osteogenic properties of miR-21. The fully biocompatible complexes consisted of 5% sodium alginate functionalized with miR-21 were placed in the centre of parietal bones (Fig. 6A, B). Two weeks after the operation, SEM–EDX analyses revealed elevated concentrations of phosphorus (P) and calcium (Ca) within defect sites after miR-21 application (Fig. 6D, F, G). Importantly, X-ray computed microtomography (μ-CT) analyses indicated the higher contribution of newly created bone tissue in SAM/P6 mice after miR-21 treatment. (Fig. 6C, E). In addition, the transcript levels of *miR-21-5p*, *miR-124-3p* and *Runx-2* were

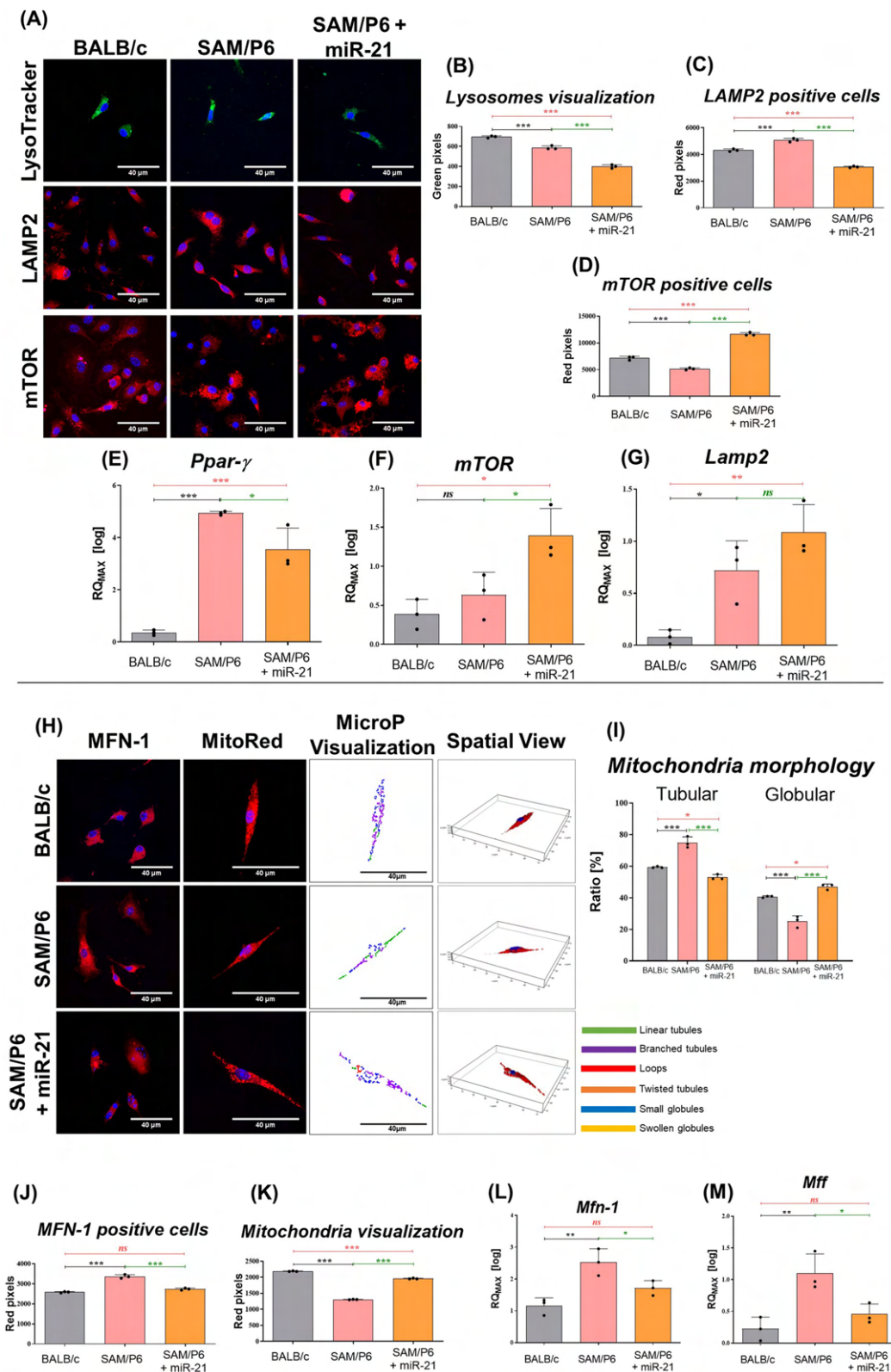


Fig. 2 (See legend on previous page.)

upregulated, while *Trap* was downregulated in the defect site. Obtained results were comparable to analyses using BMSCs model and indicated enhanced bone regeneration after miR-21 application (Fig. 6H–K).

Discussion

Osteoporosis is reaching epidemic levels among the elderly worldwide, leading to serious health complications, including bone fractures [31]. Numerous molecular pathways have been identified to play a critical role in regulating osteoporosis, including those regulated by miRNAs [32, 33]. In this study, for the first time, we have investigated the rejuvenating role of miR-21-5p in the course of senile osteoporosis. We have determined the influence of miR-21 upregulation on mitochondria network dynamics as well as impaired osteogenic differentiation of BMSCs isolated from osteoporotic SAM/P6 senile mice. Previously, miR-21-5p was widely considered a potential diagnostic and therapeutic tool that may find application during skeletal system disabilities, including osteoporosis-related fractures [20, 28, 34, 35]. Here, we have discovered that miR-21-5p drives the mitochondria dynamic, reversing the senile phenotype and improving the osteogenic differentiation potential of osteoporotic mice derived BMSC_{SAM/P6}, as well as promote bone regeneration in tissue milieu in a bilateral cranial defect in SAMP/P6 mice.

Our previous study showed that BMSC_{SAM/P6} are characterised by impaired multilineage differentiation potential, increased senescence, lowered stemness, as well as decreased proliferative activity, confirming the diseased phenotype of BMSCs isolated from osteoporotic patients [25, 36]. Additionally, the senescent BMSCs are characterised by depolarization of mitochondrial membrane that affects disturbed metabolic activity and clearly indicates an impaired ability of SAM/P6 derived BMSCs to produce a properly mineralized extracellular matrix. For that reason, there is a huge need to investigate the molecular mechanisms that must be improved in order to restore BMSCs proper functions. Here, we have shown that miR-21-5p upregulated viability and proliferative potential of senile osteoporotic BMSCs. It was evidenced by decreased *Bax/Bcl-2* ratio, as well as a

greater accumulation of Ki67 protein, which serves as a marker of actively dividing cells [37]. Moreover, the confocal analysis of the accumulation of cell surface markers, such as CD44, CD73, CD90 and CD105, confirmed the senile-like phenotype and loss of “stemness” in BMSCs delivered from SAM/P6 mice [38–42].

Further, we confirmed that miR-21-5p significantly regulates the dynamics of the mitochondria network, evidenced by the intensification of their fission processes. The ratio of elongated tubular-shape mitochondria decreased in favour of globular-shape mitochondria in BMSC_{SAM/P6+miR-21}, compared to osteoporotic BMSC_{SAM/P6}. More specifically, the percentage of distinguished mitochondria subtypes i.e. simple tubes, branching tubes and small globules in BMSC_{SAM/P6+miR-21} became identical to healthy BMSC_{BALB/c}. The reconstruction of mitochondria morphology was also noted in the general mitochondria quantity in examined BMSCs. Interestingly, the expression of both *Mfn-1* (mitofusin-1) and *Mff* (mitochondrial fission factor), the master regulators of mitochondria's fission and fusion, became downregulated. *Mfn-1* and *Mfn-2* mediate the fusion of outer mitochondria membrane, while the optic atrophy protein 1 (OPA1) mediates the fusion of inner membrane. Although the mitochondria fission is mediated by DRP1 (dynamin-related GTPase), it is recruited through four transmembrane receptors: MFF, FIS1 (mitochondrial fission 1 protein), MiD49 and MiD50 (mitochondrial kinetic protein 49 and 50). Essentially, the mitochondria division contributes to ensure their proper quality that allows to maintain the cells in a healthy state [43]. It has been proven that the presence of fragmented (globular) mitochondria is characteristic for vital and pluripotent cells with high self-renewal potential [44]. Moreover, miR-21-5p impedes autophagy processes in BMSC_{SAM/P6}, evidenced by decreased accumulation of lysosomes and LAMP2 protein. The high activity of lysosomes, accompanied with LAMP2 accumulation, is widely associated with the progression of selected autophagy [45, 46]. In addition, the level of *Ppar-γ* was downregulated, while expression of *mTOR* raised, which confirms the potential of miR-21 in autophagy

(See figure on next page.)

Fig. 3 MiR-21 improves osteogenic differentiation of BMSCs isolated from senile osteoporotic SAM/P6 mice. **A** The representative images of BMSCs isolated from BALB/c and SAM/P6 mice cultured under osteogenic conditions. The images were taken using an inverted light microscope under 100-fold magnification and the scale bar is equal 200 μm. The staining signals of visualised calcium deposits were presented as a bar graph **(C)**. **B** The representative images (z-stacks) of cells' nuclei, actin cytoskeleton and RUNX-2 protein in BMSCs isolated from BALB/c and SAM/P6 mice. The confocal microscope photographs were taken under 630-fold magnification and the scale bar is equal to 40 μm. The staining intensity of RUNX-2 protein was presented as a bar graph **(D)**. The RT-qPCR technique was used to present the gene expression of **E** *Runx-2*, **F** *Coll-1*, **G** *Alpl*, **H** *Bmp-2*, **I** *Opn*, **J** *Opg* and **K** *Ocl*. The RT-qPCR measurements were performed using RQMAX method and presented in a log scale. **L** The gating procedure of BMSCs isolated from BALB/c and SAM/P6 mice. **M** The histograms presenting the positively stained population of cells (red line) for RUNX-2 protein. Each measurement was performed for 1000 events. Significant differences between groups are indicated with asterisk: **p* < 0.05, ***p* < 0.01, ****p* < 0.001. Non-significant differences are marked as *ns*

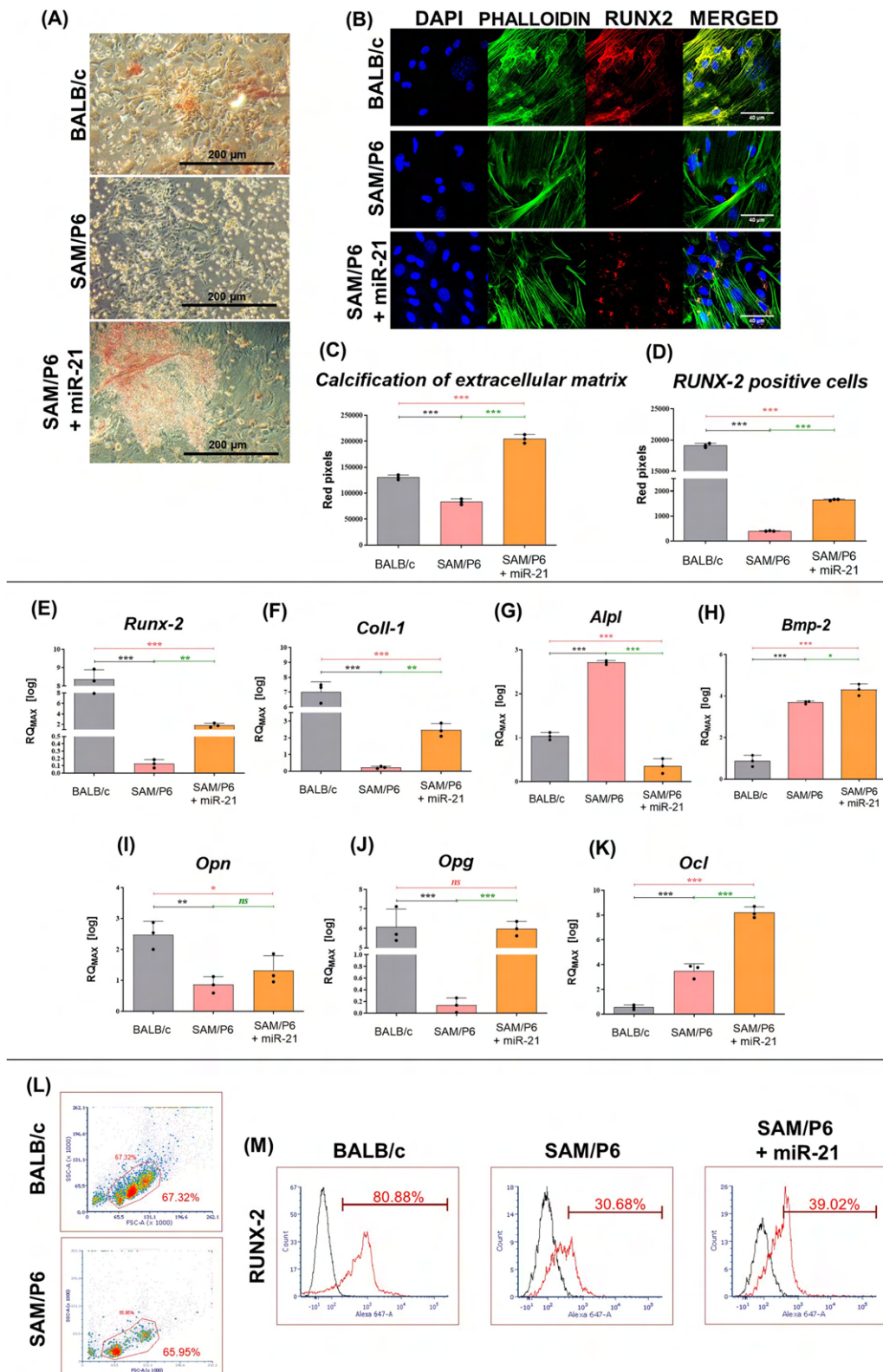


Fig. 3 (See legend on previous page.)

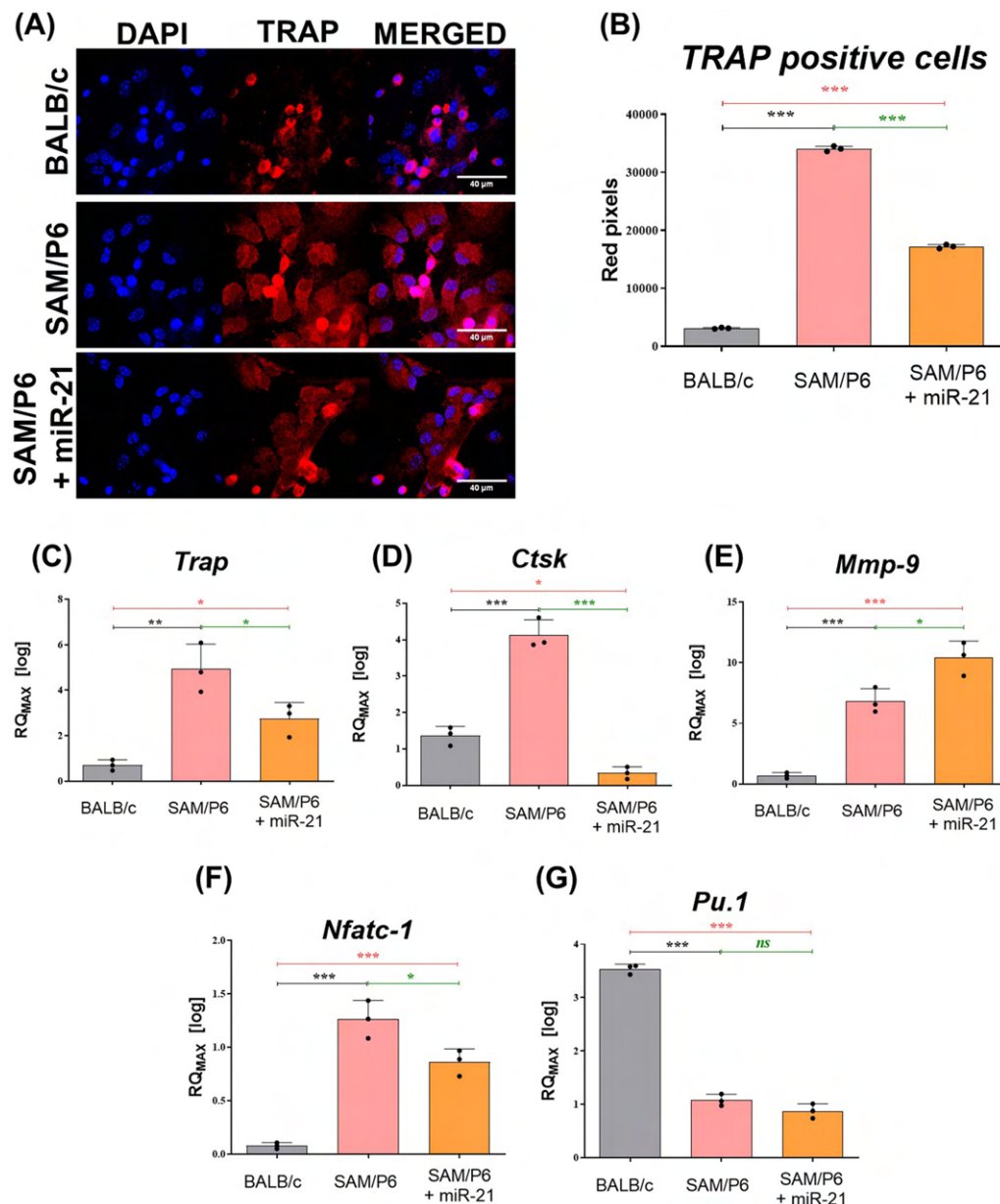


Fig. 4 MiR-21 inhibits osteoclastogenesis in BMSCs isolated from senile osteoporotic SAM/P6 mice. **A** The representative images (z-stacks) of cells' nuclei, actin cytoskeleton and TRAP protein in BMSCs isolated from BALB/c and SAM/P6 mice. The confocal microscope photographs were taken under 630-fold magnification and the scale bar is equal to 40 μ m. The staining intensity of TRAP protein was presented as a bar graph (**B**). The RT-qPCR technique was used to present the gene expression of **C** *Trap*, **D** *Ctsk*, **E** *Mmp-9*, **F** *Nfatc-1* and **G** *Pu.1*. The RT-qPCR measurements were performed using RQMAX method and presented in a log scale. Significant differences between groups are indicated with asterisk: * $p < 0.05$, ** $p < 0.01$, *** $p < 0.001$. Non-significant differences are marked as *ns*

regulation [45]. Previously, it was proven that the activation of mTOR pathway inhibits autophagy induction and prevents pathological expression of lysosomal and autophagy genes [47, 48]. Moreover, the PI3K/Akt/mTOR pathway plays a crucial role in regulating the cell cycle. Its overregulation by miR-21 may release the BMSCs from cell cycle arrest while promotes the cells proliferation.

We have found significantly enhanced expression of *Runx-2*, *Coll-1*, *Bmp-2*, *Opg* and *Ocl* in differentiated BMSC_{SAM/P6} with upregulated miR-21. It seems that miR-21-5p activates both early and late osteogenic-related markers. RUNX-2 has been previously shown to be a master regulator of osteoblast differentiation, matrix production and mineralization, making it a critical early osteogenesis marker [49]. Moreover, RUNX-2 regulates

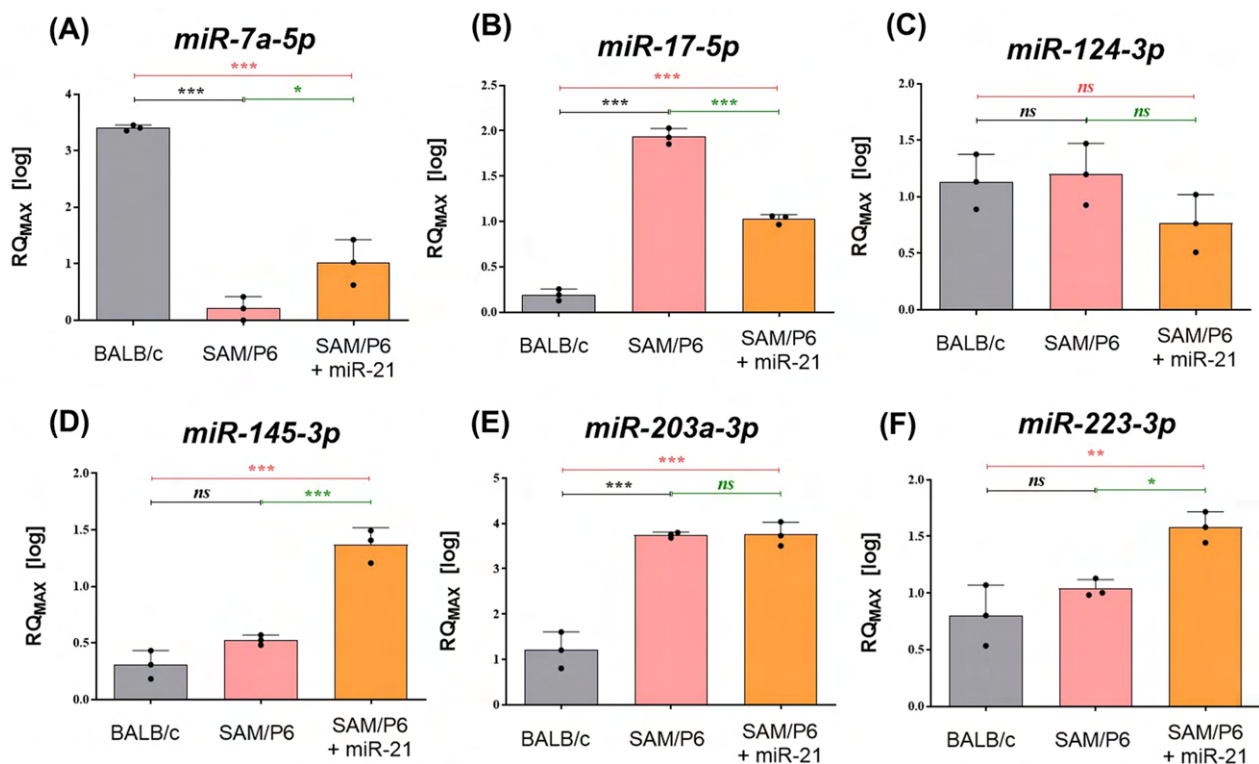


Fig. 5 MiR-21 affects the expression of non-protein-coding RNAs in BMSCs isolated from senile osteoporotic SAM/P6 mice. The RT-qPCR technique was used to present the gene expression of **A** *miR-7a-5p*, **B** *miR-17-5p*, **C** *miR-124-3p*, **D** *miR-145-3p*, **E** *miR-203a-3p* and **F** *miR-223-3p*. The RT-qPCR measurements were performed using RQMAX method and presented in a log scale. Significant differences between groups are indicated with asterisk: * $p < 0.05$, ** $p < 0.01$, *** $p < 0.001$. Non-significant differences are marked as *ns*

other major osteoblasts specific downstream transcripts, including COL1, OPN and OCL. Obtained data strongly correlates with enhanced extracellular matrix formation accompanied with calcium deposits accumulation in BMSC_{SAM/P6+miR-21}. The presented results stay in line with our previous studies regarding the pro-osteogenic activity of miR-21. We have shown that downregulation of miR-21 hampers the proper extracellular matrix reconstruction during osteogenic differentiation in murine MC3T3-E1 cell line [20]. Conversely, upregulation of miR-21 combined with miR-124 and nanohydroxyapatite (nHAp), improves the osteogenic differentiation of MC3T3-E1 cells and murine BMSCs

[28, 50]. Positive effect of miR-21-5p on osteogenesis in BMSC process has also been confirmed by other authors that found activation of Smad7-Smad1/5/8-Runx-2 pathway in miR-21-KO mice model [51]. Interestingly, recent data indicate a beneficial role of miR-21 as a regulator of osteogenic differentiation of periodontal ligament stem cells by targeting Smad5 [52]. On the other hand, OPG belongs to the tumour necrosis factor receptor (TNFR) superfamily and its inhibitory effect on osteoclasts proliferation and maturation has been shown previously [53]. Moreover, recent data suggest that OPG knockout mice develop osteoporosis and are characterised by an enhanced number of osteoclasts. Furthermore, their

(See figure on next page.)

Fig. 6 MiR-21 improves regenerative potential of BMSCs in senile osteoporotic SAM/P6 mice strain in vivo. During the procedure, two mice ($n = 2$) were operated. **A** The photograph of critical-size cranial defects during the mice operation. **B** The RTG images of SAM/P6 mice 2 weeks after the procedure. The defects were marked on the images using red circles. Scale bar is equal to 5 mm. **C** The external and internal photographs obtained during μ CT analyses of the defects in SAM/P6 mice. The ratio of newly formed tissue to the initial defect area was presented as a bar graph (**E**) and the new bone was indicated with red arrows. **D** The SEM-EDX analyses of the defects, as well as calcium and phosphorus distribution in SAM/P6 mice. The images were captured under 35-fold magnification and the scale bar is equal to 200 μ m. The SEM-EDX signal of calcium and phosphorus concentration were measured and presented as bar graphs (**F**, **G**). The mRNA level of **H** *miR-21-5p*, **I** *miR-124-3p*, **J** *Runx-2* and **K** *Trap* within the defect site. Significant differences between groups are indicated with asterisk: * $p < 0.05$, ** $p < 0.01$, *** $p < 0.001$. Non-significant differences are marked as *ns*

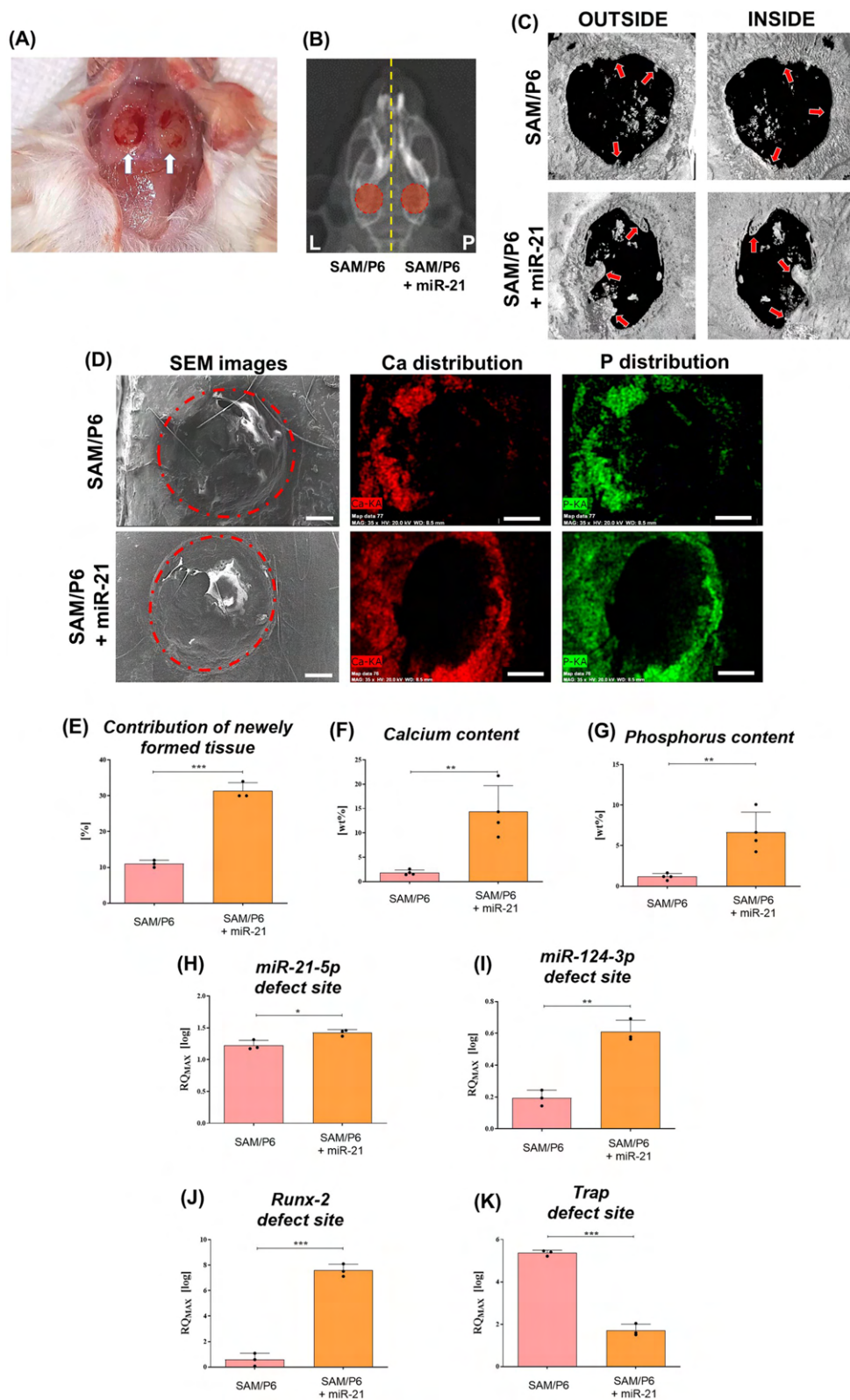


Fig. 6 (See legend on previous page.)

BMSCs exhibit high expression of adipogenic related markers leading to accumulation of adipocytes within bone marrow [53]. Contrary, the *Alpl* (alkaline phosphatase) level was downregulated after miR-21 addition. *Alpl* is considered as a crucial marker of early osteogenesis. Therefore, we hypothesise that it might be a signal of accelerated differentiating processes proven by a greater expansion of ECM in $BMSC_{SAM/P6+miR-21}$ and accumulation of transcripts considered as late markers of osteogenesis. The changeable expression profile of *Alpl* during osteogenic differentiation was noted previously by other authors [54, 55].

Simultaneously, miR-21 upregulation negatively affected *Trap*, *Ctsk* and *Nfatc-1* expression, thus, rescues osteoporotic $BMSC_{SAM/P6}$ from their osteoclastic-like nature. TRAP has been shown to be a critical cytochemical marker of osteoclasts and its high level in patients' serum corresponds with bone resorption process in menopausal women [56]. TRAP has been identified as a critical regulator of skeleton development and bone mineralization, collagen synthesis and degradation, production of dendritic cells, as well as macrophages recruitment [15]. Conversely, miR-21 did not change significantly the expression of *Pu.1*; however, we noticed its higher level in $BMSC_{SAM/P6}$ compared to $BMSC_{BALB/c}$. Obtained results stay in line with previous studies that illustrated the important role of *Nfatc-1* and *Pu.1* during osteoclast maturation in murine BMSCs and RAW264.7

cell lines. Essentially, the inadequate level of both transcripts may also be the cause of osteoporosis progression [57–59]. Inhibiting osteoclasts activity might be an important strategy for protection of bone resorption, thus, protection against osteoporosis development.

The activity of particular miRNAs regulating gene expression has been identified as a critical phenomenon that might significantly affect bone formation and bone resorption. In this study, we have found that miR-21-5p increases the expression of miR-7a-5p, miR-145-3p and miR-223-3p in $BMSC_{SAM/P6+miR-21}$. Their enhanced expression might be considered as a good prognosis for miR-21 application due to their significant involvement in maintaining bone formation [2, 60–62]. Interestingly, in this study we observed a dual function of miR-21. Its upregulation resulted in a higher expression of transcripts involved in osteoblast formation in $BMSC_{SAM/P6}$. On the other hand, a reduced expression of miR-17-5p and miR-124-3p that are involved in osteoporosis progression has been evidenced [63–65].

In order to verify the therapeutic potential of miR-21-5p, we performed in vivo bilateral cranial defect model using osteoporotic SAM/P6 mice. Since SAM/P6 mice represent the model of senile osteoporosis with low bone mass and reduced BMD index (bone mineral density), verification of clinical effectiveness using this particular model is fully justified. We observed a higher accumulation of calcium and phosphorus within

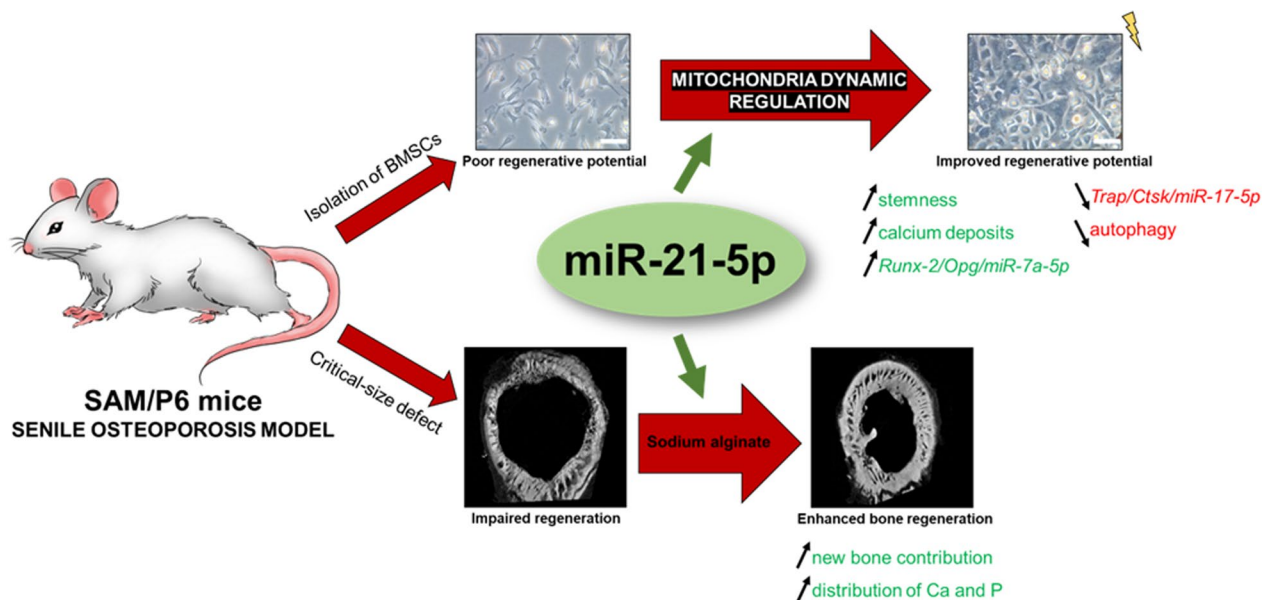


Fig. 7 A graphical abstract of performed experiment. Upregulation of miR-21-5p regulates the dynamic of mitochondria network, thus, positively affects the proper mineralization of extracellular matrix in $BMSC_{SAM/P6}$ and accumulation of proteins crucial for bone homeostasis maintenance. MiR-21 decreases the deteriorated autophagy and regulates mitochondrial network dynamic in BMSCs. In vivo study confirms the results obtained during ex vivo experiments, evidenced by enhanced bone regeneration and greater accumulation of Ca and P. All images and illustrations depicted in this figure were prepared by the Authors

the defect sites in SAM/P6_{miR-21} group two weeks after the procedure. Additionally, the contribution of newly formed tissue was significantly higher in SAM/P6_{miR-21} when compared to SAM/P6_{CTRL}. When combined, these results indicate improved osteogenesis in SAM/P6_{miR-21}, resulting in the intensified formation of functional, highly mineralized bone tissue. Obtained results show the osteoinductive properties of miR-21 confirmed on critical-size cranial defect model. In this study, we have proposed the potential mechanism of miR-21 action indicating its potential targets at mRNA level. We believe that the obtained data sheds a promising light on the potential therapeutic application of miR-21-5p in osteoporotic fractures treatment [50, 66].

Conclusions

Here, we demonstrated for the first time that upregulation of miR-21-5p in BMSCs derived from unique model of senile osteoporotic SAM/P6 mice results in modulation of mitochondria network dynamic, thus rejuvenation of cells' phenotype and improved bone-forming capability (Fig. 7). We have proven that miR-21 upregulation positively affects the proper mineralization of extracellular matrix in BMSC_{SAM/P6} and accumulation of proteins crucial for bone homeostasis maintenance. Importantly, miR-21 regulates the deteriorated autophagy of BMSCs. Performed *in vivo* study confirms the results obtained during *ex vivo* experiments. Obtained results stay in line with our previous papers concerning the effect of miR-21 in murine MC3T3-E1 cell line and BMSCs [20, 28, 50]. However, for the first time the rejuvenating role of miR-21 was identified using BMSCs isolated from senile accelerated SAM/P6 mice, as well as focused on mitochondria metabolism. We believe that obtained results may serve as an important factor during investigations in terms of osteoporosis diagnosis and treatment.

Abbreviations

ALPL	Alkaline phosphatase
BALB/c	Healthy BALB/c mice strain
BAX	Bcl-2-associated X protein
BCL-2	B-cell lymphoma 2
BMP-2	Bone morphogenetic protein 2
BMSCs	Bone marrow-derived mesenchymal stem/stromal cells
COLL-1	Collagen type 1
CSD	Critical-size cranial defect
CTSK	Cathepsin K
DRP1	Dynamamin-related GTPase 1
ECM	Extracellular matrix
FBS	Fetal bovine serum
FIS1	Mitochondrial fission 1 protein
HAp	Hydroxyapatite
HBSS	Hank's balanced salt solution
IOF	International Osteoporosis Foundation
LAMP2	Lysosome-associated membrane protein 2
MFF	Mitochondrial fission factor

MFN-1	Mitofusin-1
MFN-2	Mitofusin-2
MiD49 & MiD50	Mitochondrial kinetic protein 49 and 50
miRNA/microRNA	Small non-protein-coding RNA
miR-21/miR-21-5p	MicroRNA-21-5p
MMP-9	matrix metalloproteinase 9
MSCs	Mesenchymal stem cells
mTOR	Mammalian target of rapamycin kinase
NFATC-1	Nuclear factor of activated T-cells, cytoplasmic 1
OCL	Osteocalcin
OP	Osteoporosis
OPA1	Optic atrophy protein 1
OPG	Osteoprotegerin
OPN	Osteopontin
PFA	Paraformaldehyde
PU.1	Transcription factor PU.1
PPAR-γ	Peroxisome proliferator-activated receptor gamma
P/S	Penicillin & streptomycin antibiotic
RUNX-2	Runt-related transcription factor 2
RT-qPCR	Reverse transcription followed by a quantitative polymerase chain reaction
SAM/P6	Senescence-accelerated mice prone 6
SEM-EDX	Scanning electron microscope with energy-dispersive X-ray analysis
TRAP	Tartrate-resistant acid phosphatase
WHO	World Health Organization
μ-CT	X-ray computed microtomography

Supplementary Information

The online version contains supplementary material available at <https://doi.org/10.1186/s13287-023-03271-1>.

Additional file 1: Figure S1. MiR-21 regulates the number and phenotype of mitochondria in BMSCs isolated from osteoporotic SAM/P6 mice. Detailed MicroP analysis of mitochondria number (A) as well as mitochondria morphology classified as simple tubes (B), branching tubes (C) and small globes (D). The results are presented as bar graphs. Significant differences between groups are indicated with asterisk: * $p < 0.05$, ** $p < 0.01$, *** $p < 0.001$. Non-significant differences are marked as ns.

Acknowledgements

Not applicable.

Author contributions

MS was involved in methodology (equal), software (equal), validation (equal), investigation (equal), formal analysis (equal), resources (equal), data curation (equal), writing—original draft preparation (equal), writing—review and editing (equal), visualisation (equal); AS helped in conceptualisation (equal), methodology (equal), software (equal), validation (equal), investigation (equal), formal analysis (equal), resources (equal), data curation (equal), writing—original draft preparation (equal), writing—review and editing (equal), visualisation (equal), supervision (equal); AP contributed to methodology (equal), software (equal), validation (equal), formal analysis (equal), resources (equal), writing—original draft preparation (equal), writing—review and editing (equal), visualisation (equal); KM was involved in conceptualisation (equal), validation (equal), writing—original draft preparation (equal), writing—review and editing (equal), supervision (equal), project administration (lead), funding acquisition (lead). All authors read and approved the final manuscript.

Funding

This work was financed by Harmonia 9 project titled "New, two-stage scaffolds based on calcium nanoapatite (nHAP) incorporated with iron nanooxides (Fe₂O₃/Fe₃O₄) with the function of controlled release of miRNA in a static magnetic field for the regeneration of bone fractures in osteoporotic patients" (Grant No. UMO 2017/26/M/NZ5/01184). This work was supported by the Wrocław University of Environmental and Life Sciences (Poland) as the Ph.D. research programme "Innowacyjny Doktorat", no. N070/0006/21. The publication is financed under the Leading Research Groups support project from the subsidy increased for

the period 2020–2025 in the amount of 2% of the subsidy referred to Art. 387 (3) of the Law of 20 July 2018 on Higher Education and Science, obtained in 2019. The funding bodies played no role in the design of the study and collection, analysis and interpretation of data and in writing the manuscript.

Availability of data and materials

The datasets generated during and/or analysed during the current study are available from the corresponding author on reasonable request. The accession numbers presented in Table 1 refer to specific nucleotides and can be found in the official database of National Center for Biotechnology Information (<https://www.ncbi.nlm.nih.gov/>).

Declarations

Ethics approval and consent to participate

The in vivo study was conducted with the full approval of the Local Ethics Committee for Animal Experiments in Wrocław (Resolution no.069/2020/P1, 9.12.2020). The title of ethical approved project: “*New, two-stage scaffolds based on calcium nanoapatite (nHAP) incorporated with iron nanooxides (Fe₂O₃/Fe₃O₄) with the function of controlled release of miRNA in a static magnetic field for the regeneration of bone fractures in osteoporotic patients. In vivo assessment of the osteogenic properties of the obtained materials using the model of critical-size cranial defect in SAMP6 mice.*” The guidelines included in the Act on the Protection of Animals Used for Scientific or Educational Purposes from 15 of January 2015, which implements Directive 2010/63/EU of the European Parliament and the Council of 22 September 2010, were fully followed during the study. Moreover, the procedures of PN-EN ISO 10993–2:2006 standards were used. The manuscript has been checked in accordance with ARRIVE guidelines (Animal Research: Reporting of In Vivo Experiments) in order to improve the reporting of research involving animals, as well as maximise the quality and reliability of published research.

Consent for publication

Not applicable.

Competing interests

The authors declare that they have no competing interests.

Author details

¹Department of Experimental Biology, The Faculty of Biology and Animal Science, University of Environmental and Life Sciences Wrocław, Norwida 27B St, 50-375 Wrocław, Poland. ²Department of Medicine and Epidemiology, School of Veterinary Medicine, University of California, One Shields Avenue, Davis, CA 95616-8739, USA. ³International Institute of Translational Medicine, Jesionowa 11 Street, 55-124 Malin, Poland.

Received: 5 April 2022 Accepted: 8 March 2023

Published online: 29 March 2023

References

- Parra-Torres AY, Valdés-Flores M, Velázquez-Cruz LO and R. Molecular aspects of bone remodeling [Internet]. Topics in osteoporosis. IntechOpen; 2013 [cited 2021 Sep 20]. <https://www.intechopen.com/chapters/44505>
- Sikora M, Marycz K, Śmieszek A. Small and long non-coding RNAs as functional regulators of bone homeostasis, acting alone or cooperatively. *Mol Ther Nucleic Acids*. 2020;21:792–803.
- Chen K, Jiao Y, Liu L, Huang M, He C, He W, et al. Communications between bone marrow macrophages and bone cells in bone remodeling. *Front Cell Dev Biol*. 2020;8: 598263.
- WHO_Technical_Report.pdf [Internet]. [cited 2021 Sep 21]. https://www.sheffield.ac.uk/FRAX/pdfs/WHO_Technical_Report.pdf
- Gullberg B, Johnell O, Kanis JA. World-wide projections for hip fracture. *Osteoporos Int J Establ Result Coop Eur Found Osteoporos Natl Osteoporos Found USA*. 1997;7(5):407–13.
- Sander R. Asymptomatic osteoporosis masks the importance of taking medication. *Nurs Older People*. 2007;19(10):23.
- Jin Z, Chen J, Shu B, Xiao Y, Tang D. Bone mesenchymal stem cell therapy for ovariectomized osteoporotic rats: a systematic review and meta-analysis. *BMC Musculoskelet Disord*. 2019;20(1):556.
- Sikora M, Śmieszek A, Marycz K. Bone marrow stromal cells (BMSCs CD45⁻/CD44⁺/CD73⁺/CD90⁺) isolated from osteoporotic mice SAM/P6 as a novel model for osteoporosis investigation. *J Cell Mol Med*. 2021;25(14):6634–51.
- Mohamed-Ahmed S, Yassin MA, Rashad A, Espedal H, Idris SB, Finne-Wistrand A, et al. Comparison of bone regenerative capacity of donor-matched human adipose-derived and bone marrow mesenchymal stem cells. *Cell Tissue Res*. 2021;383(3):1061–75.
- Arthur A, Gronthos S. Clinical application of bone marrow mesenchymal stem/stromal cells to repair skeletal tissue. *Int J Mol Sci*. 2020;21(24):E9759.
- Sun Y, Yuan Y, Wu W, Lei L, Zhang L. The effects of locomotion on bone marrow mesenchymal stem cell fate: insight into mechanical regulation and bone formation. *Cell Biosci*. 2021;11(1):88.
- Marędziaś M, Marycz K, Tomaszewski KA, Kornicka K, Henry BM. The influence of aging on the regenerative potential of human adipose derived mesenchymal stem cells. *Stem Cells Int*. 2016;2016: e2152435.
- Kornicka K, Houston J, Marycz K. Dysfunction of mesenchymal stem cells isolated from metabolic syndrome and type 2 diabetic patients as result of oxidative stress and autophagy may limit their potential therapeutic use. *Stem Cell Rev Rep*. 2018;14(3):337–45.
- Alicka M, Major P, Wysocki M, Marycz K. Adipose-derived mesenchymal stem cells isolated from patients with type 2 diabetes show reduced “stemness” through an altered secretome profile, impaired anti-oxidative protection, and mitochondrial dynamics deterioration. *J Clin Med*. 2019;8(6):765.
- Hayman AR. Tartrate-resistant acid phosphatase (TRAP) and the osteoclast/immune cell dichotomy. *Autoimmunity*. 2008;41(3):218–23.
- Park JK, Rosen A, Saffitz JE, Asimaki A, Litovsky SH, Mackey-Bojack SM, et al. Expression of cathepsin K and tartrate-resistant acid phosphatase is not confined to osteoclasts but is a general feature of multinucleated giant cells: systematic analysis. *Rheumatology*. 2013;52(8):1529–33.
- Ginaldi L, Di Benedetto MC, De Martinis M. Osteoporosis, inflammation and ageing. *Immun Ageing A*. 2005;2:14.
- Ell B, Kang Y. MicroRNAs as regulators of bone homeostasis and bone metastasis. *BoneKey Rep*. 2014;3:549.
- Zhao Z, Li X, Zou D, Lian Y, Tian S, Dou Z. Expression of microRNA-21 in osteoporotic patients and its involvement in the regulation of osteogenic differentiation. *Exp Ther Med*. 2019;17(1):709–14.
- Śmieszek A, Marcinkowska K, Pielok A, Sikora M, Valihrach L, Marycz K. The role of miR-21 in osteoblasts-osteoclasts coupling in vitro. *Cells*. 2020;9(2):479.
- Seweryn A, Pielok A, Lawniczak-Jablonska K, Pietruszka R, Marcinkowska K, Sikora M, et al. Zirconium oxide thin films obtained by atomic layer deposition technology abolish the anti-osteogenic effect resulting from miR-21 inhibition in the pre-osteoblastic MC3T3 cell line. *Int J Nanomed*. 2020;15:1595–610.
- Ichioka N, Inaba M, Kushida T, Esumi T, Takahara K, Inaba K, et al. Prevention of senile osteoporosis in SAMP6 mice by intrabone marrow injection of allogeneic bone marrow cells. *Stem Cells*. 2002;20(6):542–51.
- Chen H, Zhou X, Emura S, Shoumura S. Site-specific bone loss in senescence-accelerated mouse (SAMP6): a murine model for senile osteoporosis. *Exp Gerontol*. 2009;44(12):792–8.
- Niimi K, Takahashi E. Characterization of senescence-accelerated mouse prone 6 (SAMP6) as an animal model for brain research. *Exp Anim*. 2014;63(1):1–9.
- Sikora M, Śmieszek A, Marycz K. Bone marrow stromal cells (BMSCs CD45⁻/CD44⁺/CD73⁺/CD90⁺) isolated from osteoporotic mice SAM/P6 as a novel model for osteoporosis investigation. *J Cell Mol Med*. 2021;25:6634–51. <https://doi.org/10.1111/jcmm.16667>.
- Śmieszek A, Czyrek A, Basinska K, Trynda J, Skaradzińska A, Siudzińska A, et al. Effect of metformin on viability, morphology, and ultrastructure of mouse bone marrow-derived multipotent mesenchymal stromal cells and Balb/3T3 embryonic fibroblast cell line. *BioMed Res Int*. 2015;2015: e769402.

27. Soleimani M, Nadri S. A protocol for isolation and culture of mesenchymal stem cells from mouse bone marrow. *Nat Protoc.* 2009;4(1):102–6.
28. Marycz K, Śmieszek A, Marcinkowska K, Sikora M, Turlej E, Sobierajska P, et al. Nanohydroxyapatite (nHAp) doped with iron oxide nanoparticles (IO), miR-21 and miR-124 under magnetic field conditions modulates osteoblast viability, reduces inflammation and inhibits the growth of osteoclast—a novel concept for osteoporosis treatment: part 1. *Int J Nanomedicine.* 2021;16:3429–56.
29. Peng JY, Lin CC, Chen YJ, Kao LS, Liu YC, Chou CC, et al. Automatic morphological subtyping reveals new roles of caspases in mitochondrial dynamics. *PLoS Comput Biol.* 2011;7(10): e1002212.
30. Śmieszek A, Tomaszewski K, Kornicka K, Marycz K. Metformin promotes osteogenic differentiation of adipose-derived stromal cells and exerts pro-osteogenic effect stimulating bone regeneration. *J Clin Med.* 2018;7(12):482.
31. Porter JL, Varacallo M. Osteoporosis. In: StatPearls [Internet]. Treasure Island (FL): StatPearls Publishing; 2021 [cited 2021 Sep 20]. <http://www.ncbi.nlm.nih.gov/books/NBK441901/>
32. Zhang Y, Wang N, Zhang C. Exosome derived from bone marrow mesenchymal stem cells pre-treated with curcumin alleviates osteoporosis by promoting osteogenic differentiation via regulating the METTL3/microRNA-320/RUNX2 signaling pathway. *Arch Med Sci [Internet].* 2021 Apr 18 [cited 2021 Sep 20]; <https://www.archivesofmedicalscience.com/Exosome-derived-from-bone-marrow-mesenchymal-stem-cells-pre-treated-with-curcumin.125788.0.2.html>
33. Huai Y, Zhang W, Chen Z, Zhao F, Wang W, Dang K, et al. A comprehensive analysis of microRNAs in human osteoporosis. *Front Endocrinol.* 2020;11: 516213.
34. Liu Y, Liu J, Xia T, Mi BB, Xiong Y, Hu LC, et al. MiR-21 promotes fracture healing by activating the PI3K/Akt signaling pathway. *Eur Rev Med Pharmacol Sci.* 2019;23(7):2727–33.
35. Sun X, Li X, Qi H, Hou X, Zhao J, Yuan X, et al. MiR-21 nanocapsules promote early bone repair of osteoporotic fractures by stimulating the osteogenic differentiation of bone marrow mesenchymal stem cells. *J Orthop Transl.* 2020;24:76–87.
36. Rodríguez J, Astudillo P, Ríos S, Pino M. Involvement of adipogenic potential of human bone marrow mesenchymal stem cells (MSCs) in osteoporosis. *Curr Stem Cell Res Ther.* 2008;3:208–18.
37. Sobecki M, Mrouj K, Camasses A, Parisis N, Nicolas E, Llères D, et al. The cell proliferation antigen Ki-67 organises heterochromatin. *Watt FM, editor. eLife.* 2016;5:e13722.
38. Wagner W, Horn P, Castoldi M, Diehlmann A, Bork S, Saffrich R, et al. Replicative senescence of mesenchymal stem cells: a continuous and organized process. *PLoS ONE.* 2008;3(5): e2213.
39. Iordache F, Constantinescu A, Andrei E, Amuzescu B, Halitzchi F, Savu L, et al. Electrophysiology, immunophenotype, and gene expression characterization of senescent and cryopreserved human amniotic fluid stem cells. *J Physiol Sci.* 2016;66(6):463–76.
40. Airini R, Iordache F, Alexandru D, Savu L, Epureanu FB, Mihailescu D, et al. Senescence-induced immunophenotype, gene expression and electrophysiology changes in human amniocytes. *J Cell Mol Med.* 2019;23(11):7233–45.
41. Liu J, Ding Y, Liu Z, Liang X. Senescence in mesenchymal stem cells: functional alterations, molecular mechanisms, and rejuvenation strategies. *Front Cell Dev Biol.* 2020;8:258. <https://doi.org/10.3389/fcell.2020.00258>.
42. Martini H, Iacovoni JS, Maggiorani D, Dutaur M, Marsal DJ, Roncalli J, et al. Aging induces cardiac mesenchymal stromal cell senescence and promotes endothelial cell fate of the CD90 + subset. *Aging Cell.* 2019;18(5): e13015.
43. Seo BJ, Yoon SH, Do JT. Mitochondrial dynamics in stem cells and differentiation. *Int J Mol Sci.* 2018;19(12):3893.
44. Ren L, Chen X, Chen X, Li J, Cheng B, Xia J. Mitochondrial dynamics: fission and fusion in fate determination of mesenchymal stem cells. *Front Cell Dev Biol.* 2020;8: 580070.
45. Soto-Avellaneda A, Morrison BE. Signaling and other functions of lipids in autophagy: a review. *Lipids Health Dis.* 2020;19(1):214.
46. Yim WWY, Mizushima N. Lysosome biology in autophagy. *Cell Discov.* 2020;6(1):1–12.
47. Kim YC, Guan KL. mTOR: a pharmacologic target for autophagy regulation. *J Clin Invest.* 2015;125(1):25–32.
48. Ramhormozi P, Mohajer Ansari J, Simorgh S, Nobakht M. Bone marrow-derived mesenchymal stem cells combined with simvastatin accelerates burn wound healing by activation of the Akt/mTOR pathway. *J Burn Care Res Off Publ Am Burn Assoc.* 2020;41(5):1069–78.
49. Choi JW, Shin S, Lee CY, Lee J, Seo HH, Lim S, et al. Rapid induction of osteogenic markers in mesenchymal stem cells by adipose-derived stromal vascular fraction cells. *Cell Physiol Biochem Int J Exp Cell Physiol Biochem Pharmacol.* 2017;44(1):53–65.
50. Marycz K, Śmieszek A, Kornicka-Garbowska K, Pielok A, Janeczek M, Lipińska A, et al. Novel nanohydroxyapatite (nHAp)-based scaffold doped with iron oxide nanoparticles (IO), functionalized with small non-coding RNA (miR-21/124) modulates expression of runt-related transcriptional factor 2 and osteopontin, promoting regeneration of osteoporotic bone in bilateral cranial defects in a senescence-accelerated mouse model (SAM/P6). PART 2. *Int J Nanomedicine.* 2021;16:6049–65.
51. Li X, Guo L, Liu Y, Su Y, Xie Y, Du J, et al. MicroRNA-21 promotes osteogenesis of bone marrow mesenchymal stem cells via the Smad7-Smad1/5/8-Runx2 pathway. *Biochem Biophys Res Commun.* 2017;493(2):928–33.
52. Wei F, Yang S, Guo Q, Zhang X, Ren D, Lv T, et al. MicroRNA-21 regulates osteogenic differentiation of periodontal ligament stem cells by targeting Smad5. *Sci Rep.* 2017;7(1):16608.
53. Zhang L, Liu M, Zhou X, Liu Y, Jing B, Wang X, et al. Role of osteoprotegerin (OPG) in bone marrow adipogenesis. *Cell Physiol Biochem.* 2016;40(3–4):681–92.
54. Phunikom N, Boonmuen N, Kheolamai P, Suksen K, Manochantr S, Tantrawatpan C, et al. Andrographolide promotes proliferative and osteogenic potentials of human placenta-derived mesenchymal stem cells through the activation of Wnt/ β -catenin signaling. *Stem Cell Res Ther.* 2021;12(1):241.
55. Tsai MT, Li WJ, Tuan RS, Chang WH. Modulation of osteogenesis in human mesenchymal stem cells by specific pulsed electromagnetic field stimulation. *J Orthop Res Off Publ Orthop Res Soc.* 2009;27(9):1169–74.
56. Ballanti P, Minisola S, Pacitti MT, Scarnecchia L, Rosso R, Mazzuoli GF, et al. Tartrate-resistant acid phosphate activity as osteoclastic marker: sensitivity of cytochemical assessment and serum assay in comparison with standardized osteoclast histomorphometry. *Osteoporos Int J Establ Result Coop Eur Found Osteoporos Natl Osteoporos Found USA.* 1997;7(1):39–43.
57. Zhou F, Shen Y, Liu B, Chen X, Wan L, Peng D. Gastrodin inhibits osteoclastogenesis via down-regulating the NFATc1 signaling pathway and stimulates osseointegration in vitro. *Biochem Biophys Res Commun.* 2017;484(4):820–6.
58. Crotti TN, Sharma SM, Fleming JD, Flannery MR, Ostrowski MC, Goldring SR, et al. PU.1 and NFATc1 mediate osteoclastic induction of the mouse beta3 integrin promoter. *J Cell Physiol.* 2008;215(3):636–44.
59. Ishiyama K, Yashiro T, Nakano N, Kasakura K, Miura R, Hara M, et al. Involvement of PU.1 in NFATc1 promoter function in osteoclast development. *Allergol Int.* 2015;64(3):241–7.
60. Ghafouri-Fard S, Abak A, Tavakkoli Avval S, Rahmani S, Shoorei H, Taheri M, et al. Contribution of miRNAs and lncRNAs in osteogenesis and related disorders. *Biomed Pharmacother.* 2021;142: 111942.
61. Tang Z, Xu T, Li Y, Fei W, Yang G, Hong Y. Inhibition of CRY2 by STAT3/miRNA-7-5p promotes osteoblast differentiation through upregulation of CLOCK/BMAL1/P300 expression. *Mol Ther Nucleic Acids.* 2020;19:865–76.
62. Sun K, Wang J, Liu F, Ji Z, Guo Z, Zhang C, et al. Ossotide promotes cell differentiation of human osteoblasts from osteogenesis imperfecta patients by up-regulating miR-145. *Biomed Pharmacother Biomedecine Pharmacother.* 2016;83:1105–10.
63. Wan S, Chen X, He Y, Yu X. Novel functions of microRNA-17-92 cluster in the endocrine system. *Curr Drug Targets.* 2018;19(2):191–200.
64. Li H, Li T, Wang S, Wei J, Fan J, Li J, et al. miR-17-5p and miR-106a are involved in the balance between osteogenic and adipogenic differentiation of adipose-derived mesenchymal stem cells. *Stem Cell Res.* 2013;10(3):313–24.
65. Tang J, Lin X, Zhong J, Xu F, Wu F, Liao X, et al. miR-124 regulates the osteogenic differentiation of bone marrow-derived mesenchymal stem cells by targeting Sp7. *Mol Med Rep.* 2019;19:3807–14.
66. Yang C, Liu X, Zhao K, Zhu Y, Hu B, Zhou Y, et al. miRNA-21 promotes osteogenesis via the PTEN/PI3K/Akt/HIF-1 α pathway and enhances bone regeneration in critical size defects. *Stem Cell Res Ther.* 2019;10(1):65.

Publisher's Note

Springer Nature remains neutral with regard to jurisdictional claims in published maps and institutional affiliations.